Department of Petroleum Engineering

Identification of fault and top seal effectiveness through an integration of hydrodynamic and capillary analysis techniques.

James Ross Underschultz

This thesis is presented for the Degree of

Doctor of Philosophy
of
Curtin University of Technology

January 2009

Student:	James Ross Underschultz (ID No. 13232760)
Course:	Doctor of Philosophy – Petroleum Engineering
Committee:	Dr. B. Evans (chairperson), Dr. A. Tait (supervisor), Dr. C. Otto (co-supervisor at Shell International Exploration and Production).

1. Declaration

To the best of my knowledge and belief this thesis contains no material previously published by any other person except where due acknowledgment has been made. This thesis contains no material which has been accepted for the award of any other degree or diploma in any university.

2. Abstract

Fault and top seal effectiveness has proved to be a significant risk in exploration success, and creates a large uncertainty in predicting reservoir performance. This is particularly true in the Australian context, but equally applies to exploration provinces worldwide.

Seals can be broadly classified into fault, intraformational, and top seal. For geological time-scale processes, intraformational and top seals are typically characterised by their membrane seal capacity and fracture threshold pressure. Fault seals are typically characterised by fault geometry, juxtaposition, membrane seal capacity, and reactivation potential. At the production time scale, subtle variations in the permeability distribution within a reservoir can lead to compartmentalization. These are typically characterised by dynamic reservoir models which assume hydrostatic conditions prior to commencement of production. There are few references in the seals literature concerning the integration of hydrodynamic techniques with the various aspects of seal evaluation.

The research for this PhD thesis by published papers includes: Methodology for characterising formation water flow systems in faulted strata at exploration and production time scales; a new theory of hydrodynamics and membrane (capillary) seal

capacity; and case study evaluations demonstrating integrated multidisciplinary techniques for the evaluation of seal capacity (fault, intraformational and top seal) that demonstrate the new theory in practice. By incorporating hydrodynamic processes in the evaluation of total seal capacity, the evidence shows that existing shale gouge ratio – across fault pressure difference (SGR-AFPD) calibration plots need adjustment resulting in the calibration envelopes shifting to the centre of the plot. This adjustment sharpens the predictive capacity for membrane seal analysis in the pre-drill scenario.

This PhD thesis presents the background and rationale for the thesis topic, presents each published paper to be included as part of the thesis and its contribution to the body of work addressing the thesis topic, and presents related published papers that are not included in the thesis but which support the body of published work on the thesis topic. The result of the thesis is a new theory and approach to characterising membrane seal capacity for the total seal thickness, and has implications for an adjusted SGR-AFPD calibration to be applied in pre-drill evaluations of seal capacity.
A large portion of the resources and data required to conduct the research were made available by CSIRO and its associated project sponsors including the CO2CRC.

3. Acknowledgements

I would like to acknowledge CSIRO Petroleum for providing support which allowed my project work to contribute towards this thesis. A large part of the work presented here was conducted within the IPETS research consortia, whose support I greatly appreciate. Project work from within the CO2CRC has contributed to the thesis, and I gratefully acknowledge their support. A case study is included that was sponsored by BHP Billiton Petroleum for which I am grateful. I thank my thesis committee for guidance and support, in particular Dr. Claus Otto for being a mentor and colleague during the process of writing this thesis. I want to thank my wife Jenny and son Simon for their encouragement, patience, forbearance and support during the course of this study. I would like to thank my co-authors for collaboration on many interesting projects and discussing ideas and concepts that had impact on the subject of my thesis. This thesis has gained from editorial review by Dr. Ian Lee and Dianne Elizabeth Budd and technical review by Dr. Claus Otto. I gratefully thank my

examiners Dr. G.W. O'Brien and Dr. J.M. Verweij for their thoughtful and constructive review which has improved this thesis.

4. List of publications included as part of the thesis

1. **Underschultz, J.R**., Otto, C.J. and Bartlett, R. (2005), Formation fluids in faulted aquifers: examples from the foothills of Western Canada and the North West Shelf of Australia. *In:* Boult, P. and Kaldi, J. (eds.), Evaluating fault and cap rock seals: *American Association of Petroleum Geologists, Hedberg Series*, 2, pp. 247-260.

2. **Underschultz, J.R**., Otto, C. and Hennig, A. (2007), Application of hydrodynamics to Sub-Basin-Scale static and dynamic reservoir models. *Journal of Petroleum Science and Engineering*. 57/1-2, pp. 92-105.

3. **Underschultz, J.R**. (2007). Hydrodynamics and membrane seal capacity: *Geofluids Journal*, 7, pp. 148-158.

4. Bailey, W.R., **Underschultz J.,** Dewhurst D.N., Kovack G., Mildren S. and Raven M. (2006). Multi-disciplinary approach to fault and top seal appraisal; Pyrenees-Macedon oil and gas fields, Exmouth Sub-basin, Australian Northwest Shelf. *Marine and Petroleum Geology*, 23, pp. 241-259.

5. **Underschultz, J.R**., Hill, R.A. and Easton, S. (2008). The Hydrodynamics of Fields in the Macedon, Pyrenees and Barrow Sands, Exmouth Sub-Basin: Identifying Seals and Compartments. *Australian Society of Exploration Geophysicists*, 39, pp. 85-93.

6. Gibson-Poole, C.M., Svendsen, L., **Underschultz, J**., Watson, M.N., Ennis-King, J., van Ruth, P.J., Nelson, E.J., Daniel, R.F., and Cinar, Y. (2007). Site Characterisation of a Basin-Scale CO_2 Geological Storage System: Gippsland Basin, Southeast Australia. *Journal of Environmental Geology*. On-line publication not yet in print. http://www.springerlink.com/content/0r4v8l4j846t5308/

7. Gibson-Poole, C.M., Svendsen, L., **Underschultz, J**., Watson, M.N., Ennis-King, J., van Ruth, P., Nelson, E., Daniel, R., and Cinar, Y. (2006). Gippsland Basin Geosequestration: A potential solution for the Latrobe Valley brown coal CO_2 emissions. *Australian Petroleum Production and Exploration Association Journal*, 46 (1), pp. 241-259.

5. Statement of Contribution of Others

Of the papers included as part of this thesis (listed in the previous section), I was the sole author of paper 3. I am the first author on papers 1, 2 and 5. These papers were each based on project work in which I was the principal investigator, but which included collaboration with my co-authors. I wrote these papers myself, having discussions with and technical review by my co-authors. See comments from my co-authors in Appendix 1. Papers 4, 6 and 7 are the result of multidisciplinary projects where the hydrodynamics component was integral, but secondary to the geology. Whilst I contributed text based on my hydrodynamic analysis, the bulk of the papers were written by the first author. See comments from my co-authors in Appendix 1.

6. List of additional publications by the candidate relevant to the thesis but not forming part of it

1. **Underschultz, J.R.**, Ellis, G.K., Hennig, A., Bekele, E., and Otto, C. (2002). Estimating formation water salinity from wireline pressure data: Case study in the Vulcan Sub-basin. *In*: Keep, M. and Moss, S.J. (eds.), The Sedimentary Basins of Western Australia 3: Proceedings of the *Petroleum Exploration Society of Australia Symposium*, Perth, WA, pp. 285-303.

2. Otto, C., **Underschultz, J**., Hennig, A. and Roy, V. (2001). Hydrodynamic analysis of flow systems and fault seal integrity in the Northwest Shelf of Australia: *Australian Petroleum Production and Exploration Association Journal*. 41 (1), pp. 347-365.

3. Hennig, A., **Underschultz, J.R.** and Otto, C.J. (2002). Hydrodynamic analysis of the Early Cretaceous aquifers in the Barrow Sub-basin in relation to hydraulic continuity and fault seal. *In:* Keep, M. and Moss, S.J. (eds.), The Sedimentary Basins of Western Australia 3*:* Proceedings of the *Petroleum Exploration Society of Australia Symposium*, Perth, WA, pp. 305-320.

4. **Underschultz, J.R**., Otto C.J. and Cruse T. (2003). Hydrodynamics to assess hydrocarbon migration in faulted strata - methodology and a case study from the Northwest Shelf of Australia. *Journal of Geochemical Exploration*, 78-79, pp. 469-474.

5. **Underschultz, J**. (2005). Pressure distribution in a reservoir affected by capillarity and hydrodynamic drive: Griffin Field, North West Shelf, Australia. *Geofluids Journal*, 5, pp. 221-235.

6. Gartrell, A., Lisk, M. and **Underschultz, J.** (2002). Controls on trap integrity of the Skua Oil Field, Timor Sea. *In:* Keep, M., and Moss, S.J., (eds), The Sedimentary Basins of Western Australia 3: Proceedings of the *Petroleum Society of Australia Symposium*, Perth, WA, pp. 389-407.

7. **Underschultz, J.R.** and Boult P. (2004). Top seal and reservoir continuity: Hydrodynamic evaluation of the Hutton-Birkhead Reservoir, Gidgealpa Oilfield. In *Eastern Australian Basins Symposium*, 2, pp. 473-482.

8. Simmelink, H.J., **Underschultz, J.R**., Verweij, J.M., Hennig, A., Pagnier, H.J.M., Otto, C.J. (2003). A pressure and fluid dynamic study of the Southern North Sea Basin: *Journal of Geochemical Exploration*, 78-79, pp. 187-190.

Table of contents

7. Introduction and Overview

Fault and top seal effectiveness has proven to be a significant risk in exploration success, and a large uncertainty in predicting reservoir performance within the oil and gas industry. This is particularly true in the Australian context, but equally applies to exploration provinces worldwide.

In Australia's Northwest Shelf for example, late stage convergence resulted in the reactivation of some structures, and basin inversion. This forms an exploration challenge, particularly in the Timor Sea region, because the main period of hydrocarbon generation and trap charge occurred prior to reactivation of the structures (O'Brien et al. 1993). The late stage reactivation has resulted in some previously filled traps leaking some, or all, of their hydrocarbons. Predicting which structures have leaked, and which are likely to have retained their hydrocarbons, has proved to be difficult. Recent research on this problem has focused on fault seal processes.

It has been recognized that fault intersections, where the main structural grain is crosscut at a high angle by deep-seated transfer faults, are at high risk of experiencing leakage and seal breach (Gartrell et al., 2002; Cowley and O'Brien, 2000). Fault intersections that establish either "across-fault", or "up-fault" hydraulic communication, should have signatures identifiable in the formation pressure distribution. Fault zone permeability as related to Shale Gouge Ratio (SGR) has only recently been examined in the Australian context (e.g. Bailey et al. 2006). The SGR can be correlated to the expected across fault pressure differences observed in the fluid phase (Breton et al. 2003). This correlation has not yet been calibrated for any Australian basin, and the existing calibrations for other basins assume a hydrostatic water phase. The likelihood of fault reactivation has been shown to be related to the in-situ stress and the mechanical strength of the fault zone (Jones and Hillis 2003, and Mildren et al. 2002). The effective stress varies with changing pore pressure, which can be induced by a change in the fluid phase as a trap fills. Also, a change in the hydrodynamic driving forces within a basin can lead to changing pore pressure. Either of these conditions can lead to fault reactivation and seal breach.

In the example of Australia's Northwest Shelf, top seals are normally considered to be a very low leakage risk. Top seal breach can occur, however, when either the seal capacity or the fracture threshold of the seal is overcome (Kovack et al. 2004). For example, Bailey et al. (2006) have demonstrated that the base Muderong seal at the Pyrenees-Macedon field area has been compromised with gas migration into the overlying Windalia Radiolarite. The vertical formation pressure distribution can be directly related to the continuity of various fluid phases.

Whilst extensive research exists with regard to capillarity and seals (e.g. Schowalter 1979, Fulljames et al. 1997, Bjorkum et al. 1998 and Brown 2003), and some work has been published on hydrostatic pressure distributions relative to seal capacity and fault reactivation potential (e.g. Mildren et al., 2002), there has been little published work that applies hydrodynamic techniques to membrane seal analysis. Furthermore, since capillary and stress related processes, such as fault reactivation or top seal fracturing, have a direct relation to the movement of subsurface fluids, the development of integrated hydrodynamic and seal evaluation techniques has the potential to significantly advance the understanding and prediction of seal behaviour at both the geological and human (production) time scales.

The thesis presented here is by "published papers" in peer-reviewed technical journals. Each paper seeks to clarify the relationship between hydrodynamic and capillary processes, or identify signatures attributable to a particular type of seal behaviour. This is done through a theoretical approach backed by case study examples. This document describes how each paper addresses an aspect of the thesis topic and summarizes the results.

7.1 Objectives

The overall objective of this research is to develop methodologies and workflows for using hydrodynamic analysis in seal evaluation. This could apply both in the exploration and production realm of the oil and gas industry, but applications can also be highlighted in other areas such as geosequestration of CO_2, characterization of groundwater resources from deep aquifer systems, and geothermal energy.

The objectives are addressed by a series of papers on the following topics, with case study examples where appropriate:

- Fundamental hydrodynamic processes in faulted sedimentary basins and methodologies for the characterisation of flow systems in faulted aquifers.
- The application of hydrodynamic analysis to static and dynamic reservoir models, and the evaluation of production induced aquifer depletion at the sub-basin scale (human time-scale seals processes).
- Signatures of capillarity in pressure distribution for dynamic aquifer systems.
- Theoretical integration of hydrodynamic processes with seal analysis techniques.
- Case study examples of the above points.
- Integrated hydrodynamic workflows linked with seal analysis techniques.

7.2 Significance:

The research forming this thesis has substantial economic and environmental significance to Australia and has further application world wide.

7.2.1 Hydrocarbon Reserves

According to the "2008 Oil and Gas Review" by the Department of Industry and Resources Western Australia, the value of petroleum sales from Western Australia in 2007 was $16.7 billion, of which 44% was crude oil. But crude oil and condensate sales by volume have been declining since 2002. This trend can only be offset by a combination of new discoveries, increased recoverability and a shift to reliance on natural gas. The exploration expenditure by petroleum companies in Western Australia for 2007 was $1.9 billion, more than double that of 2006. With the cost of offshore wells in the multi-millions of dollars, reducing exploration risk can have a significant impact on the finding cost of new discoveries.

The research conducted as part of this thesis has potential impact on both reducing exploration risk, and increasing recoverability.

7.2.2 Environment

The research described in this thesis has direct application to the environmental risking and due diligence associated with carbon capture and geological sequestration.

In particular, estimation of CO_2 storage capacity often depends on the top or fault seal capacity of a CO_2 storage site. The evaluation of CO_2 containment security is related to the seal capacity, fracture threshold and fault reactivation threshold of a storage site. An example of this is the proposed ChevronTexaco Gorgon gas development, which is tied to a successful application for CO_2 sequestration beneath Barrow Island in Western Australia. Key aspects of this evaluation related to top seal capacity and reactivation potential of faults.

The thesis has application to groundwater resources in deep aquifer systems where faults compartmentalise the flow systems such as the Gippsland Basin in Victoria. Finally, an understanding of seal capacity and reservoir compartmentalisation as described in this thesis is important for the evaluation of geothermal energy resources.

7.3 Research Method

To achieve the objectives of this thesis, research was carried out with theoretical analysis of key processes backed by case study examples. This thesis examines various seal-related processes and integrates hydrodynamic techniques with the standard evaluation of each of these processes.

7.3.1 Flow Driving Mechanisms

There are numerous geological processes that drive flow in sedimentary basins including; topographic variation of the water table, horizontal tectonic stress, vertical tectonic loading, burial and compaction, hydrocarbon generation, and erosion related isostatic rebound (Bekele et al. 2001). Some of these processes, such as topographic drive and erosional rebound, have been well documented (e.g. Bachu and Underschultz, 1995), but there remains a degree of uncertainty as to the relative contributions of each, in particular, fluid flow related to tectonics (Bachu, 1999). This is principally due to few hydrodynamic characterisations in faulted strata. The case studies used in this thesis to exemplify various seal processes have been selected from a range of tectonic settings in order to demonstrate hydrodynamic relations to seal capacity under various flow driving mechanisms.

7.3.2 Characterisation of Hydrodynamics in Faulted Aquifers

Standard hydrodynamic approaches to characterizing flow systems in unfaulted aquifers include the analysis of pressure data, both in vertical profile (e.g. pressure-elevation plot), and within the plane of the aquifer after conversion to hydraulic head. Pressure data are supplemented with formation water analysis and formation temperature data to aid in the evaluation of the flow system. Bachu and Michael (2002), Otto et al. (2001), Bachu (1995), and Dahlburg (1995) provide an overview of hydrodynamic analysis techniques. Evaluation techniques for the culling and analysis of formation water samples are described by Underschultz et al. (2002), and Hitchon and Brulotte (1994). Techniques for the evaluation of formation temperature are described by Bachu et al. (1995), and Bachu and Burwash (1991).

A fault zone may compartmentalise an aquifer, yet cause localised hydraulic communication with other stratigraphic levels. Therefore, both juxtaposition and fault zone rock properties need to be considered. Since pressure data from a fault zone itself are not typically available, inferences about the hydraulic nature of the fault need to be made by evaluating the pressure data in the aquifer near the fault. Yassir and Otto (1997), and Underschultz et al. (2005) describe some theoretical patterns of hydraulic head in faulted aquifers for various flow conditions, and pressure gradients on pressure elevation plots for faults with various hydraulic properties. For faulted aquifers, the hydraulic head distribution is first characterised in unfaulted blocks of the aquifer. Then the hydraulic head distributions in adjacent blocks are compared, and built as a patchwork into a flow model that is representative of the faulted strata as a whole (Underschultz et al. 2005, and Underschultz et al. 2003).

7.3.3 Fault Seal and Shale Gouge Ratio (SGR)

Several not entirely independent precursors to SGR have been proposed such as CSP (Clay Smear Potential, Bouvier et al. 1989, Fulljames et al. 1997) and SSF (Shale Smear factor, Lindsay et al. 1993). However, the SGR method has become standard, largely due to the robustness of the algorithm which will estimate a SGR irrespective of data quality, making it ideal for operation with indiscrete data such as a Vshale log. Additionally, the SGR method will still generate a comparable estimate from the detailed layer defined data required to calculate CSP and SSF if required.

For any given point on a fault surface, SGR is equal to the net shale content of the rocks which has moved past the point. Shale Gouge Ratio calculations can be conducted according to Yielding et al. (1977), and these can be related to fault zone permeability (Sperrevik et al. 2002 and Gibson et al. 1998). The standard approach for calculating across fault pressure difference is to use the pressure profile on either side of the fault and regardless of the fluid type (gas, oil or formation water), simply calculate the difference in pressure at a given elevation. Yielding (2000) presents an extensive set of field pressure data from globally distributed basins where the across-fault pressure difference is plotted against the SGR. There is a good correlation between the experimentally determined oil-water threshold pressure and the field across-fault pressure difference. Since pressure data from a fault zone itself is not typically available, inferences about the hydraulic nature of the fault are made by evaluating the pressure data in the aquifer near the fault. Calibration of the SGR-permeability relation can be achieved by examining across fault pressure differences defined by hydrodynamic analysis techniques (Underschultz 2007).

7.3.4 Fault Seal and Juxtaposition

Juxtaposition diagrams form a staple of fault seal analysis; however, case studies such as Bailey et al. (2006), show that juxtaposition alone does not describe the seal potential of a fault. Hydrodynamic analysis in faulted strata (Underschultz et al. 2005, and Underschultz et al. 2003), can be combined with juxtaposition diagrams to determine if additional fault seal analysis is required for adequate risking of seal capacity.

7.3.5 Fault Seal and In-Situ Stress

The likelihood of reactivation of a fault zone can be evaluated by examining the fault zone orientation, the in-situ stress, and the pore pressure (Mildren et al. 2002). The areas most often at risk are fault bends that are orientated at critical angles to the stress field. As pore pressure changes, the effective stress changes correspondingly, and the fault zone moves towards failure. Hydrodynamic techniques can be employed to characterise the pore pressure distribution, and the change in pore pressure over time.

7.3.6 Fault Seal and Structural Geometry

The risk of seal breach can be determined by analysing key leak points on fault systems (e.g. Gartrell et al 2002). These often occur at the intersection of high angle steeply dipping faults (Craw 2000) or at relay zones (Underschultz et al. 2003) where the continuity of the fault plane is interrupted. These leak points have characteristic signatures, often identifiable with hydrodynamic analysis (Underschultz et al. 2005), where they form anomalies in the pressure, water chemistry and temperature distributions.

7.3.7 Top Seal and Capillarity

Top seal capacity is normally evaluated with Mercury Injection Capillary Pressure (MICP) tests (Kovack et al. 2004). However, the resulting seal capacity estimate does not represent a continuum, because it is related to the permeability of the top seal. Hydrodynamic analysis calibrated to MICP data may help to solve this problem. Hydraulic head difference maps across an aquitard are qualitatively related to its seal capacity, and the hydraulic head distribution is a continuum with spatial predictability.

7.3.8 Top Seal, Rock Strength, and In-Situ Stress

The fracture threshold pressure of a top seal can be measured in the laboratory (Kovack et al., 2004), and the in-situ stress can be estimated from leak-off tests and well bore breakouts. When a trap fills with hydrocarbons, the density contrast between the initially water filled pore space, and the now hydrocarbon filled pore space, causes an increase in pore pressure (Brown, 2003). Therefore, maximum column heights that can be held prior to failure of the top seal can be estimated.

7.3.9 Sub-Basin Scale Seal Behaviour at Production Time-Scales

Standard reservoir models are typically separated into a static model that defines some initial condition for the pre-production state of a reservoir, and a dynamic model for the period that the field is producing (Crick et al., 1996). They tend to represent a field, or cluster of fields, and link the pressure in the reservoir to the underlying aquifer through some form of transmissivity factor, assuming the aquifer has a fixed volume (Singh et al., 2005, Craft at al., 1991). The reality is that not only the initial condition of the aquifer system is dynamic, but the aquifer system may respond in a transient fashion at the sub-basin scale to the ongoing production of hydrocarbons,

thus fundamentally changing the fluid dynamics within the basin over a period of time. At the production time-scale, subtle hydraulic barriers can become important for compartmentalization of the reservoir system. Sub-basin scale hydrodynamic assessment of the pressure transient systems can help to identify these barriers.

8. Thesis publications and their relation to the thesis topic

The main aspects of the thesis topic are addressed through a series of 7 publications in peer reviewed technical journals. These are overviewed in this section with a description of how each relates to the thesis subject. In general, the publications fall into three categories: methodology for characterising various aspects of seals analysis; theoretical aspects of hydrodynamics and seals analysis; and case studies demonstrating the application of seals analysis techniques.

> **Underschultz, J.R**., Otto, C.J. and Bartlett, R. (2005), Formation fluids in faulted aquifers: examples from the foothills of Western Canada and the Northwest Shelf of Australia. *In*: Boult, P. and Kaldi, J. (eds.), Evaluating fault and cap rock seals: *American Association of Petroleum Geologists, Hedberg Series*, 2, pp. 247-260.

The characterisation of fluid flow in fractured media is a topic of extensive research; however, the characterisation of regional flow systems in faulted strata is not described in the literature beyond some initial assessments by Wilkinson (1995) and Otto and Yassir (1997). The characterisation of formation water flow systems in faulted strata is an essential and fundamental requirement to understanding the impact of hydrodynamics on the membrane seal capacity of faults and the likelihood of up-fault leakage. As such, it was necessary to define an approach for mapping the flow of formation water in aquifers that have been faulted to various degrees. This paper presents a workflow for determining and representing the flow regime in faulted strata. It identifies signatures in the hydraulic head distribution that are indicative of sealing and leaking faults. Case study examples are presented from the Western Canada Sedimentary Basin and the Northwest Shelf of Australia that demonstrate the application of the described techniques. These demonstrate that the approach described, is valid for both foreland basin compressional tectonic settings, as well as passive margin settings where the fault zones have been reactivated by late stage

inversion. There are inferences made regarding the relation of the structural setting and stress regime, fault geometry and up/down fault leakage, and the across-fault sealing or leaking nature of the fault systems. This paper also provides insight on the flow driving mechanisms within thrust fold belts previously only speculated on in the literature (eg. Bachu, 1999). This paper provides a critical enabling step towards understanding fault seal processes related to hydrodynamic systems.

Underschultz, J.R., Otto, C. and Hennig, A. (2007), Application of hydrodynamics to Sub-Basin-Scale static and dynamic reservoir models. *Journal of Petroleum Science and Engineering*. 57/1-2, pp. 92-105.

The nature of fault and top seal capacity is different at the geological time scale relevant to the migration and trapping of oil and gas, than it is at the human time scale relevant to production and development of hydrocarbon resources. In the Australian context, there are several oil and gas provinces where the majority of the existing oil and gas resources are being produced from a single reservoir horizon. For example the Gippsland Basin in Victoria mainly produces from the Latrobe Aquifer, the Vulcan Sub-Basin on Australia's Northwest Shelf produces mainly from Plover and equivalent strata, and the Barrow Sub-Basin produces mainly from the Barrow and equivalent strata. In many cases, long term multi-field production from a single reservoir unit has led to the regional depressuring of the regional aquifer system. This paper describes the application of hydrodynamic techniques to static and dynamic reservoir issues at the production (human) time scale. This in turn can be used to evaluate production time-scale compartmentalisation applied to both producing fields and CO_2 storage.

Underschultz, J.R. (2007). Hydrodynamics and membrane seal capacity: *Geofluids Journal*, 7, pp. 148-158.

The previous two papers provide the foundation for evaluating hydrodynamic effects on membrane seal capacity. This third paper describes a theoretical analysis of the membrane seal capacity of the total seal thickness under hydrodynamic conditions for both fault and top seal scenarios. When considering the entire seal thickness the

formation water pore pressure distribution resulting from the hydrodynamic regime can have significant impact on the membrane seal capacity. The importance of understanding the hydrodynamic component to membrane seal capacity is greatest when calibrating seal capacity estimation techniques, such as SGR applied to fault seal capacity, and Mercury Injection Capillary Pressure (MICP) measurements applied to top seal capacity. The theoretical analysis of membrane seal capacity described in this paper forms the backbone of this thesis. Not only has this new theory of hydrodynamics and membrane seal capacity been scrutinized in the peer review process (of which Dr. Quentin Fisher from RDR at the University of Leeds, and a recognized world authority on fault seal analysis, was a reviewer) but the author has subsequently had extensive personal communication with Dr. Peter Bretan and Dr. Graham Yielding at Badley Geoscience Ltd. in Lincolnshire England, who have authored landmark papers on SGR and membrane seal capacity calibration (Yielding et al. 1997, Yielding 2002, Breton et al. 2003, and Breton and Yielding, 2005). From the author's collaboration with Yielding and Breton, a co-authored conference presentation using the theory from Underschultz (2007), and case study data from Badleys was presented at the Geological Society of London reservoir compartmentalisation conference in London 2008. The theory of hydrodynamics and membrane seal capacity has also been thoroughly reviewed by the seals analysis groups from the sponsor companies of the IPETS research consortia (Chevron (Houston), Anadarko (Houston), Woodside (Australia), Santos (Australia), Origin (Australia) and Schlumberger (Paris)). The research described in Underschultz (2007) represents an original and significant step forward in better understanding membrane seal capacity for a total seal thickness.

Bailey, W.R., **Underschultz J.,** Dewhurst D.N., Kovack G., Mildren S. and Raven M. (2006). Multi-disciplinary approach to fault and top seal appraisal; Pyrenees-Macedon oil and gas fields, Exmouth Sub-basin, Australian Northwest Shelf. *Marine and Petroleum Geology,* 23, pp. 241-259.

With the theoretical context of membrane seal capacity and hydrodynamics described in the previous 3 papers, that theory is applied to a case study describing the Pyrenees-Macedon Field in the Northwest Shelf of Australia. This work requires a

significant geological input for the stratigraphic/structural characterisation. As such, a multi-authored, multidisciplinary paper is included here to give an example of the theory in practice. The Pyrenees-Macedon case study provides an example of both fault and top seal capacity issues.

Underschultz, J.R., Hill, R.A. and Easton, S. (2008). The Hydrodynamics of Fields in the Macedon, Pyrenees and Barrow Sands, Exmouth Sub-Basin: Identifying Seals and Compartments. *Australian Society of Exploration Geophysicists.* 39, pp. 85-93.

This paper provides case study examples where hydrodynamic techniques and membrane seal analysis theory are applied using oil and gas field data from the Exmouth sub-Basin. Here, the main confirmation of the theory (Underschultz, 2007) is the case of the Stybarrow Oil Field, which has an anomalously large hydrocarbon column relative to other fields in the Macedon Sand play trend. It illustrates that a location on the low hydraulic head side of a fault membrane seal has enhanced seal capacity, as predicted by the theory described in Underschultz (2007).

Gibson-Poole, C.M., Svendsen, L., **Underschultz, J**., Watson, M.N., Ennis-King, J., van Ruth, P.J., Nelson, E.J., Daniel, R.F., and Cinar, Y. (2007). Site Characterisation of a Basin-Scale CO_2 Geological Storage System: Gippsland Basin, Southeast Australia. *Journal of Environmental Geology*. On-line publication not yet in print. http://www.springerlink.com/content/0r4v8l4j846t5308/

An understanding of membrane seal capacity not only has implications for oil and gas trapping, but also for CO_2 storage capacity. This paper describes a multidisciplinary integrated methodology for site characterisation related to geological CO_2 sequestration. The hydrodynamics aspect of membrane seal capacity is an important factor in assessing storage capacity and risking containment security. This case study also describes the impact of regional pressure depletion due to extensive hydrocarbon production over the last 30 years. The transient component of the flow system has

implications for the short term migration direction of injected CO_2.

Gibson-Poole, C.M., Svendsen, L., **Underschultz, J**., Watson, M.N., Ennis-King, J., van Ruth, P., Nelson, E., Daniel, R., and Cinar, Y. (2006). Gippsland Basin Geosequestration: A potential solution for the Latrobe Valley brown coal CO_2 emissions. *Australian Petroleum Production and Exploration Association Journal*, 46 (1), pp. 241-259.

As a follow on to the previous publication, this paper looks at specific site selection criteria for emissions from the coal fired power station in the Latrobe Valley of Victoria. It represents a good example of how an understanding of hydrodynamics and membrane seal capacity can reduce the uncertainty in estimating CO_2 storage capacity and containment security.

9. Non-Thesis publications and their relation to the thesis topic

The candidate has either authored or co-authored a series of 8 papers published in peer reviewed journals that are not included as part of this "thesis by Published Paper", but which relate to the thesis topic. They are not included due to constraints on the timing of publication relative to the official period of PhD registration. However, these publications significantly contribute towards forming the intellectual property upon which the thesis subject was conceived and addressed. The papers follow a progression of subject matter related to hydrodynamics and seals analysis and build on the total body of work that addresses the thesis topic.

Underschultz, J.R., Ellis, G K., Hennig, A., Bekele, E., and Otto, C. (2002). Estimating formation water salinity from wireline pressure data: Case study in the Vulcan Sub-basin. *In*: Keep, M. and Moss, S.J. (eds.), The Sedimentary Basins of Western Australia 3: Proceedings of the *Petroleum Exploration Society of Australia Symposium*, Perth, WA, pp. 285-303.

This paper describes a method where the salinity of formation water can be determined from pressure gradient and formation temperature data. The paper compares and

contrasts the various methods of defining the formation water salinity and defines criteria for accurate estimation of formation water salinity from pressure gradient data. Mapping the distribution of formation water salinity, together with the distribution of specific ionic concentrations or ionic ratios, can be used to identify geochemical anomalies near faults. These can be used as an independent dataset to corroborate the analysis of formation water flow systems using formation pressure data.

Otto, C., **Underschultz, J**., Hennig, A. and Roy, V. (2001). Hydrodynamic analysis of flow systems and fault seal integrity in the Northwest Shelf of Australia: *Australian Petroleum Production and Exploration Association Journal.* 41 (1), pp. 347-365.

This paper provided the first published analysis of the regional formation water flow systems on the Northwest Shelf of Australia. The data and analysis define regional basin-scale flow systems and boundary conditions that establish the driving forces for formation water flow for the sedimentary pile on the Northwest Shelf. It identifies for the first time that the regional flow systems on the Northwest Shelf are often influenced by the structural grain.

Hennig, A., **Underschultz, J.R.** and Otto, C.J. (2002). Hydrodynamic analysis of the Early Cretaceous aquifers in the Barrow Sub-basin in relation to hydraulic continuity and fault seal. *In:* Keep, M. and Moss, S.J. (eds), The Sedimentary Basins of Western Australia 3*:* Proceedings of the *Petroleum Exploration Society of Australia Symposium*, Perth, WA, pp. 305-320.

This paper represents a sub-basin scale examination of hydrodynamics and fault seal in the Barrow sub-basin of Australia's Northwest Shelf. It represents a more detailed scale update of the Otto et al. (2001) paper above, with more data control. It identifies that the Barrow Sub-Basin is significantly influenced by pressure depletion from hydrocarbon production, and that transient hydrodynamic processes are an important consideration in characterising fault seals in the sub-Basin.

Underschultz, J.R., Otto C.J. and Cruse T. (2003). Hydrodynamics to assess hydrocarbon migration in faulted strata - methodology and a case study from the Northwest Shelf of Australia. *Journal of Geochemical Exploration*, 78-79, pp. 469-474.

This paper specifically looks at the likelihood of hydrocarbon migration across the Flinders Fault Zone out of the Barrow Sub-Basin and onto the adjacent shelf. It combines hydrodynamic analysis techniques with an examination of the oil show distribution to help define possible leak points along the Finders Fault System.

Underschultz, J. (2005). Pressure distribution in a reservoir affected by capillarity and hydrodynamic drive: Griffin Field, North West Shelf, Australia. *Geofluids Journal*, 5, pp. 221-235.

This paper describes how various capillary processes manifest themselves in standard hydrodynamic evaluation methods. Brown (2003b) describes the signature of capillary pressure on pressure-elevation plots and excess pressure-depth plots for hydrostatic systems. This paper takes the result of Brown (2003b) and extends the concept to describe the signature of capillary pressure on pressure-elevation and hydraulic head-elevation plots for hydrodynamic conditions. The paper exemplifies the presented theory with a case study example of the Griffin Field in Australia's Northwest Shelf and it provides the foundation for evaluating case study data relative to hydrodynamics and membrane seal capacity.

Gartrell, A., Lisk, M. and **Underschultz, J.** (2002). Controls on trap integrity of the Skua Oil Field, Timor Sea. *In:* Keep, M., and Moss, S.J., (eds), The Sedimentary Basins of Western Australia 3: Proceedings of the *Petroleum Society of Australia Symposium*, Perth, WA, pp. 389-407.

The Skua Field in the Timor Sea shows evidence of a paleo-oil column suggesting that it has previously leaked a portion of its hydrocarbons since the time of maximum fill. This paper describes an integrated multidisciplinary examination of fault seal integrity

of the Skua Field. Hydrodynamic analysis is used to support structural and oil inclusion analysis to define the traps historical fill and leakage history. It provides a case study example of workflows used in integrated fault seal analysis.

Underschultz, J.R. and Boult P. (2004). Top seal and reservoir continuity: Hydrodynamic evaluation of the Hutton-Birkhead Reservoir, Gidgealpa Oilfield. In *Eastern Australian Basins Symposium*, 2, pp. 473-482.

The Gidgealpa Field represents a series of stacked oil pools within the Hutton and Birkhead strata of the Eromanga Basin. A palaeo-oil column identified in the Hutton reservoir indicates that the Birkhead seal was breached. The interbedded sands and muds occur in an anticlinal structure but many of the pools are not filled to their structural spill point. This paper examines issues of membrane top seal capacity at the Gidgealpa Field. It provides a case study example of workflows used in hydrodynamics and top seal analysis.

Simmelink, H.J., **Underschultz, J.R**., Verweij, J.M., Hennig, A., Pagnier, H.J.M., Otto, C.J. (2003). A pressure and fluid dynamic study of the Southern North Sea Basin: *Journal of Geochemical Exploration*, 78-79, pp. 187-190.

This paper is the result of a two year project aimed at characterising the pressure distribution for the strata in the Dutch sector of the North Sea. Issues of particular interest are overpressure zones below salt beds and reservoir horizons horizontally compartmentalized by salt structures associated with faults.

10. Data and Assumptions

All the non-proprietary data used in this thesis are available through the CSIRO Petroleum PressureDB which is in Microsoft ACCESS format. The data can be viewed and exported to spreadsheet format using the CSIRO Petroleum PressurePlot software. Both the PressureDB database and PressurePlot software can be accessed free of charge through the CSIRO web site:

http://www.pressureplot.com

There are several assumptions that can be considered to apply for all discussion and analysis with respect to this thesis unless otherwise stated. These include:

- Where the pressure gradient is not hydrostatic, Darcy's Law can be used to describe the fluid potential;
- The vertical formation water pressure within an aquitard is assumed to change smoothly between the measured formation water pressure in the aquifer above and below the aquitard;
- Formation water is assumed to be the continuous fluid phase in the pore space at the scale of the sub-basin;
- The aquitard is assumed tot be isotropic and homogeneous; and
- The membrane seals are considered to be filled by hydrocarbon exactly to their seal capacity and not overfilled.

11. Review/Discussion

The 15 peer reviewed technical papers (7 forming part of the thesis and 8 related to the thesis but not included) described above form a body of work on hydrodynamics and membrane seal capacity that proposes a significant change to conventional seal analysis is required for accurate prediction of seal capacity. As a test of this theory, the IPETS industrial research consortium funded three case study evaluations of total membrane seal capacity that specifically incorporated hydrodynamics techniques. The case study analyses provided the following:

- Confirmation that SGR calibration using the theory of Underschultz (2007) resulted in consistently more accurate column height prediction than with a standard approach; and
- Determination that the theory described by Underschultz (2007) needed to extended to cases of hydrocarbon-hydrocarbon across fault pressure difference.

The case studies provided such encouraging results on seal capacity calibration that the IPETS industrial consortium decided to disallow publication of results in order to maintain a competitive advantage. However, the results and their implications can be discussed here in a generic context. The case studies fortuitously provided one example where the new calibration approach would lower the SGR-AFPD (shale gouge ratio – across fault pressure difference) calibration envelope (Case Study 3), one case where the new approach would raise the SGR-AFPD calibration envelope (Case Study 2) and one case where the calibration would not change very much (Case Study 1).

11.1 Hydrocarbon – hydrocarbon across fault pressure difference

When hydrocarbons are accumulated on both sides of a fault but their formation pressure data define separate pressure gradients, standard SGR-AFPD calibration calculates the AFPD as simply the difference between the hydrocarbon pressures at a given elevation. The fact that the hydrocarbon pressure gradients on either side of the fault define separate gradients requires the fault zone itself to be water saturated. The standard SGR-AFPD assumes that the reservoir on either side of the fault reaches irreducible water saturation, the relative permeability to water becomes zero, and the formation water pressure in the fault zone adjacent to the hydrocarbon takes on the pressure of the hydrocarbon phase. If this were the case, then the SGR observed in Case Study 2 of the IPETS program would suggest that only a small hydrocarbon column could be maintained; much smaller than that observed. Faced with this evidence we must now consider assumptions regarding irreducible water saturation and water relative permeability of zero.

There is currently debate in the literature as to which formation water pressure value should be used to estimate Threshold Pressure, and if modification of Equation (1) for Threshold Pressure (T_p) is required (Bjorkum et al. 1998; Clayton 1999; Rodgers 1999; Brown 2003; Teige et al. 2005).

$$T_p = \Delta\rho g H \quad \text{..... (1)}$$

In the case of fault seals, Brown (2003), and in the case of top seals, Clayton (1999), suggest that when moving up through the hydrocarbon column, the relative permeability of water approaches zero as water saturation drops to approach irreducible water saturation. As a result, the excess pressure (ΔP) between the hydrostatic gradient at the FWL and the hydrostatic gradient at the first pore of the seal must be incorporated into the threshold pressure (T_p) equation as:

$$T_p = \Delta\rho gH - \Delta P \quad \text{..... (2)}$$

Bjorkum et al. (1998) argue that in a water-wet system, there is a vertical pressure gradient between the aquifer at the FWL and the top of the reservoir, even within the irreducible water phase. If this is true, then there is only an infinitesimally small change in water pressure between the uppermost pore of the reservoir and the lowermost pore of the seal and thus excess pressure has no effect on calculated threshold pressure. Rodgers (1999) however, pointed out that despite the assertions of Bjorkum et al. (1998), the permeability to the water phase at the top of the reservoir would be much less than that in the aquifer or where the water saturation is above irreducible water saturation. As such, there would be some excess pressure incurred between the formation water pressure at the FWL and the formation water pressure at the top of the reservoir (Figure 1), and thus, an excess pressure correction is still required in calculating the threshold pressure. Teige et al. (2005) conducted a laboratory experiment to test if water could migrate through oil saturated rock near irreducible water saturation. They used oil under pressure to displace water out of a core plug to what was thought to be approaching irreducible water saturation. This plug was mounted in series with a low permeability, water-wet membrane that represented the sealing rock. A water pressure difference of 0.5 MPa was then applied across the core, which produced a measurable water flow through the oil saturated core and across the membrane. This supports the thesis of Bjorkum et al. (1998) that

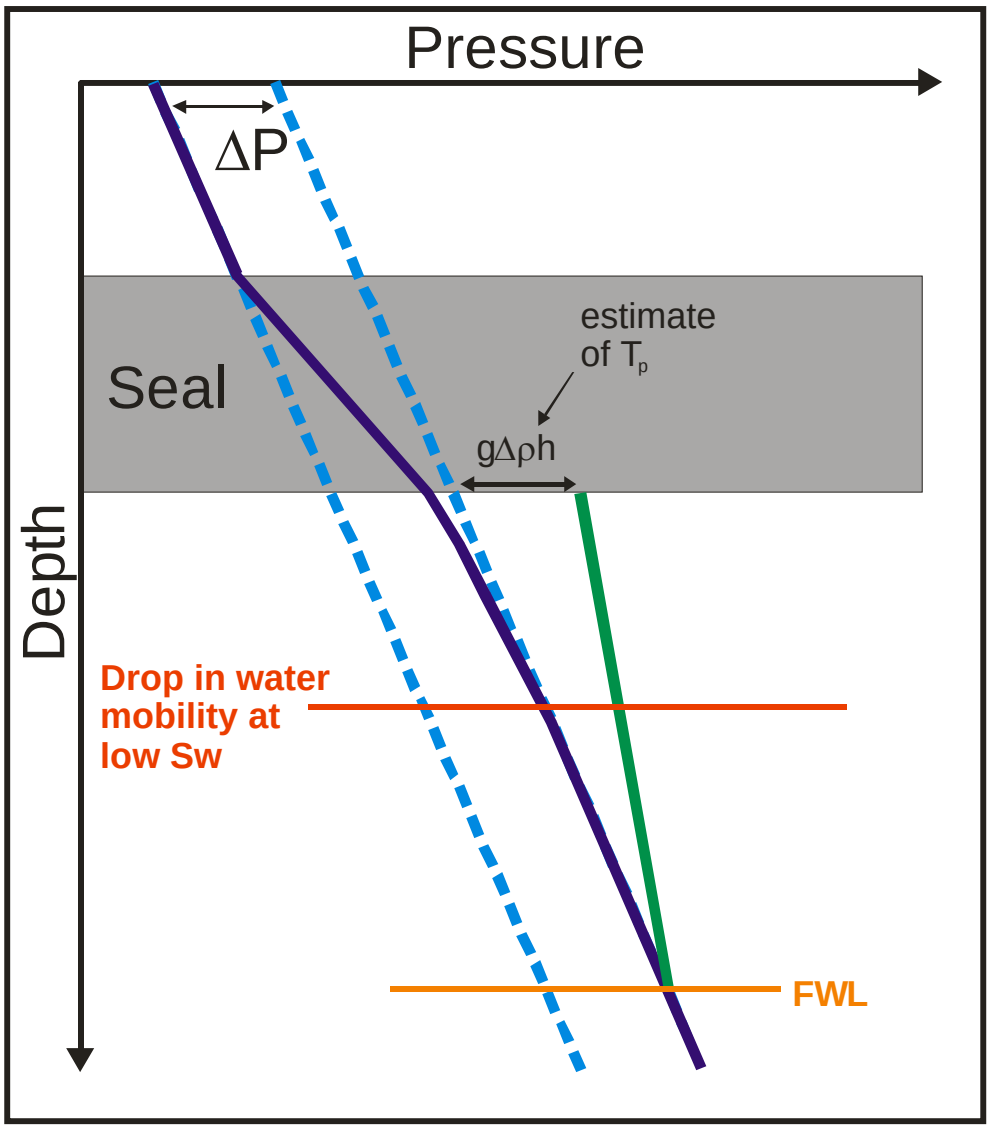

Figure 1. Pressure-Depth plot with a hydrocarbon column equal to the seals membrane capacity. In this case the capillary threshold pressure for the seal is estimated to be the difference in the hydrocarbon and water pressure at the top of the column. ΔP is the equivalent pressure difference between the hydraulic heads on either side of the seal (after Rodgers, 1999).

the water flow in the irreducible water zone of the hydrocarbon accumulation is small but not zero. Further, the calculated water permeability in the core plug experiment was 0.71 λD; significantly higher than the permeability of the seal required to hold back the hydrocarbon column (Teige et al. 2005). This suggests that the excess pressure effect described by Rodgers (1999) would be negligible because the water pressure loss in an upwards-draining system would almost all be taken up in the low permeability shale (seal). While it may be debatable if the experiment by Teige et al. (2005) achieved irreducible water saturation or only something close to irreducible

water saturation, it can be said that the water saturation achieved was certainly typical of that observed near the top of hydrocarbon accumulations where water-free production occurs. Leaving the semantics of 'irreducible water saturation' aside, the experimental results of Teige et al. (2005) have important application to understanding membrane seal capacity in hydrocarbon reservoirs. A simple extrapolation of the published experiment by Teige et al. (2005) suggests that excess pressure between the FWL and the reservoir seal interface does not have a direct impact on capillary leakage and Equation 2 is incorrect. The experimental work of Teige et al. (2005) has been followed up by further work presented in Teige et al. (2006) that supports the suggestion that relative permeability for formation water of zero does not exist in practice.

With the findings of Teige et al. (2006) in mind, we can construct a simple model to understand the processes impacting the total membrane seal capacity where there are hydrocarbons pooled on both sides of a fault seal. Figure 2 shows a schematic diagram with a geological model (Figure 2A) and a corresponding hydraulic head vs. elevation plot (Figure 2B). The top seal is assumed to have a significantly higher membrane seal capacity than the reservoir level fault seals. This means that any leakage is across-fault with no leakage occurring up the fault. For the purposes of this diagram, the reservoir and top seal are each assumed to have horizontally consistent properties but both are also assumed to be vertically heterogeneous. This assumption allows for a distribution of SGR values along the fault. Figure 2A illustrates two water saturated faults at their membrane seal capacity with identical displacement and thus similar range of SGR values. Note that the Free Water Levels (FWLs) are variable, as is the value of hydraulic head for formation water, Hw (dashed green). This allows us to test a scenario of a high hydraulic head gradient and a low hydraulic head gradient on the total membrane seal capacity similar to case study 2 and case study 3. Figure 2B shows a plot of Hw against Elevation considering the hypothetical scenario illustrated in Figure 2A, one fault supporting a small Hw gradient and the other supporting a large Hw gradient. The plot exemplifies the standard approach for Pressure Difference (ΔP) calculation where

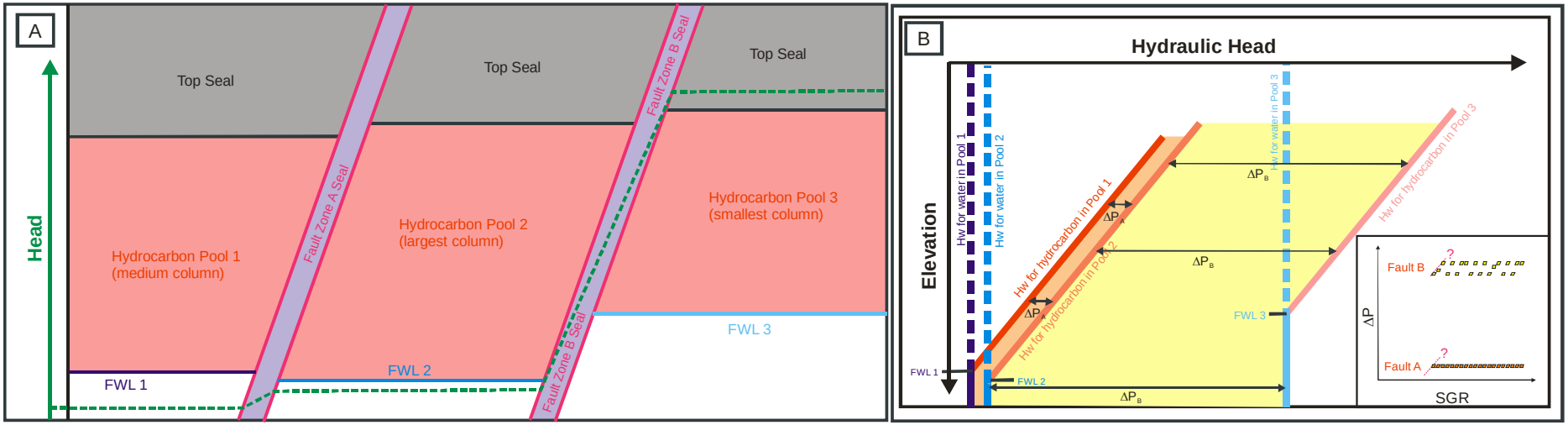

Figure 2. A schematic diagram linking a simple cross section model of three fault separated hydrocarbon pools with an associated head-elevation plot. The top seal is assumed to have a significantly higher membrane seal capacity than the reservoir level fault seals. For the purposes of this diagram, the reservoir and top seal are each assumed to have horizontally consistent properties but both are also assumed to be vertically heterogeneous. Figure 2A illustrates two water saturated faults at their membrane seal capacity with identical displacement and thus similar range of SGR values. Note that the Free Water Levels (FWLs) are variable, as is the value of hydraulic head for formation water (dashed green). Figure 2B. Plot of Hw against Elevation considering the hypothetical scenario illustrated in Figure 4A, one fault supporting a small Hw gradient and the other supporting a large Hw gradient. The plot exemplifies the standard approach for Pressure Difference (ΔP) calculation where orange shading represents ΔP_{f1} and yellow shading represents ΔP_{f2}. A ΔP-SGR calibration plot is inserted for the two cases.

orange shading represents ΔP_{f1} and yellow shading represents ΔP_{f2}. A ΔP-SGR calibration plot is inserted for the two cases. It demonstrates that the standard ΔP-SGR calibration for a situation with a small Hw gradient plots very low. This is analogous to that observed in Case Study 2. The standard ΔP-SGR calibration for a situation with a large Hw gradient plots very high. This is analogous to that observed in Case Study 3.

If the findings of Teige et al. (2005 and 2006) are taken as being correct, then the hydraulic head distribution of formation water within the system is determined by the transmissivity distribution and can be estimated by the hydraulic head in the aquifer below the reservoir in each part of the system. Using the principles of Underschultz (2007), the standard SGR calibration is adjusted where the high hydraulic head side of each fault is used to estimate the ΔP to be correlated against SGR despite there being hydrocarbon on both sides of the fault. Note that this is not correct if the two hydrocarbons define a single hydrocarbon pressure gradient. In this case the fault is already breached and the hydrocarbons must form a continuous phase across the fault at some location.

An adjusted ΔP-SGR calibration approach is depicted in Figure 3. Here the simplified geological model is identical to that in Figure 2A described previously. The corresponding hydraulic head vs. elevation plot has a modified ΔP colour shaded for each of the three reservoirs where the hydrocarbon pressure is compared with the hydraulic head on the high hydraulic head side of the fault. For Pool 2, it is obvious that the fault to the right cannot be controlling the pool size if it is at its membrane seal capacity since the hydraulic head on the high side of that fault has a pressure higher than that in the hydrocarbon column itself. Therefore, we assume that the fault to the left of the pool is the critical fault and its ΔP is considered between the hydrocarbon pressure and the hydraulic head of the formation water on the high hydraulic head side of the fault to the left. The ΔP-SGR calibration plot is inserted for the three pools and for reference the ΔP-SGR calibration data from the standard approach (Figure 2B) is also included. It can be seen that the adjusted calibration method moves the ΔP values for a given SGR towards the centre of the calibration plot. This is similar to what we observed with case study 2 and 3.

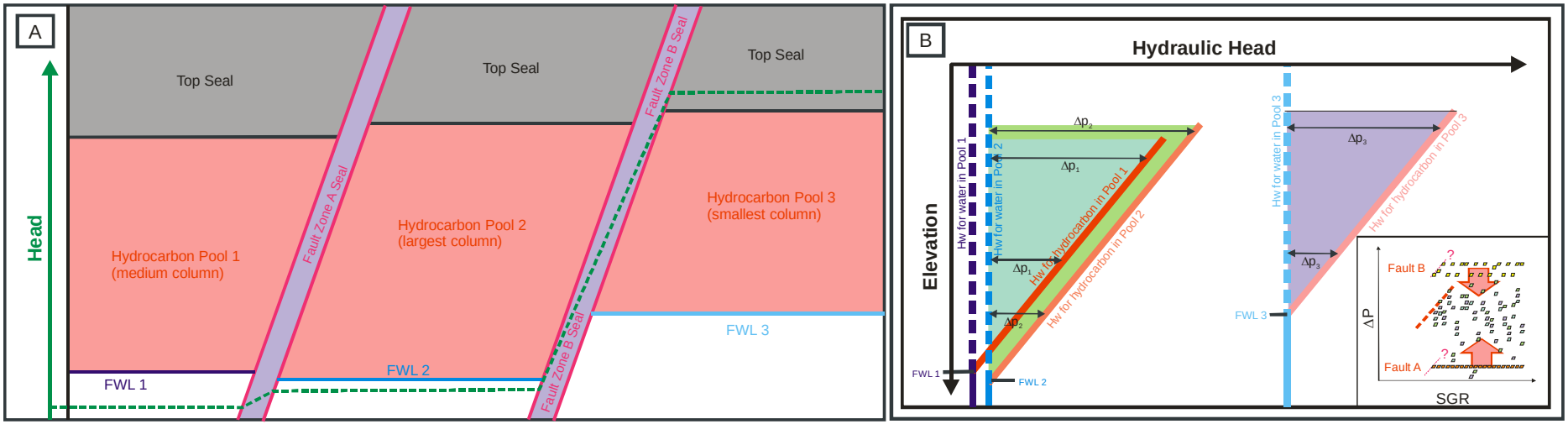

Figure 3. A schematic diagram linking a simple cross section model of three fault separated hydrocarbon pools with an associated head-elevation plot. The top seal is assumed to have a significantly higher membrane seal capacity than the reservoir level fault seals. For the purposes of this diagram, the reservoir and top seal are each assumed to have horizontally consistent properties but both are also assumed to be vertically heterogeneous. Figure 3A illustrates two water saturated faults at their membrane seal capacity with identical displacement and thus similar range of SGR values. Note that the Free Water Levels (FWLs) are variable, as is the value of hydraulic head for formation water (dashed green). Figure 3B presents a modified ΔP calculation, matt green shading for Pool 1, bright green for Pool 2 and purple for Pool 3. Note the ΔP-SGR calibration inset has the data from Figure 2B as a reference, showing how the modified approach predominantly centres the extreme values.

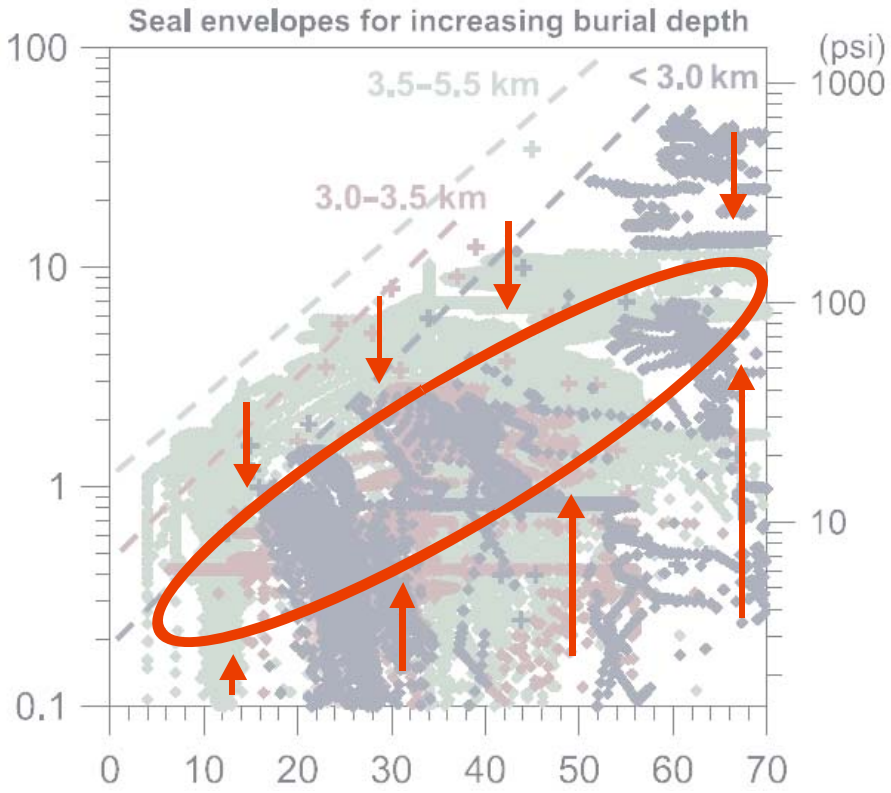

Figure 4. Schematic diagram summarising the ΔP-SGR inserts from figures 2 and 3. This is the anticipated effect of converting the global ΔP_f-SGR correlation plot to a ΔP_{fm}-SGR plot. This figure is modified from Yielding (2002).

From this extension of the Underschultz (2007) theory on hydrodynamics and membrane seal capacity into the realm of hydrocarbon on both sides of a fault and from the case study examples that appear to back the theory up, we can surmise the impact of an adjusted ΔP-SGR calibration method on the global calibration data set. Figure 4 shows the global ΔP-SGR correlation data from Yielding (2002) with the seal failure envelopes for several depths. It is anticipated that if this data set were to be re-calibrated using the modified approach described in this thesis, then the data would collapse to fall across a much more narrow range of ΔP. It may be that depth becomes irrelevant. Importantly, the data that shift downwards on the plot will change the predicted seal capacity for a given SGR value.

12. Conclusions

The seven thesis-related publications (as published in peer reviewed technical journals) form a body of work that:

- Defines a workflow and methodology for characterising formation water flow systems in faulted aquifers at geological time scales;
- Defines a workflow and methodology for characterising formation water flow systems in faulted aquifers at production time scales;
- Describes a new theory of hydrodynamic effects on membrane seal capacity; and,
- Provides various case study evaluations that exemplify the three preceding conclusions.

In addition, the eight publications (as published in peer reviewed technical journals) that are related to the thesis topic, but are not part of it, provide further background and support to the body of work in the areas of:

- Using formation water salinity data to support a hydrodynamic analysis based on formation pressure data;
- Regional evaluations of hydrodynamics and fault seal for the Northwest Shelf of Australia (with sub-basin scale evaluations of the Vulcan and Barrow sub-Basins) and the Southern North Sea Basin;
- Describes the signature of capillary effects in dynamic aquifers on pressure-elevation or head-elevation plots;
- Detailed case studies of integrated fault seal analysis; and,
- A case study of integrated top seal analysis for the Gidgealpa Field in the Eromanga Basin, Australia.

The combined body of work addresses the thesis topic; “Identification of fault and top seal effectiveness through an integration of hydrodynamic and capillary analysis techniques”.

13. List of References

Adamson, G., Crick, M., Gane, B., Gurpinar, O., Hardiman, J. and Ponting, D. (1996). Simulation throughout the life of a reservoir. *Oilfield Review*, summer 1996, pp. 16-27.

Anfort, S.J., Bachu, S.and Bentley, L.R. (2001). Regional-scale hydrogeology of the Upper Devonian–Lower Cretaceous sedimentary succession, south-central Alberta Basin, Canada. *American Association of Petroleum Geologists Bulletin*. 85 (4), pp. 637–660.

Antonellini, M. and Aydin, A. (1994). Effect of faulting on fluid flow in porous sandstones: Petrophysical Properties, *American Association of Petroleum Geologists Bulletin*, 78 (3), pp. 355-377.

Ayub, M. and Bentsen, R.G. (1999). Interfacial viscous coupling: a myth or reality? *Journal of Petroleum Science and Engineering*. 23, pp. 13-26.

Bachu, S. (1988). Analysis of heat transfer processes and geothermal pattern in the Alberta Basin, Canada, *Journal of Geophysical Research*, 93, pp. 7767-7781.

Bachu, S. (1993). Basement heat flow in the Western Canada Sedimentary Basin, *Tectonophysics*, 222, pp. 119-133.

Bachu, S. (1995a). Flow of variable-density formation water in deep sloping aquifers: review of methods of representation with case studies: *Journal of Hydrology*, 164, pp. 19-38.

Bachu, S. (1995b). Synthesis and model of formation-water flow, Alberta Basin, Canada: *American Association of Petroleum Geologists Bulletin*, 79, pp. 1159-1178.

Bachu, S. and Burwash, R.A. (1991). Regional-scale analysis of the geothermal regime in the Western Canada Sedimentary Basin, *Geothermics*, 20, pp. 387-407.

Bachu, S. and Michael, K. (2002). Flow of variable-density formation water in deep sloping aquifers: minimizing the error in representation and analysis when using hydraulic-head distributions. *Journal of Hydrology*, 259, pp. 49-65.

Bachu, S., Ramon, J.C., Villegas, M.E. and **Underschultz, J.R**. (1995). Geothermal Regime and Thermal History of the Llanos Basin, Colombia: *American Association of Petroleum Geologists Bulletin*, 79 (1), pp. 116-129.

Bachu, S., and **Underschultz, J.R.** (1995). Large-scale erosional underpressuring in the Alberta Basin: *Association of Petroleum Geologists Bulletin*, 79, pp. 989-1003.

Bailey, W.R., Manzocchi, T., Walsh, J.J., Strand, J.A., Nell, P.A., Keogh, K., Hodgetts, D., Flint, S. and Rippon, J. (2002). The effects of faults on the 3-D connectivity of reservoir bodies: a case study from the East Pennine Coalfield, U.K. *Petroleum Geoscience*, 8, pp. 263-277.

Bailey, W.R., Shannon, P., Walsh, J.J. and Unithan, V. (2003). Spatial relationships between faults and deep sea carbonate mounds: the Porcupine Basin, offshore Ireland. *Marine and Petroleum Geology*, 20, pp. 509-522.

Bailey, W.R., **Underschultz J.,** Dewhurst D.N., Kovack G., Mildren S., Raven M. (2006). Multi-disciplinary approach to fault and top seal appraisal; Pyrenees-Macedon oil and gas fields, Exmouth Sub-basin, Australian Northwest Shelf. *Marine and Petroleum Geology*, 23, pp. 241-259.

Baillie, P.W. and Jacobson, E.P. (1997). Prospectivity and Exploration history of the Barrow Sub-basin, Western Australia, *Australian Petroleum Production and Exploration Association Journal*, 37 (1), pp. 117-135.

Barson, D., Bachu, S. and Esslinger, P. (2001). Flow systems in the Mannville Group in the east-central Athabasca area and implications for steam-assisted gravity drainage (SAGD) operations for in situ bitumen production. *Bulletin of Canadian Petroleum Geology*, 49 (3), pp. 376-392.

Beacher, G.J. (1998). Pressure study of the Flacourt Formation aquifer in the Thevenard Island area of the Barrow Sub-basin, *Australian Petroleum Production and Exploration Association Journal*, 3 (1), pp. 438-452.

Bégin, N.J. and D.A. Spratt. (2002). Role of transverse faulting in along-strike termination of Limestone Mountain Culmination, Rocky Mountain thrust-and-fold belt, Alberta, Canada: *Journal of Structural Geology*, 24, pp. 689-707.

Bekele, E.B., Johnson, M. and Higgs, W. (2001). Numerical modelling of overpressure generation in the Barrow Sub-basin, Northwest Australia: *Australian Petroleum Production and Exploration Association Journal*, 41 (1), pp. 595-607.

Bense, V.F. (2004). The hydraulic properties of faults in unconsolidated sediments and their impact on groundwater flow. PhD Thesis. Vrije University Amsterdam. 143 p.

Bentsen, R.G. (2005). Effect of neglecting interfacial coupling when using vertical flow experiments to determine relative permeability. *Journal of Petroleum Science and Engineering*. 48, pp. 81-93.

Bernecker, T. and Partridge, A.D. (2001). Emperor and Golden Beach Subgroups: the onset of Late Cretaceous sedimentation in the Gippsland Basin, SE Australia. *In*: Hill, K.C. and Bernecker, T. (eds.), Eastern Australia Basins symposium: a refocused energy perspective for the future. *Petroleum Exploration Society of Australia*, Melbourne, 25-28 November, pp. 391-402.

Bernecker, T. and Partridge, A.D. (2005). Approaches to palaegeographic reconstructions of the Latrobe Group, Gippsland Basin, southeast Australia. *Australian Petroleum Production and Exploration Association Journal*, 45, pp. 581-599.

BHP Petroleum Pty Ltd. (1993). West Muiron-5 Well Completion Report Basic Data.

BHP Petroleum Pty Ltd. (1995a). Macedon-2 Basic Well Completion Report.

BHP Petroleum Pty Ltd. (1995b). Macedon-4 Basic Well Completion Report.

Bjorkum, P.A., Walderhaug, O.and Nadeau, P.H. (1998). Physical constraints on hydrocarbon leakage and trapping revisited. *Petroleum Geoscience*, 43, pp. 237-239.

Boult, P.J. (1996). An investigation of reservoir/seal couplets in the Eromanga Basin; implications for petroleum entrapment and production. Development of secondary migration and seal potential theory and investigation techniques. *PhD Thesis*. University of South Australia.

Boult, P.J., Lanzilli, E., Michaelsen, B.H., Mckirdy, D.M. and Ryan, M.J. (1998). A new model for the Hutton/Birkhead reservoir/seal couplet and the associated Birkhead-Hutton petroleum system. *Australian Petroleum Production and Exploration Association Journal.* 38, pp. 724-743.

Boult, P.J., Ryan, M. J., Michaelsen, B. H., Mckirdy, D. M., Tingate, P. R., Lanzilli, E. and Kagya, M. L. N. (1997b). The Birkhead-Hutton petroleum system of the Gidgealpa Area, Eromanga Basin, Australia. *Proceedings of the Petroleum Systems of SE Asia and Australasia Conference*, 21-23 May 1997, pp. 213-235.

Boult, P.J., Theologou, P.N. and Foden, J. (1997a). Capillary seals within the Eromanga Basin, Australia: Implications for exploration and production. *In*: Surdam, R.C. (Ed.), Seals, traps and the petroleum system, pp. 143-167.

Bouvier, J.D., Kaars-Sijpesteijn, C.H., Kluesner, D.F., Onyejekwe, C.C. and Van Der Pal, R.C. (1989). Three-dimensional seismic interpretation and fault sealing investigations, Nun River Field, Nigeria. *American Association of Petroleum Geologists Bulletin*, 73, pp. 1397-1414.

Bradshaw, J., Sayers, J., Bradshaw, M., Kneale, R., Ford, C., Spencer, L. and Lisk M. (1998). Palaeogeography and its impact on the petroleum systems of the North West Shelf, Australia, *In*: Purcell, P.G. and Purcell, R.R., (Eds.), *The Sedimentary Basins of Western Australia 2:* Proceedings of Petroleum Exploration Society of Australia, Perth, 1998, pp. 95-121.

Bredehoeft, J.D., Belitz, K. and Sharp-Hansen, S. (1992). The hydrodynamics of the Big Horn Basin; a study of the role of faults, *American Association of Petroleum Geologists Bulletin*, 76 (4), pp. 530-546.

Bretan, P.G., Nicol, A., Walsh, J. J. and Watterson, J. (1996). Origin of some conjugate or "X"-shaped fault structures. *Leading Edge*, pp. 812-816.

Bretan, P. and Yielding, G. (2005). Using Buoyancy pressure profiles to assess uncertainty in fault seal calibration. *In:* Boult, P. and Kaldi, J. (eds.), Evaluating fault and cap rock seals, *American Association of Petroleum Geologists Hedberg Series*, 2, pp. 151-162.

Bretan, P., Yielding, G. and Jones, H. (2003). Using calibrated shale gouge ratio to estimate hydrocarbon column heights. *American Association of Petroleum Geologists Bulletin*, 87, pp. 397-413.

Brincat, M., Bailey, W., Mildren, S. and Lisk, M. (2004). Integrated trap integrity analysis in a reactivated setting - examples from the Northern Bonaparte Basin, Australia. Proceedings of *EAGE Conference*, Fault and Top Seals, 26 p.

Brincat, M.P., O'Brien, G.W., Lisk, M., De Ruig, M. and George, S.C. (2001). Hydrocarbon charge history of the northern Londonderry: Implications for trap integrity and future prospectivity. *Australian Petroleum and Exploration Association Journal*. 41 (1). pp. 483-496.

Brown, A. (2003a). Improved interpretation of wireline pressure data. *American Association of Petroleum Geologists Bulletin*, 87, pp. 295–311.

Brown, A. (2003b). Capillary effects on fault-fill sealing. *American Association of Petroleum Geologists Bulletin*, 87, pp. 381-395.

Brown, A. and Fisher, Q. (2006). Detecting and evaluating hydrodynamic sealing by faults. Annual convention. *American Association of Petroleum Geologists*.

Brumley, J.C., Barton, C.M., Holdgate, G.R. and Reid, M.A. (1981). Regional Groundwater Investigation of the Latrobe Valley 1976–1981 SECV and Victorian Department of Minerals and Energy. December 1981 Reprinted March 1983.

Campbell, I.R. and Smith, D.N. (1982). Gorgon 1, Southernmost Rankin platform gas discovery. *In*: Jamieson, P.N. (Ed.), *Australian Petroleum and Exploration Association Journal*, 22(1), pp. 102-111.

Carruthers, D.J. (2003). Modeling of secondary petroleum migration using invasion percolation techniques. *In:* Duppenbecker, S. and Marzi, R. (eds.), *Multidimensional basin modelling, American Association of Petroleum Geologists datapages discovery series*. 7, pp. 21-37.

Castillo, D. A., Bishop, D.J., Donaldson, I., Kuek, D., De Ruig, M., Trupp, M. and Shuster, M.W. (2000). Trap integrity in the Laminaria High-Nancar Trough region, Timor Sea: Prediction of fault seal failure using well-constrained stress tensors and fault surfaces interpreted from 3D seismic. *Australian Petroleum Production and Exploration Association Journal*, 40, pp. 151-173.

Castillo, D. A., Hillis, R. R., Asquith, K. and Fischer, M. (1998). State of stress in the Timor Sea area, based on deep wellbore observations and frictional failure criteria: application to fault trap integrity. *In*: Purcell, P. G. and Purcell, R. R. (eds.). The Sedimentary Basins of Western Australia 2: Proceedings of *Petroleum Exploration Society of Australia Symposium*, pp. 325-341.

Childs, C., Sylta, O., Moriya, S., Walsh, J. J. and Manzocchi, T. (2002). A method for inclusing the capillary properties of faults in hydrocarbon migration models. *In*: Koestler, A.G. and Hunsdale, R. (eds.), Hydrocarbon seal quantification. Amsterdam, Elsevier, *Norwiegian Petroleum Society (NPF), Special Publication.* 11, pp. 127-139.

Clayton, C.J. (1999). Discussion: 'Physical constraints on hydrocarbon leakage and trapping revisited' by Bjørkum et al. *Petroleum Geoscience*. 5, pp. 99-101.

Clayton, C.J. and Hay, S.J. (1994). Gas migration mechanisms from accumulation to surface. *Bulletin of the Geological Society of Denmark*. 41, pp. 12-23.

CMG. (2004). IMEX: Implicit-EXplicit Black Oil Simulator User's Guide. Computer Modelling Group Ltd., Calgary, Alberta, Canada.

Collins, P.A. (2002), Geomechanics and wellbore stability design of an offshore horizontal well, North Sea. *SPE/PS-CIM/CHOA* Paper 78975.

Cooper, G. T., Barnes, C. R., Bourne, J. D. and Channon, G. J. (1998). Hydrocarbon leakage on the North West Shelf: New information from the integration of Airborne Laser Fluorosensor (ALF) and structural data. *In*: Purcell, P. G. and Purcell, R. R. (eds.). The Sedimentary Basins of Western Australia 2: Proceedings of *Petroleum Exploration Society of Australia Symposium*, pp. 255-271.

Cosse, R. (1993). Basics of reservoir engineering, oil and gas field development techniques. Editions Technip, Paris and Institut Francais du Petrole, Rueil-Malmaison, 346 p.

Cowie, P.A. (1998). A healing-reloading feedback control on the growth rate of seismogenic faults. *Journal of Structural Geology*, 20, pp. 1075-1087.

Cowley, R. and O'Brien, G.W. (2000). Identification and interpretation of leaking hydrocarbons using seismic data: A comparative montage of examples from major fields in Australia's North West Shelf and Gippsland Basin, *Australian Petroleum Production and Exploration Association Journal*, 40(1), pp. 121-150.

Craft, B.C. and Hawkins, M. (1991.). *In:* Terry, R.E. (Ed.), *Applied Petroleum Reservoir Engineering, second ed.* Prentice Hall PTR, New Jersey, 431 p.

Craw, D. (2000), Fluid flow at fault intersections in an active oblique collision zone, Southern Alps, New Zealand: *Journal of Geochemical Exploration*, 69-70, pp. 523-526.

CSIRO Petroleum. (2001). PressureQC^{TM}: A quality control method for formation pressure measurements – Instruction Manual. CSIRO Petroleum/CSIRO Land and Water. Perth. Unpublished.

Dahlberg, E.C. (1995). Applied hydrodynamics in petroleum exploration, second edition. Springer-Verlag New York Inc., pp. 1-295.

Davies, P.B. (1987). Modelling areal, variable density, ground-water flow using equivalent freshwater head - Analysis of potentially significant errors, in: Solving ground water problems with models*:* Proceedings of the *NWWA/IGWMC Conference* -. National Water Well Association, Dublin Ohio, pp. 888-903.

De Marsily, G. (1986). Quantitative Hydrogeology: groundwater hydrology for engineers. *Academic Press*, Orlando Florida. 440 p.

De Ruig, M.J., Trupp, M., Bishop, D.J., Kuek, D. and Castillo, D.A. (2000). Fault architecture and the mechanics of fault reactivation in the Nancar Trough/Laminaria area of the Timor Sea, northern Australia. *Australian Petroleum Production and Exploration Association Journal*, 40, pp. 174-193.

Dewhurst, D.N., Boult, P.J., Jones, R.M. and Barclay, S.A. (2005). Fault healing and fault sealing in impure sandstones. *In*: Boult, P. and Kaldi, J. (eds.), evaluating fault and cap rock seals: *American Association of Petroleum Geologists, Hedberg Series*, 2, pp. 37-56.

Dewhurst, D.N. and Hennig, A.L. (2003). Geomechanical properties related to top seal leakage in the Carnarvon Basin, Northwest Shelf, Australia. *Petroleum Geoscience*, 9, pp. 255-263.

Dewhurst, D.N. and Jones, R.M. (2002). Geomechanical, microstructural, and petrophysical evolution in experimentally reactivated cataclasites: Applications to fault seal prediction, *American Association of Petroleum Geologists Bulletin*, 86 (8), pp. 1383-1405.

Dewhurst, D.N., Jones, R.M. and Raven, M.D. (2002). Microstructural and petrophysical characterization of Muderong Shale: application to top seal risking. *Petroleum Geoscisnce*, 8 (4), pp. 371-383.

Dewhurst, D.N., Kovack, G.E., Hennig, A.L., Bailey, W.R., Raven, M.D. and Kaldi, J.G. (2004). Geomechanical and Lithological Controls on Top Seal Integrity on the Australian Northwest Shelf. Proceedings of the *6th North American Rock Mechanics Conference, GulfRocks04*, Houston, June, p. 8.

Dewhurst, D.N., Raven, M.D., van Ruth, P., Tingate, P.R. and Siggins, A.F. (2002b). Acoustic properties of Muderong Shale. *Australian Petroleum Production and Exploration Association Journal*, 42, pp. 241-257.

Downey, M.D. (1984). Evaluating fault seals for hydrocarbon accumulations. *The American Association of Petroleum Geologists Bulletin*, 68, pp. 1752-1763.

DPI. (2005). Minerals and Petroleum – Overview [online]. Available from http://www.dpi.vic.gov.au/dpi/nrenmp.nsf/childdocs/-C58CC29C22BD9D674A2567C4001F3676?open [accessed 1 November 2005].

Eadington, P.J., Lisk, M. and Krieger, F.W. (1996). Identifying oil well sites, United States Patent No. 5, pp. 543 616.

Ellis, G.K., Pitchford, A. and Bruce, R.H. (1999). Barrow Island Oil Field, *Australian Petroleum Production and Exploration Association Journal*, 39 (1), pp. 158-176.

Elsharkawy, A.M. (1996). A material balance solution to estimate the initial gas in-place and predict the driving mechanism for abnormally high-pressured gas reservoirs. *Journal of Petroleum Science and Engineering*, 16, pp. 33-44.

Elsharkawy, A.M. (1998). Changes in gas and oil gravity during pressure depletion of oil reservoirs. *Fuel*, 77 (8), pp. 837–845.

Ementon, N., Hill, R., Flynn, M., Motta, B., and Sinclair, S. (2004). Stybarrow oil field – from seismic to production, the integrated story so far: SPE paper, 88574, *SPE Asia Pacific Oil and Gas Conference* Perth 2004.

Ennis-King, J. and Paterson, L. (2005). Role of convective mixing in the long-term storage of carbon dioxide in deep saline formations. *SPE J* 10, pp. 349-356.

Etheridge, M.A., Mcqueen, H. and Lambeck, K. (1991). The role of intraplate stress Tertiary (and Mesozoic) deformation of the Australian continent and its margins: a key factor in petroleum trap formation, *Exploration Geophysics*, 22, pp. 123-128.

Fanchi, J.R. (2001). Integrating forward modelling into reservoir simulation. *Journal of Petroleum Science and Engineering*, 32, pp. 11-21.

Firoozabadi, A. and Ramey, H.J. (1988). Surface tension of water-hydrocarbon systems at reservoir conditions. *Journal of Canadian Petroleum Technology*, 27, pp. 41-48.

Fisher, Q.J. and Knipe R.J. (1998). Fault sealing processes in siliciclastic sediments. *In:* Jones, G., Fisher, Q.J. and Knipe, R.J. (eds.), *Faulting, fault sealing and fluid flow in hydrocarbon reservoirs: Geological Society (London) Special Publication.* 147, pp. 117-134.

Fittall A.M. and Cowley R.G. (1992). The HV11 3-D seismic survey: Skua-Swift area geology revealed, *Australian Petroleum and Exploration Association Journal*, 32 (1), pp. 159-170.

Fulljames, J.R., Zijerveld, L.J.J. and Franssen, R.C.M.W. (1997). Fault seal processes: systematic analysis of fault seals over geological and production time scales. *In:* Moller-Pedersen, P. & Koestler, A.G. (eds.), Hydrocarbon Seals, Importance for exploration and production. *Norwiegian Petroleum Society (NPF), Special Publication*, 7, pp. 51-59, Elsevier, Amsterdam.

Gartrell, A., Bailey, W.M. and Brincat, M. (2005). Strain localisation and trap geometry as key controls on hydrocarbon preservation in the Laminaria High area. *Australian Petroleum Production and Exploration Association Journal*, pp. 477-492.

Gartrell, A., Bailey, W.M. and Brincat, M. (2006). A new model for assessing trap integrity and oil preservation risks associated with postrift fault reactivation in the Timor Sea. *The American Association of Petroleum Geologists Bulletin.* 90 (12), pp. 1921-1944.

Gartrell, A. and Lisk, M. (2005). Potential new method for palaeo-stress estimation by combining 3D fault restoration and fault slip inversion techniques: First test on the Skua field, Timor Sea. *In:* P. Boult and J. Kaldi (eds.), Evaluating fault and cap rock seals, *American Association of Petroleum Geologists, Hedberg Series*, 2, pp. 23-36.

Gartrell, A., Lisk, M. and **Undershultz, J**. (2002). Controls on the trap integrity of the Skua Oil Field, Timor Sea. *In*: Keep, M. and Moss, S. J. (eds.), The Sedimentary Basins of Western Australia 3: Proceedings of *Petroleum Exploration Society of Australia,* pp. 390-407.

Gartrell, A., Zhang, Y., Lisk, M. and Dewhurst, D. (2004). Fault intersections as critical hydrocarbon leakage zones: Numerical modelling as an example from the Timor Sea, Australia. Marine and Petroleum Geology. 21. pp. 1165-1179.

George, S.C., Lisk, M., Eadington, P.J. and Quezada R. A. (1998). Geochemistry of a palaeo-oil column, Octavius-2, Vulcan Sub-basin, *In*: Purcell, P.G. and Purcell, R.R., (Eds.), The Sedimentary Basins of Western Australia: Proceedings of the *Petroleum Exploration Society of Australia*, Perth, 1998, pp. 195-210.

Gibson, R.G. (1998). Physical character and fluid-flow properties of sandstone-derived fault zones. *In:* Coward, M. P., Daltaban, T. S. & Johnson, H (eds.), Structural Geology in Reservoir Characterisation. *Geological Society, London, Special Publications*, 127, pp. 83-97.

Gibson-Poole, C.M., Root, R.S., Lang, S.C., Streit, J.E., Hennig, A.L., Otto, C.J. and **Underschultz, J.R**. (2005). Conducting comprehensive analyses of potential sites for geological CO_2 storage. *In:* Rubin, E.S., Keith, D.W. and Gilboy, C.F. (eds.), Greenhouse gas control technologies: proceedings of the *7th international conference on greenhouse gas control technologies*, I, Elsevier, Vancouver, 5-9 September, pp. 673-681.

Gibson-Poole, C.M., Svendsen, L., **Underschultz, J**., Watson, M.N., Ennis-King, J., van Ruth, P.J., Nelson, E.J., Daniel, R.F., and Cinar, Y. (2007). Site Characterisation of a Basin-Scale CO_2 Geological Storage System: Gippsland Basin, Southeast Australia. *Journal of Environmental Geology*. On-line publication not yet in print. http://www.springerlink.com/content/0r4v8l4j846t5308/.

Gibson-Poole, C.M., Svendsen, L., **Underschultz, J**., Watson, M.N., Ennis-King, J., van Ruth, P., Nelson, E., Daniel, R., and Cinar, Y. (2006). Gippsland Basin Geosequestration: A potential solution for the Latrobe Valley brown coal CO_2 emissions. *Australian Petroleum Production and Exploration Association Journal*, 46 (1), pp. 241-259.

Gomzalez, L., Herrero, C. and Kelm, U. (1998). Springhill Formation, Magellan Basin, Chile: formation water characteristics and mineralogy, *Marine and Petroleum Geology*, 15, pp. 651-666.

Gorman, I.G.D. (1990). The role of reservoir simulation in the development of the Challis and Cassini fields: *Australian Petroleum Exploration Association Journal*. 30, pp. 212-221.

Grasby, S.E. and Hutcheon, I. (2001). Controls on the distribution of thermal springs in the southern Canadian Cordillera: *Canadian Journal of Earth Sciences*, 38, pp. 427-440.

Gravestock, D.I., Griffiths, M. znd Hill, A. (1983). The Hutton Sandstone - two separate reservoirs in the Eromanga Basin, South Australia, *Australian Petroleum and Exploration Association Journal*, pp. 109-119.

Habermehl, M.A. (1996). Regional groundwater movement, hydrochemistry and hydrocarbon migration in the Eromanga Basin. *In*:: C.I. Gravestone, C.I., Moore, T.S. and Pitt, G.M. (Eds), Contributions to the Geology and Hydrocarbon Potential of the Eromanga Basin. *Geological Society of Australia Special Publication No. 12*. Sydney: Geological Society of Australia, pp. 353-376.

Hatton, T., Otto, C.J. and **Underschultz, J.R**. (2004). Falling Water Levels in the Latrobe Aquifer, Gippsland Basin: Determination of Cause and Recommendations for Future Work. CSIRO Wealth from Oceans, Open File Report 36, unpublished.

Hennig, A., **Underschultz, J.R.** and Otto, C.J. (2002). Hydrodynamic analysis of the Early Cretaceous aquifers in the Barrow Sub-basin in relation to hydraulic continuity and fault seal. *In:* Keep, M. and Moss, S.J. (eds.), The Sedimentary Basins of Western Australia 3*:* Proceedings of the *Petroleum Exploration Society of Australia Symposium*, Perth, WA, pp. 305-320.

Hennig, A., Yassir, Y., Roy, V., Powers, N., **Underschultz, J.R**. and Otto, C. (2000). The NWS hydrodynamics database: A user's guide for the quality controlled northwest Shelf Pressure Database, *CSIRO Petroleum Unrestricted Report*, No. 00-003, 40p.

Heum, O.R. (1996). A fluid dynamic classification of hydrocarbon entrapment. *Petroleum Geoscience*, 2, pp. 145-158.

Hillis, R. R. (1998). Mechanisms of dynamic seal failure in the Timor Sea and Central North Sea Basins. *In*: Purcell, P. G. and Purcell, R. R. (eds.), The Sedimentary Basins of Western Australia 2: Proceedings of *Petroleum Exploration Society of Australia Symposium*, pp. 313-324.

Hillis, R.R. and Reynolds, S.D. (2000). The Australian stress map, *Journal of the Geological Society of London*, 157, pp. 915-921.

Hillis, R.R. and Reynolds, S.D. (2003). In situ stress field of Australia. *In:* Hillis, R.R. and Müller, R.D. (eds.), Evolution and Dynamics of the Australian Plate. *Geological Society of Australia Special Publication 22 and Geological Society of America Special Paper* 372, pp. 49-60.

Hitchon, B. (2000). “Rust” contamination of formation waters from producing wells, *Applied Geochemistry*, 15, pp. 1527-1533.

Hitchon, B, and Brulotte, M. (1994), Culling criteria for “standard” formation water analyses: *Applied Geochemistry*. 9, pp. 637-645.

Hitchon, B. and Friedman, I. (1969). Geochemistry and origin of formation waters in the western Canada sedimentary basin-I. Stable isotopes of hydrogen and oxygen, *Geochimica et Cosmochimica*, 33, pp. 1321-1349.

Hitchon, B., Bachu, S. and **Underschultz, J.R**. (1990). Regional subsurface hydrogeology, Peace River Arch area, Alberta and British Columbia, *Bulletin of Canadian Petroleum Geology*, 38, pp. 196-217.

Hooper, B., Murray, L. and Gibson-Poole, C.M. (2005). Latrobe Valley CO_2 storage assessment – final report. CO2CRC Report No. RPT05-0108. http://www.co2crc.com.au/PUBFILES/OTHER05/LVCSA_FinalReport.pdf. Cited 30 November 2006.

Hubbert, M.K. (1953). Entrapment of petroleum under hydrodynamic conditions. *American Association of Petroleum Geologists Bulletin*, 37, pp. 1954-2026.

Jennings, J.B. (1987). Capillary pressure techniques: Application to exploration and development geology. *The American Association of Petroleum Geologists Bulletin*, 71, pp. 1196-1209.

Jones, G., Fisher, Q.J. and Knipe, R.J. (1998). Faulting, fault sealing and fluid flow in hydrocarbon reservoirs, *Geological Society of London special publication*, 88, 319 p.

Jones, R.M. and Hillis, R.R. (2003). An integrated, quantitative approach to assessing fault-seal risk. *The American Association of Petroleum Geologists Bulletin*, 87, pp. 507-524.

Karbøl, R.and Kabbour A. (1995). Sleipner Vest CO_2 disposal – injection of removed CO_2 into the Utsira Formation. *Energy Convers Manage* 36, pp. 509-512.

Keep, M. and Powell, C. M. B. P. W. (1998). Neogene deformation of the North West Shelf, Australia. The Sedimentary Basins of Western Australia 2: Proceedings of *Petroleum Exploration Society of Australia Symposium*, pp. 81-91.

Kennard, J.M., Deighton, I., Edwards, D.S., Colwell, J.B., O'Brien, G.W. and Boreham, C.J. (1999). Thermal history modeling and transient heat pulses: new insights into hydrocarbon expulsion and 'hot flushes' in the Vulcan Sub-basin, Timor Sea. *Australian Petroleum Production & Exploration Association Journal*, 39 (1), pp. 177-207.

Kivior, T., Kaldi, J.G. and Lang, S.C. (2002). Seal potential in Cretaceous and Late Jurassic rocks of the Vulcan Sub-basin, North West Shelf, Australia:, 42, pp. 203-224.

Kovack, G.E., Dewhurst, D.N., Raven, M.D. and Kaldi J.G. (2004). The influence of composition, diagenesis and compaction on seal capacity in the Muderong Shale, Carnarvon Basin. *Australian Petroleum Production & Exploration Association Journal*, 44, pp. 201-222.

Lang, S.C., Grech, P., Root, R.S., Hill, A. and Harrison, D. (2001). The application of sequence stratigraphy to exploration and reservoir development in the Cooper-Eromanga-Bowen-Surat Basin system. *Australian Petroleum Production & Exploration Association Journal*. 41, pp. 223-250.

Lanzilli, E. (1999). The Birkhead Formation: Reservoir characterisation of the Gidgealpa South Dome and sequence stratigraphy of the Eromanga Basin, Australia. PhD Thesis. University of South Australia.

Lerche, I. (1993). Theoretical aspects of problems in basin modelling. *In*: Dore, A.G. (ed.), Basin Modelling: Advances and Applications. *Norwegian Petroleum Society Special Publication*. 3, pp. 35-65.

Lindsay, N. G., Murphy, F. C., Walsh, J. J. and Watterson, J. (1993). Outcrop studies of shale smear on fault surfaces. *Special Publication of the International Association of Sedimentologists*. 15, pp.113-123.

Lisk, M. and Eadington, P.J. (1994). Oil migration in the Cartier Trough, Vulcan Sub-basin, *In*: Purcell, P.G. and Purcell, R.R., (Eds.), The Sedimentary Basins of Western Australia. Proceedings of *Petroleum Exploration Society of Australia Symposium*, pp. 301-312.

Lisk, M., Brincat, M. P., Eadington, P. J. and O'Brien, G. W. (1998). Hydrocarbon charge in the Vulcan Sub-basin. *In*: Purcell, P. G. and Purcell, R. R. (eds.), The Sedimentary Basins of Western Australia 2: Proceedings of *Petroleum Exploration Society of Australia Symposium*, pp. 287-303.

Lisk, M., Krieger, F., Gartrell, A. and George, S. (2002). My life before I was compressed: Fluid flow histories on the northern Australian convergent margin; *In*: Deformation History, Fluid Flow Reconstruction and Reservoir Appraisal in Foreland Fold and Thrust Belts*: American Association of Petroleum Geologists* Hedberg Conference, Palermo-Mondello, Italy. Article #90011.

Longley, I.M., Buessenschett, C., Clydsdale, L. and 8 others, (2002). The North West Shelf of Australia - a Woodside perspective. *In*: Keep, M. and Moss, S.J. (eds.), *The Sedimentary Basins of Western Australia 3*: Proceedings of the *Petroleum Exploration Society of Australia Symposium*, Perth, WA, pp. 27-88.

Lothe, A.E., Borge, H. and Sylta, Ø. (2005). Evaluation of late caprock failure and hydrocarbon entrapment using a linked pressure and stress simulator. *In*: Boult, P. and Kaldi, J. (eds.), evaluating fault and cap rock seals: *American Association of Petroleum Geologists, Hedberg Series*, 2, pp. 163-178.

Malek, R. (2004a). Barrow and Dampier aquifer depletion studies. Petroleum open day presentation, Department of Industry and Resources Western Australia.

Malek, R. (2004b). Resources branch recent activities. Petroleum in Western Australia. April. Department of Industry and Resources Western Australia, pp. 22-23.

Malek, R. and Mehin, K. (1998). Oil and Gas Resources of Victoria. Petroleum Development Unit, Victorian Department of Natural Resources and Environment. 92 p..

McKerron, A.J. Dunn, V.L., Fish, R.M, Mills, C.R. and van der Linden-Dhont, S.K. (1998). Bass Strait's Bream B reservoir development: success through a multifunctional team approach. *Australian Petroleum Production & Exploration Association Journal.* 38(1), pp. 13-35.

Meyer, V., Nicol, A., Childs, C., Walsh, J.J. and Watterson, J. (2002). Progressive Localisation of Strain During the Evolution of a Normal Fault Population. *Journal of Structural Geology*, 24, pp. 1215-1231.

Michael, K., Bachu, S. and Machel, H.G. (2000). Groundwater flow in response to ground surface topography, erosional rebound, and hydrocarbon generation in Cretaceous strata in the Alberta Basin, Canada. *Journal of Geochemical Exploration*, 69-70, pp. 657-661.

Michael, K., Machel, H.G. and Bachu, S. (2003). New insights into the origin and migration of brines in the deep Devonian aquifers, Alberta, Canada: *Journal of Geochemical Exploration*, 80, pp. 193-219.

Mildren, S.D., Hillis, R.R., Fett, T. and Robinson, P.H. (1994). Contemporary stresses in the Timor Sea: Implications for fault-trap integrity. *In*: Purcell, P.G. and Purcell, R.R. (eds.), The Sedimentary Basins of Western Australia: Proceedings of *Petroleum Exploration Society of Australia Symposium*, pp. 291-300.

Mildren, S.D., Hillis, R.R. and Kaldi, J.G. (2002). Calibrating predictions of fault seal reactivation in the Timor Sea. *Australian Petroleum Production & Exploration Association Journal.* 42(1), pp. 187-202.

Mitchelmore, L. and Smith, N. (1994). West Muiron discovery, WA-155-P – new life for an old prospect. *In:* Purcell, P.G. and R.R (eds.), The Sedimentary Basins of Western Australia: Proceedings of *Petroleum Exploration Society of Australia Symposium*, Perth, WA, pp. 584-596.

Morton-Thompson, D. and Woods A.M. (1992). Development geology reference manual. The American Association of Petroleum Geologists, *AAPG Methods in Exploration* 10.

Mudge, W.J. and Thomson, A.B. (1990). Three-dimensional geological modelling in the Kingfish and West Kingfish oil fields: the method and applications. *Australian Petroleum Production & Exploration Association Journal.* 30, pp. 342-354.

Muir-Wood, R. and King, G.C.P. (1993). Hydrological signatures of earthquake strain. *Journal of Geophysical Research*, 98, pp. 22035-22068.

Needham, D. T., Yielding, G. and Freeman, B. (1997). Analysis of fault geometry and displacement patterns. *In*: Buchanan, P.G. and Nieuwland, D.A. (eds.), Modern Development in Structural Interpretation, Validation and Modelling. *Geological Society (London) Special Publication* 99, pp. 189-199.

Needham, D.J. (1993). The structural architecture of the Timor Sea, North-Western Australia: Implications for basin development and hydrocarbon exploration. *Australian Petroleum Exploration Association Journal*, 33, pp. 258-277.

Nelson, A.W. (1989). Jabiru Field - horst, sub-horst or inverted graben?, *Australian Petroleum Exploration Association Journal*, 29(1), pp. 176-194.

Nelson, E.J. and Hillis, R.R. (2005). In situ stresses of the West Tuna area, Gippsland Basin. *Australian Journal of Earth Sciences*, 52. pp. 299-313.

Nelson, E.J., Hillis, R.R., Sandiford, M. Reynolds, S.D. and Mildren, S.D. (2006). Present-day state-of-stress of southeast Australia. *Australian Petroleum Production & Exploration Association Journal.* 46. pp. 285-305.

Newell, N.A. (1999). Water washing in the Northern Bonaparte Basin. *Australian Petroleum Production & Exploration Association Journal.* 39, pp. 227-247.

Nicol, A., Walsh, J.J., Watterson, J. and Bretan, P.G. (1995). Three-dimensional geometry and growth of conjugate normal faults. *Journal of Structural Geology*, 17, pp. 847-862.

O'Brien, G.W. and Woods E.P. (1995). Hydrocarbon-related diagenetic zones (HRDZs) in the Vulcan Sub-basin, Timor Sea: recognition and exploration implications. *Australian Petroleum Exploration Association Journal*, 35, pp. 220-252.

O'Brien, G.W., Etheridge, M.A., Willcox, J.B., Morse, M., Symonds, P., Norman, C. and Needham, D.J. (1993). The structural architecture of the Timor Sea, North-Western Australia: Implications for basin development and hydrocarbon exploration: *Australian Petroleum Exploration Association Journal*, 33, pp. 258-277.

O'Brien, G.W., Quaife, P., Cowley, R., Morse, M., Wilson, D., Fellows, M. and Lisk, M. (1998). Evaluating trap integrity in the Vulcan Sub-basin, Timor Sea, Australia, using integrated remote-sensing geochemical technologies, *In*: Purcell, P.G. and Purcell, R.R., (Eds), *The Sedimentary Basins of Western Australia 2:* Proceedings of *Petroleum Exploration Society of Australia*, Perth, 1998, pp. 237-254.

O'Brien, G.W. (1993). Some ideas on the rifting history of the Timor Sea from the integration of deep crustal seismic and other data. *Petroleum Exploration Society of Australia Journal*, 21, pp. 95-113.

O'Brien, G.W. and Woods, E.P. (1995). Hydrocarbon related diagenetic zones (HRDZs) in theVulcan Sub-basin, Timor Sea: recognition and exploration implications. *Australian Petroleum Exploration Association Journal*, 35, pp. 220-252.

O'Brien, G.W., Higgins, R., Symonds, P., Quaife, P., Colwell, J. and Blevin J. (1996). Basement control on the development of extensional systems in Australia's Timor Sea: An example of hydbrid hard linked/soft linked faulting?, *Australian Petroleum Production & Exploration Association Journal*, 36, pp. 161-200.

O'Brien, G.W., Lisk, M., Duddy, I., Eadington, P.J., Cadman, S. and Fellows, M. (1996). Late Tertiary fluid migration in the Timor Sea: a key control on thermal and diagenetic histories. *Australian Petroleum Production & Exploration Association Journal*, 36, pp. 399-427.

OPES International (2000). The Barrow Group Aquifer Depletion, Report for the Department of Mines and Energy, Western Australia, unpublished.

Osborne, M.I. (1990). The exploration and appraisal history of the Skua field, AC/P2 - Timor Sea, *Australian Petroleum Exploration Association Journal*, 30 (1), pp. 197-211.

Otto, C., Hennig, A., Roy, V., Powers, N., Yassir, N. and O'Brien, G. (1999). Evaluating trap integrity on the Northwest Shelf of Australia: An industry consortium on the hydrodynamics of seal breach. Annual Report 2, 1998-99. *CSIRO Petroleum Confidential Report* No. 99-048, *CSIRO Land and Water confidential Report* No. 99-47, 52p.

Otto, C., Hennig, A., **Underschultz, J.**, Roy, V. and O'Brien, G. (2000). Evaluating trap integrity on the Northwest Shelf of Australia: An industry consortium on the hydrodynamics of seal breach: Hydrodynamic analysis and interpretation. Unpublished CSIRO Report. 93p.

Otto, C., **Underschultz, J**., Hennig, A. and Roy, V. (2001). Hydrodynamic analysis of flow systems and fault seal integrity in the Northwest Shelf of Australia: *Australian Petroleum Production and Exploration Association Journal*. 41 (1), pp. 347-365.

Otto, C.J. (1992). Petroleum Hydrogeology of the Pechelbronn-Soultz in the Upper Rhine Graben, France - Ramifications for exploration in intermontane basins. Ph.D. Thesis, *University of Alberta, Canada*.

Otto, C.J. and Yassir, N. (1997). Hydrodynamic assessment of fault seal integrity: Ramifications for exploration and production: Geofluids II extended abstracts, Contributions to the *Second International Cconference on Fluid Evolution, Mmigration and Interaction in Sedimentary Basins and Orogenic Belts*, Belfast, Northern Ireland, pp. 129-132.

Palananthakumar, B, Childs, C. and Manzocchi, T. (2006). The effect of hydrodynamics on capillary seal capacity. Programme with abstracts, Structurally complex reservoirs meeting. *Geological Society of London.* January 2006.

Pattillo, J. and Nicholls, P.J. (1990). A tectono stratigraphic framework for the Vulcan Graben, Timor Sea region, *Australian Petroleum Exploration Association Journal*, 30(1), pp. 27-51.

Perkins, E.H. and Gunter, W.D. (1996). Mineral traps for carbon dioxide. *In:* Hitchon, B. (ed.) Aquifer Disposal of Carbon Doixide: Hydrodynamic and Mineral Trapping – Proof of Concept. *Geoscience Publishing Ltd*., pp. 93-114.

Phillips, O.M. (1991). Flow and reactions in permeable rocks, Cambridge University Press.

Pickett, G.R. (1966). A review of current techniques for determination of water saturation from logs, *Journal of Petroleum Technology*, Nov., pp. 1425-1433.

Posamentier, H.W. and Allen, G.P. (1999). Siliciclastic Sequence Stratigraphy – Concepts and Applications. *SEPM, Concepts in Sedimentology and Paleontology*, 7, p. 210.

Powder, M.R., Hill, K.C., Hoffman, N., Bernecker, T. and Norvick, M. (2001). The structural and tectonic evolution of the Gippsland Basin: results from 2D section balancing and 3D structural modelling. *In:* Hill, K.C. and Bernecker, T. (eds.), Eastern Australian Basins Symposium: A Refocused Energy Perspective for the Future. *PESA*, Melbourne, Australia, 25-28, pp. 373-384.

Prensky, S. (1992). Temperature measurements in boreholes-An overview of engineering and scientific applications, *The Log Analyst*, May-June, pp. 313-334.

Price, R. A. (1994). Cordilleran tectonics and the evolution of the Western Canada sedimentary basin. *In*: Mossop, G.D. and Shetsen, I. (eds.), Geological Atlas of Western Canada: Calgary, *Canadian Society of Petroleum Geologists/Alberta Research Council*, pp. 13-24.

Price, R.A. (2001). An evaluation of models for the kinematic evolution of thrust and fold belts: structural analysis of a transverse fault zone in the Front Ranges of the Canadian Rockies north of Banff, Alberta: *Journal of Structural Geology*, 23, pp. 1079-1088.

Pruess, K. Oldenburgh, C. and Moridis, G. (1999). TOUGH2 User's Guide, Version 2.0. Earth Sciences Division, Lawrence Berkeley National Laboratory, Technical Report LBNL-43134, unpublished.

Rahmanian, V.D., Moore, P.S., Mudge, W.J. and Spring, D.E. (1990). Sequence stratigraphy and the habitat of hydrocarbons, Gippsland Basin, Australia. *In*: Brooks, J. (ed.), Classic Petroleum Provinces. *Geological Society of London, Special Publication*. 50, pp. 525-541.

Ramsey, J.G. (1967). The Folding and Fracturing of Rocks. McGraw-Hill, New York, 568 p.

Rodgers, S. (1999). Discussion: 'Physical constraints on hydrocarbon leakage and trapping revisited' by Bjørkum et al. – further aspects. *Petroleum Geoscience.* 5, pp. 421-423.

Root, R.S., Gibson-Poole, C.M., Lang, S.C., Streit, J.E., **Underschultz, J.R**. and Ennis-King, J. (2004). Opportunities for geological storage of carbon dioxide in the offshore Gippsland Basin, SE Australia: an example from the upper Latrobe Group. *In:* Boult, P.J., Johns, D.R. and Lang, S.C. (eds.), Eastern Australasian Basins Symposium II. Special Publication, *Petroleum Exploration Society of Australia,* Adelaide, pp. 19-22 September, pp. 367-388.

Root, R.S., in prep. Geological Model Construction for Geosequestration – Gippsland Basin. Australia. PhD Thesis, The University of Adelaide, unpublished.

Ross, M.I. and Vail, P.R. (1994). Sequence stratigraphy of the lower Neocomian Barrow Delta, Exmouth Plateau, Northwestern Australia, *In*: Purcell, P.G., & Purcell R.R., (Eds.), The sedimentary basins of Western Australia*:* Proceedings of the *Petroleum Exploration Society of Australia*, Perth, 1994, pp. 435-447.

Rowe, A.M. and Chou, J.C.S. (1970). Pressure-Volume-Temperature-Concentration of aqueous NaCl solutions, *Journal of Chemical and Engineering Data*, 15, pp. 61-66.

Sagawa, A., Corbett, P.W.M. and Davies, D.R. (2000). Pressure transient analysis of reservoirs with a high permeability lens intersected by a well bore. *Journal of Petroleum Science and Engineering*, 27, pp. 165-177.

Salem, H.S. and Chilingarian, G.V. (1999). The cementation factor of Archie's equation for shaly sandstone reservoirs, *Journal of Petroleum Science and Engineering*, 23**,** pp. 83-93.

Samani, N., Kompani-Zare, M. and Barry, D.A. (2004). MODFLOW equipped with a new method for the accurate simulation of asymmetric flow. *Adv. Water Resources*. 27, pp. 31-45.

Sayers, J., Marsh C., Scott A., Cinar Y., Bradshaw J., Hennig A.L., Barclay S. and Daniel R.F. (2006). Assessment of a potential storage site for carbon dioxide: a case study, southeast Queensland, Australia. *Evironmental Geoscince* 13, pp. 123-142.

Schlumberger (1974). Fluid Conversions in Production Log Interpretation, 57p.

Schlumberger (1989). Log Interpretation Charts, 151p.

Schowalter, T.T. (1979). Mechanics of secondary hydrocarbon migration and entrapment. *American Association of Petroleum Geologists Bulletin*, 63, pp. 723-760.

Schulz-Rojahn, J.P. (1993). Calcite-cemented zones in the Eromanga Basin: clues to petroleum migration and entrapment, *Australian Petroleum Exploration Association Journal*, pp. 63-76.

Scibiorski, J.P., Micenko, M. and Lockhart, D., 2005. Recent discoveries in the Pyrenees Member, Exmouth sub-Basin: A new oil play fairway: *Australian Petroleum Production and Exploration Association Journal*, 45**,** pp. 233 – 251.

Sclater, J.G. and Christie, P.A.F. (1980). Continental stretching: an explanation of the post-Mid –Cretaceous subsidence of the Central North Sea Basin, *Journal of Geophysical Research*, 85, pp. 3711-3739.

Seeburger, D.A., Miller, N.W.D., Beacher, G.J., Schultz-Rojahn, J.P. and Popek, J.P. (1998). An evaluation of the Mardie Greensand reservoir, Thevenard Island Area, Carnarvon Basin, *In*: Purcell, P.G., & Purcell R.R., (Eds.), The sedimentary basins of Western Australia 2: Proceedings of the *Petroleum Exploration Society of Australia*, Perth, 1998, pp. 491-502.

Shuster, M.W., Eaton, S., Wakefield, L. and Kloosterman, H.J. (1998). Neogene tectonics, greater Timor Sea, offshore Australia: implications for trap risk, *Australian Petroleum Production and Exploration Association Journal*, 38 (1), pp. 351-379.

Sibson, R.H. (1996). Structural permeability of fluid-driven fault-fracture meshes. *Journal of Structural Geology*, 18, pp. 1031-1042.

Sibson, R.H., Moore, J M. and Rankin, A. H. (1975). Seismic pumping: a hydrothermal fluid transport mechanism. *Journal of the Geological Society London*, 131, pp. 653-659.

Simmelink, H.J., **Underschultz, J.R**., Verweij, J.M., Hennig, A., Pagnier, H.J.M., Otto, C.J. (2003). A pressure and fluid dynamic study of the Southern North Sea Basin: *Journal of Geochemical Exploration*, 78-79, pp. 187-190.

Singh, K., Fevang, O. and Whitson, C.H. (2005). Depletion oil recovery for systems with widely varying initial composition. *Journal of Petroleum Science and Engineering*, 46, pp. 283-297.

Smith, D.A. (1966). Theoretical considerations of sealing and non-sealing faults. *The American Association of Petroleum Geologists Bulletin*, 50, pp. 363-374.

Smith, D.A. (1980). Sealing and non-sealing faults in Louisiana Gulf Coast Salt Basin. *The American Association of Petroleum Geologists Bulletin*, 64, pp. 145-172.

Smith, G.C., Tilbury, L.A., Chatfield, A., Senycia, P. and Thompson, N. (1996). Laminaria - A new Timor Sea discovery. *Australian Petroleum Production and Exploration Association Journal*, 36, pp. 12-29.

Smith, P.M. and Sutherland, N.D. (1991). Discovery of salt in the Vulcan Graben: A geophysical and geological evaluation, *Australian Petroleum Exploration Association Journal*, 31, pp. 229-243.

Sneider, R.M., Sneider, J.S., Bolger, G.W. and Neasham, J.W. (1997). Comparison of seal capacity determinations; conventional cores vs. cuttings. *In*: Surdam, R.C. (ed.), Seals, traps, and the petroleum system, *American Association of Petroleum Geologists Memoir*, 67, pp. 1-12.

Sollie, F. and Rodgers S. (1994). Towards better measurements of logging depth. Society of Professional Well Log Analysts *Thirty-Fifth Annual Logging Symposium Transactions*, 1, D1-D15.

Sperrevik, S., Gillespie, P A., Fisher, Q. J., Halvorsen, T. and Knipe, R. J. (2002). Empirical estimation of fault rock properties. *In* : Koestler, A.G. & Hunsdale, R. (eds.), *Hydrocarbon Seal Quantification*, *NPF Special Publication* 11, pp. 109-125. Elsevier, Amsterdam.

Stagg, H.M.J. (1993). Tectonic elements of the North West Shelf Australia, scale 1:25 00000, Australian Geological Survey Organisation, Canberra.

Streit, J.E. and Hillis, R.R. (2004). Estimating fault stability and sustainable fluid pressures for underground storage of CO_2 in porous rock. *Energy*, 29(9-10), pp. 1445-56.

Struik, L. C. and D.G. MacIntyre (2001). Introduction to the special issue of Canadian Journal of Earth Sciences: The Nechako NATMAP Project of the central Canadian Cordillera: *Canadian Journal of Earth Sciences*, 38, pp. 485-494.

Teige, G.M.G. and Hermanrud, C. (2004). Seismic characteristics of fluid leakage from an underfilled and overpressured Jurassic fault trap in the Norwegian North Sea. *Petroleum Geoscience*, 10(1), pp. 35-42.

Teige, G.M.G., Hermanrud C, Thomas W.H., Wilson, O.B., Bolas, H.M.N. (2005). Capillary resistance and trapping of hydrocarbons: a laboratory experiment. *Petroleum Geoscience*, 11, pp. 125-129.

Teige, G.M.G., Thomas W.L.H., Hermanrud, C., Oren, P., Rennan, L., Wilson, O.B., Bolas, H.M.N. (2006). Relative permeability to wetting-phase water in oil reservoirs. *Journal of Geophysical Research*, 111, B12204, doi:10.1029/2005JB003804..

Tenchov, G.G. (1998). Evaluation of electrical conductivity of shaly sands using the theory of mixtures, *Journal of Petroleum Science and Engineering*, 21, pp. 263-271.

Thomas, H., Bernecker, T. and Driscoll, J. (2003). Hydrocarbon Prospectivity of Areas V03-3 and V03-4, Offshore Gippsland Basin, Victoria, Australia: 2003 Acreage Release. Department of Primary Industries, Victorian Initiative for Minerals and Petroleum Report 80.

Tindale, K., Newell, N., Keall, J. and Smith, N. (1998). Structural evolution and charge history of the Exmouth Sub-basin, Northern Carnarvon Basin, Western Australia. *In:* Purcell, P.G. and R.R (eds.), The Sedimentary Basins of Western Australia 2: Proceedings of *Petroleum Exploration Society of Australia Symposium*, Perth, WA, pp. 447-472.

Tingate, P. R., Wrightstone, A., Dewhurst, D., Dodds, K., Khaksar, A. and Van Ruth, P. (2000), Overpressure in the Barrow sub-basin, North West Shelf, Australia. *The American Association of Petroleum Geologists Bulletin,* 84. p.1506.

TNO-NITG. (2001). Pressure and Temperature QC system-Review and applicability to Dutch subsurface- Collaboration CSIRO/TNO-NITG. TNO report NITG 01-079-B. Utrecht.

Tóth, J. (1962). A theory of groundwater motion in small drainage basins in Central Alberta, *Canada. Journal of Geophysical Research*. 67, pp. 4375–4387.

Tóth, J. and C.J. Otto (1993). Hydrogeology and oil deposits at Pechelbronn-Soultz, Upper Rhine Graben: *Acta Geologica Hungarica*, 36 (4), pp. 375-393.

Toupin, D., Eadington, P.J., Person, M., Morin, P., Wieck, J.M. and Warner, D. (1997). Petroleum hydrogeology of the Cooper and Eromanga basins, Australia; some insights from mathematical modelling and fluid inclusion data. *The American Association of Petroleum Geologists Bulletin*, 81(4), pp. 577-603.

Underschultz, J. (2005). Pressure distribution in a reservoir affected by capillarity and hydrodynamic drive: Griffin Field, North West Shelf, Australia. *Geofluids Journa*l, 5, pp. 221-235.

Underschultz, J.R. (2007). Hydrodynamics and membrane seal capacity: *Geofluids Journal* 7, pp. 148-158.

Underschultz, J.R. and Bartlett, R. (1999). Hydrodynamic controls on foothills gas pools; Mississippian strata. *Canadian Society of Petroleum Geologists Reservoir*, 26, pp. 10-11.

Underschultz, J.R. and Boult P. (2004). Top seal and reservoir continuity: Hydrodynamic evaluation of the Hutton-Birkhead Reservoir, Gidgealpa Oilfield. *In:* Boult, P.J., Johns, D.R. and Lang, S.C. (eds.), Eastern Australasian Basins Symposium II. Special Publication, *Petroleum Exploration Society of Australia*, Adelaide, 19-22 September, pp. 473-482.

Underschultz, J.R., Ellis, G. K., Hennig, A., Bekele, E. and Otto, C. (2002). Estimating formation water salinity from wireline pressure data: Case study in the Vulcan Sub-basin. *In*: Keep, M. and Moss, S.J., (Eds.), The Sedimentary Basins of Western Australia 3: Proceedings of *The Petroleum Exploration Society of Australia Symposium*, Perth, WA, 2002, pp. 285-303.

Underschultz, J.R., Hill, R.A. and Easton, S. (2008). The Hydrodynamics of Fields in the Macedon, Pyrenees and Barrow Sands, Exmouth Sub-Basin: Identifying Seals and Compartments. *Australian Society of Exploration Geophysicists.* 39, pp. 85-93.

Underschultz, J.R., Otto, C.J. and Bartlett R. (2005), Formation fluids in faulted aquifers: examples from the foothills of Western Canada and the North West Shelf of Australia. *In:* P. Boult and J. Kaldi (eds.), Evaluating fault and cap rock seals, *American Association of Petroleum Geologists, Hedberg Series*, 2, pp. 247-260.

Underschultz, J.R., Otto C.J. and Cruse T. (2003). Hydrodynamics to assess hydrocarbon migration in faulted strata - methodology and a case study from the Northwest Shelf of Australia. *Journal of Geochemical Exploration*, 78-79, pp. 469-474.

Underschultz, J.R., Otto, C. and Hennig, A. (2007), Application of hydrodynamics to Sub-Basin-Scale static and dynamic reservoir models. *Journal of Petroleum Science and Engineering*. 57/1-2, pp. 92-105.

Underschultz, J.R., Otto, C.J. and Roy, V. (2003). Regional Hydrodynamic Analysis on the Gippsland Basin. CSIRO Petroleum, APCRC Confidential Report No. 03-04. 28 p., unpublished.

Ursin, J.R. (2000). Fault block modelling – a material balance model for the early production forecasting from strongly compartmentalised gas reservoirs. *Journal of Petroleum Science and Engineering*, 27, pp. 179-195.

Vanwagoner, J.C., Mitchum, J.R.M., Campion, K.M. and Rahmanian, V.D. (1990). Siliciclastic Sequence Stratigraphy in Well Logs, Core and Outcrops: Concepts for High-Resolution Correlation of Time Facies. *American Association of Petroleum Geologists, Methods in Exploration Series*, 7, 55.

Vavra, C.L. Kaldi, J.G. and Sneider, R.M. (1992). Geological applications of capillary pressure: a review. *American Association of Petroleum Geologists Bulletin*, 76(6) pp. 840-850.

Veevers, J.J. (1988). Morphotectonics of Australia's Northwestern Margin – A Review. *In*: Purcell, P. G. and R. R. (eds.), *The North West Shelf Australia*: Proceedings of Petroleum Exploration Society of Australia Symposium, Perth, 1988, pp. 19-28.

Veneruso, A.F., Erlig-Economides, C and Petijean, L. (1991). Pressure gauge specification considerations in practical well testing. *66th Annual Technical Conference and Exhibition of the Society of Petroleum Engineers*. SPE Preprint 22752, pp. 865-878.

Verweij, H. (2003). Fluid flow systems analysis on geological timescales in onshore and offshore Netherlands with special reference to the Broad Fourteens basin. Doctoral Thesis Vrije Universiteit, Amsterdam. 278 p.

Verweij, J.M. and Simmelink, H.J. (2002). Geodynamic and hydrodynamic evolution of the Broad Fourteens Basin (The Netherlands) in relation to its petroleum systems. M*arine and Petroleum Geology*, 19, pp. 339-359.

Verweij. J.M. (1993). Hydrocarbon Migration Systems Analysis. Elsevier. Amsterdam.

Viessman, W., Lewis, G.L.and Knapp, J.W. (1989). Introduction to hydrogeology 3rd Edition, HarperCollins, New York.

Villegas, M.E., Bachu, S., Ramon, J.C.and **Underschultz, J.R**. (1994). Flow of formation waters in the Cretaceous-Miocene succession of the Llanos Basin, Columbia: *American Association of Petroleum Geologists Bulletin*, 78, pp. 1843-1862.

Walker, G. (1992). Effect of petroleum production on onshore groundwater aquifers in the Gippsland Basin. Proceedings of the Gippsland Basin Symposium, Melbourne, 22-23 June, pp. 235-242.

Walker, G. and Mollica, F. (1990). Review of the Groundwater Resources in the South East Region. A report to the Department of Water Resources Victoria. Report No. 54, Water Resource Management Report Series, March 1990. 68 p.

Wallace, W.E. (1969). Water production from abnormally pressured gas reservoirs in South Louisiana, *Journal of Petroleum Technology*, 21, pp. 969-983.

Walsh, J.J., Bailey, W.R., Childs, C., Nicol, A. and Bonson, C.G. (2003). Formation of segmented normal faults; a 3-D perspective. *Journal of Structural Geology*, 25, pp. 1251-1262.

Watons, M.N. and Gibson-Poole, C.M. (2005). Reservoir selection for optimised geological injection and storage of carbon dioxide: a combined geochemical and stratigraphic perspective. The fourth annual conference on carbon capture and storage. National Energy Technology Laboratory, US Department of Energy, Alexandria, 2-5 May 2005. [CD-Rom].

Watson, M.N., Boreham, C.J. and Tingate, P.R. (2004). Carbon dioxide and carbonate cements in the Otway Basin: implications for geological storage of carbon dioxide. *Australian Petroleum Production and Exploration Association Journal*, 44(1), pp. 703-20.

Watterson, J., Nicol, A. and Walsh, J.J. (1998). Strains at the intersections of synchronous conjugate normal faults. *Journal of Structural Geology*, 20, pp. 363-370.

Watts, N.L. (1987). Theoretical aspects of cap-rock and fault seals for single- and two-phase hydrocarbon columns. *Marine and Petroleum Geology*, 4, pp. 274-307.

Wilkinson, K. (1995), Is fluid flow in Paleozoic formations of west-central Alberta affected by the Rocky Mountain thrust belt? Master's Thesis, University of Alberta, Edmonton, Alberta, Canada.

Woods, E.P. (1992). Vulcan Sub-basin fault styles implications for hydrocarbon migration and entrapment, *Australian Petroleum Exploration Association Journal*, 32(1), pp. 138-158.

Woods, E.P. (1994). A salt-related detachment model for the development of the Vulcan Sub-Basin. *In*: Purcell, P.G. and R.R. (Eds.), The Sedimentary Basins of Western Australia: Proceedings of *Petroleum Exploration Society of Australia Symposium*, Perth, 1994 pp. 259-273.

Woollands, M.A. and Wong, D. (Eds.). (2001). Petroleum Atlas of Victoria, Australia. The State of Victoria, Department of Natural Resources and Environment, 208 p.

Workman, L.J., Slate, T.V. and Oke, B.F. (2002). The Griffin Development - Flying High on Infill Success. *SPE Asia Pacific Oil and Gas Conference and Exhibition*. SPE 77920.

Wormald, G.B. (1988). The geology of the Challis Oilfield Timor Sea, Australia. Proceedings of *Petroleum Exploration Society Australia Symposium*, Perth, pp. 425-437.

Yassir, N. and Otto, C.J. (1997). Hydrodynamics and fault seal assessment in the Vulcan Sub-basin, Timor Sea. *Australian Petroleum Production and Exploration Association Journal*, 37(1), pp. 380-389.

Yielding, G, Freeman, B., Needham, D.T. (1997). Quantitative fault seal prediction. *American Association of Petroleum Geologists Bulletin*, 81, pp. 897-917.

Yielding, G. (2002). Shale gouge ratio – Calibration by geohistory. *In:* Koestler, A.G. and Hunsdale (eds.), *Hydrocarbon Seal Quantification*: Amsterdam, Elesevier, *Norwegian Petroleum Society (NPF) Special Publication.* 11, pp. 1-15.

Zhao, S., Tara, J.D. and Muller, R.D. (2002). 3D finite element modeling of the northwest Australian stress field, *PESA News*, 61, pp. 42-43.

14. Published papers

17

Underschultz, J. R., C. J. Otto, and R. Bartlett, 2005, Formation fluids in faulted aquifers: Examples from the foothills of Western Canada and the North West Shelf of Australia, *in* P. Boult and J. Kaldi, eds., Evaluating fault and cap rock seals: AAPG Hedberg Series, no. 2, p. 247–260.

Formation Fluids in Faulted Aquifers: Examples from the Foothills of Western Canada and the North West Shelf of Australia

J. R. Underschultz

Commonwealth Scientific and Industrial Research Organization Petroleum, Bentley, Western Australia, Australia

C. J. Otto

Commonwealth Scientific and Industrial Research Organization Petroleum, Bentley, Western Australia, Australia

R. Bartlett

Hydro-Fax Resources Ltd., Calgary, Alberta, Canada

ABSTRACT

Faults and fault zones commonly represent key geological factors in determining migration fairways and assessing the retention and leakage history for hydrocarbons in the subsurface. Although formation pressure data are sparsely acquired from within fault zones themselves, hydrodynamic analysis of faulted aquifers can be used as an indirect indicator of the fault zone hydraulic properties. Case studies from the foothills of Western Canada and the North West Shelf of Australia are used to define a workflow for hydrodynamic analysis in faulted strata and to identify the manifestation of fault zone hydraulic properties on adjacent aquifer pressure systems for various tectonic settings.

Faults with significant displacement can form hydraulic barriers. In this case, fluid flow in the aquifer next to the fault is predominantly parallel to the structural grain, and a discontinuity occurs in the potentiometric surface for the aquifer being crosscut. Localized hydraulic communication (leakage), either across a fault in an aquifer or vertically along a fault zone between aquifers, tends to occur (1) where the fault zone

DOI:10.1306/1060768H23171

bends out of plane from the dominant stress field; (2) where the main structural grain is crosscut by steeply dipping high-angle faults; or (3) where deformation is transferred from one fault zone to another through a relay zone or transfer fault. These are manifest by chemical or thermal anomalies and potentiometric highs or lows closed against the fault trace. Although conditions of fault zone conductivity tend to be localized, they can limit the trapping potential of structural closures by allowing the leakage and further migration of hydrocarbons.

INTRODUCTION

Faults can both be barriers and conduits to flow, and because faults form key risk factors in the capture and retention of hydrocarbons, understanding their effects on mass transport processes in sedimentary basins is essential at the geological timescale. On the reservoir production timescale, faults can compartmentalize a reservoir or act as a thief to injected fluids. This chapter examines flow systems in faulted strata under a range of tectonic settings, with the aim to identify a linkage between structural style, the hydraulic behavior of faults themselves, and more generally, the impact of faults on formation water flow systems. Understanding the fault systems that make up part of the plumbing of a sedimentary basin, in turn, aids the characterization of hydrocarbon migration and trapping.

To examine the hydrodynamic behavior of faults to fluid flow, hydrodynamic analyses are presented at various scales from two basins that represent different tectonic settings. The first case study is located on the transition between undisturbed Mississippian carbonates of the west central Alberta Basin in Canada and the outboard equivalent strata in the adjacent thrust-fold belt of the Rocky Mountains. This region has extensive data to constrain the stratigraphic and structural geometry of the rock framework, as well as formation pressure and rock property data needed to define the formation water flow system. The overall tectonic setting is that of a shortened continental margin, developed through transpressional collision of the North American continent with various tectonic elements of the Pacific plate. Mississippian strata host extensive gas accumulations in the thrust-fold belt and gas and oil reserves in the adjacent foreland basin.

The second case study is a reservoir-scale evaluation located on the North West Shelf of Australia, in a contrasting tectonic setting to that of Western Canada. The North West Shelf represents a Late Devonian to Early Carboniferous rifted passive margin, with thermal subsidence to the Late Triassic. Late Jurassic to Early Cretaceous saw regional transpression and middle Miocene to Holocene reactivation of faults, because of convergence and subduction of the northern edge of the Australian continental plate margin at the Timor trough (O'Brien et al., 1993). The North West Shelf of Australia is an active exploration region with extensive geological and hydrodynamic data. The complex tectonic history with fault reactivation make fault seal issues an important regional exploration risk.

METHODOLOGY

Pressure data are obtained from drillstem (DST), wireline (WLT), and production or static gradient tests. Initially, only data from zones of formation water are used to characterize the hydraulic head distribution, but these are supplemented by preproduction hydrocarbon pressure data extrapolated to known free-water-level elevations. Data are located in a well-defined structural stratigraphic framework.

Standard hydrodynamic approaches to characterizing flow systems in unfaulted aquifer systems include the analysis of pressure data, both in vertical profile (e.g., pressure-elevation plot), and within the plane of the aquifer after conversion to hydraulic head. Pressure data are supplemented with formation-water analysis and formation-temperature data to aid in the evaluation of the flow system. Bachu (1995), Dahlberg (1995), Otto et al. (2001), and Bachu and Michael (2002) provide an overview of hydrodynamic analysis techniques. Evaluation techniques for the culling and analysis of formation water samples are described by Hitchon and Brulotte (1994) and Underschultz et al. (2002). Techniques for the evaluation of formation temperature are described by Bachu and Burwash (1991) and Bachu et al. (1995).

The hydraulic properties of a fault should be considered separately from the impact that fault may have on the aquifer it crosscuts. A fault zone may hydraulically separate the aquifer on either side yet put one side in hydraulic communication vertically with a separate stratigraphic level. Therefore, both juxtaposition and fault zone rock properties need to be considered. Because pressure data from a fault zone itself is not typically available, inferences about the hydraulic nature of the fault need to be made by evaluating the pressure data in the aquifer near the fault. Otto et al. (2001)

describe some theoretical patterns of hydraulic head in faulted aquifers and pressure gradients on pressure-elevation plots for faults with various hydraulic properties.

Although flow systems are three dimensional in nature, they are commonly visualized in more simplistic ways first and then built into a three-dimensional model. In the plane of the aquifer, the hydraulic head can be contoured to show the fluid potentials for formation water (Bachu, 1995; Bachu and Michael, 2002), provided that no significant density variations are present. For faulted aquifers in the studies described here, the hydraulic head distribution is first characterized in unfaulted blocks of the aquifer. Then, the hydraulic head distributions in adjacent blocks are compared and built as a patchwork into a flow model that is representative of the faulted strata as a whole.

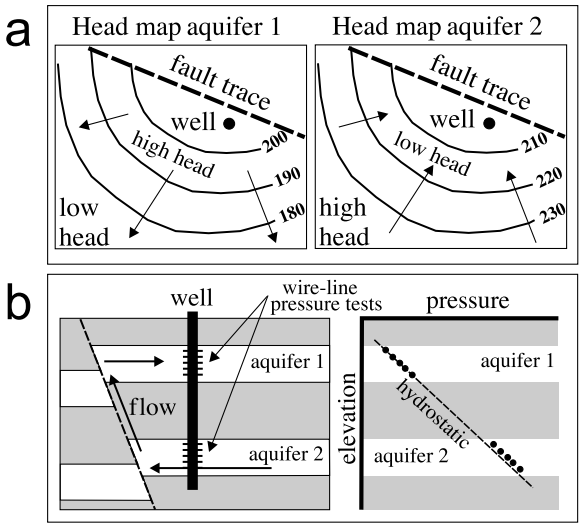

FIGURE 1. Schematic fault hydrodynamics (modified from Otto et al., 2001). (a) Hydraulic head distributions in two stacked aquifers connected by a crosscutting conduit fault; (b) cross section of the conduit fault in (a) with upfault flow, and the corresponding pressure-elevation plot of WLT data from the two aquifers at the well location.

Upfault (or Downfault) Flow

If a fault is acting as a conduit, with higher permeability along the fault than the aquifer it crosscuts, and if the fault zone permeability pathway is vertically continuous to either a separate aquifer or the land surface (or seabed), then the aquifer will see the fault as either a source or a sink for fluids. The hydraulic head distribution in the aquifer will form either a closed high or low against the fault surface, indicating that formation water is either emanating from the fault zone into the aquifer or flowing from the aquifer into the fault zone, respectively (Figure 1a). This analysis can be supplemented by evidence such as thermal springs at the land surface or thermal and chemical anomalies of the formation water in the aquifer adjacent to the fault. If, for example, a fault zone is acting as a conduit recharging an aquifer at depth, it is expected that the formation water in the aquifer would be relatively fresh and have a meteoric ionic signature, such as elevated HCO_3^- and/or SO_4^{2-}. The likelihood of an aquifer being in hydraulic communication with the land surface can be deduced by comparing the hydraulic head in the aquifer with the elevation of the water table (commonly similar to the topographic elevation). If the hydraulic head in the aquifer is similar to topographic elevation, it is possible that the water table elevation is in hydraulic communication with the aquifer.

At any one location, the vertical hydraulic communication can be examined by pressure-elevation plot analysis. If two vertically separated aquifers are in hydraulic communication via a fault zone conduit, the pressure data from the two aquifers near the fault should define a near-common hydrostatic gradient on a pressure-elevation plot (Figure 1b). In this schematic example, the hydraulic head in the deeper aquifer is slightly higher than the shallower aquifer, which allows for the flow up the fault zone. For this reason, the WLT pressure data in aquifer 2 fall slightly above the pressure gradient defined by the data in aquifer 1 on the pressure-elevation plot (Figure 1b).

Faults as Flow Barriers

When a fault zone has lower permeability than the aquifer it crosscuts, the flow direction in the aquifer adjacent to the fault will tend to be parallel to the plane of the fault (Figure 2a). This nature of the flow leads to a relatively abrupt contrast in hydraulic head values in the aquifer directly across the fault (a hydraulic head discontinuity). The more significant the fault is as a barrier, either because of juxtaposition or low fault rock permeability, the more severe is the hydraulic head discontinuity. In this schematic example (Figure 2a), there is a 70 m drop in hydraulic head across the fault zone. If the fault zone could be examined at a small scale, the discontinuity in hydraulic head would actually be a very steep hydraulic head gradient along the plane of the fault, thus leading to some flow across the fault plane, but the flux would be negligible compared to that moving parallel to the fault plane in the adjacent aquifer. Corroborating evidence for fault zone barriers are the accumulations of hydrocarbon on one side of the fault, and discontinuities in the formation water chemistry across the fault.

At any one location, the vertical hydraulic communication can be examined by pressure-elevation

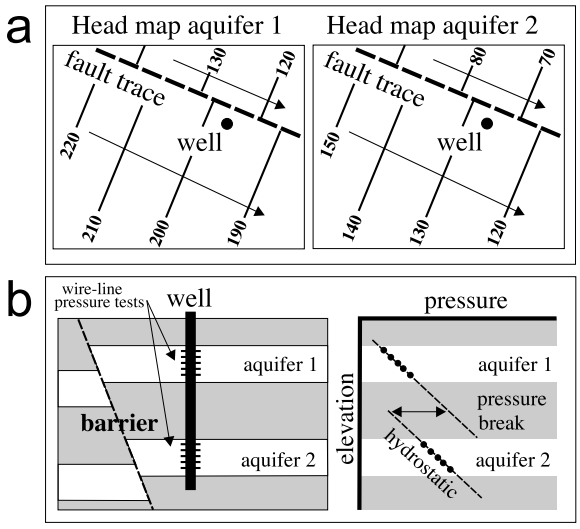

FIGURE 2. Schematic fault hydrodynamics (modified from Otto et al., 2001). (a) Hydraulic head distributions in two stacked aquifers crosscut by a barrier fault; and (b) cross section of the barrier fault in (a) with no upfault flow and the corresponding pressure-elevation plot of WLT data from the two aquifers at the well location.

plot analysis for a well near to, or crosscut by a fault (Figure 2b). Zones of low hydraulic transmissivity manifest themselves as a break in the observed pressure gradient with depth (Dahlberg, 1995).

WESTERN CANADIAN FOLD AND THRUST BELT

The western edge of the Alberta Basin is deformed by thrusting and folding in the foothills and main ranges. Further westward, allochthonous rocks make up the accreted terranes that collided with the North American craton between the Jurassic and Cretaceous. The geological history of the thrust-fold belt has been the subject of extensive investigation and is described by various authors (e.g., Price, 1994, 2001; Struik and MacIntyre, 2001; Begin and Spratt, 2002).

One of the first hydrodynamic evaluations of the foothills and main ranges of the Rocky Mountains is by Wilkinson (1995) in the Burnt Timber area. He observed abrupt changes in both hydraulic head and formation-water salinity across the main thrust faults, suggesting that they were acting as barriers to flow. Underschultz and Bartlett (1999) examined the Mississippian strata at Moose Mountain, Wildcat Hills, and Burnt Timber fields and noticed that a component of flow moved parallel to the structural grain in individual thrust sheets. Grasby and Hutcheon (2001) observed the distribution and chemistry of thermal springs in the southern Canadian Cordillera. They found springs with temperatures as much as 67°C and circulation depths of as much as about 3 km (1.8 mi).

Study Area and Structural Style

For the purpose of examining the regional characteristics of the flow system, the hydraulic head distributions for the Mississippian aquifer (Livingstone strata) have been selected (Figure 3). The area with the best data control extends from Township (Tp) 30 in the south to Tp 46 in the north, representing a distance of about 160 km (99 mi) (Figure 4). The structural trend is from southeast to northwest, so the study area was selected to be about 120 km (74 mi) wide and straddling the boundary between thrusted and undisturbed strata. At any location in the study area, moving from undisturbed strata westward, minor thrusts are encountered

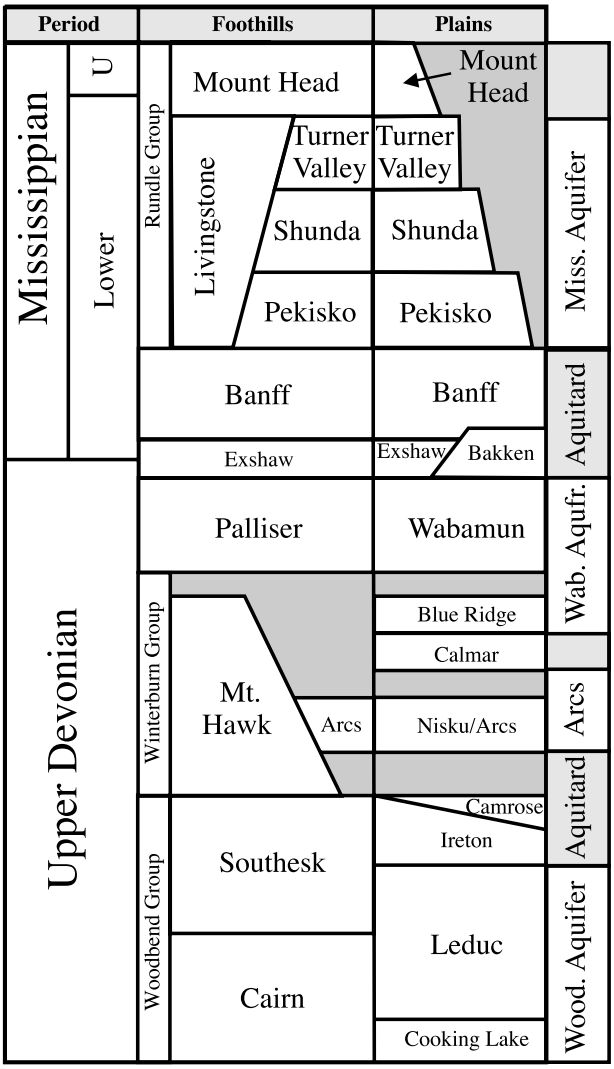

FIGURE 3. Stratigraphic and hydrostratigraphic nomenclature for the west central Alberta Basin and foothills.

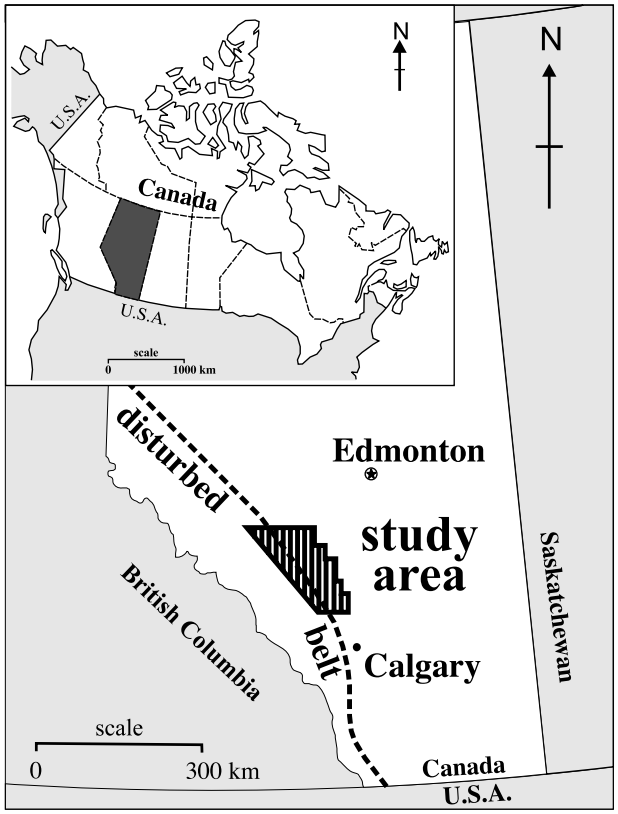

FIGURE 4. Study area for the west central Alberta Basin.

with small displacement and limited geographic extent. Typically, the maximum displacement along an individual fault is greatest in the center, decreasing to zero displacement at the ends. These minor thrust faults commonly form doubly plunging anticlines, making them excellent hydrocarbon traps. When taken in series, as displacement is lost along one thrust, it is taken up on the next subparallel thrust either to the east or west. This style of deformation is characteristic for the foothills section of the thrust-fold belt in the study area. Further west, more significant thrusts occur, such as the Bighorn and Brazeau sheets. These faults are continuous over much larger distances and also represent more significant displacement. Finally, the McConnell thrust to the west is the first regional thrust sheet, and it defines the start of the Front Ranges of the Rocky Mountains. It represents a continuous structure from one end of the study area to the other.

Hydraulic head was calculated for pressure data based on a constant density correction for formation-water salinity of 70 g/L, which is average for Paleozoic formation water in this region. More than 4000 pressure tests (DSTs, WLTs, and production and static gradient tests) and nearly 4400 formation water analyses in the Paleozoic strata of the thrust-fold belt and adjacent undeformed strata of Western Canada have been evaluated. Both the thrusted and the undeformed parts of the Alberta Basin are characterized to observe the relation between the two. Care has been taken to ensure that data used to constrain the flow model is unaffected by production, and that standard data quality assurance has been observed (Otto et al., 2001).

Mississippian Aquifer

The regional distribution of hydraulic head for Mississippian strata is shown in Figure 5. At some locations, as much as three repeat sections of Mississippian strata are present, each with its own pressure data. For display purposes, the hydraulic head distribution for the aquifer in the upper sheet (Brazeau and Bighorn) is shown in green color shade with black contours, and the aquifer repeated below is shown in blue color shade with blue contours. At North Limestone (34-11W5), a window is cut out of the green color shade of the Brazeau flow system to show the aquifer system below the Brazeau sheet. Some generalities observed in the foreland thrust belt of the Alberta Basin common to all the Paleozoic aquifers are as follows. (1) Within the same aquifer, hydraulic head generally increases westward and to structurally higher thrust sheets; (2) faults with large displacement tend to correspond to a discontinuity of hydraulic head for the aquifer displaced across the fault; and (3) in faulted aquifers, the hydraulic gradient in an unfaulted block tends to drive flow parallel to the structural grain (i.e., along strike).

In the case of the study area described here, the amount of data is much less in the thrusted part of the aquifer than in the undisturbed part of the aquifer to the east. With the additional constraint of initially contouring unfaulted blocks separately from one another, very few control points may be present in a particular contouring domain. The result is that the contour distribution is very simplistic for most parts of the thrusted strata in any individual block. With more data control, it is expected that there would be much more detail and complexity to the distribution. Nonetheless, because significant differences in hydraulic head commonly exist between one thrust sheet and the next, even a rudimentary flow model can provide significant predictive capability for the pressures and flow directions expected for individual thrust sheets.

In the undisturbed part of the Mississippian aquifer, the hydraulic head ranges from 500 to 800 m (1600 to 2600 ft). Two significant troughs of low hydraulic head extend southwestward into the foothills region. These are separated by a region (ridge) of high hydraulic head. The first extends westward to the North Limestone gas pool. In this region, a series of small thrusts form the Limestone, North Limestone, and Clearwater gas fields. The Brazeau thrust brings Paleozoic (Mississippian and Devonian) strata in a separate thrust sheet over the top of the Mississippian aquifer containing the Limestone and Clearwater pools. The

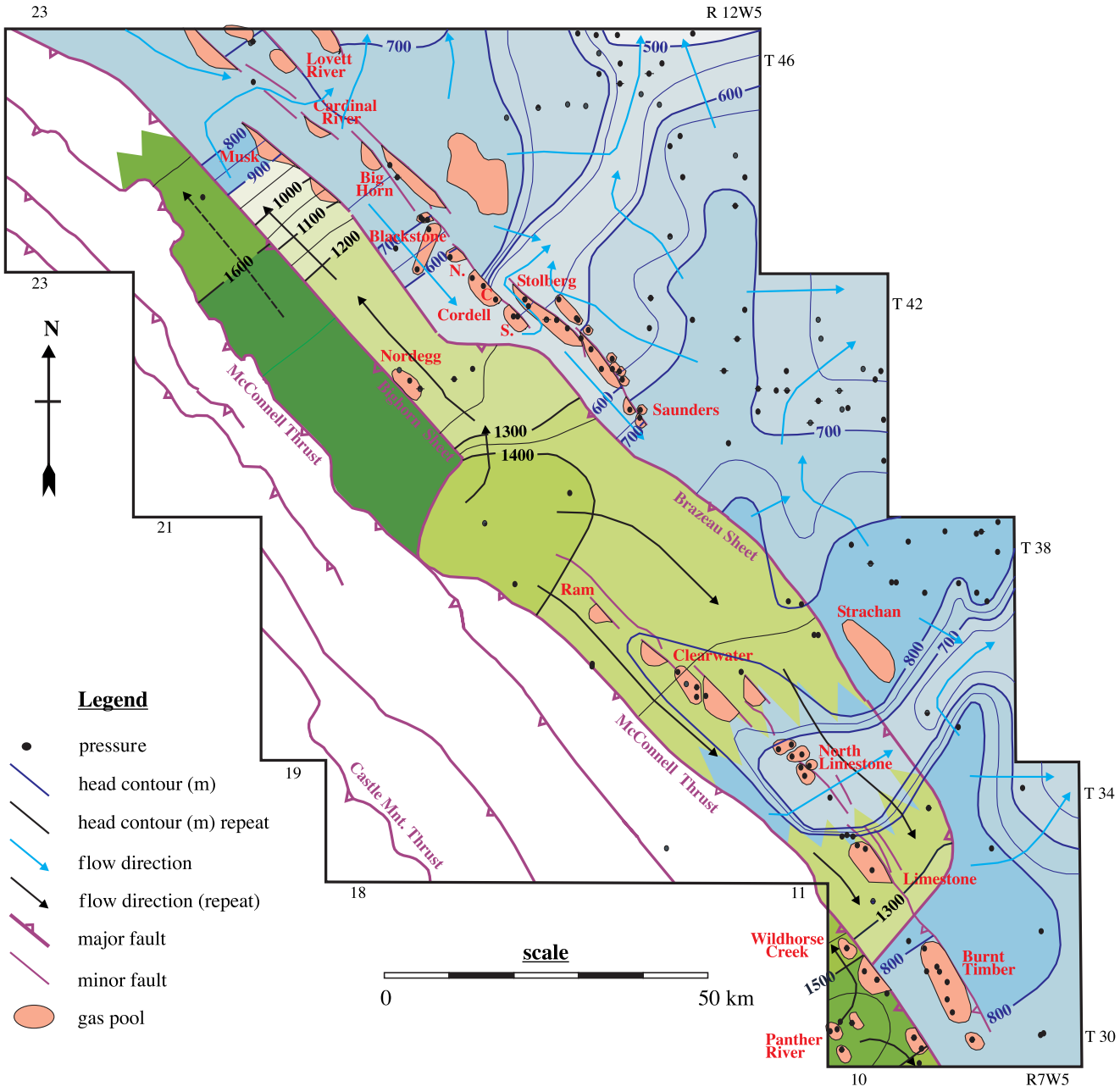

FIGURE 5. Hydraulic head (m) distribution for the Mississippian aquifer.

trough of low hydraulic head in the Mississippian aquifer below the Brazeau thrust turns parallel to the structural grain and extends northwest to the Clearwater field. The hydraulic head in this trough is between 700 and 800 m (2300 and 2600 ft), whereas the Mississippian aquifer in the Brazeau sheet above has a hydraulic head of 1300 m (4300 ft). The second trough of low hydraulic head extends southwestward to the foothills in the region of the Stolburg field. This region of low hydraulic head extends past the first small thrusts and westward at least to the edge of the Brazeau sheet. Each of these troughs of low hydraulic head channels formation-water flow like a collector system in the Mississippian aquifer, and each enters the thrust-fold belt at a location where a continuous Mississippian aquifer between small faults is present.

In the foothills and Front Ranges of the Rocky Mountains, the flow system was characterized by first examining the hydraulic head distribution in each thrust sheet separately and then combining these into a composite. For example, the Saunders to Stolburg region has northwest-directed flow between the first foothills thrusts and the leading edge of the Brazeau thrust. This flow proceeds into the trough of low hydraulic head described previously that enters the foothills belt at the north end of the Stolburg bounding

fault. From Blackstone to South Cordell, a southeast-directed flow system is present between the series of first foothills faults (that bound the Blackstone and Cordell pools) and the leading edge of the Brazeau thrust. This system decreases from 700 to 600 m (2300 to 1900 ft) of hydraulic head before joining into the Stolburg flow system around the south end of the South Cordell thrust.

Flow in the southern part of the Brazeau thrust sheet is southeastward, parallel to the trend of the structure. The hydraulic head in the Mississippian aquifer of the Brazeau sheet is 1400 m (4600 ft) in the vicinity of 39-16W5. A decrease is observed in head southeastward to about 1300 m (4300 ft) in the limestone area. From the 39-16W5 region, a decrease is also observed in hydraulic head parallel to strike northwestward, until displacement on the Brazeau thrust is lost (in the region of the Musk field). Here, the Brazeau thrust flow system comes into hydraulic equilibrium with the small discontinuous thrusts that make up the first structures on the western edge of the undisturbed strata. From Musk, the flow turns east and southeastward toward the Blackstone field described previously.

Further into the thrust-fold belt, less data exist; however, the hydraulic head in the Bighorn thrust is more than 1600 m (5200 ft) (a 200-m [660-ft] jump from the hydraulic head in the adjacent Brazeau thrust). Similarly, the hydraulic head in the Panther River region at the southern end of the study area is about 1600 m (5200 ft).

Because formation water analyses are extremely subject to contamination (Hitchon and Brulotte, 1994; Underschultz et al., 2002), the number of usable salinity data points is small. For the northern part of the undisturbed Mississippian aquifer, the formation water has salinity of as much as 70 g/L (Figure 6), but with low salinity (less than 30 g/L) at the north end of Stolberg and extending northeastward into the plains to about 45-13w5, exactly the same location as the trough of low hydraulic head described earlier. Toward the southern edge of the study area, the salinity increases to 120 g/L in the undisturbed strata. Insufficient data is observed in the Mississippian aquifer below the Brazeau sheet to contour. Based on very little data, the entire foothills region east of the Bighorn thrust sheet (northern half of the study area) appears relatively fresh (less than 30 g/L). Within the Brazeau sheet, the salinity of Mississippian aquifer increases toward the southeast to about 70 g/L (Figure 6).

Flow and Faults in the Foothills and Front Ranges

For the Mississippian aquifer in the foothills of Western Canada, it is observed that when crosscut by faults with significant displacement, an abrupt change (discontinuity) generally occurs in the hydraulic head between one side of the fault and the other, resulting in a flow parallel to structural strike. As the fault loses displacement along its length, the hydraulic head in the aquifer on either side becomes similar, and at the end of the fault where displacement becomes zero, the hydraulic head in the aquifer equilibrates, and hydraulic communication is reestablished in the aquifer. However, faults with significant displacement are not exclusively sealing to the aquifers they crosscut.

Grasby and Hutcheon (2001) demonstrated, by examining thermal springs in the southern Canadian Cordillera, that gravity-driven flow systems occur in the front and main ranges of the Rocky Mountains down to more than 3 km (1.8 mi) depth. They also showed that in the overall compressive tectonic regime, at locations of complex structure, at locations where near-vertical orthogonal structures crosscut the main structural trend, and at locations of steeply dipping lateral ramps, vertical hydraulic communication between the deep subsurface and the ground level was greatly enhanced. Because of variable fault geometry, opportunities exist for localized extensional stress in an overall compressional setting. A similar scenario is described by Craw (2000) in the compressional tectonic setting of the Southern Alps in New Zealand. He observed enhanced formation water flow with meteoric signatures at the intersection of steeply dipping extensional structures and the main fault zones.

Although discharging thermal springs indicate highly permeable pathways from depth along fault zones, the flux tends to be highly focused. Heterogeneous fault zone properties are observed worldwide. For example, in the Mesozoic- and Tertiary-age strata of the Pechelbronn–Soultz subbasin, France, Otto (1992), Toth and Otto (1993), and Otto and Yassir (1997) observed vertically ascending flow of groundwater concentrated largely through the fault zones. These constitute the main pathways for cross-formational fluid flow. However, because of the discontinuous sealing nature of the faults and fault zones, rising fluids may be deflected and forced into highly permeable sections (e.g., lenses) of strata juxtaposed onto the fault plane.

The thermal springs observed by Grasby and Hutcheon (2001) represent a discharge phenomena over an exceedingly small part of the geographic area of the foothills and main ranges, occurring as focused fluid flow enabled by particular geological conditions. Similar structural scenarios of locally extensional settings could equally be located in regions of recharge, where formation water at high topographic elevation is placed in hydraulic communication with a deep aquifer. In this case, it is expected that the formation water in the deep aquifer would have high hydraulic head (approaching that of the surface elevation) and fresh salinity, because the residency time after recharge would

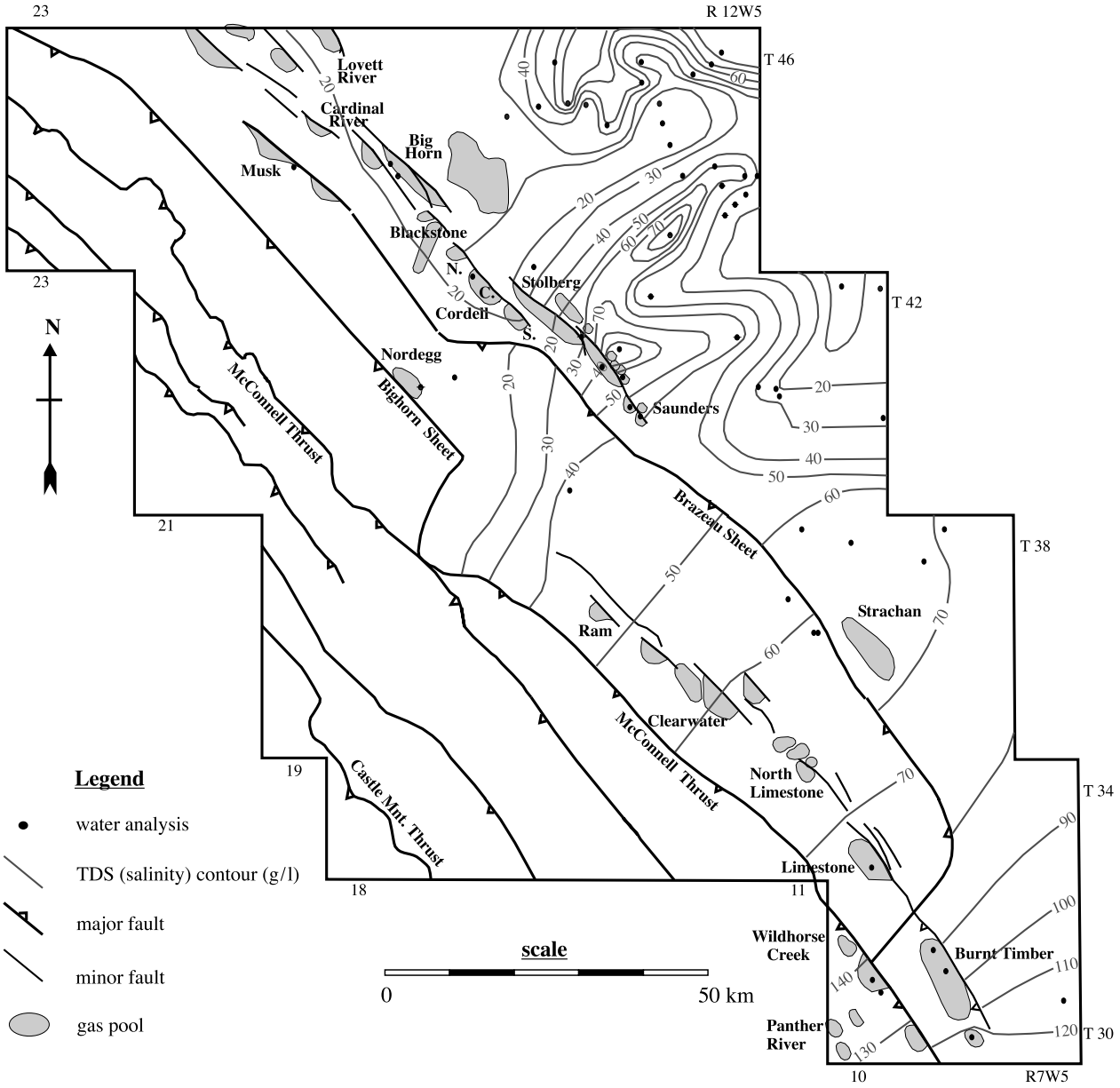

FIGURE 6. Salinity (mg/l) distribution for the Mississippian aquifer. TDS = total dissolved solids.

be short. There is evidence that this situation may exist at various locations in the foothills and main ranges, such as the lateral ramps located at the south end of the Big Horn and Brazeau thrust sheets.

The south end of the Bighorn thrust (39-17W5) forms a steeply dipping lateral ramp. The hydraulic head in the Mississippian aquifer in this region is more than 1400 m (4600 ft) and forms a closed hydraulic head high against the ramp (Figure 5). The surface elevation here is about 1600 m (5200 ft). Only sparse formation water salinity data exist, but values at Nordegg are less than 20 g/L (Figure 6). The flow path from Nordegg is directed northwestward parallel to strike, then around the termination of the Brazeau thrust at the Musk field and southwestward past Cordell in a convoluted path through the foothills belt for more than 120 km (74 mi), before entering into the undisturbed strata at Stolberg. By the exit point from the foothills, the hydraulic head has dropped to less than 600 m (2000 ft), and the salinity is nearly 30 g/L.

A similar situation of focused recharge occurs at the south end of the Brazeau thrust. This region is where the southern end of the Brazeau thrust sheet forms a steeply dipping lateral ramp. Begin and Spratt (2002) interpreted and described a detailed structural geometry for this area. The hydraulic head in the Mississippian aquifer in the Brazeau sheet appears to be controlled by the high hydraulic head near the lateral

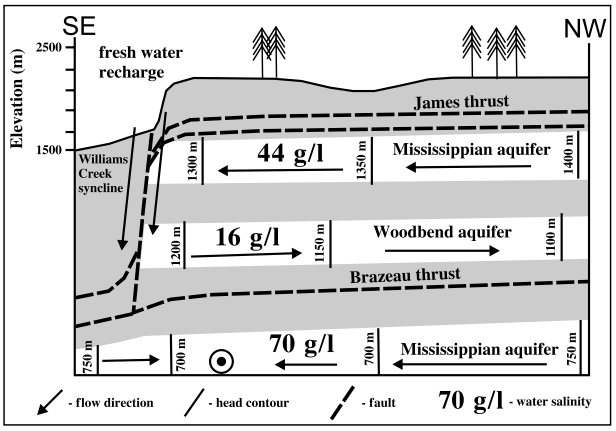

FIGURE 7. Schematic strike cross section of the Brazeau thrust sheet (based on Begin and Spratt, 2002).

ramp in the Bighorn sheet discussed previously. In addition to the flow system previously described, a component of flow migrates southeastward parallel to strike in the Mississippian aquifer of the Brazeau sheet. At the southern end of the Brazeau sheet near the lateral ramp, the hydraulic head has dropped to about 1300 m (4300 ft) (Figure 5). The question that follows is where does this formation water go once it reaches the southern end of the Brazeau sheet? It cannot discharge to the land surface, because the topographic elevation around the base of the Brazeau thrust is about 1500 m (5000 ft), and the hydraulic head in the Mississippian aquifer at the southern end of the Brazeau thrust is less than 1300 m (4300 ft). It probably does not enter the relatively undisturbed Mississippian aquifer underlying the Brazeau sheet, because the hydraulic head in the Clearwater region is about 750 m (2500 ft). This large difference suggests that a hydraulic barrier is present between the two aquifers. More likely, focused recharge is present from the land surface down the steeply dipping lateral ramp at the southern end of the Brazeau sheet. This fresh meteoric water is mixed with the formation water migrating in the Mississippian aquifer in the Brazeau sheet. The formation water recharging down the lateral ramp probably emerges in the Devonian Woodbend aquifer (Figure 3) in the Brazeau sheet, where the hydraulic head is about 1200 m (3900 ft). It then migrates northwestward parallel to strike in the Woodbend aquifer of the Brazeau sheet. The Brazeau thrust itself, at the base of the Brazeau sheet, prevents hydraulic communication between its aquifers and the next Mississippian aquifer below (Limestone to Clearwater region). A formation-water analysis from within the Arcs strata (see Figure 3) of the Brazeau sheet, has a salinity of just 16 g/L, fitting well with the idea of recently recharged formation water. A schematic cross section (based on Begin and Spratt, 2002) illustrating this system is shown in Figure 7. In this case, the valley floor is at a sufficient elevation to act as a focused recharge site.

The final evidence for focused recharge at the Brazeau lateral ramp is the topography and drainage at the land surface. The lateral ramp helps form a valley orientated southwest–northeast, perpendicular to the structural grain, and forms a break in the linear topographic highs above the Brazeau thrust (Limestone and Marble Mountains). The next similar valley to the south hosts the Red Deer River system that flows from a large drainage basin in the foothills and front ranges. No such equivalent drainage is present from the valley at the south end of the Brazeau sheet (Figure 8) other than a small creek that is the headwater of the relatively minor James River. This suggests that a large portion of the precipitation and snowmelt goes to recharge down the Brazeau lateral ramp, leaving little for surface runoff.

Thrusts in the foothills and main ranges of the Rocky Mountains typically act as hydraulic barriers, separating the aquifer in one thrust sheet from the next. This is evidenced by the large differences in hydraulic head and water chemistry between one thrust sheet and the next. There is evidence, however, of significant vertical hydraulic communication with both focused discharge (thermal springs) and recharge as much as 3 km (1.8 mi) deep, particularly at lateral ramps and locations where there are steeply dipping, high-angle structures crosscutting the main structural grain. These are locations where local extensional stress occurs in an overall compressive tectonic regime, and fault zone permeability is high. The result is that the flow paths from the zones of focused recharge to undisturbed aquifers in the plains can be long and convoluted. Regions along the foothills front where formation water enters the undisturbed aquifers are of a restricted nature. This is an important aspect to

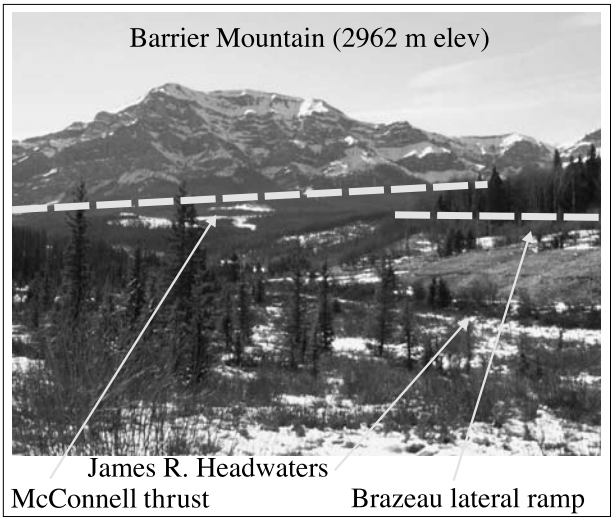

Figure 8. Barrier Mountain and the topographic valley at the south end of the Brazeau thrust sheet lateral ramp.

understanding the flow and transport mechanisms in faulted aquifers, because much of the flux is directed parallel to strike, whereas interpretations of various processes are commonly interpreted and published on dip-oriented cross sections. These invariably indicate no hydraulic connection along the line of section between one sheet and the next; however, eventual communication may well be present out of the plane of the section.

NORTH WEST SHELF OF AUSTRALIA

The North West Shelf of Australia can be broadly characterized as a rift margin with thermal sag. Late-stage convergence resulted in the reactivation of some structures and basin inversion. This has proved to be an exploration challenge, particularly in the Timor Sea region, because the main period of hydrocarbon generation and trap charge occurred prior to reactivation of the structures. The late-stage reactivation has resulted in some previously filled traps leaking some, or all, of their hydrocarbons. Predicting which structures have leaked and which are likely to have retained their hydrocarbons has proven to be difficult and is the subject of significant efforts in fault seal research. It has been recognized that fault intersections where the main structural grain is crosscut at a high angle by deep-seated transfer faults are a high risk for leakage and seal breach (Cowley and O'Brien, 2000; Gartrell et al., 2002). A review of some published studies and a hydrodynamic interpretation of the Challis oil field in the Vulcan subbasin is presented here to illustrate how fault zone hydraulic properties can be deduced from aquifer hydrodynamics. Figure 9 shows a location map of Australia's North West Shelf with the main basin outlines and the Australian coastline.

Commonwealth Scientific and Industrial Research Organization Petroleum conducted the first regional hydrodynamic evaluation of the North West Shelf strata from 1998 to 2001. With the support of an industry consortium, a database was developed of more than 5000 pressure tests and 800 water chemistry analyses. Otto et al. (2001) define the regional hydrostratigraphy across the entire North West Shelf and provide a regional flow system characterization that includes pressure, temperature, and water-salinity data. Two subbasin-scale studies have been completed that examine the influence of faults on regional flow systems, one in the Vulcan subbasin (Underschultz et al., 2002) and one in the Barrow and Dampier subbasins (Underschultz et al., 2003).

Underschultz et al. (2002) show flow systems in the Plover strata of the Vulcan subbasin (Figure 9) to be similarly affected by faulting as those previously

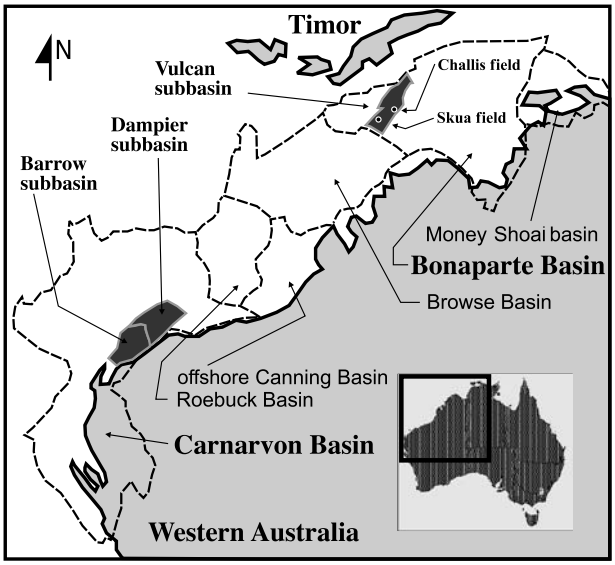

FIGURE 9. Basins on the North West Shelf of Australia modified from Geoscience Australia Map (modified after Kennard, 2004).

described for the Mississippian strata of the Alberta Basin. Outboard faults that form continuous zones of displacement separate flow systems, which is evidenced by discontinuities both in hydraulic head and formation-water salinity across the faults. In these regions, formation water migration is parallel to the structural grain. Nearer to shore, the faults are less continuous. Here, tortuous flow paths are defined, which feed regions of low hydraulic head. These drain the aquifer to the basin margins and eventual discharge.

A hydraulic head distribution for the Barrow strata (Underschultz et al., 2003) was updated from Hennig et al. (2002) for the Barrow and Dampier subbasins (Figure 9). Underschultz et al. (2003) evaluated the likelihood of oil migration from source rocks in the central part of the basin to the south and east across the basin-edge Flinders fault zone and onto the adjacent margin. The basin-edge fault pattern has a change in character north and south of 21°S latitude. To the south, the faults have a general orientation of southwest–northeast; they are closely spaced; and they are interconnected. North of 21°S latitude, the faults change to a north–south orientation (at high angle to regional stress); they become widely spaced; and few connecting structures between the main fault zones are present. Underschultz et al. (2003) conclude that north of 21°S latitude, the faults act as barriers, except for specific locations where transfer zones shift displacement from one fault to the next. Conversely, south of 21°S latitude, the complex fault orientations and interconnectedness give opportunity for the faults to contain conductive pathways.

Some field-scale examples are present where faults locally provide zones of vertical hydraulic communication. Gartrell et al. (2002) show how the intersection

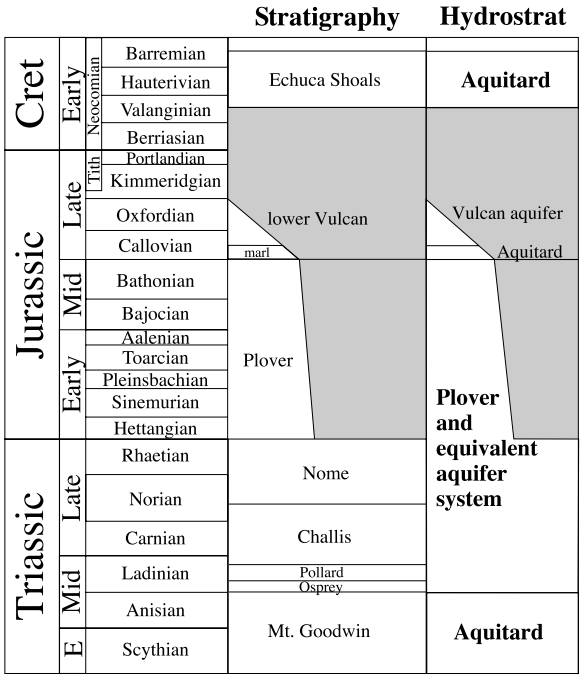

FIGURE 10. Stratigraphic and hydrostratigraphic nomenclature for the Challis Field.

of southwest–northeast-orientated Late Jurassic rift faults and north–south-orientated late Proterozoic basement faults may have controlled the leakage history for the Skua oil field (Figure 9). This interpretation is supported by a structural analysis and restoration, charge history analysis, and an evaluation of the hydraulic communication using hydrodynamic techniques. The intersections of steeply dipping, high-angle basement faults with basin-forming faults create zones of vertical hydraulic communication. A second field in the Vulcan subbasin that shows evidence for vertical hydraulic communication is Challis (Figure 9).

CHALLIS FIELD

The Challis oil field was discovered in 1984 when Challis-1 encountered a 29-m (95-ft) gross oil column in Triassic sandstones immediately below the base Cretaceous unconformity. The Challis-11ST1 well completion report indicates that a thin Jurassic sand exists between the base of the seal and the Triassic sands, but pressure data from the Jurassic and Triassic sands form a common gradient and are considered the same aquifer. Top seal is provided by Cretaceous claystones of the Echuca Shoals Formation (Figure 10) and is reliant on fault juxtaposition for lateral seal. The seal capacity of the top seal is excellent, with Kivior et al. (2002) showing it capable of holding more than 400 m (1300 ft) of oil column. The trap is heavily faulted and is both structurally and sedimentologically complex. With the top seal thickness of about 10 m (33 ft) and fault throws locally in excess of this amount, the structural seal integrity is the main sealing risk. Gorman (1990) and Wormald (1988) describe the structural geometry of the Challis field. The study area extends slightly southwest of the field itself to include Cassini-1 (Figure 11). Within the Challis field horst block, the Jurassic sands are mainly eroded, so the stratigraphic horizons containing the bulk of the hydrodynamic data are the Triassic Challis and Pollard formations (Figure 10). In the vicinity surrounding the Challis field where Jurassic sands occur, the Middle to Early Jurassic sands of the Plover Formation form a single aquifer system with the Triassic sands below and are jointly termed the Plover aquifer system by Underschultz et al. (2002). This is demonstrated by the pressure-elevation profile for Cypress-1, just north of the Challis field (Figure 12). Here, the Late Jurassic sands of the Vulcan Formation have slightly lower hydraulic head than the Middle to Early Jurassic and Triassic sands of the Plover aquifer system.

Of the 18 wells in the study area, 15 have pressure data either from DSTs or WLTs. Eleven of the wells with

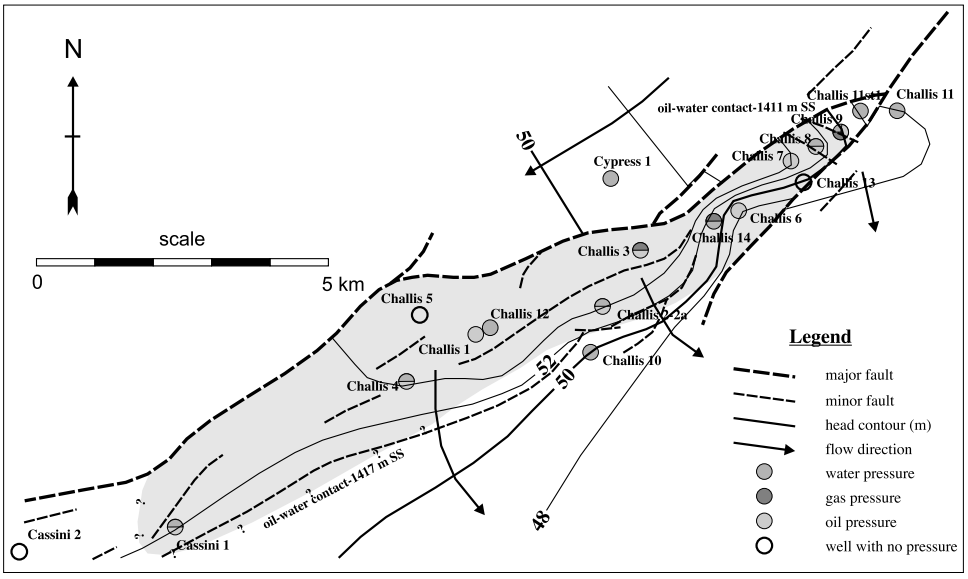

FIGURE 11. Hydraulic head (m) distribution for the Triassic sands at the Challis field.

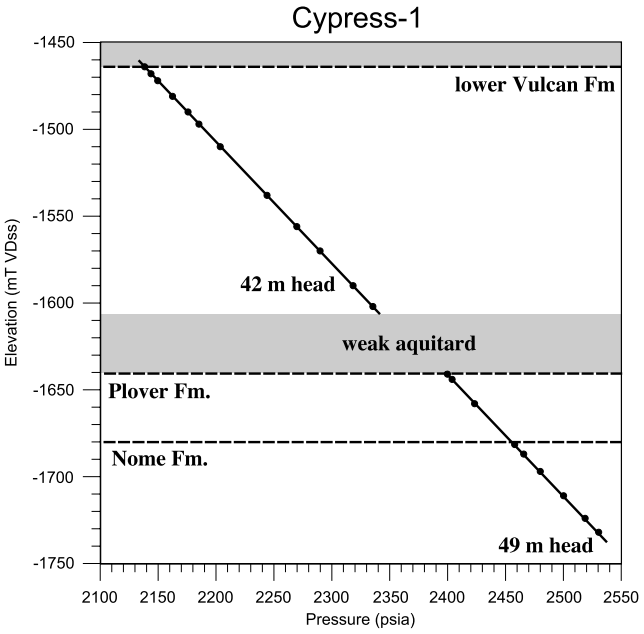

FIGURE 12. Pressure-elevation profile for Cypress-1.

pressure data record information directly on the formation water system. For the four wells with pressure measurements only in the hydrocarbon phase, the pressure was extrapolated down to the estimated hydrocarbon-water contact to gain information on the water system at these locations. To accomplish this, an estimate of the hydrocarbon water contact elevation was made from a combination of WLT data at nearby wells and log analyses from the well completion reports. Formation-water analyses were not found for any of the wells in the study area, but there are production water analyses from Cassini-1, Challis-1, and Challis-2A. Supplementing these data are log analyses values and water salinity estimated from the hydrostatic water pressure gradient recorded by WLTs (Underschultz et al., 2002) in the aquifer.

It has previously been recognized (Yassir and Otto, 1997) and confirmed in this evaluation that production from the Challis field has impacted the pressure recorded at wells drilled into the field after about 1990 (Challis 9–14).

Hydraulic Head

Hydraulic head values for the Triassic sands were calculated based on freshwater density (Figure 11). The dashed lines on the base map represent the position of faults obtained from Wormald (1988). The predominant feature of the map is the closed hydraulic head high in the aquifer beneath the Challis field, against the main Challis-bounding fault. A drop in hydraulic head is present to the north side of the fault, as defined by Cypress-1. No other data control points in the study area are present on the north side of the fault, so a hydraulic gradient on this information alone cannot be established. By examining regional hydraulic head maps from Underschultz et al. (2002), it appears that groundwater flow on the north side of the Challis-bounding fault in the Plover aquifer system is roughly parallel to strike and toward the west.

Within the aquifer, at the base of the Challis field, the fault bounding the north side of the field appears to be a hydraulic barrier. The hydraulic head distribution on the south side of the fault defines a system where flow emanates from the fault and migrates away in a radial fashion to the southwest, south, and east. This pattern is a field example of the idealized transmissive fault described by Otto et al. (2001) and shown in Figure 1a. The formation water must be flowing vertically, from above or below, along the Challis-bounding fault or a subsidiary fault and into the aquifer at the base of the Challis field. The only well that has formation water pressure data above the Challis aquifer is Cypress-1, which defines a value of 42 m (137 ft) head in the Late Jurassic sands of the Vulcan Formation. If this value of hydraulic head is representative, it would suggest that an upward hydraulic gradient is present. Therefore, the formation water traveling along the Challis-bounding fault is likely to be originating from a deeper aquifer. This is broadly consistent with a dewatering compacting basin. From the regional hydrodynamic assessment (Underschultz et al., 2002), the salinity of the Plover aquifer system is described as being 30–45 g/L in the vicinity of the Challis field. If the formation water from deeper in the stratigraphic column was migrating up the Challis fault zone and appearing in the sands at the base of the field, then the salinity would be higher than the regional values in the Plover aquifer system. The pressure-derived salinity for the Challis wells range from 48 to 63 g/L, slightly higher than would have been predicted from the regional trend. Further, at 1510-m (4954-ft) TVDss elevation, the estimated formation-water salinity is only 38 g/L at Cypress-1 on the north side of the Challis fault, fitting well with the low salinity predicted from the regional study of Underschultz et al. (2002). The limited evidence suggests that the source of the formation water entering the aquifer at the base of the Challis field is most likely to be from below. If the Challis fault zone becomes sealing as it passes through the claystone at the top of the Challis field, it would explain the maintenance of the hydrocarbon accumulation.

CONCLUSIONS

When mapping the potential energy distribution in faulted aquifers, unfaulted regions of aquifer are initially considered separately, and then unfaulted

blocks are combined in a patchwork to form a regional flow model. In this way, the impact of the faults on the aquifer system can be assessed. Through the examination of hydrodynamic systems in faulted strata from various regions and tectonic regimes, there emerges some commonality to the impact of faults on hydrodynamic systems. These are as follows.

- Aquifer flow tends to be parallel to the structural grain where faults are sealing.
- Vertical hydraulic communication tends to occur where (1) fault orientation bends out of plane from the dominant stress regime; (2) fault intersections are present, particularly where one fault set is steeply dipping and at a high angle to the other fault set; and (3) at relay zones and transfer faults.
- Flow along conductive faults, instead of an entire fault plane, is likely to be focused.

Conditions of fault zone transmissivity can be identified if sufficient pressure data is available in the aquifer adjacent to the fault. Features that identify a fault zone as being of lower permeability than the reservoir horizon and thus having the potential to be sealing are

- hydraulic head discontinuity across a fault
- flow directions in the aquifer adjacent to the fault, which are parallel with the structural grain
- formation water chemistry discontinuity across a fault
- a vertical break in the pressure gradient on a pressure-elevation plot for wells adjacent to or crosscut by a fault

Features that identify a fault zone as being leaky are

- hydraulic head at depth and adjacent to a fault being similar to topographic elevation and accompanied by low-salinity formation water with elevated CO_3^{2-} or SO_4^{2-}
- hydraulic head highs or lows in the aquifer closing onto the plane of the fault and accompanied by anomalous formation-water chemistry
- a vertically continuous pressure gradient on a pressure-elevation plot for wells adjacent to or crosscut by a fault

ACKNOWLEDGMENTS

We thank Commonwealth Scientific and Industrial Research Organization Petroleum and Hydro-Fax Resources Ltd for supporting the publication of this work. Appreciation is due to Pat Ward, who instigated the initial hydrodynamic work at Moose Mountain. We are grateful for thought-provoking discussions with Allison Hennig, Dan Barson, and Kent Wilkinson. Comments from Jennifer Adams, Jenny Stedmon, and Tim Wood and technical reviews by Barb Tilley, Neil Tupper, and John Kaldi helped improve this chapter.

REFERENCES CITED

Bachu, S., 1995, Flow of variable-density formation water in deep sloping aquifers: Review of methods of representation with case studies: Journal of Hydrology, v. 164, p. 19–38.

Bachu, S., and R. A. Burwash, 1991, Regional-scale analysis of the geothermal regime in the Western Canada sedimentary basin: Geothermics, v. 20, p. 387–407.

Bachu, S., and K. Michael, 2002, Flow of variable-density formation water in deep sloping aquifers: Minimizing the error in representation and analysis when using hydraulic-head distributions: Journal of Hydrology, v. 259, p. 49–65.

Bachu, S., J. C. Ramon, M. E. Villegas, and J. R. Underschultz, 1995, Geothermal regime and thermal history of the Llanos basin, Colombia: AAPG Bulletin, v. 79, p. 116–129.

Begin, N. J., and D. A. Spratt, 2002, Role of transverse faulting in along-strike termination of Limestone Mountain culmination, Rocky Mountain thrust-and-fold belt, Alberta, Canada: Journal of Structural Geology, v. 24, p. 689–707.

Cowley, R., and G. W. O'Brien, 2000, Identification and interpretation of leaking hydrocarbons using seismic data: A comparative montage of examples from major fields in Australia's North West Shelf and Gippsland basin: Australian Petroleum Production and Exploration Association Journal, v. 40, p. 121–150.

Craw, D., 2000, Fluid flow at fault intersections in an active oblique collision zone, Southern Alps, New Zealand: Journal of Geochemical Exploration, v. 69–70, p. 523–526.

Dahlberg, E. C., 1995, Applied hydrodynamics in petroleum exploration: New York, Springer-Verlag, Inc., 295 p.

Gartrell, A., M. Lisk, and J. R. Underschultz, 2002, Controls on the trap integrity of the Skua oil field, Timor Sea, *in* The sedimentary basins of Western Australia: 3. Proceedings of the Petroleum Exploration Society of Australia Symposium, Perth, Western Australia, p. 389–407.

Gorman, I. G. D., 1990, The role of reservoir simulation in the development of the Challis and Cassini fields: Australian Petroleum Exploration Association Journal, v. 30, p. 212–221.

Grasby, S. E., and I. Hutcheon, 2001, Controls on the distribution of thermal springs in the southern Canadian Cordillera: Canadian Journal of Earth Sciences, v. 38, p. 427–440.

Hennig, A., J. R. Underschultz, and C. J. Otto, 2002, Hydrodynamic analysis of the Early Cretaceous aquifers in the Barrow sub-basin in relation to hydraulic continuity and fault seal, *in* The sedimentary basins of Western

Australia: 3. Proceedings of the Petroleum Exploration Society of Australia Symposium, Perth, Western Australia, p. 305–320.

Hitchon, B., and M. Brulotte, 1994, Culling criteria for ''standard'' formation water analyses: Applied Geochemistry, v. 9, p. 637–645.

Kennard, J., 2004, Geoscience Australia: http://www.agso.gov.au/oceans/projects/nwr.jsp (accessed April 2004).

Kivior, T., J. G. Kaldi, and S. C. Lang, 2002, Seal potential in Cretaceous and Late Jurassic rocks of the Vulcan sub-basin, North West Shelf, Australia: Australian Petroleum Production and Exploration Association Journal, v. 42, p. 203–224.

O'Brien, G. W., M. A. Etheridge, J. B. Willcox, M. Morse, P. Symonds, C. Norman, and D. J. Needham, 1993, The structural architecture of the Timor Sea, North-Western Australia: Implications for basin development and hydrocarbon exploration: Australian Petroleum Exploration Association Journal, v. 33, p. 258–277.

Otto, C. J., 1992, Petroleum hydrogeology of the Pechelbronn–Soultz in the Upper Rhine Graben, France—Ramifications for exploration in intermontane basins. Ph.D. Thesis, University of Alberta, Canada, 357 p.

Otto, C. J., and N. Yassir, 1997, Hydrodynamic assessment of fault seal integrity: Ramifications for exploration and production (abs.), *in* Contributions to the Second International Conference on Fluid Evolution, Migration and Interaction in Sedimentary Basins and Orogenic Belts, Belfast, Northern Ireland: Geofluids II Extended Abstracts, p. 129–132.

Otto, C., J. Underschultz, A. Hennig, and V. Roy, 2001, Hydrodynamic analysis of flow systems and fault seal integrity in the North West Shelf of Australia: Australian Petroleum Production and Exploration Association Journal, v. 41, p. 347–365.

Price, R. A., 1994, Cordilleran tectonics and the evolution of the Western Canada sedimentary basin, *in* G. D. Mossop and I. Shetsen, eds., Geological atlas of Western Canada: Calgary, Canadian Society of Petroleum Geologists/Alberta Research Council, p. 13–24.

Price, R. A., 2001, An evaluation of models for the kinematic evolution of thrust and fold belts: Structural analysis of a transverse fault zone in the Front Ranges of the Canadian Rockies north of Banff, Alberta: Journal of Structural Geology, v. 23, p. 1079–1088.

Struik, L. C., and D. G. MacIntyre, 2001, Introduction to the special issue of Canadian Journal of Earth Sciences: The Nechako NATMAP Project of the central Canadian Cordillera: Canadian Journal of Earth Sciences, v. 38, p. 485–494.

Toth, J., and C. J. Otto, 1993, Hydrogeology and oil deposits at Pechelbronn–Soultz, Upper Rhine Graben: Acta Geologica Hungarica, v. 36, no. 4, p. 375–393.

Underschultz, J. R., and R. Bartlett, 1999, Hydrodynamic controls on foothills gas pools; Mississippian strata: Canadian Society of Petroleum Geologists Reservoir, v. 26, p. 10–11.

Underschultz, J. R., G. K. Ellis, A. Hennig, E. Bekele, and C. Otto, 2002, Estimating formation water salinity from wireline pressure data: Case study in the Vulcan sub-basin, *in* The sedimentary basins of Western Australia: 3. Proceedings of the Petroleum Exploration Society of Australia Symposium, Perth, Western Australia, p. 285–303.

Underschultz, J. R., C. J. Otto, and T. Cruse, 2003, Hydrodynamics to assess hydrocarbon migration in faulted strata—Methodology and a case study from the North West Shelf of Australia: Journal of Geochemical Exploration, v. 78–79, p. 469–474.

Wilkinson, K., 1995, Is fluid flow in Paleozoic formations of west-central Alberta affected by the Rocky Mountain thrust belt? Master's thesis, University of Alberta, Edmonton, Alberta, Canada, 122 p.

Wormald, G. B., 1988, The geology of the Challis oil field, Timor Sea, Australia: Proceedings of Petroleum Exploration Society Australia Symposium, Perth, p. 425–437.

Yassir, N., and C. J. Otto, 1997, Hydrodynamics and fault seal assessment in the Vulcan sub-basin, Timor Sea: Australian Petroleum Production and Exploration Association Journal, v. 37, part 1, p. 380–389.

Available online at www.sciencedirect.com
ScienceDirect
Journal of Petroleum Science and Engineering 57 (2007) 92 – 105
JOURNAL OF PETROLEUM SCIENCE & ENGINEERING
www.elsevier.com/locate/petrol

Application of hydrodynamics to sub-basin-scale static and dynamic reservoir models

J.R. Underschultz *, C. Otto, A. Hennig

Jim Underschultz, CSIRO Petroleum PO Box 1130, Bentley WA. 6102, Australia

Received 1 July 2005; accepted 3 October 2005

Abstract

In mature hydrocarbon provinces, the impact of production induced pressure depletion on un-produced or undiscovered reserves is a concern. Reduced formation pressure has an adverse effect on recoverability, but more problematic are accumulations that are filled to spill, where a reduction of formation pressure results either in gas exsolution or gas cap expansion and loss of liquids from the trap. In the Australian context, the latter is of significant concern owing to the gas rich nature of many of its sedimentary basins. Standard reservoir engineering techniques have been used to evaluate the impact of pressure depletion with mixed results.

There are three assumptions typically made in the reservoir models that are normally valid for a single pool, but can add significant uncertainty when applied to a region of several pools, or worse yet, at the sub-basin or basin-scale. The first assumption is that the virgin pressure state of the aquifer at the base of the hydrocarbon column can be approximated by an average hydrostatic formation water pressure gradient. The second is that all pressure data can be referenced to a common reservoir datum by correcting each measured formation pressure using an assumed fluid pressure gradient. The third is that the aquifer which supports one or more hydrocarbon pools has a fixed volume.

The study of basin hydrodynamics uses techniques that take into account the fact that, while the pre-production trapped hydrocarbon phase is static, the aquifer at the base of the hydrocarbon accumulation is dynamic. Regional boundary conditions can be identified that drive formation water flow and help define formation water influx and discharge from an aquifer system rather than assuming a fixed aquifer volume. Pressures in an aquifer may therefore vary for a given depth, due to variations in the hydraulic potential field resulting from differences in aquifer properties across a sub-basin. Hydrodynamic techniques also characterise formation pressure data using a hydraulic head to avoid the requirement of referencing a formation pressure to a depth datum. It removes the need to assume a particular fluid pressure gradient when the fluid composition is not known. This paper describes how hydrodynamic techniques can be incorporated into the static and dynamic reservoir models to reduce errors and uncertainty in the model results. These include the use of a potentiometric energy distribution for the aquifer to obtain aquifer pressure rather than an average hydrostatic gradient and a basin wide depth datum, and the characterisation of natural inflows and discharges rather than assuming a fixed aquifer volume. The approach is exemplified with data from various basins.

Keywords: Hydrodynamics; Reservoir models; Aquifers; Pressure; Depletion

1. Introduction

For sedimentary basins that have multiple hydrocarbon accumulations within the same reservoir horizon, a

* Corresponding author. Tel.: +61 8 6436 8747; fax: +61 8 6436 8555.
E-mail address: james.underschultz@csiro.au (J.R. Underschultz).

0920-4105/$ - see front matter © 2007 Elsevier B.V. All rights reserved.
doi:10.1016/j.petrol.2005.10.014

long term holistic development strategy is required to mitigate the effects of sub-basin scale (10's to 100 km distances) aquifer pressure depletion on unproduced and undiscovered reserves. The West Australian Department of Industry and Resources (DOIR) state in "Petroleum in Western Australia" (2004), that observations from newly discovered fields in the Exmouth, Barrow and Dampier Sub-basins of Western Australia (Fig. 1) suggest sub-basin scale pressure depletion has occurred. Yassir and Otto (1997) describe pressure depletion of the aquifer in the Challis Field region of the Vulcan Sub-basin in the Timor Sea, and sub-basin scale pressure depletion of the Latrobe Group strata in the Gippsland Basin (Fig. 1) has been documented by Walker (1992) Gibson-Poole et al. (2004), Hatton et al. (2004), and Root et al. (2004).

Regionally reduced aquifer pressure has a generally adverse effect on oil and gas recoverability, since there is less pressure support from water influx. More problematic, are single phase reservoirs that are near to the bubble point, or two phase accumulations that are filled to spill. In the case of a single phase reservoir, if the reservoir pressure falls below the bubble point, a gas phase will come out of solution (Craft et al., 1991). With the volumetric expansion, some of the oil may be lost from the trap if it was filled to spill. Similarly, a reduction of reservoir pressure for a two phase reservoir results in gas cap expansion and the potential loss of liquids from the trap. In the Australian context, the latter is of significant concern owing to the gas rich nature of many of its sedimentary basins and the fact that many of its basins have the bulk of their hydrocarbon production from only a few reservoir horizons. Malek (2004a,b) suggest that the potential loss in state royalties due to

Table 1
Estimated royalty loss from the Carnarvon Basin by 2030 due to aquifer pressure depletion assuming 10% royalty and a $50/bbl (AUS) oil price (summarized from Malek (2004a,b)).

	Possible royalty loss $million (AUS)		
Assumed volume of unproduced oil in place (MMSTB)	15 psi depletion	50 psi depletion	500 psi depletion
3200	30	130	2080
6050	60	240	3930

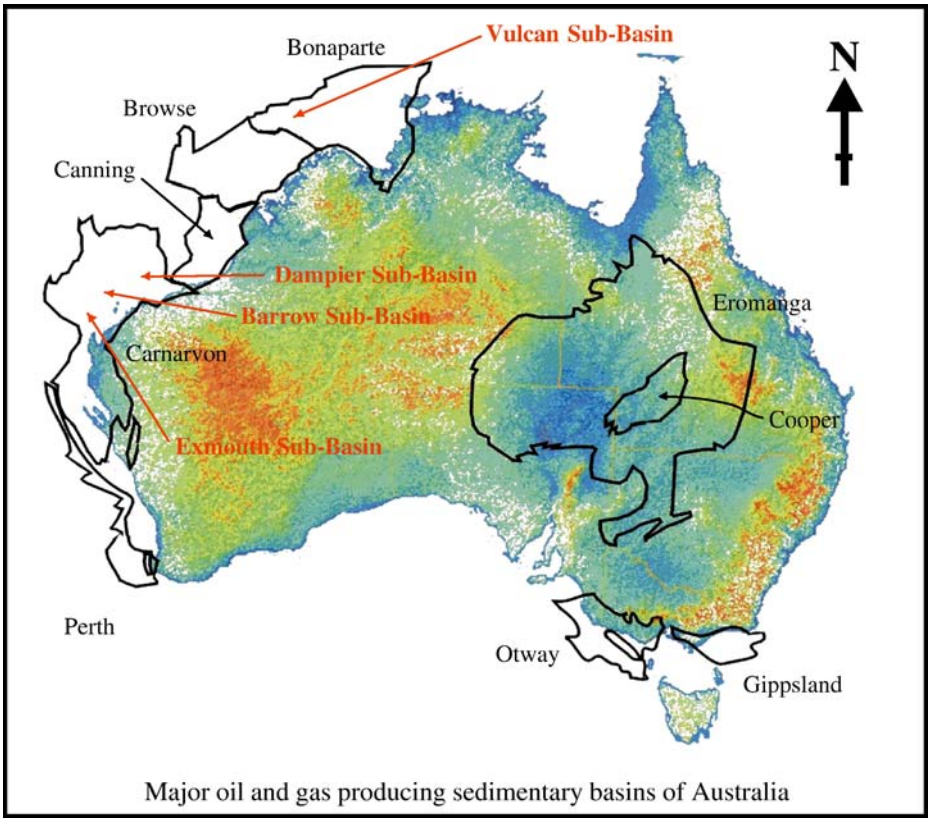

Fig. 1. Major oil and gas producing sedimentary basins of Australia.

lower recovery and lost reserves from gas cap expansion may be greater than 30 million Australian dollars by 2030, as a result of aquifer pressure depletion (Table 1).

It is, therefore, of interest to characterise, model, and predict aquifer pressure depletion based on historical and proposed production. The impact of aquifer pressure reduction on unproduced and undiscovered reserves can then be assessed, and mitigation plans adopted. Standard reservoir engineering techniques, however, are inadequate to fully characterise these processes. In a laterally connected aquifer system it is critical to evaluate the virgin state of the pressure system at the sub-basin to basin-scale in order to provide a basis of comparison to post production pressure values. Only then is it reasonable to determine which pressure observations have been impacted by human activity (production or injection) and which are part of the natural system. A sub-basin to basin-scale hydrodynamic characterisation that captures the variation of potential energy for the aquifer system could be incorporated in the static model to reduce uncertainty in the initial condition of reservoir pressure. Moreover, the dynamic model should include natural influxes and discharges from the aquifer (including cross-formational flow). This will more realistically predict sub-basin scale aquifer response to human activity (injection and production). This paper provides an examination of the standard reservoir modelling approach as applied to the sub-basin scale and describes how a hydrodynamics model could be incorporated to reduce uncertainty.

2. Reservoir engineering approach

Historically, reservoir engineering has focused on understanding the state of crude oil, natural gas and formation water in the reservoir and well bore during production. The division of the well and reservoir fluids between the various states is primarily a function of pressure and temperature (Craft et al., 1991; Cosse, 1993). In order to understand the behaviour of a reservoir over production time, the standard approach is to first build a "static model" that incorporates a definition of the rock framework and its contained fluids (Adamson et al., 1996). The transient behaviour of the reservoir is then predicted using a "dynamic model" that incorporates the multi-phase flow equation and an understanding of the phase behaviour of the reservoir fluid composition. A numerical simulation can be used that solves the material balance and Darcy's law (Adamson et al., 1996). A simulation can be calibrated to observed reservoir pressure over the production history of a field, and can be used to predict reservoir response to various development scenarios.

2.1. Static reservoir model

The complexity of the static reservoir model is dependant on the amount of data that are available to characterise the reservoir. The static reservoir model characterises essentially the initial conditions of the reservoir prior to the start of production. This includes the geometry of the rock framework, the distribution of rock properties (porosity, permeability and compressibility), and the initial pressure and temperature conditions. The static model estimates the initial volume of hydrocarbon in the reservoir, and its phase distribution at initial conditions. It can be done either by the volumetric method or the material balance method (Elsharkawy, 1996).

The rock framework can be defined by a seismic volume tied to well data (Fanchi, 2001). Depending on the nature of the reservoir, special consideration may need to be given to the lithostratigraphic geometry, such as permeable lenses (Sagawa et al., 2000) or fault block geometries (Ursin, 2000). The properties of the rock framework such as porosity, permeability and compressibity (Adamson et al., 1996) are required as spatial distributions. These require either gridding or a scaling up processes of core or petrophysical data.

The fluid attributes of primary concern are the composition, volume, compressibility, viscosity, pressure and temperature of the various reservoir fluids (Adamson et al., 1996). Fluid sample analysis can define most of these, while down hole measurements are required to define the reservoir pressure and temperature. The volume estimate of the various reservoir fluids relies on a combination of the framework model that quantifies the pore space, and the distribution of fluid saturations. Fluid saturation is commonly estimated from petrophysical log analysis linked with reservoir pressure data. The fluid attributes and the rock framework are linked by capillarity and relative permeability (Adamson et al., 1996; Underschultz, 2005).

2.2. Dynamic reservoir model

Once the static reservoir model is established, the dynamic model is developed with the purpose of predicting reservoir response to production, and to optimise a development strategy (Cosse, 1993). When a field is put on production, the dynamic model can be calibrated to match the observed reservoir response. Most reservoir simulators solve the continuity equation (conservation of mass), the equation of flow (Darcy's law) and the equation of state (Adamson et al., 1996). The complexity of the solution required for solving the equations of

state depends on the number of fluid phases present in the reservoir, and the likelihood of the temperature or fluid composition in the reservoir changing with time (Elsharkawy, 1998; Fanchi, 2001; Singh et al., 2005). Most dynamic reservoir models use a numerical simulation approach, where the coupled equations are solved for discrete blocks (elements) of the reservoir over a number of time steps.

Once production from the reservoir commences and the reservoir pressure falls, the PVT behaviour of the reservoir fluids, influx of water from the aquifer, influx of fluids from the sealing formations, and compaction of the rock framework needs to be considered (Adamson et al., 1996; Elsharkawy, 1996; Ursin, 2000; Singh et al., 2005). If the reservoir is subject to temperature variation with location or with time, then a more complex simulation coupled with thermodynamic equations may be required (Adamson et al., 1996). This is most often the case when steam or water injection is required for stimulation or enhanced recovery.

2.3. Application to the sub-basin scale

For the problem of sub-basin scale aquifer depletion, the standard reservoir modelling approach requires some basic assumptions related to the aquifer. For most reservoir simulators the aquifer is characterized by an aquifer volume and an initial aquifer pressure. Most reservoir simulators have a static model defined with a single aquifer pressure. This is commonly obtained from the average aquifer pressure at a field datum elevation (Craft et al., 1991; Singh et al., 2005). In a field that has multiple well penetrations to different depths, an average aquifer pressure can be obtained by first extrapolating each formation pressure measurement to a common datum. The variation of pressure with depth is defined as its hydrostatic gradient (Grad P) and is related to the density of the fluid (Underschultz et al., 2002) according to:

$$\text{Grad } P = \rho g$$

where ρ is the fluid density and g is the gravitational constant. If a formation pressure is obtained within a hydrocarbon phase it must first be extrapolated on the hydrocarbon hydrostatic gradient downwards to the Free Water Level (FWL), and then along the formation water hydrostatic gradient to the field datum. The FWL is defined by the intersection of the hydrocarbon and formation water hydrostatic gradients (Brown, 2003a; Underschultz, 2005). This can be different than the hydrocarbon-water contact, depending on the effects of capillarity (Brown, 2003b; Underschultz, 2005). In a three-phase system the extrapolation may be required to occur down a gas hydrostatic gradient to the Free-Oil-Level (FOL), then down the oil hydrostatic gradient to the FWL, and finally along the formation water hydrostatic gradient to the field datum. Once all pressure measurements for a field have been corrected to a field datum, the average of those pressures is used for the aquifer pressure in the reservoir simulation. For many hydrocarbon fields, the variation in pre-production reservoir pressure from the average is small, and it represents a small error in reservoir simulation (Craft et al., 1991). At the sub-basin scale this variation could be large.

As the reservoir is produced and the formation pressure is reduced in the hydrocarbon phase, there is a response in the aquifer resulting in reduced aquifer pressure. The reduced aquifer pressure causes an influx of formation water that provides pressure support to the production. The extent of pressure support is assumed to depend on the size (pore volume) of the aquifer, the compressibility of the various fluids and rock framework, and the hydraulic conductivity or mobility, which is a product of permeability and fluid viscosity (Elsharkawy, 1996; Sagawa et al., 2000). The assumption is that the initial pore volume of the aquifer is fixed. In effect, a fixed aquifer volume at an initial hydrostatic pressure is attached to several field scale reservoirs as a series of tanks, where withdrawal of hydrocarbons from each tank impacts the common aquifer. Calibration of the dynamic reservoir model is often obtained by adjusting the aquifer volume and permeability distribution. The resulting aquifer response is then evaluated with regard to its impact on undiscovered or unproduced reserves (Malek, 2004a,b). The simplifications of a fixed volume hydrostatic aquifer at initial conditions can be overcome if a hydrodynamic characterisation is incorporated which will capture the non-hydrostatic nature of aquifers at the sub-basin scale. For the dynamic model, the hydrodynamic characterisation addresses the natural influxes and discharges of formation from the aquifer in addition to the human impact of production or injection.

3. Hydrodynamic approach

The study of hydrodynamics seeks to characterize the pressure distribution in sedimentary basins through an understanding of the formation water flow systems. It has been shown that various geological processes can result in transient changes to the formation pressure in a basin. These typically include compaction, thermal processes,

hydrocarbon generation and phase changes, tectonic compression or extension, density-induced fluid movements, and gravitational effects such as topography on the water table (Bachu, 1995b; Bekele et al., 2001). Formation water, which forms the continuous fluid phase in the subsurface, responds to changing formation pressure by flowing. The rate at which formation water moves is a function of the rock permeability, viscosity of the water, and the magnitude of the driving force. The hydrodynamic system within a sedimentary basin, therefore, varies over geological time in response to geological processes. Thus, the pre-production state of the formation water is not hydrostatic (eg. Tóth, 1962; Villegas et al., 1994; Bachu, 1995b; Barson et al., 2001; Anfort et al., 2001; Verweij and Simmelink, 2002; Hennig et al., 2002; Underschultz et al., 2003) even though the oil and gas trapped in reservoirs are. The hydraulic gradient tends to be low in high permeability aquifers (reservoirs) and high across zones of low permeability such as aquitards (seals). Uncertainty in the lithostratigraphic and structural geometry can therefore lead to uncertainty in the potentiometric surface geometry.

Standard hydrodynamic approaches to characterizing flow systems in aquifers include the analysis of pressure data, both in vertical profile (e.g. pressure-elevation plot), and within the plane of the aquifer by conversion to hydraulic head. Pressure data are supplemented with formation water analysis and formation temperature data to aid in the evaluation of the flow system as these parameters can be related to hydrodynamic processes. Bachu and Michael (2002), Otto et al. (2001), Bachu (1995a), and Dahlberg (1995) provide an overview of hydrodynamic analysis techniques. Evaluation techniques for the culling and analysis of formation water samples are described by Hitchon and Brulotte (1994), Underschultz et al. (2002). Techniques for the evaluation of formation temperature are described by Bachu and Burwash (1991), Bachu et al. (1995).

3.1. Pre-production hydrodynamic model

In a laterally connected aquifer system, the virgin state of the pressure system at the sub-basin to basin scale is characterised. This provides the baseline used to determine which post production pressure observations have been impacted by human activity (production or injection) and which remain unaffected and still part of the natural system.

To demonstrate that an average aquifer pressure gradient is not an adequate characterisation of an aquifer's initial pressure condition at the sub-basin scale, the pressure data from a single aquifer horizon in three separate basins are examined. The average pressure gradient for each basin is plotted with an indicator bar quantifying the typical range of pre production formation pressure in a sample aquifer system.

Fig. 2 shows the pressure data from the Rotliegend strata in the Dutch sector of the North Sea, which are known for their overpressure (Simmelink et al., 2003; Verweij, 2003). The high pressures are related to burial compaction of strata having a high percentage of evaporate horizons that prevent dewatering. It is evident from Fig. 2 that there is a wide range of possible formation pressures within the Rotliegend strata, and the basin average gradient is not meaningful for identifying the formation pressure at a given depth. The data set shows a total range in pressure of more than 3000 psi for a particular depth (between 2.5 to 4 km). If the clearly overpressured strata are ignored, the remainder of the data show a spread of more than 500 psi about the average pressure gradient.

In Australia's Gippsland Basin (Fig. 1), oil and gas has been produced in the offshore, mainly from the

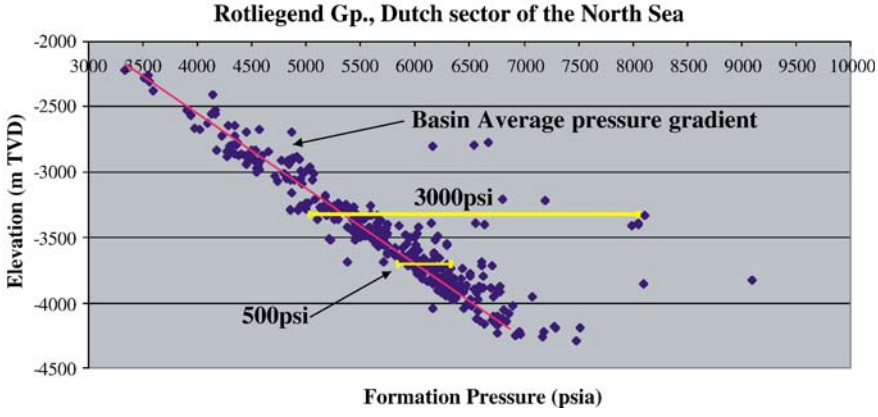

Fig. 2. Pre-production formation pressure data from the Dutch sector of the North Sea.

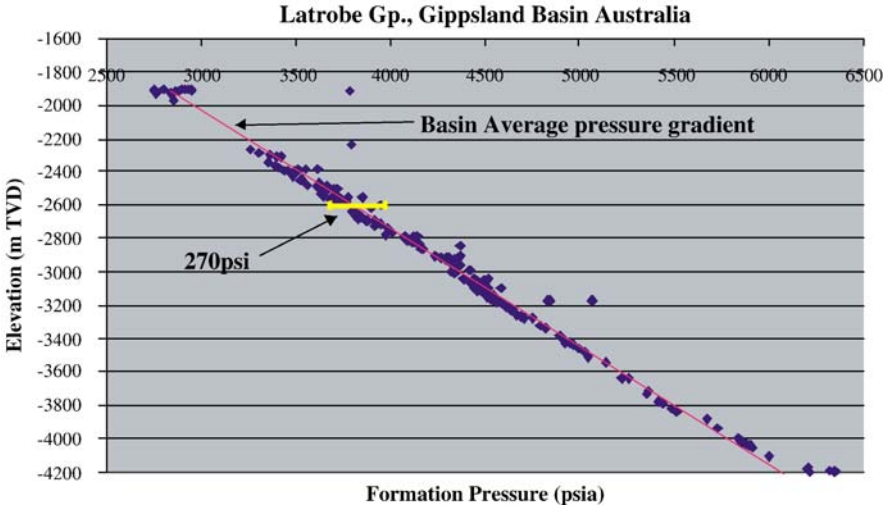

Fig. 3. Pre-production formation pressure data from the Gippsland Basin, Australia.

Latrobe Group, since the late 1960's (Hatton et al., 2004). Pressure data from the Latrobe Gp. are shown in Fig. 3. In this case, the typical range in pressure at a particular depth is about 270 psi about the average basin gradient.

The Bonaparte Basin is located on Australia's North West Shelf (Fig. 1), with production occurring mainly from Triassic and Jurassic age reservoirs. Extensive exploration has led to a large pressure database. The pre production pressure data from the Plover and equivalent strata are plotted with a basin average pressure gradient in Fig. 4. This shows the bulk of the data falling within a band of 500 psi at any given depth.

From the basin examples above, it is clear that the expected range in pre-production pressure data for a particular depth can vary substantially. All of the examples are from off-shore basins where there is little if any influence by topographically controlled flow systems. In the case of topographically controlled flow systems, even more variation could be expected. If an average pressure gradient is used to represent the static model for an aquifer that has a range in pressure for a particular depth of 270 psi (i.e. Gippsland Basin), then the dynamic model can only distinguish a pressure drop of more than 135 psi as being the result of production. Anything less, could be due to either production induced pressure depletion or simply the natural variation of pressure within the aquifer. Given the potential implications of even a 50 psi aquifer pressure drop (Table 1), characterizing the pressure of an aquifer system with an average pressure gradient is not adequate.

A better approach than using an average pressure gradient is to map the distribution of hydraulic head for individual aquifer systems. The use of hydraulic head (or fluid potential) to analyse fluid flow and pressure regimes

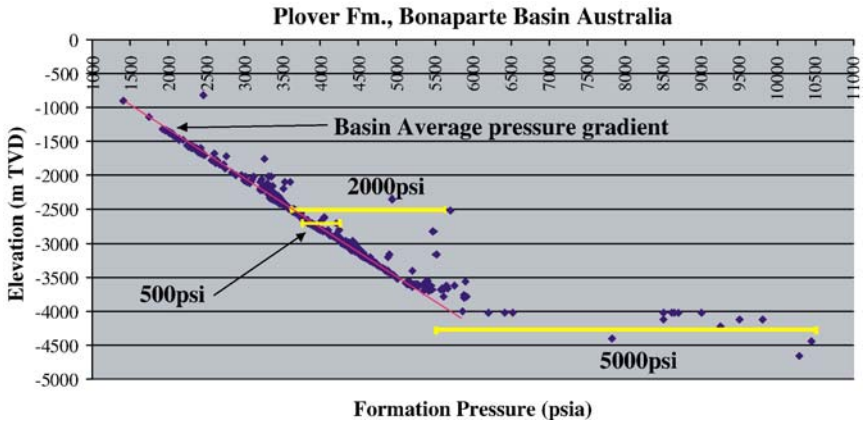

Fig. 4. Pre-production formation pressure data from the Bonaparte Basin, Australia.

has several advantages over pressure data. Perhaps the most important of these is that head values are "normalised" by depth and salinity gradients. This means that the calculated head value will automatically indicate the degree of abnormality of a pressure value without the necessity of relating it to depth first. It therefore allows direct comparison between different wells. The second advantage is that head gradients automatically indicate flow potential in any direction, for example toward a leaking fault. Thirdly, they can provide an indication of the origin of the pressure regime (boundary condition of the flow system), for example, connection to a recharge area.

Hydraulic head is calculated using the following equation:

$$H = P/(\rho g) + z$$

where H is hydraulic head (measured in meters), P is the estimated formation pressure, ρ is the fluid density, g is the gravitational constant and z is the recorder elevation. The formation water system can then be characterised with a combination of techniques including the analysis of pressure data, both in vertical profile (e.g. pressure–elevation plot), and within the plane of the aquifer after conversion to hydraulic head. Pressure data are supplemented with formation water analysis and formation temperature data to aid in the evaluation of the flow system. The above approach assumes variations in formation water density can be neglected. When formation water density variations are significant, buoyancy effects can be evaluated using the driving force ratio approach described by Bachu (1995a,b) and Bachu and Michael (2002).

For the static reservoir model, the hydraulic head can be converted to a pre-production formation pressure representative of the aquifer at that location by rearranging the hydraulic head equation to solve for formation pressure according to:

$$P = \rho g(H - Z)$$

Using this approach, an estimate of aquifer pressure can be obtained at any geographic location which captures the natural variability in the aquifer.

3.2. Post-production hydrodynamic model

The formation water flow system response to production can be predicted using numerical single phase flow simulators that solve the flow equation and express the formation pressure distributions as hydraulic head. These can include producing wells, injection wells, hydraulic communication between aquifer horizons, recharge, and discharge. This avoids the need to assume that the aquifer system has a limited pore volume, and takes account of natural inflows and outflows as well as producing or injection wells (Samani et al., 2004). The numerical modelling approach normally uses the pre-production hydrodynamic characterisation as an initial condition. If post production pressure measurements are available, these can be used to calibrate the numerical simulation. If sufficient post production pressure data are available, rather than a numerical simulation, a series of time slice maps of hydraulic head can be constructed for an aquifer and compared. A case study of the time-slice approach is discussed below.

3.3. Application to the sub-basin scale

For the problem of sub-basin scale aquifer depletion, the hydrodynamic approach can be used to reduce uncertainty in three areas of reservoir characterisation. Firstly, by using hydraulic head, there is an avoidance of the requirement to adjust measured formation pressure to a sub-basin wide elevation datum. Secondly, by characterising the potential energy distribution, the hydrodynamic approach removes the error associated with a reservoir model based on a basin average water hydrostatic gradient, since the formation pressure can be obtained at any geographic location from the hydraulic head map. Finally, the assumption that various reservoirs interact with an aquifer of fixed fluid volume does not account for natural inflows and outflows. By characterising the distribution of hydraulic head in the various aquifers, both at the pre-production time and subsequently at various times during the sub-basin production history, the natural inflow and outflows are captured and can be incorporated as part of the aquifer response to production. An example of sub-basin scale aquifer depletion where there is sufficient pressure data over time to define the potential energy distribution at different times, is the Gippsland Basin located off the southeast coast of Victoria (Fig. 1).

3.4. Data

Offshore, the only source of publicly available pressure data for the Gippsland Basin are Well Completion Reports (WCR) from oil and gas wells (normally for wells older than 2 yr). For this example, the dataset used by Hatton et al. (2004) was updated with an additional 26 wells, making a control set of 88 wells in total from the offshore area of the Gippsland Basin. The formation pressure values are comprised mainly from Wireline Formation Test (WFT) type pressure measurements. Data were entered in a relational pressure database, and have been passed through a quality control procedure called

Table 2
Statistics on pressure test data

Test type	Number of data points	% of total
DST	55	2.3
FITP	182	7.7
RFT	2131	90.0
KICK	1	0.04

PressureQC™ (Otto et al., 2000) to establish the degree of reliability for each pressure value. From the 88 wells, a total of 2369 quality-controlled pressure data points have been entered into the database (Table 2).

3.5. Pre production hydrodynamic system

In understanding sub-basin scale pressure depletion, the starting point is to characterise the range in potential energy of the system prior to production. Formation pressure data that can be used for constraining the pre production flow system fall in two categories: pressure recorded prior to any production; and, pressure recorded post production but geographically far enough away from the production that it is not affected in terms of pressure depletion. The latter category needs to be scrutinized closely. If there have been several formation pressure measurements of the same aquifer over time, and from close geographic proximity, the date at which pressure starts to decline can be identified. This will be variable for different locations within the sub-basin, with locations closer to production responding sooner than those further away. If there is insufficient pressure data over time to determine a date for initiation of pressure decline, then formation pressure values can only be used as a minimum constraint on the pre production flow system (i.e. the pre production pressure must have been at least as high as the measured formation pressure). The formation pressure values used in the pre production flow system characterisation need to be converted to hydraulic head to map the potentiometric surface.

Before making the simplifying assumption of constant density formation water, the driving force ratio (Bachu and Michael, 2002) test must be applied to ensure that buoyancy driven flow can be neglected. The formation water salinity in the Upper Latrobe Aquifer system within the study area ranges from about 10 000 mg/L along the coast line to about 50 000 mg/L near the Halibut Field (Root et al., 2004). The average salinity is about 30 000 mg/L, and when converted to in situ temperature and pressure conditions (Underschultz et al., 2002), the formation water density is 1.0 g/cc. In the case of the Offshore Gippsland Basin the DFR values are about 0.25 making the assumption of a constant

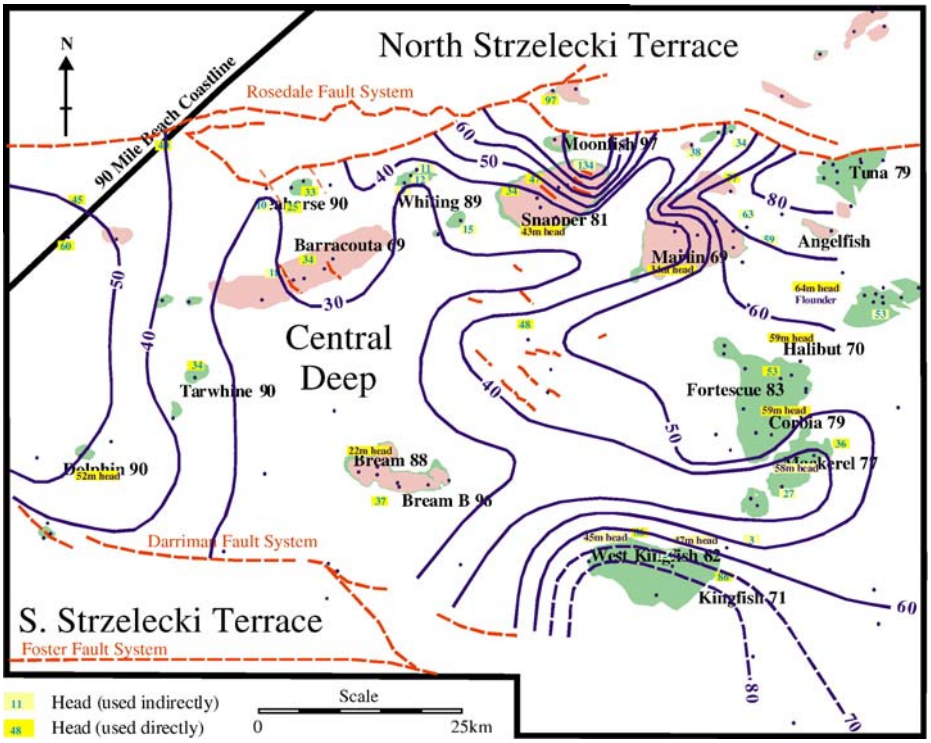

Fig. 5. Pre-Production hydraulic head distribution for the Upper Latrobe Aquifer System.

density hydraulic head valid (Bachu, 1995a,b). This may not be the case in aquifers with large salinity gradients.

The pre production distribution of hydraulic head for the Upper Latrobe Aquifer is shown in Fig. 5. The year each field began producing is indicated (e.g. Barracouta 69). Occasionally, no well pressure data is known within a pool, but only the pre-production pool pressure is known. These values were also converted to hydraulic head, and used to constrain the hydraulic head distribution. It was assumed that the pre-production pool pressure was valid at the time of the earliest well drilled for the field. In some cases there is a large time gap between field discovery and initiation of production. In these situations the quoted initial field pressure was used only at the discovery date, not for the date production actually began.

As described in Hatton et al. (2004), the virgin head distribution (Fig. 5) shows that there are competing basin-scale driving forces in the offshore Gippsland Basin. High hydraulic head extending eastwards from onshore subcrop reflects gravity driven freshwater recharge from the west. This is prominent on the western part of the Central Deep, where hydraulic head values above 50 m extend to the Dolphin Field. Compaction driven dewatering of the offshore sedimentary pile is expressed as regions of high hydraulic head (roughly those areas greater than 50 m head) in the eastern half of the study area (Fig. 5). In the central part of the Central Deep, there is a region of less than 40 m of hydraulic head that forms a sink into which the formation water flows. The sink has several interconnected "arms" of low hydraulic head, which extend to the north and east. These tend to pass between the main hydrocarbon pools. A major arm extends northwards between the Snapper and Marlin fields, and a second one extends eastwards between Fortescue and Kingfish fields. The sink appears to be connected to Darriman Fault system on the southern edge of the Central Deep (Hatton et al., 2004). It is postulated that formation water discharges up the Darriman Fault System either to an upper aquifer, or even to the seabed where it may discharge.

3.6. Mid 1980's hydrodynamic system

The distribution of hydraulic head for the Upper Latrobe Aquifer System in the mid 1980's is shown in Fig. 6. Pressure data used to control the contour distribution in this case are from wells drilled during the mid 1980's. This map shows that production from the Halibut, Fortescue, Corbia, Mackerel and Kingfish fields has resulted in a depression of the hydraulic head surface in the Upper Latrobe Aquifer. In the area of Fortescue, the depression reaches about −50 m of hydraulic head, and about −20 m at Kingfish. At this

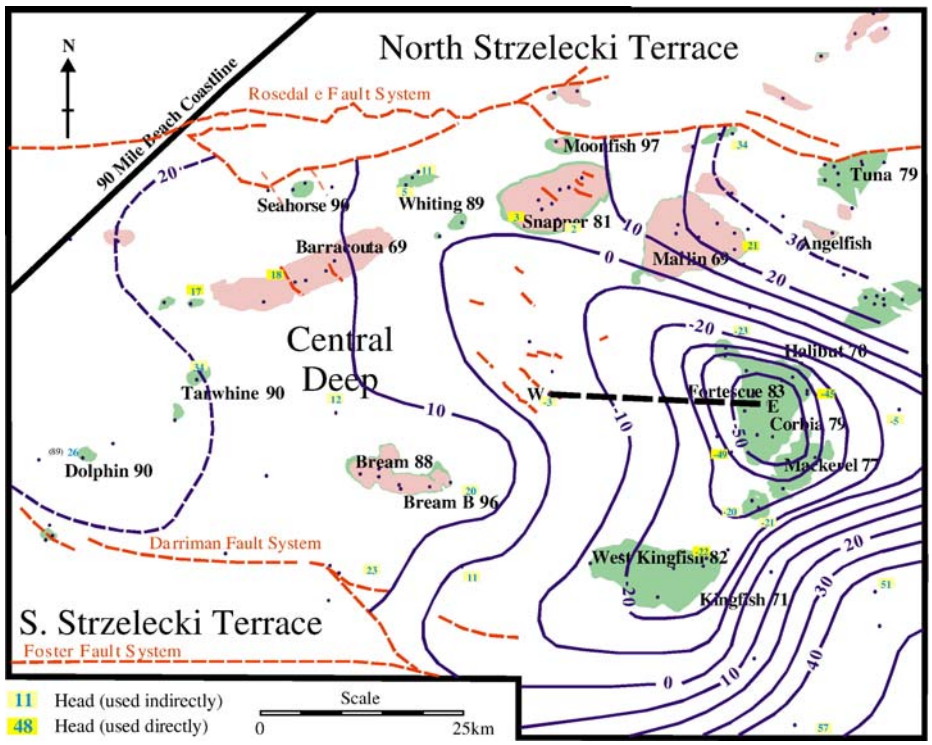

Fig. 6. Mid 1980's hydraulic head distribution for the Upper Latrobe Aquifer System.

time, the depression is somewhat localized, with the wells in the far southeast corner of the study area relatively unaffected, still having hydraulic head of more than 50 m. This is probably due to the stratigraphic architecture where individual units within the Latrobe Gp. aquifer subcrop in sequentially older units towards the southeast.

By the mid 1980's, production from the various fields has resulted in a profound change in the aquifer hydrodynamics, not just in the vicinity of the fields, but at a sub-basin scale. The impact, however, is geographically dependant. Whilst the hydraulic head along the western edge of the study area has diminished somewhat, there remains a ridge of high hydraulic head extending out to the Dolphin Field. This ridge is probably partially supported by active recharge to the aquifer system in onshore regions of the basin, where the Latrobe strata subcrop near the surface. Hatton et al. (2004) suggest that fault zone architecture and fault zone permeability may have an important role in the partial compartmentalization of production induced pressure decline. Faults may also allow hydraulic communication between the Upper Latrobe Aquifer system and adjacent aquifers. The pressure decline in the Upper Latrobe Aquifer system may induce increased vertical leakage into the Latrobe from the adjacent aquifers. These geological factors influence the aquifer response to production. It is interesting to note that the Darramin Fault discharge point previously noted for the pre-production state of the aquifer (Fig. 5), may have switched to a recharge point by the mid 1980's, with the pressure depletion at Kingfish and Fortescue causing a reversal of flow direction (Fig. 6). The hydraulic head just north of the Darramin Fault System discharge point at the Bream Field now shows a slight ridge of greater than 10 m. The resilience of a slight ridge of high hydraulic head in this region is consistent with the previous discharge region now acting as recharge to the aquifer system from shallower depths due to a reversal of the hydraulic gradient.

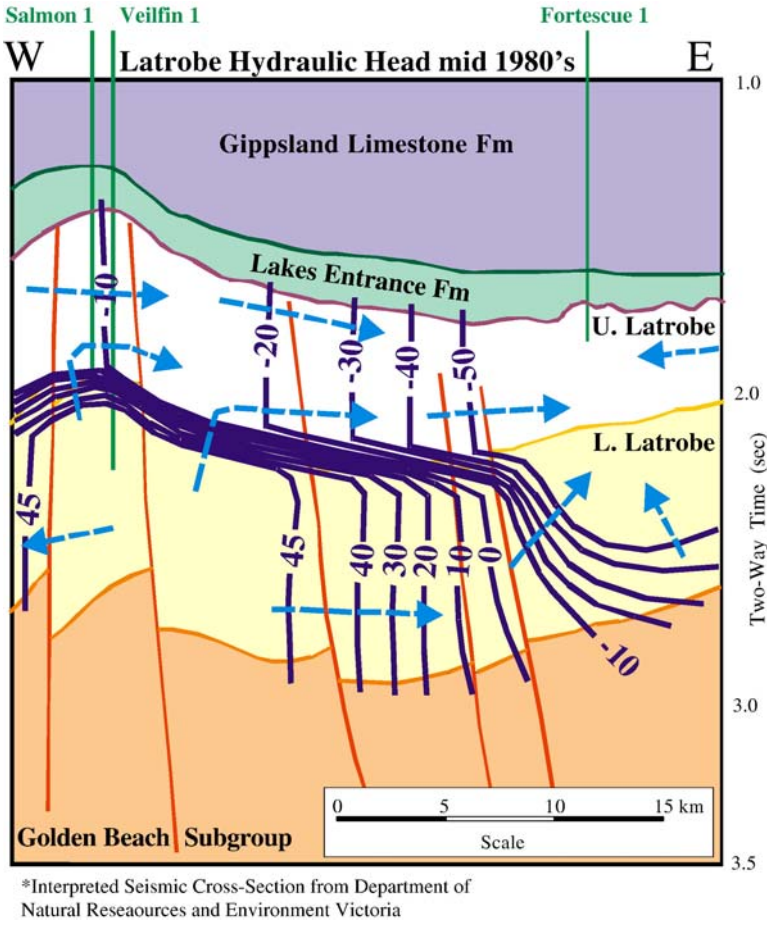

Fig. 7. Schematic cross-section of hydraulic head west from the Fortescue Field showing the Upper and Lower Latrobe Aquifer Systems in white and yellow respectively.

To test the possibility of water influx from the adjacent aquifer, pressure data was examined along a cross section between the Fortescue and Bream fields (Fig. 6) for both the pre-production time and for the mid 1980's. Data is from the upper and lower Latrobe aquifer systems, which are separated by a mudstone dominated Mid Latrobe Aquitard System (Root et al., 2004). Fig. 7 shows the hydraulic head distribution along the line of cross section for the mid 1980's. It is evident that production from the Upper Latrobe Aquifer System has a localized impact on the Lower Latrobe Aquifer System. Note that production has occurred only from the Upper Latrobe Strata. While the reduction in hydraulic head is not as pronounced in the Lower Latrobe as it is in the Upper Latrobe, there is clearly cross formational inflow of formation water from the Lower Latrobe Aquifer System induced by pressure depletion in the oil fields. If the system were to be modelled as a fixed aquifer volume for the Upper Latrobe, the cross formational flow would remain unaccounted.

4. Discussion

By linking a hydrodynamic characterisation with a reservoir engineering approach the main sources of modelling uncertainty can be reduced. These include: avoiding the need to extrapolate pressure data to a common datum; defining the pressure distribution with hydraulic head rather than using an average hydrostatic gradient for an initial condition of the aquifer system; and, characterisation of natural inflows and outflows which impact pressure support rather than assuming a fixed aquifer volume.

4.1. Pressure extrapolation

In the example of the offshore Gippsland Basin, the top of the Latrobe is shown by Gibson-Poole et al. (2004) to range between less than 1200 and greater than 2400 m below sea level. If a datum was selected at 1800 m below sea level (average depth of the top of the aquifer), pressure data from the aquifer system would need extrapolation over as much as 600 m. If a formation pressure value is known to be representing formation water but water density was not known, an uncertainty in the hydrostatic gradient of 0.2 kPa/m (0.03 psi/m) results in an uncertainty of 124 kPa (18 psi) after extrapolation across 600 m. Furthermore, if the formation fluid is unknown (eg. a DST mud recovery), then the uncertainty in the hydrostatic gradient and resulting extrapolated pressure is even greater.

With the hydrodynamic approach to characterising the Latrobe Aquifer System, formation pressure values are converted to a constant density hydraulic head. Formation pressure from an aquifer (water saturated) is converted directly to hydraulic head, while formation pressure from a hydrocarbon column is corrected down the hydrocarbon pressure gradient to the FWL, and then converted to hydraulic head. In this case, the uncertainty associated with the pressure extrapolation is limited to that incurred over the small distance to the FWL. This can be up to about 200 m or about one third the uncertainty associated with using a basin average pressure datum. Hydraulic head values are then mapped for different times during the history of production. The difference between the maps represents the drop in hydraulic head over the time period between maps, and the difference can be converted to an equivalent pressure drop at each location. This approach removes the need to extrapolate all pressure data from an entire sub-basin to a common datum elevation.

4.2. Average Hydrostatic Gradient

For the initial condition of the dynamic model the standard engineering approach characterizes the aquifer with an average hydrostatic gradient. In the example of the Gippsland Basin, the regional pressure elevation profile of all data (Fig. 3) shows a typical range in pressure values at a given depth of 270 psi, or a possible variation of 135 psi from a basin average hydrostatic gradient. This variation is in the same order of magnitude as the expected pressure depletion from production, making a pressure variation due to production indistinguishable from natural pressure variations in the aquifer. The pre-production hydraulic head distribution for the Latrobe aquifer defines the geographic distribution of the potentiometric energy for the Latrobe Aquifer (Fig. 5). With modern temperature compensated quartz gauges and for non-deviated wells, typical gauge and depth error (Veneruso et al., 1991; Sollie and Rodgers, 1994) is on the order of 30 kPa (~4.0 psi) or 3 m of hydraulic head. From the hydraulic head map, the formation pressure can be calculated at any geographic location and elevation within the aquifer. The uncertainty in the pre-production pressure predicted at any particular location is much therefore much less than the typical uncertainty (135 psi in this case) associated with the average hydrostatic gradient. The resulting distribution of pressure can be incorporated in the dynamic reservoir model rather than assuming an average aquifer pressure.

4.3. Aquifer volume

The dynamic reservoir model is normally characterized by simulating production from a reservoir that is linked to an aquifer of fixed volume. Since the reservoir volume is normally a small fraction of the aquifer volume, this

characterisation is appropriate, and the aquifer volume in combination with the permeability distribution is often adjusted to calibrate the simulation with the observed reservoir pressure decline. The concept of a fixed aquifer volume becomes problematic when simulating the sub-basin scale with multiple reservoirs, since there are natural influxes and discharges of formation water from the aquifer across its geographic distribution linked to the geological boundary conditions of the basin and the hydrologic cycle.

The Gippsland Basin case provides a good example of how geological processes such as aquifer recharge, sediment compaction and dewatering, vertical leakage between aquifers, and hydraulic communication along fault zones can contribute influxes and discharges of formation water to the aquifer at the sub-basin scale within the production lifetime of hydrocarbon fields. The slope of the potentiometric surface for the aquifer (grad$H$) is related to the specific discharge of formation water (q) through the hydraulic conductivity (K) where:

$$q = -K\,\mathrm{grad}H$$

As a further complication, the specific discharge may increase with time if production from reservoirs causes the hydraulic gradient (grad$H$) to increase. For example, in the case of the Gippsland Basin, the cross formational flow of formation water from the Lower Latrobe Aquifer System into the Upper Latrobe Aquifer System can be estimated from the vertical hydraulic gradient between the aquifers (Fig. 7) and an estimate of the hydraulic conductivity for the intervening aquitard. By mapping (or modelling) the aquifer response through time with a time series of hydraulic head distributions, the inflows and outflows of formation water for the aquifer can be estimated and incorporated in the dynamic reservoir model, eliminating the assumption of a fixed aquifer volume. For the Gippsland Basin, groundwater studies such as those by Brumley et al. (1981), Walker and Mollica (1990) and Hatton et al. (2004) estimate recharge to the Latrobe aquifer system and vertical leakage from adjacent aquifers to total on the order of 80 000 mL/yr (Hatton et al., 2004).

4.4. Integrated approach

An integrated hydrodynamic and reservoir engineering approach is advocated to reduce uncertainty in the dynamic reservoir model used at the sub-basin scale. The hydrodynamic approach can be used to characterise the initial condition of the aquifer system, and its response to production. The hydrodynamic model for the aquifer can be used to constrain the aquifer pressure through time at each field location. With the hydrodynamic characterisation as input, the dynamic reservoir model can be applied without the need for large pressure extrapolations, assumption of a basin average pressure gradient, or the assumption of a fixed volume aquifer. With reduced uncertainty in the initial condition from which aquifer depletion occurs, and a better characterisation of aquifer response to production, the confidence in reserves loss estimates should increase. The integrated approach also allows for the calculated risk of reserves loss to be geographically dependant, rather than a single risk for the entire sub-basin.

5. Conclusions

At the sub-basin scale, the standard reservoir engineering approach is inadequate for characterising regional aquifer depletion in response to long term production. In particular, the requirement of pressure extrapolation over large vertical distances to a basin wide datum, the assumption that the initial condition of the aquifer can be represented by an average pressure gradient, and the assumption that the regional aquifer responds to production as a fixed volume, lead to significant uncertainty in modelling results. If the standard approach is modified to incorporate a hydrodynamic characterisation, these uncertainties could be reduced.

6. Symbols

g	Gravitational constant
grad$H$	Hydraulic gradient
Grad P	Pressure gradient
H	Hydraulic head
K	Hydraulic conductivity
P	Formation pressure
q	Specific discharge
ρ	Formation water density
Z	Elevation TVD

Acknowledgements

The authors would like to acknowledge the helpful technical reviews of Wayne Cox and Erik Simmelink.

References

Adamson, G., Crick, M., Gane, B., Gurpinar, O., Hardiman, J., Ponting, D., 1996. Simulation throughout the life of a reservoir. Oilfield Rev. 16–27 summer 1996.

Anfort, S.J., Bachu, S., Bentley, L.R., 2001. Regional-scale hydrogeology of the Upper Devonian–Lower Cretaceous sedimentary succession, south-central Alberta Basin, Canada. AAPG Bull. 85 (4), 637–660.

Bachu, S, 1995a. Flow of variable-density formation water in deep sloping aquifers: review of methods of representation with case studies. J. Hydrol. 164, 19–38.

Bachu, S., 1995b. Synthesis and model of formation-water flow, Alberta Basin, Canada. AAPG Bull. 79, 1159–1178.

Bachu, S., Burwash, R.A., 1991. Regional-scale analysis of the geothermal regime in the Western Canada Sedimentary Basin. Geothermics 20, 387–407.

Bachu, S., Michael, K., 2002. Flow of variable-density formation water in deep sloping aquifers: minimizing the error in representation and analysis when using hydraulic-head distributions. J. Hydrol. 259, 49–65.

Bachu, S., Ramon, J.C., Villegas, M.E., Underschultz, J.R., 1995. Geothermal regime and thermal history of the Llanos Basin, Colombia. AAPG Bull. 79, 116–129.

Barson, D., Bachu, S., Esslinger, P., 2001. Flow systems in the Mannville Group in the east-central Athabasca area and implications for steam-assisted gravity drainage (SAGD) operations for in situ bitumen production. Bull. Can. Pet. Geol. 49 (3), 376–392.

Bekele, E.B., Johnson, M., Higgs, W., 2001. Numerical modelling of overpressure generation in the Barrow sub-basin, Northwest Australia. APPEA J. 41, 595–607.

Brown, A., 2003a. Improved interpretation of wireline pressure data. AAPG Bull. 87, 295–311.

Brown, A., 2003b. Capillary effects on fault-fill sealing. AAPG Bull. 87, 381–395.

Brumley, J.C., Barton, C.M., Holdgate, G.R., Reid, M.A., 1981. Regional Groundwater Investigation of the Latrobe Valley 1976–1981 SECV and Victorian Department of Minerals and Energy. December 1981 Reprinted March 1983.

Cosse, R., 1993. Basics of reservoir engineering, oil and gas field development techniques. Editions Technip, Paris and Institut Francais du Petrole, Rueil-Malmaison, 346.

Craft, B.C., Hawkins, M., 1991. In: Terry, R.E. (Ed.), Applied Petroleum Reservoir Engineering, second ed. Prentice Hall PTR, New Jersey, p. 431.

Dahlberg, E.C., 1995. Applied hydrodynamics in petroleum exploration. Springer-Verlag New York Inc, New York.

Elsharkawy, A.M., 1996. A material balance solution to estimate the initial gas in-place and predict the driving mechanism for abnormally high-pressured gas reservoirs. J. Pet. Sci. Eng. 16, 33–44.

Elsharkawy, A.M., 1998. Changes in gas and oil gravity during pressure depletion of oil reservoirs. Fuel 77 (8), 837–845.

Fanchi, J.R., 2001. Integrating forward modelling into reservoir simulation. J. Pet. Sci. Eng. 32, 11–21.

Gibson-Poole, C.M., Root, R.S., Lang, S.C., Streit, J.E., Hennig, A.L., Otto, C.J., Underschultz, J., 2004. Conducting comprehensive analyses of potential sites for geological CO_2 storage. 7th International Conference on Greenhouse Gas Control Technologies, Sept. 2004, Vancouver.

Hatton, T., Otto, C., Underschultz, J., 2004. Falling water levels in the Latrobe Aquifer, Gippsland Basin. Determination of cause and recommendations for future work.

Hennig, A.L., Underschultz, J.R., Otto, C.J., 2002. Hydrodynamic analysis of the Early Cretaceous aquifers in the Barrow sub-basin in relation to hydraulic continuity and fault seal. In: Keep, M., Moss, S.J. (Eds.), The Sedimentary Basins of Western Australia 3: Proceedings of the Petroleum Exploration Society of Australia Symposium, Perth, pp. 305–320.

Hitchon, B., Brulotte, M., 1994. Culling criteria for "standard" formation water analyses. Appl. Geochem. 9, 637–645.

Malek, R., 2004a. Barrow and Dampier aquifer depletion studies. Petroleum open day presentation, Department of Industry and Resources Western Australia.

Malek, R., 2004b. Resources branch recent activities. Petroleum in Western Australia. April. Department of Industry and Resources Western Australia, pp. 22–23.

Otto, C., Hennig, A., Underschultz, J., Roy, V., O'Brien, G., 2000. Evaluating trap integrity on the Northwest Shelf of Australia: An industry consortium on the hydrodynamics of seal breach: Hydrodynamic analysis and interpretation. Final Report.

Otto, C., Underschultz, J., Hennig, A., Roy, V., 2001. Hydrodynamic analysis of flow systems and fault seal integrity in the Northwest Shelf of Australia. APPEA J. 41, 347–365.

Root, R.S., Gibson-Poole, C.M., Lang, S.C., Streit, J.E., Underschultz, J., Ennis-King, J., 2004. Opportunities for geological storage of carbon dioxide in the offshore Gippsland Basin, SE Australia: an example from the upper Latrobe Group. PESA Eastern Australian Basins Symposium II, pp. 367–388.

Sagawa, A., Corbett, P.W.M., Davies, D.R., 2000. Pressure transient analysis of reservoirs with a high permeability lens intersected by a well bore. J. Pet. Sci. Eng. 27, 165–177.

Samani, N., Kompani-Zare, M., Barry, D.A., 2004. MODFLOW equipped with a new method for the accurate simulation of axisymmetric flow. Adv. Water Resour. 27, 31–45.

Simmelink, H.J., Underschultz, J.R., Verweij, J.M., Hennig, A., Pagnier, H.J.M., Otto, C.J., 2003. A pressure and fluid dynamic study of the Southern North Sea Basin. J. Geochem. Explor. 78–79, 187–190.

Singh, K., Fevang, O., Whitson, C.H., 2005. Depletion oil recovery for systems with widely varying initial composition. J. Pet. Sci. Eng. 46, 283–297.

Sollie, F., Rodgers, S., 1994. Towards better measurements of logging depth. Society of Professional Well Log Analysts Thirty-Fifth Annual Logging Symposium Transactions, vol. 1, pp. D1–D15.

Tóth, J., 1962. A theory of groundwater motion in small drainage basins in Central Alberta, Canada. J. Geophys. Res. 67, 4375–4387.

Underschultz, J., 2005. Pressure distribution in a reservoir affected by capillarity and hydrodynamic drive: Griffin Field, North West Shelf, Australia. Geofluids J. 5, 221–235.

Underschultz, J.R., Ellis, G.K., Hennig, A., Bekele, E., Otto, C., 2002. Estimating formation water salinity from wireline pressure data: case study in the Vulcan sub-basin. In: Keep, M., Moss, S.J. (Eds.), The Sedimentary Basins of Western Australia 3: Proceedings of the Petroleum Exploration Society of Australia Symposium, Perth, pp. 285–303.

Underschultz, J.R., Otto, C.J., Cruse, T., 2003. Hydrodynamics to assess hydrocarbon migration in faulted strata- methodology and a case study from the Northwest Shelf of Australia. J. Geochem. Explor. 78–79, 469–474.

Ursin, J.R., 2000. Fault block modelling — a material balance model for the early production forecasting from strongly compartmentalised gas reservoirs. J. Pet. Sci. Eng. 27, 179–195.

Veneruso, A.F., Erlig-Economides, C., Petijean, L., 1991. Pressure gauge specification considerations in practical well testing. 66th Annual Technical Conference and Exhibition of the Society of Petroleum Engineers. SPE Preprint, vol. 22752, pp. 865–878.

Verweij, H., 2003. Fluid flow systems analysis on geological timescales in onshore and offshore Netherlands with special reference to the Broad Fourteens basin. Doctoral Thesis Vrije Universiteit, Amsterdam. 278.

Verweij, J.M., Simmelink, H.J., 2002. Geodynamic and hydrodynamic evolution of the Broad Fourteens Basin (The Netherlands) in relation to its petroleum systems. Mar. Pet. Geol. 19, 339–359.

Villegas, M.E., Bachu, S., Ramon, J.C., Underschultz, J.R., 1994. Flow of formation waters in the Cretaceous–Miocene succession of the Llanos Basin, Columbia. AAPG Bull. 78, 1843–1862.

Walker, G., 1992. Effect of petroleum production on onshore groundwater aquifers in the Gippsland Basin. Proceedings of the Gippsland Basin Symposium, Melbourne, 22–23 June, pp. 235–242.

Walker, G., 1990. Review of the Groundwater Resources in the South East Region. A report to the Department of Water Resources Victoria. Report No. 54, Water Resource Management Report Series. March 1990, 68 pp.

Yassir, N., Otto, C.J., 1997. Hydrodynamics and fault seal assessment in the Vulcan Sub-basin, Timor Sea. APPEA J. 37, 380–389.

Geofluids (2007) 7, 148–158 doi: 10.1111/j.1468-8123.2007.00170.x

Hydrodynamics and membrane seal capacity

J. UNDERSCHULTZ
CSIRO Petroleum, Bentley, WA, Australia

ABSTRACT

The impact of hydrodynamic groundwater movement on the capacity of seals is currently in debate. There is an extensive record of publication on seals analysis and a similar history on petroleum hydrodynamics yet little work addresses the links between the two. Understanding and quantifying the effects of hydrodynamic flow has important implications for calibrating commonly used seal capacity estimation techniques. These are often based on measurements such as shale gouge, clay smear or mercury porosimitry where membrane sealing is thought to occur. For standard membrane seal analysis, seal capacity is estimated by quantifying capillary pressure-related measurements and calibrating them with a large observational database of hydrocarbon column heights and measured buoyancy pressures. The seal capacity estimation process has historically been adjusted to account for a number of different generic trapping geometries. We define the characteristics of these geometries from a hydrodynamics viewpoint in order to fine-tune the seal capacity calibration process. From theoretical analyses of several simplified trapping geometries, it can be concluded that generally, the high pressure side of the seal should be used as the water pressure gradient with which to calculate buoyancy pressure. Secondly, trap geometries where hydrocarbon is reservoired on both sides of a fault are not useful for estimating across fault seal capacity.

Key words: fault seal, hydrodynamics, seal capacity, shale gouge ratio, top seal

Received 1 June 2006; accepted 20 December 2006

Corresponding author: Jim Underschultz, CSIRO Petroleum, PO Box 1130, Bentley, WA 6102, Australia.
Email: james.underschultz@csiro.au. Tel: 61 8 6436 8747. Fax: 61 8 6436 8555

Geofluids (2007) 7, 148–158

INTRODUCTION

The effect of hydrodynamics as a driving force on the movement of hydrocarbons within carrier beds or reservoirs was described by Hubbert (1953) and has since been documented with field examples throughout the world. Methods for characterization of hydrodynamic systems in faulted strata have been described amongst others by Yassir & Otto (1997), Otto *et al.* (2001) and Underschultz *et al.* (2003, 2005a). Schowalter (1979) discussed how hydrodynamic conditions might affect secondary migration of hydrocarbon and impact on top or fault seal capacity. Little has been published since with regards to understanding hydrodynamics and seal capacity.

Seals have been classified into various types depending on the sealing mechanism (e.g. Watts 1987; Heum 1996; Bretan *et al.* 2003; Brown 2003). Commonly used terms that will be adopted in this paper are 'membrane seals' that rely on capillary processes and 'hydraulic resistance seals' that rely on low leakage rates. Top or fault seals may fail mechanically if the formation pressure below the seal exceeds the mechanical strength of the seal rock leading to fracturing or fault reactivation. It has been suggested that faults may represent membrane seals either through juxtaposition of reservoir against a seal or by the low permeability of the fault zone itself (Watts 1987). This paper will focus on understanding the seal capacity of membrane seals for both top and fault seal geometries.

Membrane seals

For a membrane seal, capillary pressure is simply the difference between the pressure in the wetting phase (normally water) and that in the non-wetting phase (normally hydrocarbon). At a sealing interface where there is a change of permeability from reservoir rock to seal rock, the non-wetting phase is trapped until the capillary entry pressure is

exceeded. The capillary entry pressure of a seal (P_{ce}) is defined by:

$$P_{ce} = \frac{2\gamma \cos \Theta}{r_t} \quad (1)$$

where γ is the interfacial tension, Θ is the contact angle of hydrocarbon and water against the solid and r_t is the radius of pore throats in the cap rock (e.g. Schowalter 1979). As such, the seal capacity is site-specific and dependent on the local fluid and rock properties. Unfortunately, these rock properties are not commonly available in standard oil field data sets. Brown (2003) describes the capillary threshold pressure (T_P) to be slightly higher than the capillary entry pressure, and the pressure at which 'a continuous thread of non-wetting fluid extends across the sample'. If a trap is filled to its seal capacity, the threshold pressure of the seal is balanced by the upwards buoyancy pressure of the hydrocarbon, leading to:

$$T_P = \Delta\rho g H \quad (2)$$

where $\Delta\rho$ is the density contrast between the formation water and the hydrocarbon, g is the gravitational constant and H is the height of the hydrocarbon column above the free water level (FWL) at the point the seal is breached. These parameters are often more readily obtained than those in Eqn (1) and T_P is more closely related to seal capacity.

Estimates of the capacity of top seals or juxtaposition fault seals can be obtained from mercury injection capillary pressure (MICP) measurements on core samples from the seal rock (e.g. Schowalter 1979; Fisher & Knipe 1998; Dewhurst *et al.* 2002; Kovack *et al.* 2004; Bailey *et al.* 2006), and estimates of fault seal capacity where the fault zone is the seal can be obtained by combining MICP with shale gouge ratio (SGR) calculations (Yielding *et al.* 1997; Bretan *et al.* 2003; Bailey *et al.* 2006). As neither of these derives all of the parameters in Eqn (1), they need to be calibrated to obtain an equivalent seal capacity value. In previous studies, hydrocarbon traps that are thought to be filled to their membrane seal capacity (i.e. traps with adequate charge, but not filled to structural spill point) have been used via Eqn (2) to calibrate seal capacity measurements (e.g. Bretan *et al.* 2003). If a demonstrable relation is established between SGR and seal capacity, for example, the SGR can be used as a predictive tool.

Equation (2) assumes that the formation water pressure relevant to understanding column height (H) is the pressure at the FWL. However, there is currently debate in the literature as to which formation water pressure value should be used, and if modification of Eqn (2) is required (Bjorkum *et al.* 1998; Clayton 1999; Rodgers 1999; Brown 2003; Teige *et al.* 2005). For the purpose of discussion here, excess pressure (ΔP) is defined as the difference between the water pressure at the FWL and the water pressure in the pores of the seal. In the case of fault seals, Brown (2003), and in the case of top seals, Clayton (1999), suggest that when moving up through the hydrocarbon column, the relative permeability of water approaches zero as water saturation drops to approach irreducible water saturation. As a result, the excess pressure between the hydrostatic gradient at the FWL and the hydrostatic gradient at the first pore of the seal must be incorporated into the threshold pressure (T_P) equation as:

$$T_P = \Delta\rho g H - \Delta P \quad (3)$$

Bjorkum *et al.* (1998) argue that in a water-wet system, there is a vertical pressure gradient between the aquifer at the FWL and the top of the reservoir, even within the irreducible water phase. If this is true, then there is only an infinitesimally small change in water pressure between the uppermost pore of the reservoir and the lowermost pore of the seal and thus excess pressure has no effect on calculated threshold pressure.

Rodgers (1999) however, pointed out that despite the assertions of Bjorkum *et al.* (1998), the permeability to the water phase at the top of the reservoir would be much less than that in the aquifer or where the water saturation is above irreducible water saturation. As such, there would be some excess pressure incurred between the formation water pressure at the FWL and the formation water pressure at the top of the reservoir (Fig. 1), and thus, an excess pressure correction is still required in calculating the threshold pressure.

Teige *et al.* (2005) conducted a laboratory experiment to test if water could migrate through oil saturated rock near irreducible water saturation. They used oil under pressure to displace water out of a core plug to what was thought to be approaching irreducible water saturation. This plug was then mounted in series with a low permeability, water-wet membrane that represented the sealing rock. A water pressure difference of 0.5 MPa was then applied across the core, which produced a measurable water flow through the oil saturated core and across the membrane. This supports the thesis of Bjorkum *et al.* (1998) that the water flow in the irreducible water zone of the hydrocarbon accumulation is small but not zero. Further, the calculated water permeability in the core plug experiment was 0.71 μD, significantly higher than the permeability of the seal required to hold back the hydrocarbon column (Teige *et al.* 2005). This suggests that the excess pressure effect described by Rodgers (1999) would be negligible because the water pressure loss in an upwards-draining system would almost all be taken up in the low permeability shale (seal).

While it may be debatable if the experiment by Teige *et al.* (2005) achieved irreducible water saturation or only something close to irreducible water saturation, it can be said that the water saturation achieved was certainly typical

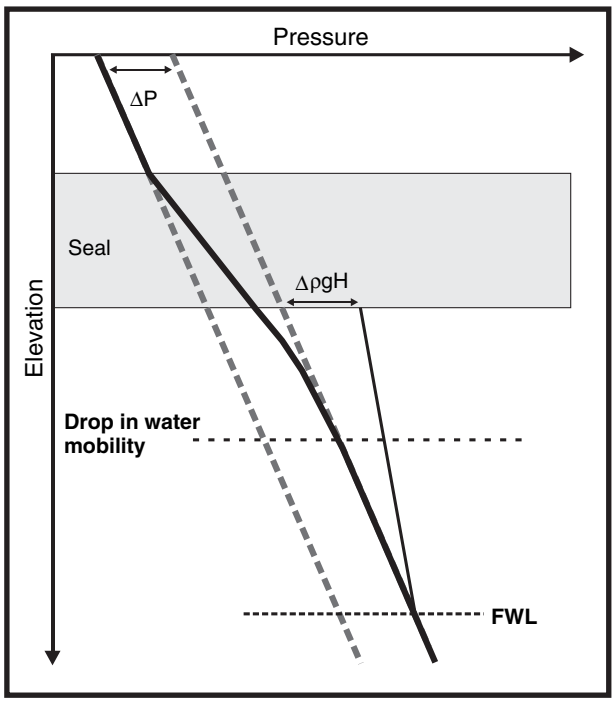

Fig. 1. Excess pressure within a hydrocarbon column (after Rodgers 1999). The drop in water mobility occurs at the top of the transition zone where the reservoir approaches irreducible water saturation. The FWL is located at the intersection of the formation water pressure gradient (thick solid line) and the hydrocarbon pressure gradient (thin solid line). The buoyancy pressure ($\Delta\rho gH$) at the top of the hydrocarbon column is calculated using the formation water pressure gradient extrapolated upwards from the FWL. The assumed excess pressure (ΔP) is the pressure difference between the hydrostatic formation water pressure gradients above and below the seal. The thick solid line is the actual formation water pressure gradient including that portion through the hydrocarbon column and seal.

of that observed near the top of hydrocarbon accumulations where water-free production occurs. Leaving the semantics of 'irreducible water saturation' aside, the experimental results of Teige *et al.* (2005) have important application to understanding membrane seal capacity in hydrocarbon reservoirs. A simple extrapolation of the published experiment by Teige *et al.* (2005) suggests that excess pressure between the FWL and the reservoir seal interface does not have a direct impact on capillary leakage and Eqn 3 is incorrect.

HYDRODYNAMICS AND MEMBRANE SEALS

The work of Bjorkum *et al.* (1998), supported by the experiment of Teige *et al.* (2005), imply that the hydrodynamic regime will not impact capillary leakage as the excess pressure term in Eqn 3 is not required. However, these papers only deal with the boundary between the uppermost pore of the reservoir and the lowermost pore of the seal. In an exploration sense, a seal has failed only if hydrocarbons have breached its entire thickness (assuming that the volume of hydrocarbon charge is not a limiting factor). In order to better predict the behaviour of petroleum systems it is worthwhile using the principles established by Bjorkum *et al.* (1998) and Teige *et al.* (2005) to re-examine the relation between hydrodynamics and membrane seals for the entire seal thickness. To do this, we consider a simple geometry of two aquifers separated by a seal. Various seal excess pressure conditions are considered along with their effect on seal capacity. We assume that the seal is of uniform permeability and that it has a particular seal capacity expressed as a hydrocarbon buoyancy pressure equal to the capillary threshold pressure. Examining a simple case allows us to understand the relative importance of various processes affecting seal capacity. In reality, both top and fault seals are heterogeneous and this adds further complications to seal capacity calibrations (e.g. Bretan & Yeilding 2005).

Excess pressure below the seal (Case 1)

Figure 2 shows a water pressure profile through a homogeneous seal with hydraulic head in the upper aquifer less than that in the lower aquifer (i.e. the case of excess pressure below the seal). As a hydrocarbon column accumulates below the seal, the hydrocarbon buoyancy pressure increases until it equals the capillary threshold. At this point hydrocarbon enters the lowermost pores of the seal. The next vertical increment in the seal will have infinitesimally less excess pressure than the lowermost pores as the formation water pressure vertically through the seal is following the pressure profile shown in Fig. 2B. This suggests that the first pores at the base of the seal are the critical part of the seals capacity and once overcome, a filament of the hydrocarbon will percolate freely and migrate across the seal. Put simply, seal thickness has no effect on seal capacity in this case. The cap rock, previously a membrane seal, becomes a hydraulic resistance seal as soon as hydrocarbon invasion commences. If we assume that any additional hydrocarbon charge is at a similar rate as leakage, the implication is that the seal will have low hydrocarbon saturation even after breach, as the hydrocarbon buoyancy pressure will never much exceed the capillary threshold pressure.

Excess pressure above the seal (Case 2)

Figure 3 shows the opposite case to Fig. 2 with higher hydraulic head in the upper aquifer. As a hydrocarbon column accumulates below the seal, the hydrocarbon buoyancy pressure increases until it equals the capillary threshold (Eqn 2). At this point hydrocarbon enters the lowermost pores of the seal. The next pores vertically within the seal will have slightly higher excess pressure than the lowermost pores as the formation water pressure through the seal is following the pressure profile shown in Fig. 3B. This suggests that the

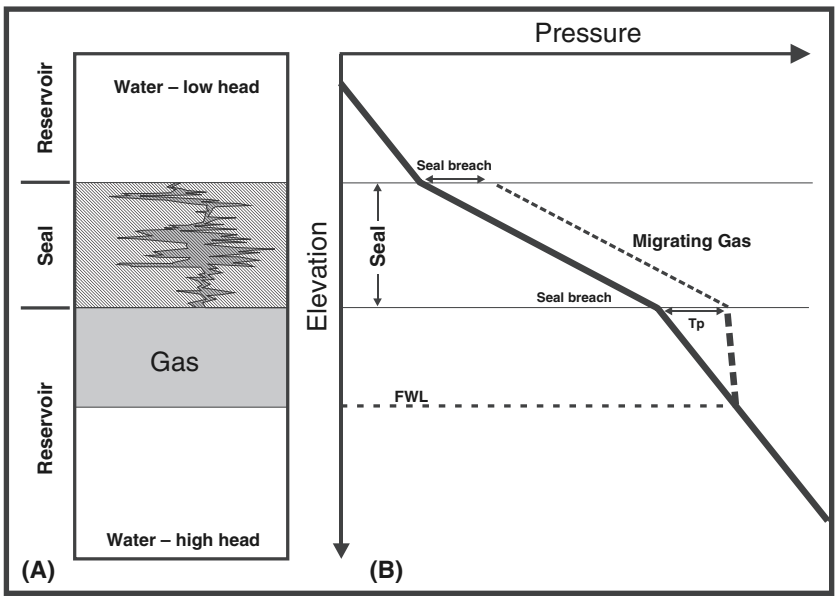

Fig. 2. Schematic diagram of Case 1 showing: (A) a model of hydrocarbon below a seal at the threshold pressure; and (B) a corresponding pressure elevation profile with excess pressure below the seal. The threshold pressure of the lowermost pores of the seal (T_P) defines the total seal capacity and is balanced by the buoyancy pressure of the hydrocarbon column.

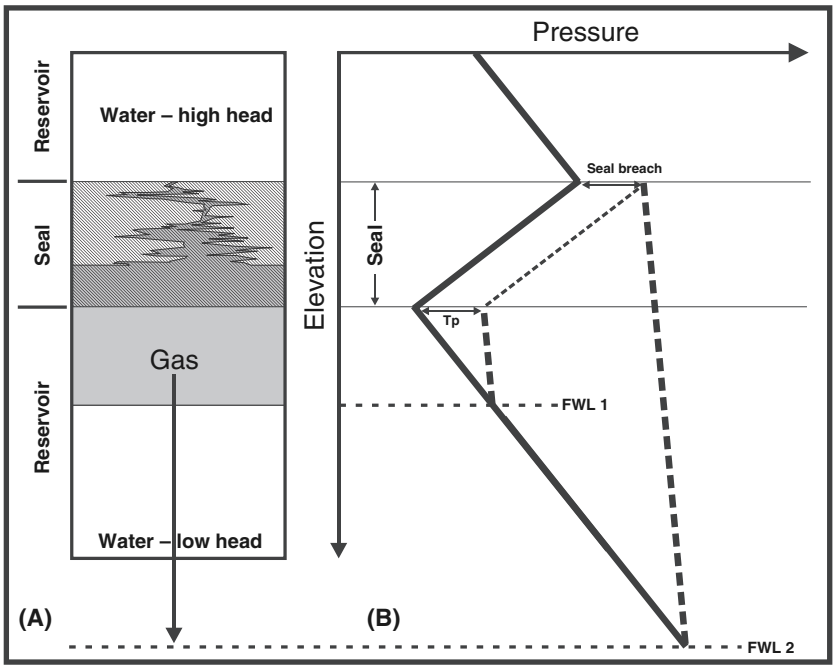

Fig. 3. Schematic diagram of Case 2 showing: (A) a model of hydrocarbon below a seal at the threshold pressure; and (B) a corresponding pressure elevation profile with excess pressure above the seal. The threshold pressure of the lowermost pores of the seal (T_P) underestimates the total seal capacity due to the water pressure profile through the seal (thick solid line). The total seal capacity is determined by the uppermost pores of the seal which is balanced by the buoyancy pressure of the hydrocarbon column defined by FWL 2.

uppermost pores at the top of the seal form the critical part of the seal defining its total membrane seal capacity.

In the case where excess pressure occurs above the seal (Fig. 3), a larger hydrocarbon column (below the base of the seal) can be held prior to complete seal breach than that expected from the threshold pressure at the base of the seal. At the point of maximum hydrocarbon column prior to seal breach, the capillary pressure in the lower part of the seal will be well above the threshold pressure for the lowermost pores of the seal. This suggests that the hydrocarbon saturation in the lower part of the seal will be more significant than Case 1, as the capillary pressure will be higher and consequently more of the pores will be invaded by the non-wetting fluid during the percolation process. Figure 3A shows schematically how the lower part of the seal may have a high hydrocarbon saturation which then decreases upwards. Underschultz & Boult (2004) describe a case study for the Gidgealpa oil field in the Cooper-Eromanga Basin of Australia where the hydrocarbon fill history is thought to have occurred in a situation analogous to our second case, that is, with overpressure in the aquifer above the sealing horizon.

Case 2 highlights a situation where standard seals analysis would attribute the observed hydrocarbon column to a buoyancy pressure calculated with the water pressure gradient from the FWL 2 (Fig. 3B). This would result in the calibration of an erroneously high seal capacity to the measured threshold pressure from MICP data. To be done correctly, the buoyancy pressure in this case should be calculated with the water pressure gradient in the aquifer above the seal.

An overpressured seal actively compacting and dewatering (Case 3)

Commonly, a seal may be actively compacting and dewatering with excess pressure build-up occurring within the low permeability sealing strata (e.g. Otto *et al.* 2001; Hennig *et al.* 2002), while near normal pressure conditions prevail in the aquifers above and below due to the relatively high hydraulic conductivity in the aquifers. In this case, the maximum excess pressure occurs in the central part of the seal (Fig. 4B), therefore a larger hydrocarbon column can be held prior to seal breach than expected from the threshold pressure at the base of the seal. At the point of maximum hydrocarbon column, the capillary pressure in the lower part of the seal will be somewhere between that in Case 1 and 2.

As with Case 2, standard seals analysis would attribute the observed hydrocarbon column to a buoyancy pressure calculated with the water pressure gradient from the FWL 2 (Fig. 4B). This would result in the calibration of an erroneously high seal capacity to the measured threshold pressure from MICP data. To be done correctly, the buoyancy pressure in this case should be calculated with the water pressure in the centre of the seal.

Excess pressure above seal to balance buoyancy pressure (Case 4)

There is a situation intermediate between Case 1 and 2, where the amount of excess pressure in the aquifer above the seal exactly balances the buoyancy pressure of the hydrocarbon column. The geometry required for this condition is shown in Fig. 5, where the hydraulic head in the upper aquifer is higher than in the lower aquifer, thus defining downwards vertical flux across the seal. The head difference across the seal is the particular condition that defines a vertical water pressure gradient within the seal exactly equal to the hydrostatic gradient of the trapped hydrocarbon.

As a hydrocarbon column accumulates below the seal, the hydrocarbon buoyancy pressure increases until it equals the capillary threshold pressure (Eqn 2). At this point hydrocarbon enters the lowermost pores of the seal. The next pores vertically in the seal will again have slightly higher excess pressure than the lowermost pore but this time the increase will be equal to the hydrocarbon hydrostatic pressure gradient, as shown in Fig. 5B. This suggests that the entire seal thickness requires the same threshold pressure at the base of the seal for it to be breached. If we assume that any additional hydrocarbon charge is at a similar rate as leakage, the implication is that the seal will have low hydrocarbon saturation even after breach, as the hydrocarbon buoyancy pressure at the base of the seal will never much exceed the capillary threshold pressure (the same as Case 1).

Case 4 marks the point at which any additional excess pressure in the aquifer above the seal will increase the seal capacity. Further, the critical hydraulic head contrast across

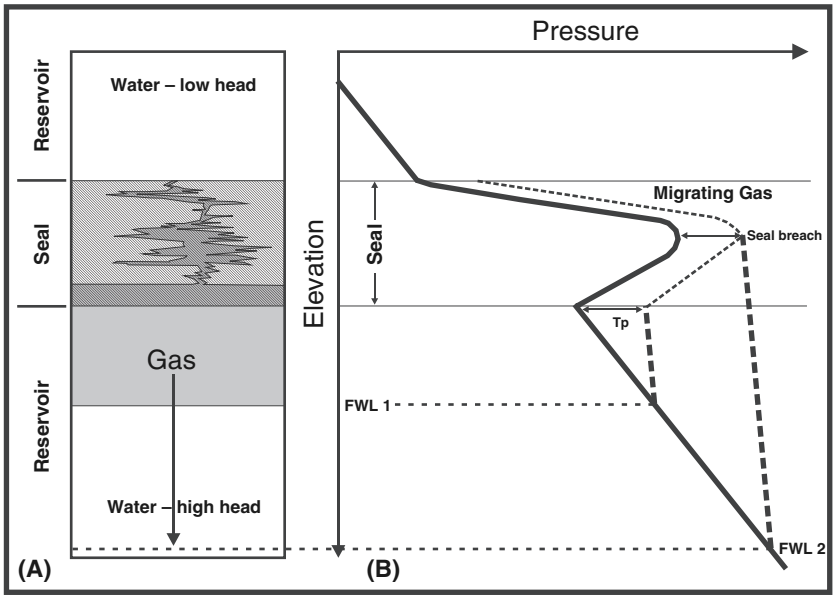

Fig. 4. Schematic diagram of Case 3 showing: (A) a model of hydrocarbon below a seal at the threshold pressure; and (B) a corresponding pressure elevation profile with excess pressure in the centre of the seal. The threshold pressure of the lowermost pores of the seal (T_P) underestimates the total seal capacity due to the water pressure profile through the seal (thick solid line). The total seal capacity is determined by the central pores of the seal which is balanced by the buoyancy pressure of the hydrocarbon column defined by FWL 2.

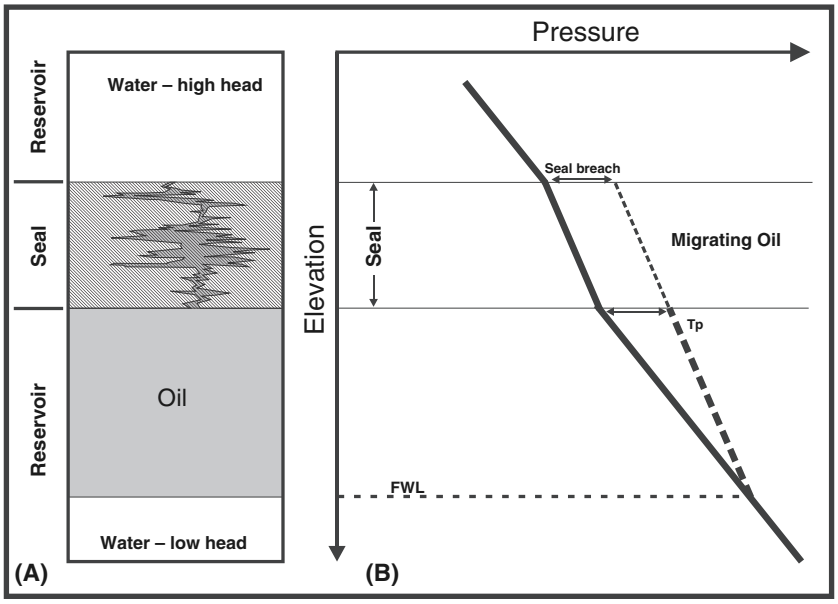

Fig. 5. Schematic diagram of Case 4 showing: (A) a model of hydrocarbon below a seal at the threshold pressure; and (B) a corresponding pressure elevation profile with excess pressure above the seal matching the critical Δh. Here the water pressure gradient through the seal (thick solid line) exactly matches the hydrocarbon hydrostatic pressure gradient (dashed line).

the seal (Δh) required to match this condition can be calculated according to:

$$\Delta h = \frac{\Delta \rho D}{\rho_w} \quad (4)$$

where $\Delta\rho$ is the density contrast between the formation water and the hydrocarbon, D is the seal thickness and ρ_w is the formation water density. Knowing this condition has application for exploration as excess pressure conditions exceeding that of Eqn (4) will enhance seal capacity. The Δh value is also important for top seal capacity calibrations as situations with seal excess pressure less than Δh have seal capacity controlled by aquifer pressure at the FWL, while situations with seal excess pressure greater than Δh have seal capacity controlled by aquifer pressure on the high pressure side of the seal. Note that the seals most affected by the head gradient effects will be the thinnest seals (small D value in Eqn 4), where the analysis of top seal risk is most critical.

Excess pressure on the hydrocarbon side of a fault seal (Case 5)

In the case of a fault seal where the aquifer on the hydrocarbon side of the fault has higher hydraulic head than the aquifer on the other side, the pressure profile can be represented by data from two wells, one on either side of the fault. Figure 6 shows a conceptual model of a faulted aquifer and the corresponding pressure-elevation plot. We assume the fault zone has low uniform isotropic permeability, there is no up-fault leakage, and the seal capacity of the fault zone is less than the top seal. For the part of the plot where the two wells are on the same side of the fault there is a small difference in the pressure gradient (Fig. 6B). This is the result of a small variation in hydraulic head between the two well locations (flow is from left to right).

The formation water flow in Fig. 6 is parallel to bedding. As the beds are shown to be dipping, it follows that there is a slight vertical component to flow recorded by a vertical well. This results in the pressure gradients defined by vertical wells having a slope slightly different from hydrostatic (shallower than hydrostatic for up-dip flow and steeper than hydrostatic for down-dip flow). To understand seal capacity, the pressure profile is required along each edge of the fault zone. In this simple example, the hydraulic head between the top and the base of the aquifer along the surface of the fault would be the same as this surface is perpendicular to the flow direction. Thus, the entire flux moves parallel to bedding and across the fault zone (arrow in Fig. 6). The thin pressure gradient lines representing the formation water pressure on either side of the fault (Fig. 6B) are parallel to the hydrostatic gradient, and at a slight angle to the pressure gradients recorded by the vertical wells. Also, the two thin pressure gradients intersect the pressure gradient from Well 2 where it crosses either side of the fault zone.

As a hydrocarbon column accumulates to the left of the fault, the hydrocarbon buoyancy pressure increases until it equals the capillary threshold of the fault rock. As the top of the reservoir has an offset across the fault, the critical leak point occurs at the highest elevation of aquifer–aquifer juxtaposition (Fig. 6A). Given that the permeability of the aquifer is much higher than the permeability of the fault zone, most of the potential energy change will occur within the fault zone. The thin solid line is the correct

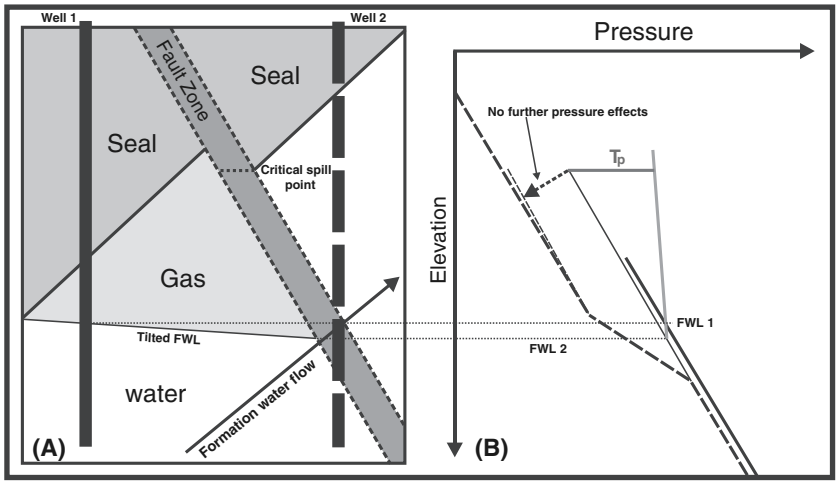

Fig. 6. Schematic diagram of Case 5 showing: (A) a fault seal geometry with two wells and up-dip flow across the fault; and (B) a corresponding pressure-elevation profile for the wells. The pressure profile for Well 1 is shown as a thick solid line while the pressure profile for Well 2 is shown as a thick dashed line. The water pressure within the fault is described by the lower part of the thick dashed line over the elevation interval where Well 2 intersects the fault. The thin dashed line represents the formation water pressure perpendicular to bedding on the right side of the fault and the thin solid line represents the formation water pressure perpendicular to bedding on the left side of the fault. The threshold pressure of the leftmost pores of the seal (T_P) defines the total seal capacity and is balanced by the buoyancy pressure of the hydrocarbon column.

water pressure gradient to use for understanding breach of the first pore of the fault seal. The thin dashed line is the correct water pressure gradient to use for understanding breach of the last pore of the fault seal.

Once hydrocarbon enters the leftmost pore of the fault seal at the elevation of the critical leak point (where buoyancy pressure equals T_P relative to the thin solid line in Fig. 6B), the next pore through the fault seal will have infinitesimally less excess pressure than the leftmost pore as the formation water pressure through the seal is following the pressure profile shown by the thick dashed line (Fig. 6B) for that portion of the well where it crosses the fault seal. This suggests that the first pore at the left of the fault seal at the critical leak point controls the fault seal capacity and once overcome, a filament of the hydrocarbon is free to migrate across the seal, and the fault zone, previously a membrane seal, becomes a hydraulic resistance seal. Also, note that the position of the FWL defined by the water pressure at the edge of the fault zone (thin solid line) is different from that at Well 1 due to a variation in hydraulic head in the aquifer at the base of the pool (i.e. a tilted FWL).

Excess pressure on the aquifer side of a fault seal (Case 6)

Figure 7 shows the opposite to Case 5, with higher aquifer pressures on the aquifer side of the fault than in the compartment containing the hydrocarbon column. With flow in the opposite direction, the relative slope between the thin and thick dashed lines is opposite to that in Fig. 6 and the direction of tilt to the FWL is correspondingly in the opposite direction. As a hydrocarbon column accumulates against the fault and top seal, the hydrocarbon buoyancy pressure increases until it equals the capillary threshold pressure of the fault seal at the top of the structure (shown by FWL 1 in Fig. 7B). At this point, hydrocarbon enters the leftmost pore of the fault seal. The next pore through the fault seal will have slightly larger excess pressure than the leftmost pore as the formation water pressure through the seal follows a pressure profile like the thick dashed line in Fig. 7B (for that part of Well 2 where it crosses the fault zone). This suggests that the last pore at the right of the fault seal at the critical leak point elevation determines the total seal capacity. The hydrocarbon column required to generate sufficiently high buoyancy pressure to balance this total seal capacity is defined by FWL 3 in Fig. 7B. By comparing Case 5 with Case 6, it can be seen that there is a significant change in the total seal capacity as the result of a difference in the excess pressure distribution across the seal. Interestingly, for Case 6 (Fig. 7) the fault zone itself would become partially saturated with hydrocarbon during the percolation process. Figure 7B shows an example of the saturated area outlined by the white line. As with Case 2 and 3, standard seals analysis would overestimate the seal capacity attributed to the measured rock properties (SGR), in this case.

Similar to the case for the top seal demonstrated in Fig. 5 (Case 4), there is one condition of excess pressure in the aquifer across the fault from the hydrocarbon where the increase in pressure across the fault zone exactly balances the hydrocarbon buoyancy pressure. It is only after this excess pressure condition is exceeded, that the seal capacity

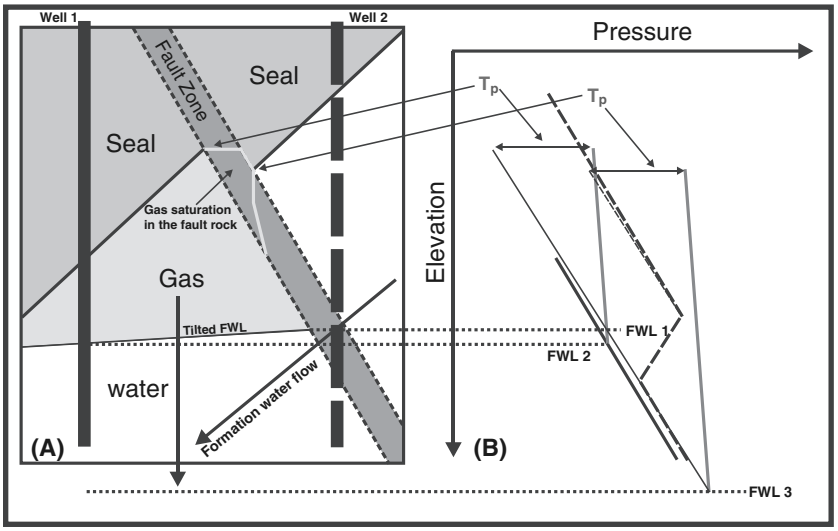

Fig. 7. Schematic diagram of Case 6 showing: (A) a fault seal geometry with two wells and down-dip flow across the fault; and (B) a corresponding pressure-elevation profile for the wells. The pressure profile for Well 1 is shown as a thick solid line while the pressure profile for Well 2 is shown as a thick dashed line. The water pressure within the fault is described by the lower part of the thick dashed line over the elevation interval where Well 2 intersects the fault. The thin dashed line represents the formation water pressure perpendicular to bedding on the right side of the fault and the thin solid line represents the formation water pressure perpendicular to bedding on the left side of the fault. The threshold pressure of the leftmost pores of the seal (T_P) underestimates the total seal capacity due to the water pressure profile through the seal (thick dashed line). The total seal capacity is determined by the rightmost pores of the seal which is balanced by the buoyancy pressure of the hydrocarbon column defined by FWL 3.

increases. In theory, the critical hydraulic head contrast (Δh) across the fault required to balance the buoyancy pressure can be calculated according to Eqn (4). In practice, the fault zone thickness (seal thickness D) will be small and thus the head contrast required to reach Δh will be negligible. Because of this, the aquifer pressure gradient on the high pressure side of the seal should always be used to calculate buoyancy pressure for seal capacity calibration.

Different free water levels across a fault zone (Cases 7–9)

Fault seal SGR calibrations are often made for situations where there is a hydrocarbon accumulation on both sides of a fault, but where the FWL on either side of the fault is different (e.g. Bretan *et al.* 2003). From a hydrodynamics point of view there are three fundamentally different pressure patterns possible on a pressure-elevation plot for this FWL geometry: (i) a single hydrocarbon pressure gradient for both sides of the fault (continuous hydrocarbon phase across the fault), but with different water pressure gradients on either side (Fig. 8, Case 7); (ii) different hydrocarbon pressure gradients on either side of the fault with different water pressure gradients (Fig. 9, Case 8); or (iii) different hydrocarbon pressure gradients on either side of the fault with the same water pressure gradient (Fig. 10, Case 9).

Case 7 has the same hydrocarbon pressure gradient on both sides of the fault (Fig. 8). This means that at some point within the fault zone there has been a breach and a continuous hydrocarbon phase now exists across the fault. Furthermore, the hydrocarbon must have reached static equilibrium (i.e. no current migration across the fault zone), and therefore, the different FWLs must be related to different hydraulic head values in the aquifer on either side of the fault (i.e. different hydrostatic gradients).

This situation is not useful for across-fault seal capacity calibration, as it is not clear at what point in the fill history the seal was breached. Therefore, the current capillary pressure of the hydrocarbon column may far exceed the threshold pressure of the fault rock. If there has been sufficient charge to fill the structure and the geometry is that shown in Fig. 8 (i.e. not filled to spill), then the control on pool size must be related to either up-fault or top seal leakage. If the up-fault or top seal leakage is controlled by membrane seal capacity then the threshold pressure could be estimated if the aquifer pressure above the seal is known. The two buoyancy pressures (one can be calculated for each side of the fault) could be estimated using the appropriate water pressure gradient and the higher of the two is the best estimate of top seal capacity.

In the situation where the hydrocarbon pressure gradient is different on either side of the fault and the hydrocarbon has reached static equilibrium (Fig. 9, Case 8), the fault core must be water saturated (i.e. the across-fault seal has not been breached and buoyancy pressure is less than the across-fault seal capacity). In this case, if there has been

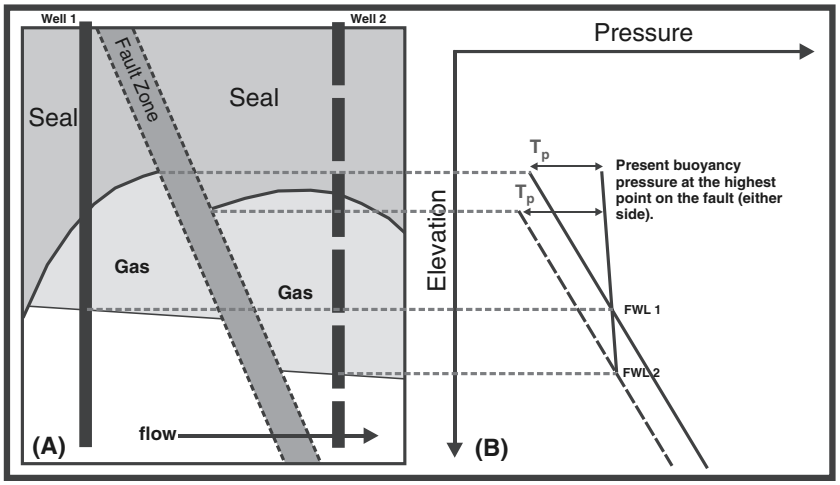

Fig. 8. Schematic diagram of Case 7 for: (A) a continuous hydrocarbon phase but different FWLs on either side of a fault; and (B) a corresponding pressure-elevation plot. The pressure profile for Well 1 is shown as a thick solid line while the pressure profile for Well 2 is shown as a thick dashed line.

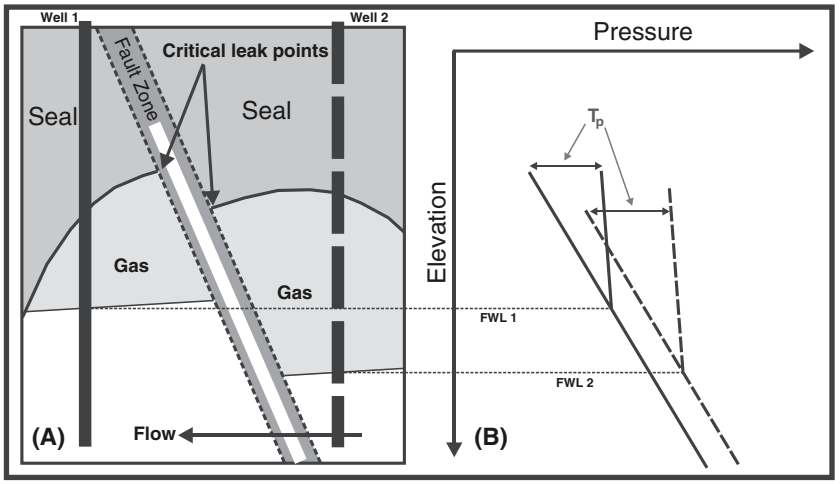

Fig. 9. Schematic diagram of Case 8 for: (A) a discontinuous hydrocarbon phase and different FWLs on either side of a fault; and (B) a corresponding pressure-elevation plot. The pressure profile for Well 1 is shown as a thick solid line while the pressure profile for Well 2 is shown as a thick dashed line.

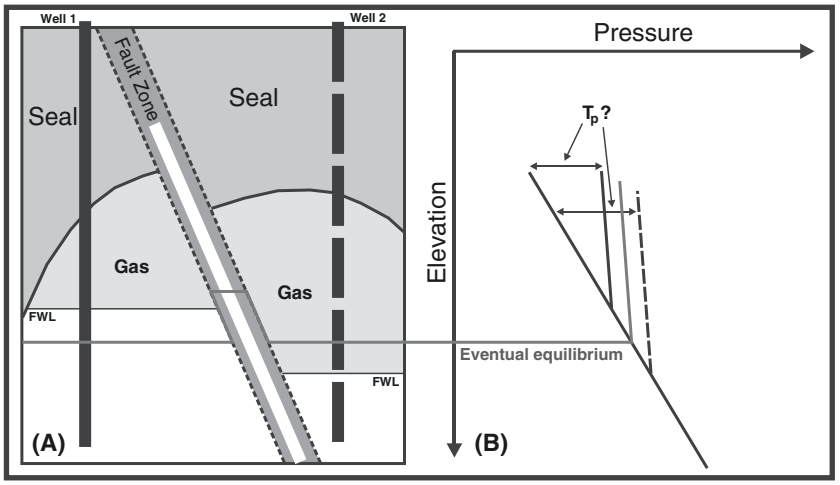

Fig. 10. Schematic diagram of Case 9 for: (A) a discontinuous hydrocarbon phase and different FWLs on either side of a fault but a constant water pressure gradient; and (B) a corresponding pressure-elevation plot. The pressure profile for Well 1 is shown as a thick solid line while the pressure profile for Well 2 is shown as a thick dashed line.

sufficient charge and the structure remains not filled to spill, leakage must be occurring either up-fault or through the top seal. If the up-fault or top seal leakage is controlled by membrane seal capacity, then the threshold pressure may be different at each side due to heterogeneities in the fault zone or top seal.

For the situation where the aquifer pressure falls on the same hydrostatic gradient for both sides of the fault,

but the FWLs are different (Fig. 10, Case 9), the hydrocarbon pressure gradients must be different and the fault zone is water saturated (Fig. 10). The difference between Case 8 and 9 is that for Case 9 the water pressure on either side of the fault is the same. This may arise if the aquifer is hydraulically connected around the fault tips (e.g. Underschultz *et al.* 2005a). Here, the fault may not have a large geographic extent. Alternatively, the fault may lose displacement and die out downwards within the aquifer below the pool.

Case 8 and 9 could alternatively be explained by a dynamic hydrocarbon phase actively migrating across the fault zone that will eventually find an equilibrium position (Fig. 10B) given sufficient time. In this situation, neither would form a useful situation for SGR calibration as breach has previously occurred and the present geometry is a transient one not related to the initial seal capacity.

DISCUSSION

From the analysis of some simple trapping geometries it can be seen that hydrocarbon pools observed to be at static equilibrium and filled to membrane seal capacity are not necessarily controlled by the threshold pressure at the reservoir–seal interface, but rather by the threshold pressure at the high water pressure side of the seal if critical hydraulic head contrast (Δh) is exceeded. This applies to both top and fault seals, but for fault seals Δh is typically negligible. Where the higher pressure side occurs on the opposite side of the seal to the hydrocarbon, a traditional approach of calculating the buoyancy pressure based on the FWL and column height will overestimate the seal capacity and result in an erroneous definition of the 'seal failure envelope' (e.g. Bretan *et al.* 2003).

None of the geometries where hydrocarbon occurs on both sides of the fault are useful for across-fault seal capacity calibration unless we have more information about how that distribution of fluids came about. Case 8 and 9 give a minimum seal capacity in that we know the across fault seal capacity has yet to be reached, but this does not further enhance a seal capacity calibration data set. If we know that the system is not charge limited and that the hydrocarbon is static (not currently migrating), these geometries can be used to infer about either up fault or top seal capacity, assuming a membrane seal exists.

The Δh value is critical for top seal capacity calibrations as situations with excess pressure less than Δh have seal capacity controlled by aquifer pressure at the FWL, while situations with excess pressure greater than Δh have seal capacity controlled by aquifer pressure on the high pressure side of the seal.

Processes unrelated to capillarity that may have an additional impact on total seal capacity include hydrodynamic trapping (Ayub & Bentsen 1999; Carruthers 2003; Bentsen 2005; Underschultz 2005b; Brown & Fisher 2006; Palananthakumar *et al.* 2006), hydraulic resistance sealing (e.g. Brown 2003) and fracture threshold pressure (Watts 1987; Lerche 1993; Clayton & Hay 1994; Bjorkum *et al.* 1998; Teige *et al.* 2005). Also, withdrawal-secondary injection hysteresis on relative permeability curves may result in variable membrane seal capacity over the fill/leakage history of a trap (e.g. Brown 2003). If any of these processes is contributing to the total seal capacity, they need to be accounted for when calibrating estimates of membrane seal capacity to observed column height.

CONCLUSIONS

When calculating buoyancy pressure to estimate membrane seal capacity the following guidelines are proposed:

1. For fault seals, the water pressure on the high pressure side of the seal should be used.
2. For top seals with seal excess pressure less than the critical hydraulic head contrast (Δh), seal capacity should be estimated using aquifer pressure at the FWL.
3. For top seals with seal excess pressure greater than the critical hydraulic head contrast (Δh), seal capacity should be estimated using the aquifer pressure on the high pressure side of the seal.
4. Trapping geometries where hydrocarbons are trapped on both sides of a fault seal cannot be used to estimate across-fault seal capacity unless details of the fill history are known.
5. Processes such as hydrodynamic trapping, seal mechanical strength, and hydraulic resistance sealing that are unrelated to capillarity but which may have a contribution to the total seal capacity, need to be considered prior to attribution the entire observed seal capacity from the hydrocarbon column height to membrane sealing.

Only with these procedures in place, can the SGR seal failure envelopes defined by a numerous buoyancy pressure measurements, and calibration of MICP data to seal capacity estimates, be more accurately constrained.

ACKNOWLEDGMENTS

I gratefully acknowledge the support of the IPETS consortium (Woodside Energy Limited, Santos, Origin Energy, Kerr-McGee Oil and Gas Corporation, Department of Primary Industry and Resources South Australia (PIRSA), Schlumberger and Chevron Australia) in funding and giving permission to publish this work. I would like to acknowledge the valuable technical input and discussions I had with Ben Clennell, Mark Brincat, Wayne Bailey and Dave Dewhurst. This manuscript has benefited greatly from the technical reviews of Quentin Fisher and Andrew Aplin.

NOMENCLATURE

D	Seal thickness
$\Delta\rho$	Density contrast between the formation water and the hydrocarbon
ρ_w	Formation water density
g	Gravitational constant
H	Height of the hydrocarbon column above the FWL
Δh	Critical hydraulic head contrast across a seal required to balance buoyancy pressure
γ	Interfacial tension
P_{ce}	Capillary entry pressure
r_t	Radii of pore throats
Θ	Contact angle of hydrocarbon and water against the solid
ΔP	Excess pressure (dierence in water pressure between that of the seal and that at the FWL)
T_P	Capillary threshold pressure

REFERENCES

Ayub M, Bentsen RG (1999) Interfacial viscous coupling: a myth or reality? *Journal of Petroleum Science and Engineering*, **23**, 13–26.

Bailey WR, Underschultz J, Dewhurst DN, Kovack G, Mildren S, Raven M (2006) Multi-disciplinary approach to fault and top seal appraisal; Pyrenees-Macedon oil and gas fields, Exmouth Sub-basin, Australian Northwest Shelf. *Marine and Petroleum Geology*, **23**, 241–59.

Bentsen RG (2005) Effect of neglecting interfacial coupling when using vertical flow experiments to determine relative permeability. *Journal of Petroleum Science and Engineering*, **48**, 81–93.

Bjorkum PA, Walderhaug O, Nadeau PH (1998) Physical constraints on hydrocarbon leakage and trapping revisited. *Petroleum Geoscience*, **43**, 237–9.

Bretan P, Yeilding G. (2005) Using buoyancy pressure profiles to assess uncertainty in fault seal calibration. In: *Evaluating Fault and Cap Rock Seals* (eds Boult P, Kaldi J). *American Association of Petroleum Geologists Hedberg Series*, **2**, 151–62.

Bretan P, Yielding G, Jones H (2003) Using calibrated shale gouge ratio to estimate hydrocarbon column heights. *American Association of Petroleum Geologists Bulletin*, **87**, 397–413.

Brown A (2003) Capillary effects on fault-fill sealing. *AAPG Bulletin*, **87**, 381–95.

Brown A, Fisher Q (2006) Detecting and evaluating hydrodynamic sealing by faults. Annual convention. *American Association of Petroleum Geologists*, **16**, p. 15.

Carruthers DJ (2003) Modeling of secondary petroleum migration using invasion percolation techniques. In: *Multidimensional Basin Modelling* (eds Duppenbecker S, Marzi R). *American Association of Petroleum Geologists Datapages Discovery Series*, 7, 21–37.

Clayton CJ (1999) Discussion: 'Physical constraints on hydrocarbon leakage and trapping revisited' by Bjørkum et al. *Petroleum Geoscience*, **5**, 99–101.

Clayton CJ Hay, SJ (1994) Gas migration mechanisms from accumulation to surface. *Bulletin of the Geological Society of Denmark*, **41**, 12–23.

Dewhurst DN, Jones RM, Raven MD (2002). Microstructural and petrophysical characterisation of Muderong Shale: application to top seal risking. *Petroleum Geoscience*, **8**, 371–83.

Fisher QJ, Knipe RJ (1998) Fault sealing processes in siliciclastic sediments. In: *Faulting, Fault Sealing and Fluid Flow in Hydrocarbon Reservoirs* (eds Jones G, Fisher QJ, Knipe RJ), *Geological Society (London) Special Publication*, **147**, 117–34.

Hennig A, Underschultz JR, Otto CJ (2002) Hydrodynamic analysis of the Early Cretaceous aquifers in the Barrow Sub-basin in relation to hydraulic continuity and fault seal. In: *The Sedimentary Basins of Western Australia 3: Proceedings of the Petroleum Exploration Society of Australia Symposium* (eds Keep M, Moss SJ), Perth, Australia, pp. 305–20.

Heum OR (1996) A fluid dynamic classification of hydrocarbon entrapment. *Petroleum Geoscience*, **2**, 145–58.

Hubbert MK (1953) Entrapment of petroleum under hydrodynamic conditions. *AAPG Bulletin*, **37**, 1954–2026.

Kovack GE, Dewhurst DN, Raven MD, Kaldi JG (2004) The influence of composition, diagenesis and compaction on the seal capacity in the Muderong Shale, Carnarvon Basin. *Australia Petroleum Production & Exploration Association Journal*, **44**, 201–21.

Lerche I (1993) Theoretical aspects of problems in basin modelling. In: *Basin Modelling: Advances and Applications* (ed. Dore AG). *Norwegian Petroleum Society Special Publication*, **3**, 35–65.

Otto CJ, Underschultz JR, Hennig AL, Roy VJ (2001) Hydrodynamic analysis of flow systems and fault seal integrity in the Northwest Shelf of Australia. *APPEA Journal*, **41**, 347–65.

Palananthakumar B, Childs C, Manzocchi T (2006) The effect of hydrodynamics on capillary seal capacity. Programme with abstracts, structurally complex reservoirs meeting. *Geological Society of London*, p. 40. January.

Rodgers S (1999) Discussion: 'Physical constraints on hydrocarbon leakage and trapping revisited' by Bjørkum et al. – further aspects. *Petroleum Geoscience*, **5**, 421–3.

Schowalter TT (1979) Mechanics of secondary hydrocarbon migration and entrapment. *American Association of Petroleum Geologists Bulletin*, **63**, 723–60.

Teige GMG, Hermanrud C, Thomas WH, Wilson OB, Bolas HMN (2005) Capillary resistance and trapping of hydrocarbons: a laboratory experiment. *Petroleum Geoscience*, **11**, 125–9.

Underschultz JR (2005b) Pressure distribution in a reservoir affected by capillarity and hydrodynamic drive: Griffin Field, North West Shelf Australia. *Geofluids Journal*, **5**, 221–35.

Underschultz JR, Boult P (2004) Top seal and reservoir continuity: hydrodynamic evaluation of the Hutton-Birkhead Reservoir, Gidgealpa Oilfield. *Eastern Australian Basins Symposium*, **2**, 473–82.

Underschultz JR, Otto CJ, Cruse T (2003) Hydrodynamics to assess hydrocarbon migration in faulted strata – methodology and a case study from the Northwest Shelf of Australia. *Journal of Geochemical Exploration*, **78–79**, 469–74.

Underschultz JR, Otto CJ, Bartlett R (2005a) Formation fluids in faulted aquifers; Examples from the foothills of Western Canada and the North West Shelf of Australia. In: *Evaluating Fault and Cap Rock Seals* (eds Boult P, Kaldi J), *American Association of Petroleum Geologists Hedberg Series*, **2**, 247–60.

Watts NL (1987) Theoretical aspects of cap-rock and fault seals for single- and two-phase hydrocarbon columns. *Marine and Petroleum Geology*, **4**, 274–307.

Yassir N, Otto CJ (1997) Hydrodynamics and fault seal assessment in the Vulcan Sub-basin, Timor Sea. *Australia Petroleum Production & Exploration Association Journal*, **37**, 380–9.

Yielding G, Freeman B, Needham DT (1997) Quantitative fault seal prediction. *American Association of Petroleum Geologists Bulletin*, **81**, 897–917.

ELSEVIER

Marine and Petroleum Geology 23 (2006) 241–259

Marine and Petroleum Geology

www.elsevier.com/locate/marpetgeo

Multi-disciplinary approach to fault and top seal appraisal; Pyrenees–Macedon oil and gas fields, Exmouth Sub-basin, Australian Northwest Shelf

Wayne R. Bailey [a,d,*], Jim Underschultz [a,d], David N. Dewhurst [a,d], Gillian Kovack [b,d,1], Scott Mildren [b,d,2], Mark Raven [c]

[a] *CSIRO Petroleum, P.O. Box 1130, Bentley WA. 6102, Australia*
[b] *Australian School of Petroleum, University of Adelaide, Australia*
[c] *CSIRO Land and Water, PMB 2, Glen Osmond, SA 5064, Australia*
[d] *Australian Petroleum Co-operative Research Centre (Seals Program), Australia*

Received 16 November 2004; received in revised form 23 August 2005; accepted 26 August 2005

Abstract

The Pyrenees–Macedon (P–M) fields in the Exmouth Sub-basin of the Northern Carnarvon Basin, Australian Northwest Shelf are currently under-filled relative to available closure despite being a regional focal point for Cretaceous to recent charge. Late structural development of the P–M trap with respect to charge was thought to be the reason for under-filling. However, seismic amplitude anomalies and gas shows above the reservoir suggest vertical leakage may have controlled column heights. Hydrodynamic analysis of pressure data also suggests that faults separating the fields act as barriers to the migration of hydrocarbons and water, whilst faults within the Macedon Field do not.

The reasons for hydrocarbon leakage and the difference in fault seal capacities are investigated by integrating field observations, analysis of pressure and stress data, the appraisal of top (mercury porosimetry measurements) and fault (Shale Gouge Ratios; SGR) membrane seal capacities, constraining geomechanical properties (top and fault seals) and well-based fracture analysis. The top seals are at a low risk of capillary failure, but vertical leakage is possible via dynamic failure along pre-existing faults and conductive fractures, and lateral leakage across reservoir against thief zone fault juxtapositions. The difference in observed fault seal capacities between different faults is explained by a combination of the spatial distributions of SGR and buoyancy pressure. The procedure presented delivers a robust description of the key risks concerning reservoir connectivity and the integrity and capacity of seals where static (geological timescale migration) and dynamic (tectonically related flow) conditions must be considered.

Keywords: Seal capacity; Seal integrity; Geomechanics; Fault seal; Top seal

1. Introduction

Evaluation of trap capacity and integrity is a critical facet of exploration risk assessment. The size of a hydrocarbon accumulation can be controlled by numerous factors and accurate risk evaluation requires identification of the most critical mechanism(s) that control(s) column heights. Retention of the initial hydrocarbon charge can be controlled by trap geometry, properties of top and fault seals (e.g. Schowalter, 1979; Watts, 1987), and other processes such as in situ alteration. Here we present an integrated work flow to investigate a well characterised hydrocarbon trap through combined application of a wide range of complementary techniques in order to better understand the controls on seal behaviour. The structure chosen contains the juxtaposed Pyrenees (oil and gas) and Macedon (gas) (P–M) fields (Mitchelmore and Smith, 1994) on the West Muiron structural high in the Northern Carnarvon Basin on the Australian Northwest Shelf (Figs. 1 and 2). The West Muiron structure is heavily faulted and compartmentalised as indicated by different free-water levels and fluid compositions. The fields are not filled to spill despite the system not being considered

* Corresponding author. Address: CSIRO Petroleum, P.O. Box 1130, Bentley WA. 6102, Australia. Tel.: +61 8 64368538; fax: +61 8 64368555
E-mail address: wayne.bailey@csiro.au (W.R. Bailey).
[1] Current address: Alberta Geological Survey, 4999 50th Ave, Edmonton, Alberta, Canada T6B 2X3.
[2] Current address: JRS Petroleum Research, 45 Woodforde Road, Magill, SA 5072, Australia.

0264-8172/$ - see front matter © 2005 Elsevier Ltd. All rights reserved.
doi:10.1016/j.marpetgeo.2005.08.004

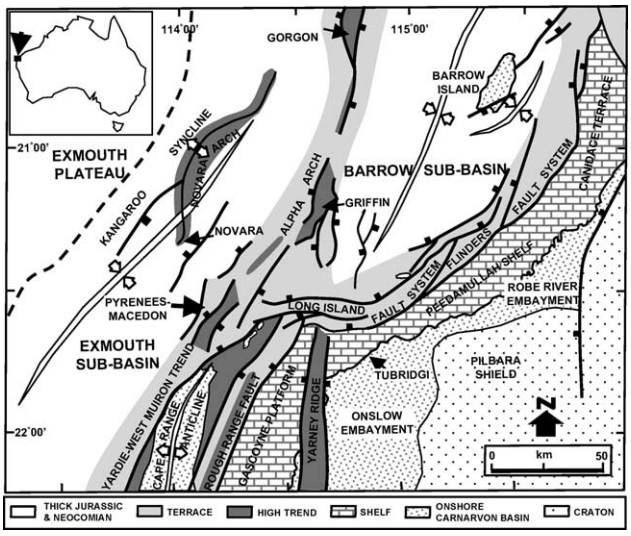

Fig. 1. Regional map for the Exmouth and Barrow Sub-basins of the Carnarvon Basin (from Mitchelmore and Smith, 1994).

charge limited and the West Muiron structure being a focal point for regional migration (Tindale et al., 1998). The presence of gas-bearing units above the regionally recognised top seal (Muderong Shale), coupled with features observed on 3D seismic and seabed surveys, suggests that some vertical leakage has occurred (Mitchelmore and Smith, 1994; Cowley and O'Brien, 2000), but the mechanisms responsible for leakage have not been clearly defined. The aim of the approach adopted here is to provide a comprehensive evaluation of the fault and top seals in terms of their geometry, capacity and integrity to deliver a basis for risking lateral and vertical leakage, and compartmentalisation.

2. Regional tectonic setting

The West Muiron structure is located in the Exmouth Sub-basin, Northern Carnarvon Basin, and comprises a broad faulted anticline overlying the NE-striking Yardie-West Muiron structural high (Fig. 1; Mitchelmore and Smith, 1994). Comprehensive descriptions of the regional geological evolution is provided by Mitchelmore and Smith (1994) and Tindale et al. (1998), but is summarised below. The area has experienced multiple tectonic events and is located at a complex structural juncture between NE- and E–W-trending basement features (Fig. 1). Late Carboniferous to Early Permian rifting and subsequent Triassic thermal subsidence resulted in the formation of a wide basin that was subsequently overprinted by a narrow basin during Early–Middle Jurassic rifting associated with deposition of the Upper Jurassic Dingo Claystone, which constitutes the main source rock for the region (Fig. 3). Extensional reactivation followed in the Late Jurassic and Early Cretaceous as Greater India separated from Australia. During this stage, Lower Cretaceous Barrow Group sediments (Fig. 3), which comprise the main reservoir units in the area, were deposited during northward progradation across the Exmouth Sub-basin. NE–SW trending syn-sedimentary

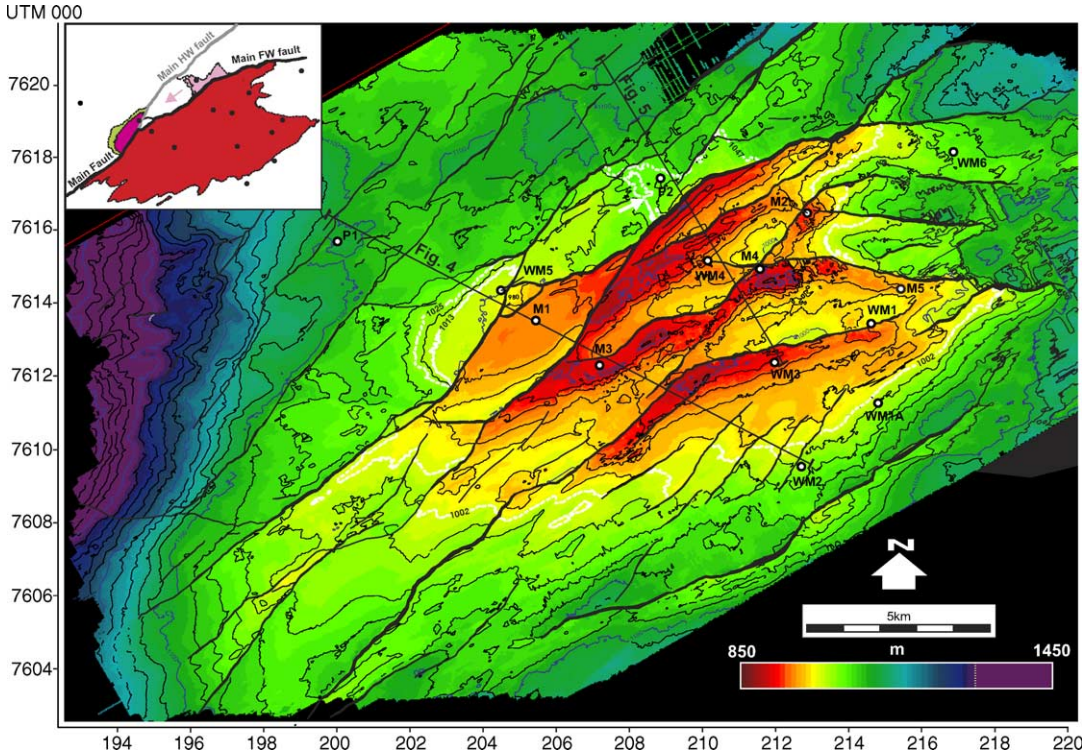

Fig. 2. Top Barrow reservoir (Base Muderong) depth structure map (20 m contours). Free water (FWL; white dashed) and free oil (FOL; white solid) levels are shown and extents of the separate hydrocarbon pools are shown in the inset: Red = Macedon gas field; dark pink and green = Pyrenees gas and oil (respectively) field; pink = Pyrenees-2 gas field. The western limit of the Pyrenee-2 accumulation is uncertain and is either bound by a structural saddle (white arrow) or may extend west (illustrated by pink arrow; inset) to the fault east of West Muiron-5.

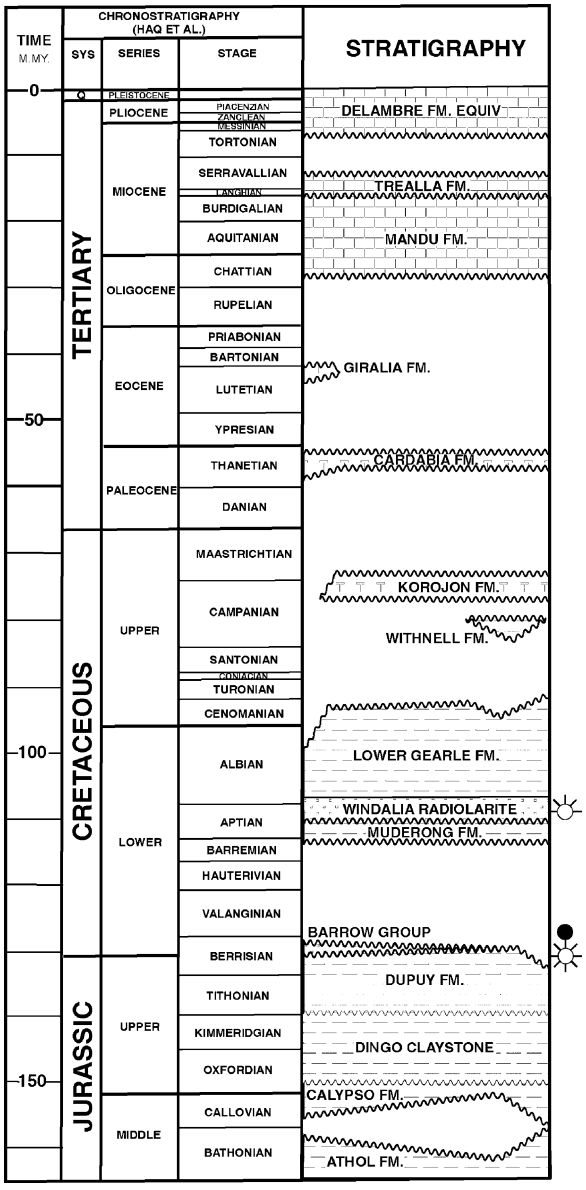

Fig. 3. (a) Stratigraphic column for P–M (from Mitchelmore and Smith, 1994).

faults transect the Barrow Group sediments, and therefore, document this rift episode. Continued separation of India from Australia in the Valanginian (Veevers, 1988) is correlated with uplift and erosion of the Barrow Group at the southern end of the West Muiron structure. The structural expression of Late Jurassic-Cretaceous rifting and uplift is a series of southerly tilted fault blocks bound by northward-dipping faults (Figs. 2, 4 and 5).

The Muderong Shale comprises the regional top seal in the Northern Carnarvon Basin, sealing the majority of discoveries (Longley et al., 2002). It was deposited during thermal relaxation in the Early Cretaceous and is overlain by the Windalia Radiolarite, a porous, but low permeability thief zone. Above the radiolarite is a thick sequence of Albian to mid-Cenomanian claystones and siltstones (Lower Gearle Formation), which were deposited in an outer shelf environment and are considered to be the effective top seal at P–M (Mitchelmore and Smith, 1994). Mild inversion is recorded in the Late Cretaceous (Santonian) resulting in uplift of the Novara Arch and N–S buckling (Fig. 1; Tindale et al., 1998). This phase at P–M is coincident with a series of E–W trending faults that hard link with the underlying NE–SW Jurassic-Cretaceous faults. The latest phase of tectonism is recorded in the Late Miocene by gross tilting of the margin to the west due to progradation of a thick Tertiary carbonate wedge and fault reactivation.

Results of 1- and 2-D maturation modelling of the Exmouth Sub-basin, reported by Tindale et al. (1998) and referred to by Scibiorski et al. (2005), suggests peak oil expulsion from the Dingo Claystone in the Early Cretaceous prior to seal deposition and trap formation at P–M. Therefore, the preferred oil charge model to P–M involves long distance migration from central and northern parts of the Sub-basin where the Dingo reached maturity later (Tindale et al., 1998; Scibiorski et al., 2005). The Pyrenees Field, as with other more recent oil discoveries to the west, is a fault-bound subcrop play beneath the Muderong seal (Scibiorski et al., 2005). In contrast, the Macedon Field relies on an anticlinal closure that formed in the Tertiary *subsequent* to peak oil generation (Mitchelmore and

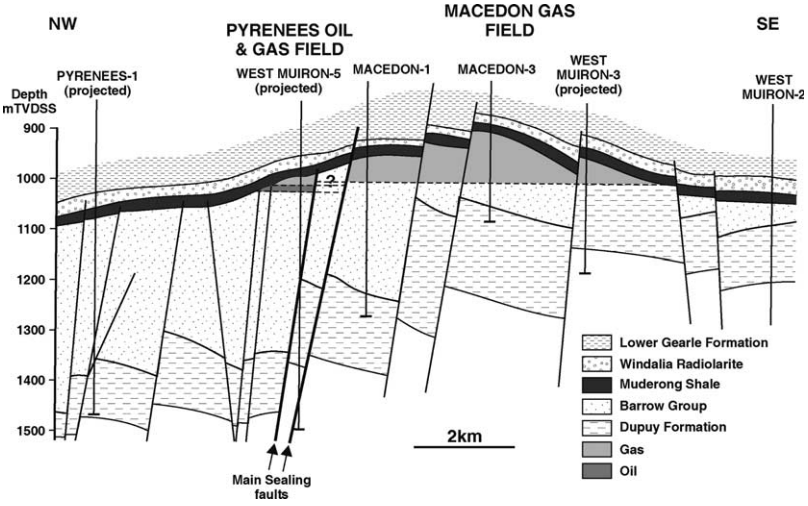

Fig. 4. Schematic cross-section through the P-M fields (modified from Mitchelmore and Smith, 1994). Position of section shown in Fig. 2.

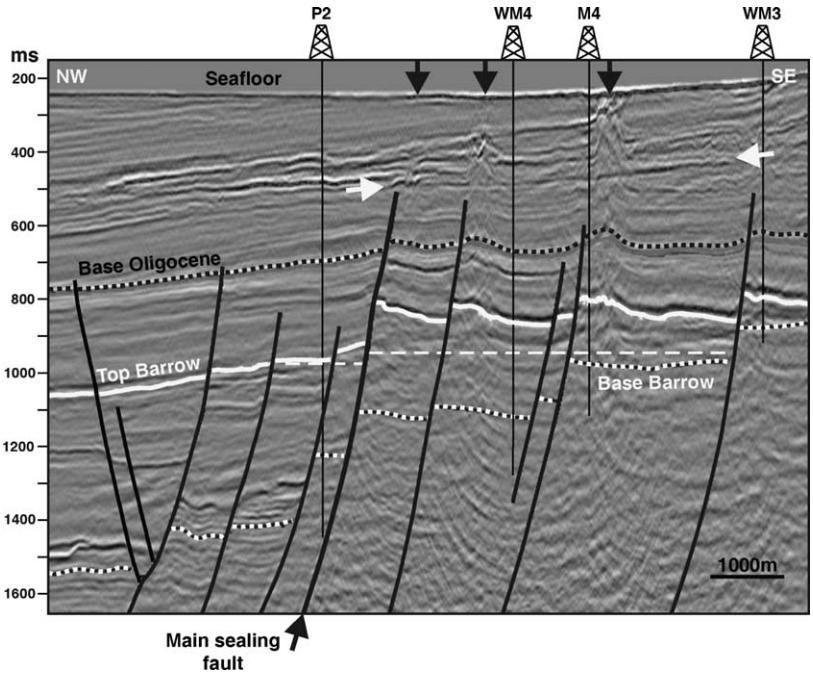

Fig. 5. Seismic section through Pyrenees-2 and Macedon gas fields (approximate positions of FWLs shown as white dashed lines). Vertical black arrows point to shallow level amplitude anomalies or 'reefs' (see text). White arrows show high amplitude reflector beneath the 'reefs'. Note the high seismic amplitudes immediately above the Top Barrow reflector interpreted as resulting from Windalia gas charge. Wells P2 = Pyrenees-2; WM4 = West Muiron-4; M4 = Macedon-4; WM3 = West Muiron-3. Position of section shown in Fig. 2.

Smith, 1994). Slow and steady gas (and minor oil) expulsion and migration from the Late Cretaceous and throughout the Tertiary coincided with regional tilting down to the east. This directed regional migration pathways towards the eastern margin of the Exmouth Sub-basin and towards P–M with gas most likely supplied from the immediate north or possibly underlying the area (Mitchelmore and Smith, 1994; Tindale et al., 1998). As a consequence, the traps are unlikely to be charge limited with respect to gas. The currently reservoired gas is dry and heavily biodegraded (Tindale et al., 1998).

3. The Pyrenees–Macedon fields

The main hydrocarbon bearing interval at P–M is the Lower Cretaceous Barrow Group (sandstones and siltstones), which is unconformably overlain by the regionally extensive Muderong and Lower Gearle Formation claystone and siltstone top seals (Fig. 4). Three main hydrocarbon compartments comprise the Pyrenees Field (oil and gas), the Macedon Field (gas) and the Pyrenees-2 (gas) accumulation (Figs. 2, 4 and 6). The Pyrenees oil and gas field tested by West Muiron-5 is characterised by a free-water level (FWL) at 1025 mTVDSS and free-oil level (FOL) at 1013 mTVDSS (Fig. 6). This accumulation is separated from the Macedon gas field (FWL at 1002 mTVDSS) to the SE by an ENE-trending fault (Figs. 2, 4 and 5). Pyrenees-2 is located on the northern side of this fault and sampled a deeper FWL at 1047 mTVDSS, thereby defining a separate gas accumulation. The FWL coincides with a structural saddle to the south-west of Pyrenees-2 (Fig. 2) and may constitute a geometric spill point controlling the size of the column (further charge would result in gas migration towards the Pyrenees Field to the SW). These three fields combine to only partially fill the available closure; the depth of the deepest closing contour, however, is outside of the area of seismic data coverage, and is therefore, unknown.

Trap compartmentalisation is also reflected in the underlying aquifer pressures. Water pressures are relatively consistent over the area with Macedon and Pyrenees-2 water legs defining a similar trend (gradient = 0.01 MPa/m; 0.1 bar/m or 1.45 psi/m; water density 1.02 g/cc; Fig. 6). In contrast, the Pyrenees Field (West Murion-5 well) water leg displays the same gradient, but pressure values are shifted approximately 0.1 MPa (14.5 psi; 1 bar) higher for a given depth than for data for the rest of the area (Fig. 6). For wells not significantly deviated, depth conversion error could be expected to be about 0.03% (Sollie and Rodgers, 1994) or about 7 kPa (1 psi), and gauge error for temperature compensated quartz gauges is about 14 kPa or 2.0 psi (Veneruso et al., 1991). The hydraulic head distribution for the aquifer at the base of the Pyrenees and Macedon fields is shown in Fig. 7. In keeping with the regional aquifer trend (Otto et al., 2001; Hennig et al., 2002; Underschultz et al., 2003), the potentiometric surface in Fig. 7 defines a hydraulic gradient and flow toward the northeast parallel to the structural grain. Despite the significant degree of faulting in the Macedon Field, the hydraulic head in the underlying aquifer is consistent at 69 m, with only a slight increase on the northern edge of the field to a maximum of 72 m recorded at West Muiron-4. A dramatic shift in hydraulic head occurs across the northern Macedon bounding fault. There is insufficient data to determine if the hydraulic head in

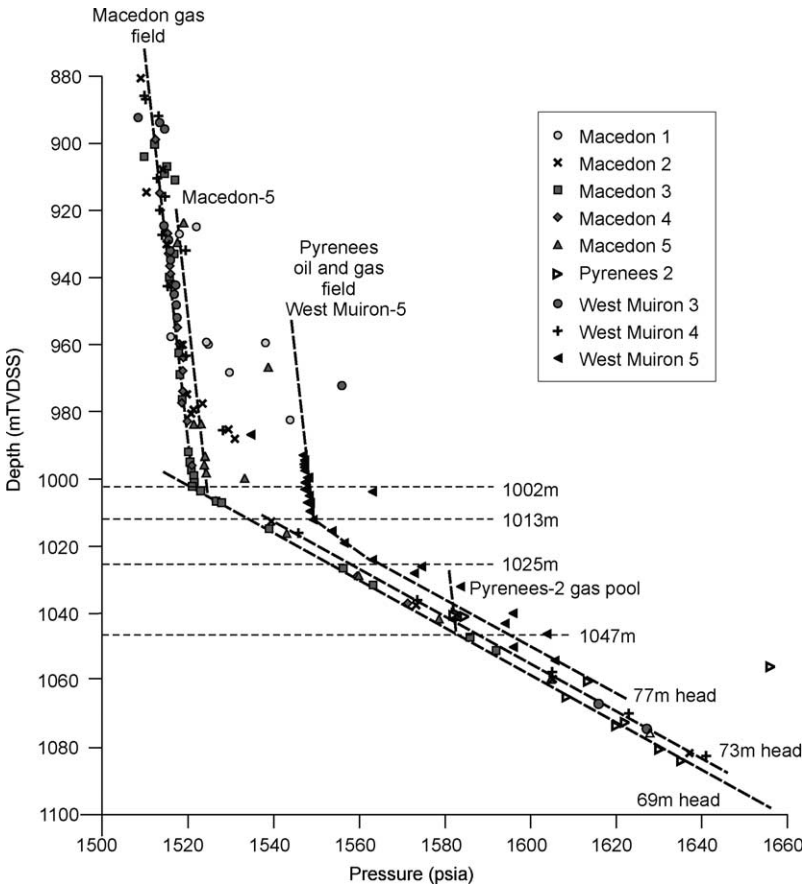

Fig. 6. Composite pressure elevation plot for the P–M fields.

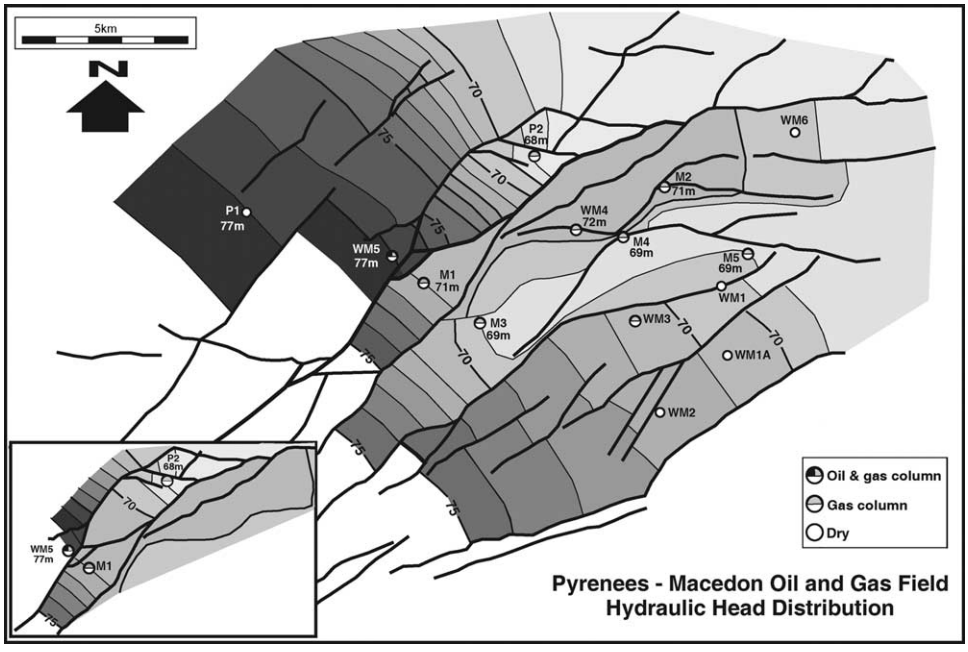

Fig. 7. Hydraulic head distribution map for the Barrow aquifer for the P–M fields. Inset shows alternative interpretation for head distribution in the compartment between Pyrenees-2 and West Muiron-5.

the Pyrenees-2 fault block is controlled by the aquifer on the Macedon Field or Pyrenees Field sides of the Macedon bounding fault, so both alternatives are shown (Fig. 7). However, the hydraulic head in the West Muiron-5 fault block (Pyrenees oil and gas field) defines a separate local flow system about 6 m higher than at the Macedon gas field to the southeast. From the regional data constraints and known reservoir characteristics of the P–M fields, it is expected that the bulk of the 6 m head difference is taken up within the fault zone. While this then defines some streamlines that cross the fault zone from the Pyrenees to the Macedon side, the flux will be small compared to that in the aquifer on either side. Thus for clarity of presentation, the fault zone is shown as a discontinuity for the potentiometric surface.

In the vertical sense, pressure data supports fluid communication between gas pools in the Barrow reservoir and overlying Windalia Radiolarite. Where available, pressure data at Windalia level (West Muiron-4 (Fig. 8) and Macedon-5) lie on the same pressure gradient as gas data from the Barrow (0.0006 MPa/m), which suggests that they define a gas-saturated interval either connected by faults or the pore network of the intervening Muderong Formation. Mitchelmore and Smith (1994) cite an absence of gas saturations in the Windalia at West Muiron-5 as evidence for the main sealing fault acting as a 'permeability barrier' between the Pyrenees and Macedon fields. However, we note that gas is documented in the Windalia at this location (BHP Petroleum, 1993) and is associated with a kick in total gas (C1) and C2 in the mudgas log.

A number of observations characterise the complexity of the current fluid and pressure distributions, which are likely to be controlled, at least in part, by variable top and fault seal properties. These include:

- Underfilling of both the Macedon and Pyrenees fields (assuming that the fields are not charge limited as suggested by published maturation and migration modelling results (Tindale et al., 1998)).
- Separation of the Pyrenees and Pyrenees-2 accumulations from the Macedon Field across the main fault, but a lack of compartmentalisation in the Macedon Field despite significant faulting.
- Evidence for shallow gas-charge.

Collectively, these observations suggest that a more comprehensive evaluation of fault and top seals is required in order to better understand the retention of hydrocarbons in this field and similar structures throughout the Carnarvon Basin.

3.1. Retention history

Whilst the observed current hydrocarbon distribution can potentially be explained by a combination of trap timing

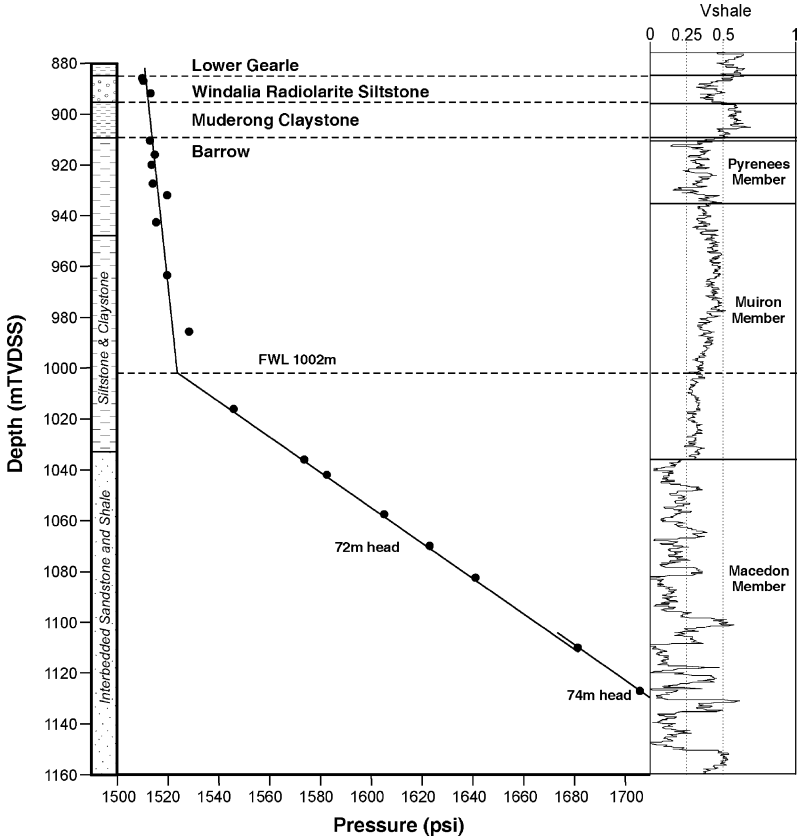

Fig. 8. Pressure-depth plot for West Muiron-4 showing pressure communication between the Barrow Group (Macedon, Muiron and Pyrenees Members) and Windalia Radiolarite.

and maturation history (oil charge pre-, and gas charge syn-post Macedon trap formation; Mitchelmore and Smith, 1994; Tindale et al., 1998), the presence of hydrocarbons above the Muderong Shale top seal does imply some component of vertical leakage (Mitchelmore and Smith, 1994). Gas shows, for example, have been widely reported in the Windalia Radiolarite (Fig. 3) overlying the Macedon Field, with faulting of the Muderong Shale assumed to be the cause of vertical leakage, and the Lower Gearle Formation claystones providing the ultimate top seal to the field (Mitchelmore and Smith, 1994). However, the mechanism(s) responsible for leakage are not proven.

In addition to gas within the Windalia, there are a variety of indicators that point to potential leakage into the shallow section above the Lower Gearle Formation. These include seismic amplitude anomalies and irregularities on the sea-bed (Mitchelmore and Smith, 1994; Cowley and O'Brien, 2000). Shallow seismic amplitude anomalies in the Tertiary section are located above and along the footwall side of the main Macedon Field faults (Figs. 5 and 9(a)). In cross-section, the anomalies appear as mounded features, characterised by internally chaotic reflectors with varying amplitudes (vertical arrows; Fig. 5), that overly a sharp, sub-horizontal high amplitude (horizontal arrows; Fig. 5) event that can be traced laterally away from the anomalies as an erosional unconformity. These characteristics are comparable to buried carbonate build-ups or reefs observed in other areas (e.g. Bailey et al., 2003) and are referred to as such ('Miocene reefs'; Trealla Formation) by BHP Petroleum (1995a). This interpretation is supported by significant drilling problems noted at Macedon-2 where the drill bit commonly dropped several metres through 'large caverns' whilst drilling this section. Degradation of the seismic quality beneath the 'reefs' allows identification of their spatial distributions on lower reflectors and demonstrates that they are parallel to the Macedon Field faults (Fig. 9). Supporting evidence for these features being related to vertical hydrocarbon migration is based on their position at the crest of the Macedon gas field, they are parallel to faults and there is a general coincidence between their distribution and the extent of the field. This spatial association has been used to suggest that the anomalies represent hydrocarbon-related diagenetic zones (HRDZs from O'Brien and Woods, 1995; Cowley and O'Brien, 2000). However, without sampling and isotope analysis of their cements, their origin remains speculative. Pockmarks and 'irregularities' (BHP Petroleum, 1995b) are noted on the seabed above the seismic 'reef' anomalies (Cowley and O'Brien, 2000), but it remains uncertain if they relate to leakage of thermogenic hydrocarbons.

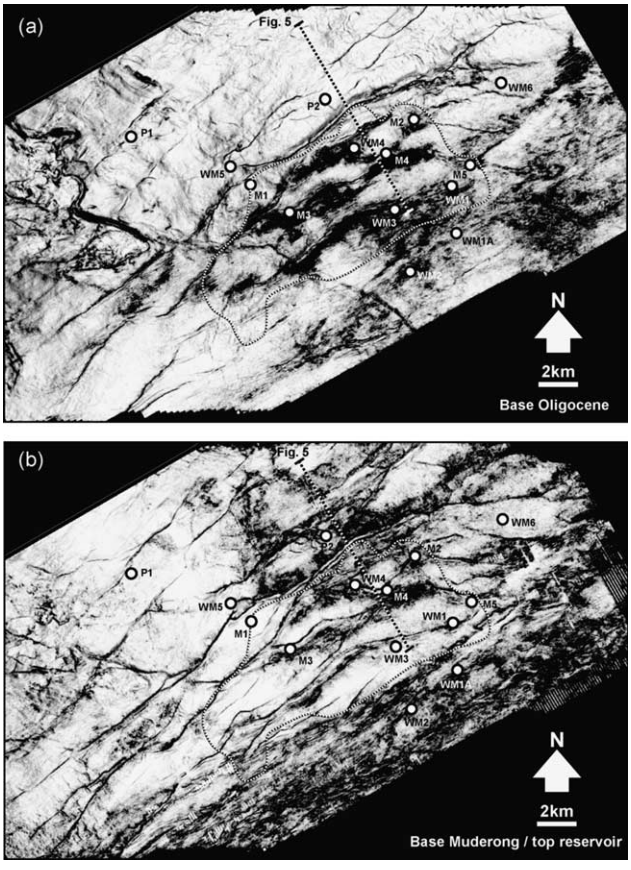

Fig. 9. Variance (coherence) maps. (a) Base Oligocene reflector (Fig. 5). Faults represented as linear discontinuities and seismic amplitude anomalies (possibly related to leakage, see text) as black amorphous patches on the FW side of Macedon field faults. Curvilinear feature in the west is a channel. (b) Top Barrow Group reflector clearly showing positions of faults (see Fig. 2). Dotted line in (a) and (b) delineates the extent of the sub-horizontal, high amplitude erosive surface underlying the 'reef' anomalies shown in Fig. 5.

4. Seal potential—introduction

Hydrocarbon seals are lithologies that halt or retard flow and can take the form of cap rocks, non-reservoir units faulted against the reservoir or fault rocks (e.g. Watts, 1987). Evaluation of the effectiveness of fault and top seals involves consideration of three principal elements: geometry, capacity and integrity (e.g. Jones and Hillis, 2003). Furthermore, investigation of the single- and multi-phase flow properties of seals in a tectonically active setting, such as the Australian Northwest Shelf, can be sub-divided into static or dynamic cases. Seals in a *static* environment (fluid migration takes place over long (geological) timescales) can take the form of hydraulic or membrane seals. Hydraulic seals are those that possess capillary threshold pressures so high that they fracture before capillary failure. Membrane seals exist where the capillary threshold pressure for the seal is high enough to withstand the buoyancy pressure exerted by a hydrocarbon column, but would eventually leak if buoyancy pressures reach a threshold level (Smith, 1966; 1980; Downey, 1984). Fault membrane seals are either 'juxtaposition seals' where reservoir units are juxtaposed against tight, non-reservoir units or 'fault rock seals' where the fault rock petrophysical properties control the column height. In a *dynamic* environment, rapidly changing properties of seals can facilitate flow. For example, fault reactivation may result in the re-distribution of large volumes of fluid over a seismic–inter-seismic cycle (e.g. Sibson et al., 1975). The mechanisms associated with dynamic failure and fluid flow resulting from seismic faulting are poorly

understood and could be related to faulting/fracturing of a top seal or fault rock and channelling flow up or across the main fault zones.

4.1. Seal geometry

The West Muiron structure is a broad faulted anticline that relies on top and fault seal elements to provide valid traps. General characteristics of top seal and reservoir connectivity can be understood by consideration of the relative size distribution of faults and sedimentary bodies (e.g. Bailey et al., 2002). Stratigraphic intervals thicker than the maximum fault displacement cannot be completely offset by faulting. For a fault to completely offset a stratigraphic interval it must be more laterally extensive than the interval, and possess displacements along the length of offset greater than the interval thickness. The Barrow Group reservoir is of variable thickness (40 m at West Murion-3 to 550 m at Pyrenees-2) over the West Muiron structure due to a combination of growth faulting and footwall erosion (Fig. 4). The overlying Muderong Shale (top seal) and Windalia Radiolarite (thief zone), on the other hand, possess relatively uniform thicknesses of approximately 20 and 18 m, respectively. The shallower Lower Gearle (top seal) Formation is much thicker, generally varying between 100 and 140 m. These details constrain the following guidelines:

- Throws less than 40 m will result in areas of Barrow reservoir self-juxtaposition.
- Throws between 20 and 40 m will offset the Muderong top seal and juxtapose the Barrow Group against the Windalia Radiolarite (thief zone).
- Throws greater than 40 m will result in Barrow-Lower Gearle juxtaposition seals.
- Throws greater than 100 m are required to completely offset the Lower Gearle top seal.

Areas of Barrow self-juxtaposition and Barrow-Windalia juxtaposition are potential across-fault hydrocarbon migration pathways, but leakage will only occur if the intervening fault rocks have suitable two-phase flow properties (appraised below). Clearly, the above geometric guidelines are a simplification and faults are complex zones along which displacements vary considerably and different areas of the fault will display different juxtaposition relationships.

Maximum displacement and trace length data for all seismically resolvable faults are shown in Fig. 10. The majority of Macedon Field faults have maximum displacements greater than 20 m at Top Barrow level and thus widespread potential Windalia-Barrow juxtaposition leak windows are anticipated. These faults typically have lengths shorter than the (NE-) strike dimension of the field (ca. 10 km). This has the result of most faults linking with others along high-angle branch-lines, some at displacement lows, whilst a few faults tip out within the extent of the field. In combination, these geometries and maximum displacements mean that throws less than 20 m are likely to be widespread, allowing

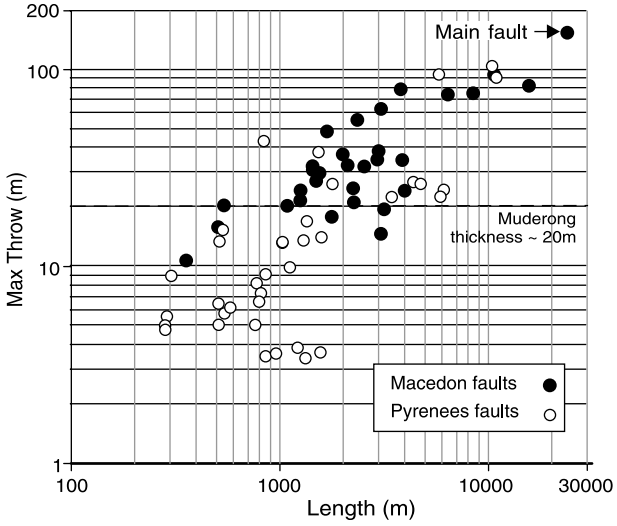

Fig. 10. Maximum throw-trace length plot for all faults at Top Barrow level. All throws above the horizontal dashed line will offset the ca. 20 m thick Muderong Shale. The main fault (FW segment) is labelled.

Barrow self-juxtaposition and favouring good connectivity, which is supported by the hydrodynamic assessment of the field (Figs. 6 and 7). Visual inspection of Fig. 2 corroborates this assumption and shows that most of the Macedon wells can be connected to one another, albeit by a tortuous path, through displacement lows associated with branch-lines and around fault tips. The compartment sampled by Macedon-2, however, is the only well that is not easily connected to another compartment and its communication with the rest of the field relies on the petrophysical properties of the intervening fault rocks.

The main difference between the main sealing fault that separates the Macedon Field from the Pyrenees and Pyrenees-2 accumulations compared to the intra-Macedon Field faults is that it is demonstrably larger in terms of both length and displacement at both top and base reservoir levels (Fig. 10). The large displacements along the main fault (typically >60 m at Top Barrow level) cause reservoir in the footwall to be juxtaposed against hangingwall shales (Muderong and Lower Gearle Formations) over the majority of its area; thereby creating an effective juxtaposition seal. This explains the separation of the Macedon Field from the Pyrenees-2 gas accumulation. However, the main intervening fault between the Pyrenees (oil and gas) and Macedon (gas) fields locally displays low displacements (<40 m), caused by it branching into two segments (Fig. 2), resulting in reservoir self-juxtaposition and Barrow-Windalia juxtapositions. The sealing character of this fault, therefore, must (at least in part) be controlled by the petrophysical properties of the fault rocks. Here, the southern ENE-striking branch (herein referred to as the footwall (FW) segment) is the dominant fault at top Barrow (black fault, inset, Fig. 2), but the northern, NE-striking branch (hangingwall (HW) segment), is dominant at base Barrow level (grey fault, inset, Fig. 2). Near the sub-vertical branch-line, the HW fault displacement at top Barrow is as low as 10 m and the FW (southern) fault displacement as low as 20 m; both of

which result in reservoir self-juxtaposition. However, displacements at this locality are poorly constrained because of significant erosion of the top reservoir level, as demonstrated by the absence of the uppermost Barrow Group (Pyrenees Member) in the footwall at Macedon-1. Synchronous erosion and syn-sedimentary faulting results in an incomplete displacement record at the top of the reservoir. This is exacerbated at this locality by poor seismic expression of the faults at top Barrow level. Therefore, the displacements recorded at this level are an underestimate. The absence of continuous reflectors within the Barrow precludes a more accurate estimate of syn-sedimentary displacements. Nevertheless, accurate mapping of the fault structure is possible using top and base Barrow reflectors and minor discontinuous intra-Barrow reflectors. Projection of the stratigraphy from West Muiron-5 and Macedon-1 allows across-fault stratigraphic juxtaposition geometries to be mapped.

Importantly, none of the mapped faults above the reservoir have throws greater than the 100 m required to completely offset the Lower Gearle top seal, confirming this unit as an effective juxtaposition seal if capillary threshold pressures are consistently high. In contrast, widespread offset of the Muderong Shale results in common Barrow-Windalia juxtapositions and produces numerous potential leak windows that could allow across-fault migration of hydrocarbons out of the main reservoir and into the thief zone if the bounding fault rocks possess sufficiently low capillary threshold pressures. Overall, top seal geometry is confirmed (for the Lower Gearle Formation), but the capacity of both the top and fault seals need to be evaluated further.

4.2. Seal capacity

The capacity of top and fault seals reflects the capillary nature of material opposing hydrocarbon flow. For top seals, the capillary entry pressure is typically recorded using Mercury Injection Capillary Pressure (MICP) measurements on representative samples. Capillary properties of fault rocks can also be measured in this manner, but no fault rock samples are available. Therefore, the seal capacity of fault rocks can be estimated using well-described algorithms (e.g. Bouvier et al., 1989; Yielding et al., 1997).

4.2.1. Top seal composition and capacity

Capillary failure of the Muderong Shale top seal will occur if the buoyancy pressure exerted by the underlying hydrocarbon column exceeds the threshold pressure of the seal. Capillary properties of top seals can be determined from MICP data, although sample representativeness can be a limitation of this approach (Downey, 1984). This risk can be reduced if samples are characterized mineralogically, demonstrating uniform composition for example, or where variations can be linked to wireline log response. In this study, the composition of samples of Muderong Shale taken from Macedon-5 and West Muiron-5 (Fig. 2) has been determined by XRD analyses. Distinct compositional differences (Table 1) are noted between shale samples taken from these two wells, which are located on either side of the main sealing fault. Whole rock illite–smectite (I–S) content in Macedon-5 is ~35%, with a low kaolinite (5–10%) content. In the two shale samples from West Muiron-5, the whole rock mixed layer I–S content is much lower (10–14%) than that seen at Macedon-5, but the kaolinite content is much higher (36–44%). Quartz is the other dominant mineral present at ~30%. The composition of the mixed layer I–S in Macedon-5 is ~$Sm_{80}I_{20}$, while that in West Muiron-5 is ~$I_{80}Sm_{20}$. Collectively, these analyses define significant variations in seal rock composition, particularly with respect to clay mineral types. These differences are likely to influence both the capillary seal properties as well as the geomechanical properties of the top seals (Dewhurst et al., 2004) and potentially also the fault rocks.

Table 1
Grain size (<2 μm fraction), composition (% illite-smectite, kaolinite, quartz), capillary threshold pressure (*P*th) and seal capacity to gas (Col. height) for samples of Muderong Shale from West Muiron-5 and Macedon-5 wells

Sample location: (depth mTVDSS)	<2 μm	% I–S	% Kao	% Qz	*P*th (MPa)	Col. height (m)
WM5-1018	50%	10	44	28	16.9	290
WM5-1010	47%	14	35	29	9.75	168
Macedon-5 (973–979)	51%	35	10	18	4.83	87
Macedon-5 (967–973)	46%	33	5	35	24.4	441

Muderong Shale used in this study was recovered from core samples in West Muiron-5 and from cuttings in Macedon-5. Cores generally give the most reliable results as cuttings generally underestimate threshold pressures (Sneider et al., 1997). Seal capacity was interpreted from mercury porosimetry data converted to appropriate reservoir fluids and conditions using the methods outlined by Schowalter (1979), although interfacial tensions were determined from more recent data of Firoozabadi and Ramey (1988). Full details of XRD and MICP experimental procedures are contained in Dewhurst et al. (2002a,b).

The Muderong Shale from West Muiron-5 has high air-mercury entry pressures, ranging from ~9.75 to 16.9 MPa. Threshold pressures determined on the Macedon-5 cuttings samples are distinctly different. Macedon-5 (967–973 mTVDSS) has a threshold pressure of 24.4 MPa, whereas samples from 948 to 954 mTVDSS have a threshold pressure of 4.83 MPa. As the whole rock mineralogy of the two Macedon samples are very similar (948–954 mTVDSS has slightly more clay), it is likely that the low value is erroneous due to factors such as improper preservation of the cuttings samples, cracking, drilling mud contamination and small sample size. A large conformance was noted for this sample, which also indicates that sample damage is likely. Hence, the higher value here is believed to be more representative of the Muderong Shale. These values of air-mercury threshold pressure are also consistent with basin-wide data from Kovack et al. (2004), which indicate that the Muderong Shale is a good capillary top seal, despite considerable regional variation in seal capacity.

Additionally, the majority of Northern Carnarvon Basin discoveries are located sub-Muderong, suggesting it is a good capillary seal. Laboratory air/mercury pressures may be converted to the brine/hydrocarbon system allowing seal capacity and column heights to be reflective of reservoir pressure-temperature conditions (see Schowalter, 1979; Watts, 1987). Apart from one sample, the seal capacities to gas for both Macedon-5 and West Muiron-5 are in excess of 150 m, which essentially signifies little risk of capillary breakthrough in these areas. One sample (Macedon-5 973–979 mTVDSS) has a lower seal capacity of 87 m, most likely the result of poor sample preservation rather than any geological differences. The column height estimates for Macedon-5 should be regarded as minimum in situ static values, in that they are, in general, taken from cuttings, which almost always underestimate seal capacity. The 'static' condition is also important, as the values estimated are for present day conditions. Charge may have occurred under different conditions in the past when seal capacity may have been different. Estimating these effects, however, is beyond the scope of this paper. Current top seal capacity to both gas and oil are in excess of the columns found in the fields at the present day (maximum of 102 m at Macedon-5), indicating that top seal capillary failure is unlikely to be the cause of the observed leakage indicators at this field.

4.2.2. Fault seal capacity

At P–M, juxtaposition analysis presented earlier indicates that fault membrane seals are likely to play an important role in controlling the distribution of fluid types, contacts and pressures, and therefore, estimation of fault rock properties is required. Critical areas along fault surfaces are identified where detailed across-fault juxtaposition mapping and fault rock capacity calculations are required, and include:

- Juxtapositions of the Macedon Field against the Pyrenees and Pyrenees-2 hydrocarbon accumulations along the main fault(s) to explain why they form seals.
- Barrow self-juxtapositions along Macedon Field faults to explain the good reservoir communication determined from the hydrodynamic assessment.
- Barrow-Windalia juxtapositions in the Macedon Field to evaluate if they are likely to provide leak windows, thus explaining Windalia gas charge.

For across-fault leakage to occur at these juxtapositions, the hydrocarbon column(s) in contact with the fault must exert buoyancy pressures that exceed the capillary threshold pressure of the fault rock. Therefore, to appraise the seal capacities of the faults, an understanding of the likely fault rock properties and the pressure conditions is required.

4.2.2.1. Fault shale gouge ratio calculations. To estimate likely seal capacity of the faults that possess potential leak windows due to reservoir-reservoir (including thief zone) juxtapositions we use the Shale Gouge Ratio (SGR) method of Yielding et al. (1997), which is simply a measure of the amount of shale that has moved past a point on a fault:

$$\mathrm{SGR} = S(\mathrm{Vshale} * \Delta Z)/\mathrm{Throw}$$

where, for a given interval, Vshale is the volumetric shale fraction and ΔZ the interval thickness. Increasing amounts of shale that have passed a point on a fault increase the proportion of shale that can be incorporated into a gouge during faulting. Increasing fault rock shale content broadly correlates negatively with pore throat sizes and permeability, and positively correlates with capillary threshold pressures (Gibson, 1998; Sperrevik et al., 2002); thus, increasing SGR should equate to increasing seal capacity. Complications to this simple rule have been acknowledged. For example, increasing maximum depth of burial and depth during faulting broadly translate to increased seal capacities due to diaganesis and compaction effects (Bretan et al., 2003; Sperrevik et al., 2002). However, for P–M, maximum depths and depths during faulting are unlikely to be much greater than 1 km (ca. temperatures 55°C) and, therefore, compaction and diagenetic effects are not considered to be a controlling factor on fault seal (e.g. Fisher and Knipe, 1998). Calibration studies based on the relation between SGR and across-fault pressure difference or buoyancy pressure are used to assess trap capacity, and suggest that faults with SGRs $<$15–20% are potentially leaky (Yielding et al., 1997; Yielding, 2002).

Across-fault stratigraphic juxtapositions and SGRs have been mapped onto and calculated for all the main P–M fault surfaces using TrapTester software, following the methodology described by Needham et al. (1997). The Barrow Group reservoir is self-juxtaposed across all the Macedon Field faults. In contrast, the reservoir is juxtaposed against the Lower Gearle Formation along the majority of the main fault surface, apart from small areas of reservoir self-juxtaposition on the FW and HW faults between Macedon-1 and West Muiron-5 (Fig. 2). This is the lowest displacement part of the main (FW) fault and at least one of the two fault surfaces that separate the two wells must provide a fault rock seal to separate the Pyrenees and Macedon fields.

In addition to areas of Barrow self-juxtaposition, the Macedon Field faults also display large areas of FW Barrow-HW Windalia juxtaposition. These typically comprise $<$10% of fault surface area, but are volumetrically significant (e.g. 750–2500 m^2 per fault).

The results from all SGR calculations for all main fault surfaces (performed only on areas of reservoir self-juxtaposition above the observed FWLs) are summarised in Fig. 11 as curves of normalised frequency. Fig. 11(a) highlights the minimum SGR values for Barrow self-juxtaposition, considered equivalent to the most likely leak points for each fault, which are consistently $<$20% for Macedon faults, and $>$24% for the main sealing faults which, very broadly speaking, corroborates the proposed 15–20% SGR cut-off between sealing and non-sealing faults (Yielding et al., 1997). SGR calculations are subject to errors stemming from uncertainties in the input parameters and these are discussed in a later section. However, we note here that all faults were subjected to the same analysis and thus the SGR results can be

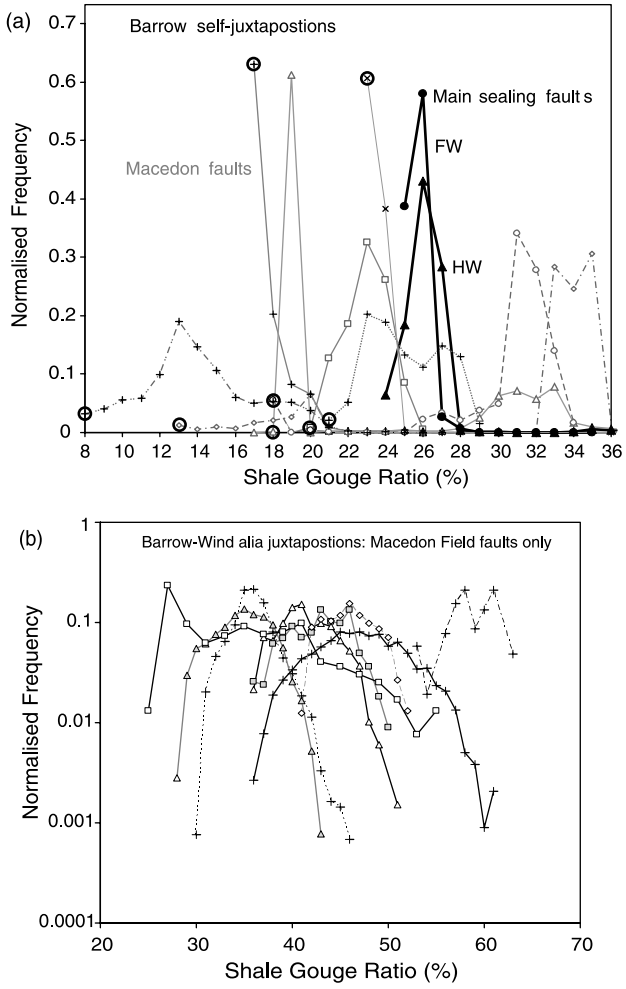

Fig. 11. Normalised frequency vs. SGR curves derived from separate faults for (a) Barrow reservoir self juxtapositions (Macedon Field (grey) and both FW and HW segments of the main 'sealing' fault (black)) and (b) FW Barrow reservoir against HW Windalia Radiolarite juxtapositions (Macedon Field faults only). Minimum values for Macedon Field faults in (a) are circled. Each fault has different ornament.

used in a relative sense to compare the different faults. The slight, but distinct, difference in SGR between the main faults and the Macedon Field faults is attributed to two contributing factors: (1) local juxtaposition of high quality sands over parts of the Macedon Field; (2) widespread occurrences of locally lower displacements (<10 m) on the Macedon faults at branch-lines and towards tip zones.

SGR distributions for Barrow-Windalia juxtapositions are higher ($>25\%$ and typically $>30\%$) than those for Barrow self-juxtapositions, which is due to the displacement of the Muderong Shale (Fig. 11(b)). Therefore, despite large areas of Barrow-Windalia juxtaposition, across-fault flow may be hindered by the relatively high seal capacity of the fault rocks. However, to determine whether or not across-fault migration is expected the pressure conditions that the faults are subjected to must be considered.

4.2.2.2. Buoyancy pressures. Determination of the pressure conditions across the Macedon Field is straightforward due to the relatively uniform pressure distribution. In contrast the pressure conditions in the compartment between the main fault FW and HW segments are unknown, and thus is an area of significant uncertainty (Figs. 2 and 4). Nevertheless, by considering the potential variations in buoyancy pressure for the different scenarios, constraints can be placed on the likely fault seal capacity. The pressure and phase conditions in this central compartment may be directly related to Macedon-1, Pyrenees-2 or West Muiron-5, or may even be free of hydrocarbons (Fig. 2). However, the structural saddle to the SW of Pyrenees-2 may limit the extent of the Pyrenees-2 gas accumulation (Fig. 2). What is certain, given the observed different FWLs, is that one or both of the FW or HW faults must support the pressures exerted by the Macedon and Pyrenees columns. Buoyancy pressures and across-fault pressure differences (AFPD) have been calculated following the procedure of Bretan et al. (2003) for all possible pressure combinations across the FW and HW segments (Fig. 12; Table 2). Where the same aquifer is presumed present either side of the fault (e.g. FW fault, Macedon-1 (FW) and

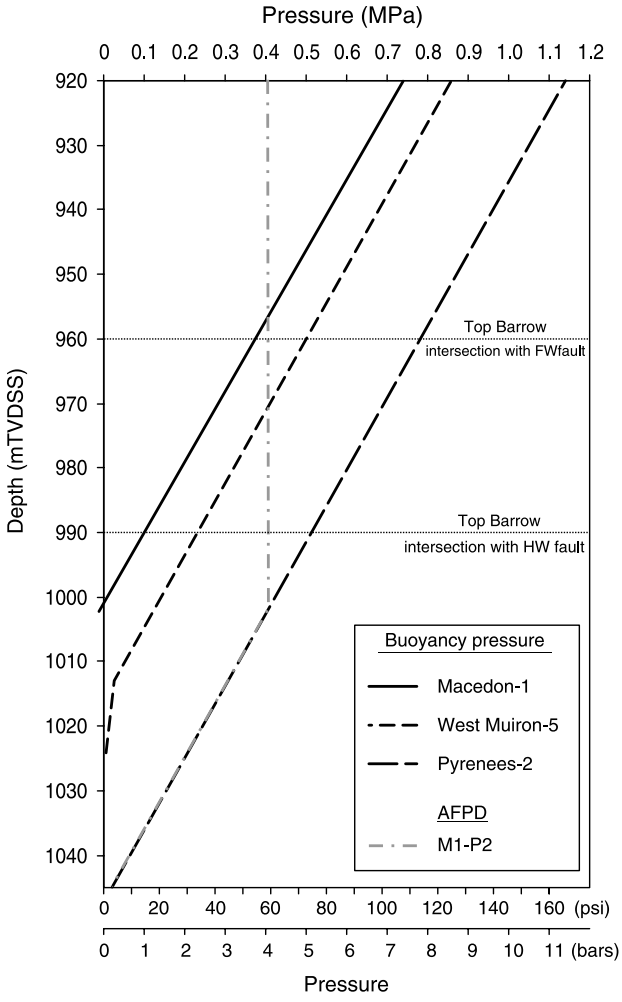

Fig. 12. Graphical summary of the variation with depth of possible buoyancy pressures or across-fault pressure differences that the main 'sealing' fault (FW and HW segments) would need to support. The main FW fault, being structurally higher than then HW fault is subjected to higher pressures.

Table 2
Maximum pressures (buoyancy (BP) or AFPD in MPa) exerted on the main sealing fault FW and HW segments at the shallowest Barrow Group self-juxtapositions for different pressure conditions in the FW and HW blocks

FW fault				HW fault			
FW block/HW block	FW BP	HW BP	AFPD	FW block/HW block	FW BP	HW BP	AFPD
M1/WM5	0.37	0.48		M1/WM5	0.15	0.22	
M1/P2			0.41	P2/WM5	0.51	0.22	
M1/Macedon water	0.37		0.37	Macedon water/WM5		0.22	
M1/Pyrenees water	0.37			Pyrenees water/WM5		0.22	0.22

Pyrenees-2 (HW)), AFPD is considered to reflect the capillary properties of the fault zone. However, where there is a different aquifer across the fault (i.e. Macedon-1 against West Muiron-5), AFPD reflects the fault properties and also hydrodynamic effects. Therefore, buoyancy pressures on both side of the fault are considered more relevant to the fault seal capacity than AFPD under the simplistic assumption that there is no pressure communication across the fault. Pressures shown in Table 2 are derived from the shallowest reservoir juxtapositions where SGR values are lowest and buoyancy pressures highest. The FW fault, if sealing, supports a maximum buoyancy pressure of 0.37 MPa exerted by the Macedon gas column. However, if West Muiron-5 (oil and gas) or Pyrenees-2 (gas) conditions exist in the HW then the pressures exerted would be higher (0.48 and 0.41 MPa, respectively; Fig. 12; Table 1). Similarly, the HW fault, if sealing, supports 0.22 MPa exerted by the Pyrenees column, but Pyrenees-2 conditions in the central compartment would exert 0.51 MPa.

No published SGR calibration data exist for circum-Australian oil or gas fields, providing a severe limitation to a calibration approach. Data for P–M have been plotted on the calibration plots of Bretan et al. (2003) that contain data from a number of fields worldwide. However, the P–M data lie within the general data distributions for sealing to non-sealing faults, and therefore, the results are not conclusive and one would not predict that the difference in a few percent in SGR between the main fault(s) and the Macedon Field faults could result in the difference between sealing to non-sealing. Explaining the difference between the apparent seal properties of the main fault(s) and the Macedon Field faults requires an understanding of the buoyancy pressures that the faults are subjected to. To illustrate this, buoyancy pressures are calculated at the shallowest Barrow Group self-juxtapositions (i.e. top Barrow Group HW-fault intersections; Fig. 13). Macedon Field faults are distributed from the crest of the structure to the FWL on the flanks, and therefore, are subjected to a range of buoyancy pressures from 0 to 0.96 MPa (0–110 m gas column). In comparison, the Barrow Group self-juxtapositions on the main sealing fault are situated down-dip of the Macedon Field crest and the maximum buoyancy pressures they support are 0.37–0.48 MPa, exerted by the Macedon and Pyrenees columns, respectively. Therefore, there is a sizeable difference ($<$0.6 MPa) in the buoyancy pressures supported by the Macedon Field and main sealing faults. This difference, combined with the lower SGR values for the Macedon Field faults compared to the main sealing faults may explain the difference in their observed sealing behaviour, a conclusion that can only be tested by deriving more calibration data from this region.

4.2.2.3. Column height calculations and errors. A better understanding of how a change of a few percent in SGR translates to seal capacity can be estimated using published SGR to column height conversions (e.g. Sperrevik et al., 2002; Bretan et al., 2003). Bretan et al. (2003) provide an empirically derived conversion where:

$$\text{Buoyancy pressure} = 10^{(\mathrm{SGR}/27C)}$$

The value of C varies as a function of depth ($<$3 km, $C=0.5$; 3–3.5 km, $C=0.25$; $>$3.5 km $C=0$). Buoyancy pressure can then be converted to column height (H) using (e.g. Jennings, 1987; Schowalter, 1979):

$$H = \mathrm{d}P/g(\rho_w \rho_h)$$

where dP is buoyancy pressure, g the acceleration due to gravity, ρ_w the pore water density and ρ_h the hydrocarbon

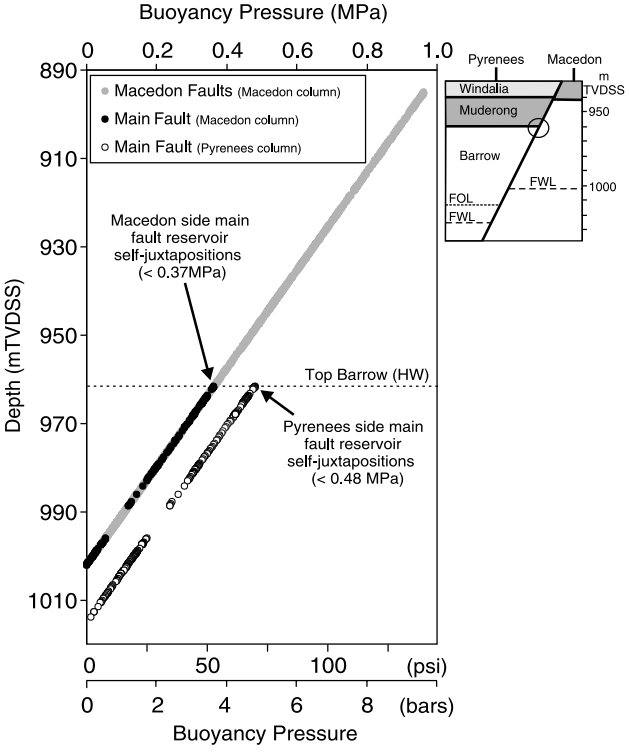

Fig. 13. Buoyancy pressures exerted by the Pyrenees and Macedon columns at the shallowest Barrow Group self-juxtapositions (shown by circle in cross-section schematic).

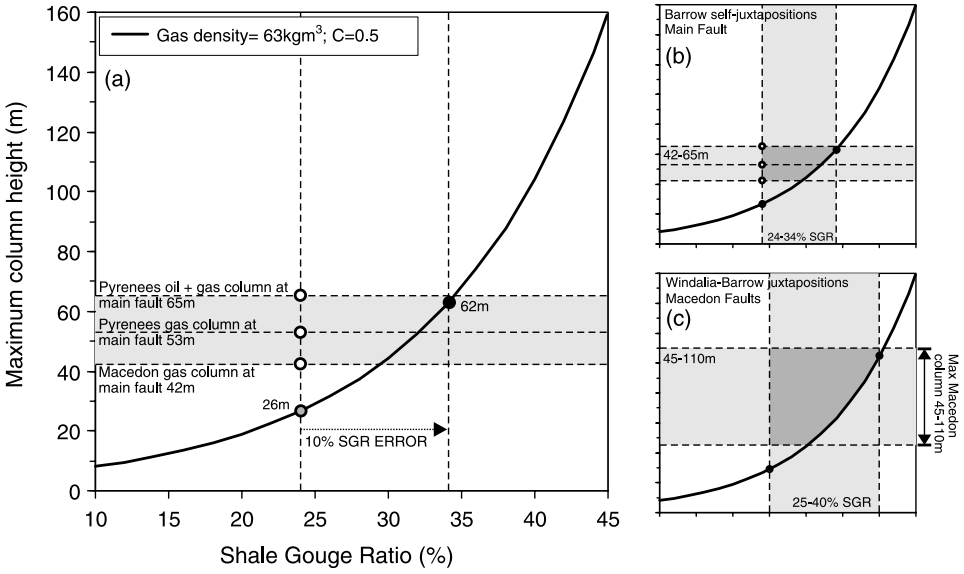

Fig. 14. SGR vs. maximum column height plots for Barrow self-juxtapositions along the main fault between Macedon-1 and West Muiron-5 (a and b) and for Windalia-Barrow juxtapositions over Macedon Field faults (c). The grey and white circles in (a) show the positions of the predicted and in situ columns, respectively, for the minimum SGR calculated on the main fault (24%, vertical dashed line). The black dot shows the position of the predicted column if there is a +10% error in the SGR calculation. The light grey areas in (a) to (c) show the heights of columns in contact with the faults (and also likely SGR distributions in (b) and (c)). Dark areas in (b) and (c) highlight the areas that represent failed seal; the relatively large area in (c) suggests some Windalia-Barrow juxtapositions are likely to allow across-fault leakage.

density. Fig. 14(a) shows a curve for maximum column height versus SGR derived using $C = 0.5$ (< 3 km burial depth). Areas below the curves represent sealing faults defined by this procedure, and above to non-sealing faults (shown as dark grey areas, Fig. 14(b) and (c)). A 26 m gas column is predicted for the minimum SGR calculated of 24%, which is less than the 42 m (Macedon gas) and 65 m (Pyrenees gas and oil rim) columns in contact with the fault. This result may suggest that the calibrations of Bretan et al. (2003) are not appropriate for these conditions (i.e. very shallow fields), or perhaps a lower C value would be more appropriate. However, application of the SGR method requires an understanding of the likely errors. The main issue with fault membrane seal analysis at P–M relates to the erosion of the top of the Barrow Group, which has removed the upper parts of the footwall stratigraphy and the displacement record of the uppermost parts of the reservoir. Reconstructing the syn- to post-reservoir geometries is uncertain due to the synchroneity of faulting and reservoir sedimentation (i.e. both the composition and thickness of the absent footwall stratigraphy are unknown). Using the displacements at base and top reservoir would overestimate and underestimate throw, respectively, and no reflectors are available to better constrain vertical throw distribution for the reservoir interval. Therefore, throw values used for the SGR calculations are derived by linear interpolation between base and top Barrow reflectors. For the critical parts of the fault near the top of the Barrow Group where throws and SGR are at their lowest and buoyancy pressures highest, throws are likely to be an underestimate. However, the limit of resolution is approximately 5–10 m and adding 10 m to the throw increases SGR by 10–15% (i.e. increasing a 10 m throw to 20 m increases SGR from 20 to 35%). As an example, increasing SGR by 10% in Fig. 14(a) and (b) results in estimates of columns that are similar in size (ca. 62 m) to those in place (42–65 m). Clearly, this demonstrates a need to consider uncertainty in seal calculations.

In a previous section we noted that the minimum SGRs for Barrow-Windalia juxtapositions are high (25–40%), which may inhibit across-fault flow of gas. As above, we compare the in situ column heights (45–110 m) with those predicted in Fig. 14(c). The columns present are as much as 85 m greater than predicted, which suggests that Windalia gas charge via across-fault flow is a distinct possibility, particularly at the crest of the trap. Note that unlike Barrow self-juxtapositions, throw values at this level are well constrained as there is no growth or erosion, and therefore, SGR calculations are only limited by the accuracy of the Vshale calculation.

4.2.2.4. Fault seal capacity—additional considerations. SGR is clearly heavily dependent on the accuracy of the Vshale input. Vshale curves used in this analysis were mainly derived from gamma logs using linear interpolation between interpreted sand-shale lines, and, as such, are susceptible to poorly constrained errors. However, the Vshale values have been cross-checked against descriptions in well completion reports and appear reasonable. Bretan et al. (2003) noted SGR calculations may be in the order of 10% different depending on the Vshale calculation used. Further analysis into the sensitivity of SGR to varying throw and stratigraphic inputs is beyond the scope of this contribution, but we note that the differences in the minimum SGR values for the main fault and the Macedon Field faults are within error, and, as such, there

may be no real difference between their seal capacities. However, we also note that the same modelling procedure was applied to all faults, the inputs were varied (principally Vshale, stratigraphy), and the main faults yield minimum SGR values consistently higher than the majority of Macedon faults (by approximately 5%).

The procedure presented above does not conclusively identify shale gouge to be the sole explanation for the apparent seal capacity differences. First, we entertain the possibility that all fault surfaces at P–M with SGRs c. 20% act as membrane seals. The only difference between the main sealing fault and the rest may be that the latter are less continuous and possess sub-resolution geometrical leak points (i.e. tip zones, relays, branch-lines). Second, the Pyrenees column exerts approximately 0.11 MPa greater buoyancy pressure than the Macedon column at the shallowest Barrow self-juxtapositions on the main sealing fault; this is close to the difference in the underlying aquifer pressures across the fault. Due to this coincidence, it is possible that the seal capacity for this fault may have been reached, i.e. the fault capillary properties and buoyancy pressures were once in equilibrium, but have since been thrown out of balance by an increase in Pyrenees pressures (e.g. by gas charge from the west) or decrease in Macedon pressures (e.g. by vertical leakage from the Macedon trap). Leakage indicators over the Macedon Field identified on seismic data coupled with Windalia gas charge suggests that vertical leakage is a risk and is explored below.

4.3. Seal integrity

In addition to considering seal capacity, investigation of the likely hydraulic behaviour of seals in a tectonically active setting, such as the Australian North West Shelf, is also required. This can be achieved by evaluation of in situ stress conditions coupled with laboratory testing to determine likely rock strength of both fault and top seals. Susceptibility to mechanical failure, resulting either in reactivation of pre-existing faults and fractures, or the generation of new fracture sets can be assessed by comparison of the failure envelope, either produced from the rock testing data or utilising a generic example, against Mohr circle constructions based on measurements of field stress conditions.

4.3.1. Muderong Shale top seal integrity

Dewhurst and Hennig (2003) presented an assessment of Muderong Shale top seal integrity by combining laboratory-based geomechanical testing of Muderong Shale samples from the southern Barrow Sub-basin with in situ stress data. They determined that whilst the shale samples were weak (2.75 MPa and a coefficient of friction of 0.34) relative to other rock types, fracturing of the intact Muderong Shale caprock does not appear to be a critical risk factor, as Mohr circles for the current in-situ stress magnitudes appear to lie comfortably beneath the peak strength failure envelope. However, pre-existing faults within the Muderong Shale are near or at the critically stressed state, suggesting reactivation of pre-existing faults in certain orientations is a significant risk for sub-Muderong traps (Dewhurst and Hennig, 2003) and that associated fractures may by hydraulically conductive. However, the degree of risk is likely to be variable across the basin as both increasing effective stress and temperature with increasing burial depth can alter shale geomechanical properties. Varying lithology may also change shale properties, especially where there is an increase in rigid grain content. As such, both coarser and more deeply buried shales may be stronger and this may change the risk perceived for such seals.

Geomechanical properties of Muderong Shale determined by (Dewhurst and Hennig (2003) were used to evaluate the risk of fault reactivation and fracture conductivity in the P-M fields. The risk has been assessed using the FAST technique (Mildren et al., 2002; Fig. 15(a)), which calculates the distance of any given fault or fracture plotted in shear and normal stress space from an input failure envelope, assuming Andersonian fault mechanics hold true. This is a simplification, given that stress trajectories are known to deflect around pre-existing discontinuities (Ramsey, 1967). Using failure envelopes derived by Dewhurst and Henning (2003), combined with the in situ stress field data, fault and fracture orientations at low and high risk of reactivation can be assessed on a polar plot (Fig. 15(b)). For P–M, steeply dipping faults and fractures striking 060°N and 120°N, and those trending E–W and dipping at ~60°, are considered to be most at risk of reactivation in the present day stress field, which broadly coincides with the observed fault orientations. Faults at top reservoir level display dominantly north-easterly strikes and moderate to steep dips (mean orientation 050/50° SE; Fig. 15(c) and (d)). A subordinate set of E–W-striking faults hard-link and transfer displacement between the dominant NE-striking set, which are parallel to the underlying Base Barrow fault system. The coincidence between the orientations of seismically resolvable faults and the planes of weakness determined by the FAST method suggest that recent gas leakage from the Barrow Group reservoir into the Windalia radiolarite, and potentially above, may be associated with critically stressed faults or fractures within the top seals.

We note that the main sealing fault has a similar trend to the others, but possesses only minor amplitude anomalies (Figs. 5 and 9), which may be attributed, at least in part, to the positions of the leakage indicators over the crest of the Macedon Field where the driving force for migration, the buoyancy pressures, are highest. Alternatively, or in combination, this may be due to a change in the mineralogy and related geomechanical properties of the top seal across the fault as discussed earlier. On the Macedon side of the fault, the Muderong Shale appears to be more smectite rich than the Pyrenees side, which is more kaolinite rich albeit based on only the two available sample locations. Smectite is generally the weakest of minerals, geomechanically speaking, while kaolinite tends to have the highest friction coefficients among the clay minerals. These differences are likely to be the result of depositional processes and may provide an explanation as to why seismic anomalies do not occur along the major sealing fault, even though its trend is similar to that of other critically stressed faults in the region.

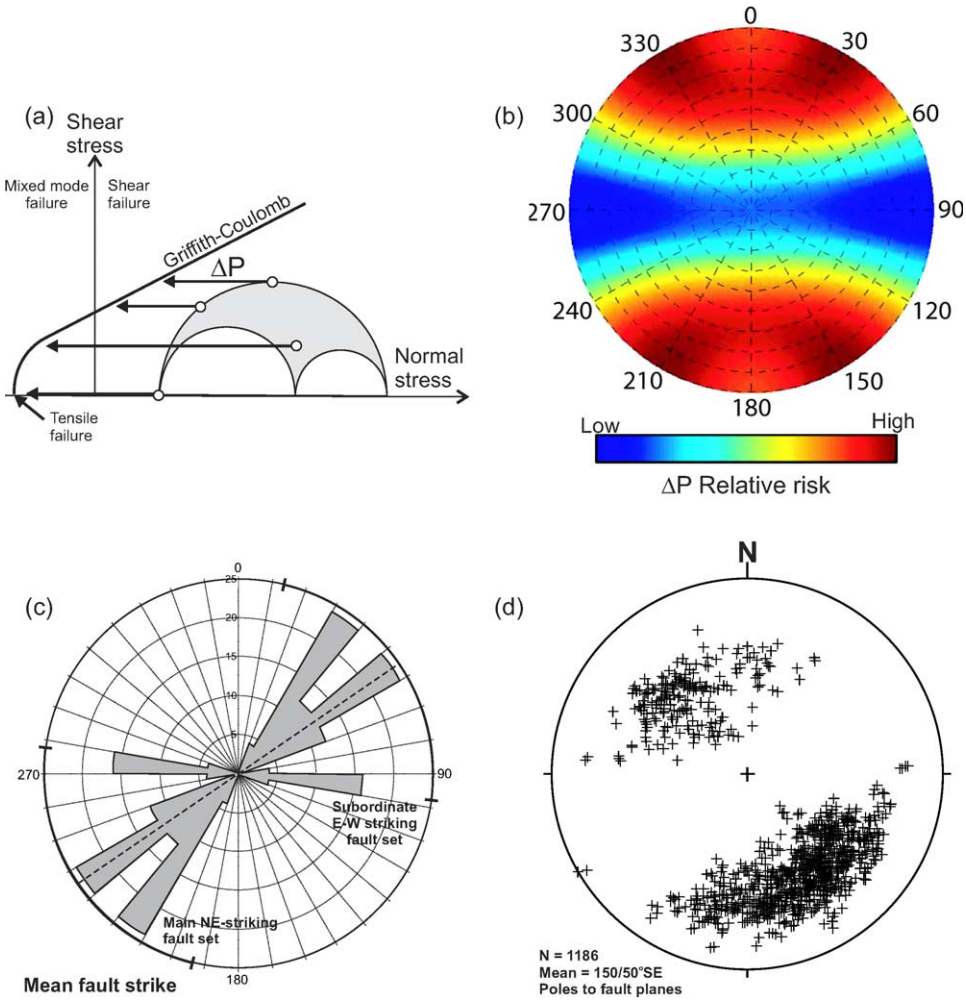

Fig. 15. (a) Graphical representation of the FAST method for risking the likelihood of fault reactivation (after Mildren et al., 2002). The lower the ΔP values, the higher the risk of reactivation. (b) Polar plot showing the distribution of ΔP values for poles to fault planes from P–M. The highest risk of reactivation (lowest ΔP; dark red) is on steeply dipping faults striking 060° and 120°, and E–W faults dipping at 60°. (c) Mean orientations of faults (radial scale is percentage of population). (d) Lower hemisphere stereonet of poles to fault surfaces sampled every 100 m along NW–SE oriented sample lines.

4.3.2. Gearle formation top seal integrity

Indirect evidence for vertical hydrocarbon leakage above the uppermost top seal, the Lower Gearle Formation (Figs. 5 and 9), indicates the need to appraise the seal integrity of this unit in addition to the Muderong Shale. Whilst no analyses have been completed at P–M, the Lower Gearle Formation in this region has a similar composition to the Muderong Shale (co-dominant mineralogies are mixed layer illite-smectite and quartz, Dewhurst et al., 2002b) and could, therefore, be assumed to have similar strength. Cohesive strengths may be derived from wireline log data using a variety of algorithms. Here we used the algorithms described by Collins (2002) to estimate the cohesive strength of the reservoir to top seal sequence sampled by Macedon-1 (Fig. 16). Our results suggest that the Lower Gearle Formation has a similar strength profile to the Muderong (Fig. 16).

Analysis of image logs at Macedon-1 shows that both the Muderong and Lower Gearle Formations contain conductive fractures, noting that fracture identification from image logs is likely to considerably under-sample their natural occurrence (Fig. 16). Development of these fractures is, however, likely to be fault related given their comparable orientations (rose diagrams in Figs. 15 and 16) and the heavily faulted nature of the West Muiron structure. The modal strike of fractures from the image logs is E–W (Fig. 16) and is parallel to the orientation of the subordinate set of seismically resolvable faults (Fig. 15). Given that the E–W faults are interpreted to accommodate displacement transfer between the NE-striking faults, which inherit their trends from lower structural levels, it is logical to assume that the E–W faults and fractures developed relatively late, and are related to the contemporary stress regime. The orientations of genetically related faults and fractures are consistent with predictions of critically stressed fault/fracture orientations from the FAST methodology. We note that, at face value, the presence of fractures observed in the Macedon-1 image log could be viewed to be at odds with the geomechanical prediction of relatively high integrity for *intact* Muderong Shale. However, the predicted and observed faulting of the Muderong is expected to be associated with fracturing/sub-seismic faulting, and therefore, testing of faulted

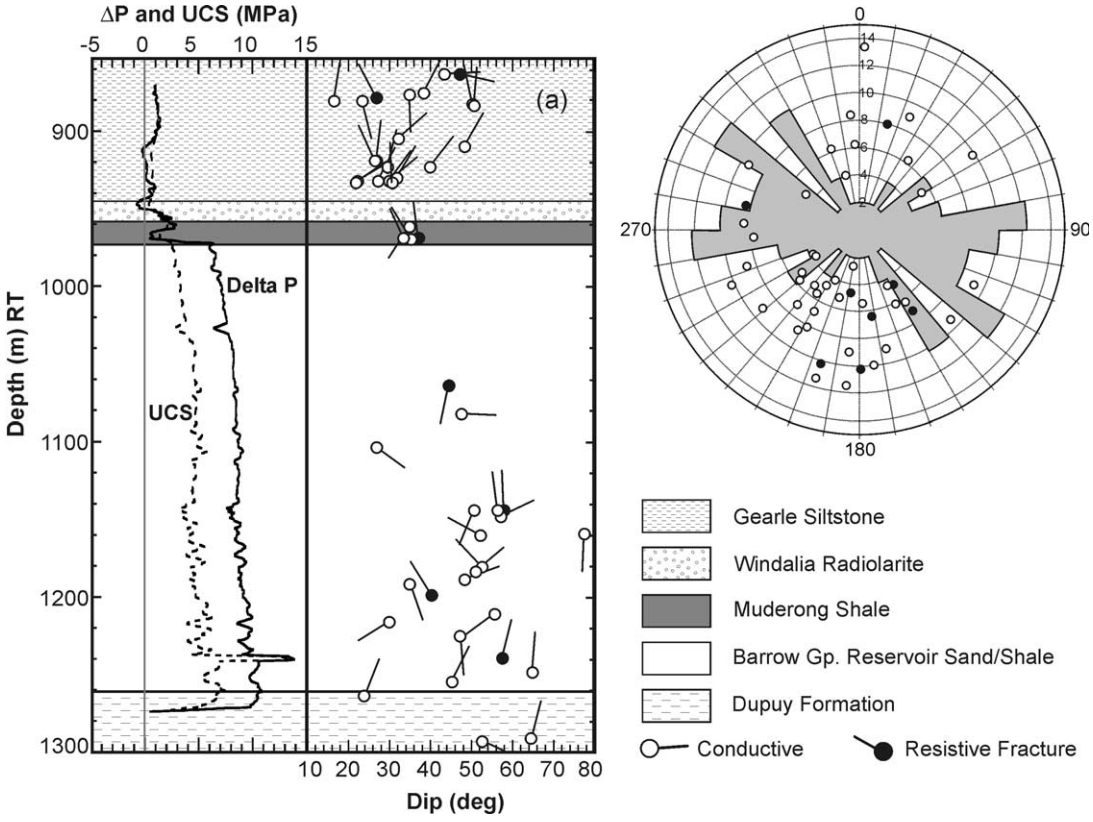

Fig. 16. Estimates of unconfined compressive strength (UCS; dashed curve) derived from wireline log data from Macedon-1. UCS is converted to a cohesive strength, using a friction coefficient of 0.34, a failure envelope is derived and a ΔP value estimated through the sequence (solid curve). Both Muderong and Lower Gearle Formations are shown to have low ΔP values consistent with high risk of critically stressed fractures in the contemporary stress field. Fractures (conductive (white) and resistive (black)) observed on image logs (right and lower hemisphere polar plot) occur in both Muderong and Lower Gearle top seals.

top seals should take the geomechanical properties of the faults into account.

5. Discussion

Assessment of the fault and top seals over the P–M fields has revealed various seal properties at specific locations that may have controlled the current-day distribution of hydrocarbons. A continuous top seal cover, which appears to have capillary properties sufficient to retain the reservoired hydrocarbons, drapes the P–M structure making it unlikely that capillary top seal failure has occurred. In contrast, faults that transect the Macedon Field do not provide significant barriers to lateral migration, with numerous tip lines and branch-lines contained within the field and relatively low calculated fault rock seal capacities for widespread reservoir self-juxtapositions. This is consistent with the common FWL sampled by the wells within the Macedon Field and the flat hydraulic head contours within the Barrow Group.

The role of the main fault that separates the Macedon Field from the Pyrenees Fields is more difficult to explain. Although this fault extends beyond the margins of the field and generally produces a juxtaposition seal (explaining separation of the Macedon Field from the Pyrenees-2 accumulation), there are regions of the fault where displacement lows, caused by branching of the fault, produce reservoir self-juxtaposition. The differences in the FWLs and hydrocarbon phase across this fault demonstrate the presence of a seal, yet evaluation of fault rock capacity, based on the SGR method, provides equivocal results as to whether this fault should provide a seal. Whilst SGR values are higher than those for the Macedon faults, the differences are nevertheless slight. A distinct limitation to the interpretation of SGR values at P–M is the paucity of calibration datasets for relatively shallow faults and the complete absence of any such datasets for the circum-Australia region. In summary, however, we conclude that the main fault has only a limited capacity to withhold a hydrocarbon column and may be close to seal capacity; the location of the fault on the flanks of the P–M closure may be the main cause of the fault forming a seal between the Pyrenees and Macedon fields.

In summary, our analysis supports a model whereby the trap at Pyrenees-2 is filled to spill with gas with further (gas) charge migrating to the west to the Pyrenees Field, which is separated from the Macedon Field by a fault that is close to, or has exceeded, its membrane seal capacity. It is possible, therefore, that gas has accessed, and may continue to access, the Macedon Field by migration through the main ‘sealing’ fault during easterly directed charge from the Exmouth Sub-basin. The reason for the observed difference in fluid contacts between the Pyrenees and Macedon fields may be due to the membrane seal capacity of the fault. Alternatively, the system is out of

equilibrium and either current-day charge to the Pyrenees Field is outpacing leakage from the Macedon Field, or just that there is loss of gas from the Macedon Field.

The assessment of fault seal capacity produces an acceptable correspondence with the observed compartmentalisation of the Barrow reservoir, but cannot provide an explanation for the under-filled nature of the structure relative to the available structural closure. The presence of gas saturation and associated seismic amplitude anomalies within the overlying Windalia Radiolarite has previously been cited as evidence of vertical leakage. The similarity in gas gradients between these two units is consistent with a connected gas phase. Capillary leakage is not supported by MICP measurements of the Muderong Shale, so the connection is likely to be facilitated by faults or fractures. Geometric analysis of the faults across the Macedon Field reveals numerous areas where Barrow-Windalia juxtaposition occurs and these potential leak windows offer a viable mechanism to allow gas migration from the main reservoir into the Windalia thief zone. SGR values from these faults indicate seal capacity that is higher than inferred for the sealing main fault, but the crestal position of the Macedon faults exposes them to a greater buoyancy pressure due to the larger column height being supported. This makes it possible that across-fault migration can explain gas in the Windalia. What is not clear is whether this conclusion represents a satisfactory explanation for the degree of underfilling.

Loss of gas from the Barrow Group into the Windalia may simply imply that the Lower Gearle Formation, and not the Muderong Shale, is the effective top seal for P–M. Whilst detailed volumetric calculations of gas volumes reservoired in the Windalia are not available, it seems unlikely that these thin and relatively poor reservoir quality siltstones contain enough gas to account for the unfilled closure at the Barrow Group level. This leaves two plausible explanations for the underfilling; lack of sufficient gas charge or another mechanism is controlling hydrocarbon retention. Potential leakage indicators above the Lower Gearle Formation and the inference that P–M has been a long-lived focal point for regional hydrocarbon migration suggest the latter option is more likely. Indications for gas leakage are inferred from seismic data and complement irregularities observed on the sea-floor. If these reflect vertical leakage then a mechanism for fluid migration is required. Simple cross fault leakage is not a viable option as fault throws are not sufficient to offset the Lower Gearle Formation. Therefore, the most likely cause of vertical leakage is loss of fault or top seal integrity, which is supported by geomechanical analyses. In the contemporary stress field, faults that transect the Macedon Field top seal are susceptible to reactivation with associated fracturing. Therefore, there is a likelihood that connected, conductive fracture networks are present in the top seals, which is supported by image log analysis at Macedon-1. Why the Macedon trap contains gas despite the expected low seal integrity is uncertain, but may be attributable to relative low rates of leakage (low gas permeability of the fracture network) and/or to recent/current gas charge.

5.1. Retrospective implications for P–M and opportunities for application elsewhere

Evaluation of seal potential has provided insights into the controls on hydrocarbon retention at P–M. This result highlights the value in adopting integrated workflows for the application to the risking of seals, but it is the ability to translate this knowledge into a predictive capability that ultimately has the greatest value.

Retrospectively, the analyses completed would identify traps to the west of the main fault as potentially disconnected from the Macedon Field and they would rely on charge from the west. This is indeed the inferred direction of migration. Had charge directions been via the Macedon Field (i.e. from the east) then it is probable that the Pyrenees traps would have been dry. A second major implication of the analyses completed is that compartmentalisation of the Macedon Field would not be expected and drilling of several appraisal wells, specifically designed to confirm connectivity, would have been considered unnecessary. However, it is unlikely that the transition between non-sealing (intra-Macedon) and sealing (segments between West Muiron-5 and Macedon-1) faults would be identified pre-drill, or early in the appraisal phase, given the slight difference in their calculated seal capacities (SGR). This is attributed to both the errors inherent in fault seal analysis and also to a lack of calibration data in this region. However, the weakest point along the main fault is interpreted as being close to or at capillary failure and, therefore, we speculate that this part of the fault could constitute a migration path for gas entering the Macedon Field from the west.

At a regional scale, this analysis has strengthened the confidence that can be placed on the significance of remote leakage indicators to accurately detect breached traps. A limitation is that, in this instance, P–M may have been ranked as high risk, despite the presence of hydrocarbon columns at the current day. This makes it clear that the assignment of pre-drill risk values needs to not only predict the presence or absence of hydrocarbons, but also consider the degree of fill needed to make the volumes economic. For the Northern Carnarvon Basin, particularly where the Muderong is thin, the experience of this study suggests that careful mapping of fault juxtapositions is required to properly evaluate the role of thief zones, such as the Windalia Radiolarite.

5.2. Future challenges

In such a complex environment, where hydrocarbon retention is being risked, great advances would be made if better constraints could be imposed on the mechanisms of vertical fault-related leakage and on the relative rates of charge and leakage. This can only be addressed with coupled charge-seal workflows (see also Gartrell et al., 2002) and simulations (e.g. Childs et al., 2002; Lothe et al., in press). To this end, this paper forms half a research project, involving charge history analysis and structural restoration studies, which is currently ongoing. A question remains as to whether or not the application of fault membrane seal calculations are valid in

this and other reactivated settings worldwide. Understanding this problem requires calibration of fault seal calculations with pressure data, using better constrained examples than that presented here. In an exploration context, our provisional results suggest that consideration of fault membrane seal properties is important, as the size of the Pyrenees Field could have been estimated pre-drill. However, in this type of environment where dynamic seal failure and the presence of conductive fracture networks in the top seal are risks, membrane seal capacities are likely to over estimate column heights. This demonstrates that holistic evaluations of seals, integrating a range of techniques, are required to underpin prospect risk assessments in structurally complex settings.

6. Conclusions

- Underfilling of the P–M traps can be attributed to late structural development (Mitchelmore and Smith, 1994), but there is clear evidence that vertical leakage may have at least influenced the column heights preserved.
- Despite being heavily faulted, pressure data in the Macedon gas field suggests that it is not compartmentalised. SGR calculations compared to published calibration datasets support the idea of good Macedon reservoir communication via capillary failure of the fault rocks. Furthermore, fault tips, and possibly also branch-lines, within the extent of the field favour good communication, albeit via tortuous flow paths. The fault that separates the Macedon Field from the Pyrenees Field is interpreted to be close to seal capacity and ultimately does not control the volumetric capacity the whole trap.
- The Muderong Shale, despite having suitable seal capacity to retain the observed hydrocarbon column, does not represent the effective seal to P–M. Instead fault offsets have produced potential leak windows that may allow gas to be lost into the Windalia Radiolarite, with the overlying Lower Gearle Formation acting as the principal seal.
- Cross fault leakage has played a role in redistributing gas charge, but ultimately the Macedon Field size is most likely controlled by limitations in the integrity of the Lower Gearle Formation, which, although thick and with high seal capacity, has been compromised by the formation of hydraulically conductive fractures during periods of fault reactivation.
- The use of integrated workflows that address all aspects of seal potential are critical to properly assign trap integrity risks, particularly for complex fields such as P–M.

Acknowledgements

This paper stems from work completed during the APCRC Seals research programme. The company sponsors, Anadarko, ExxonMobil, BHP Billiton, ChevronTexaco, OMV, Marathon, Origin Energy, Santos, Statoil and Woodside, and past member JNOC are thanked for their support and permission to publish. BHP Billiton is thanked for the contribution of data, invaluable discussions and permission to publish.

Badleys, UK are thanked for the provision of TrapTester v.5.2 and FAPS v3 and for their support. Schlumberger Oilfield Australia Pty Ltd is thanked for the provision of GeoFrame™.

Mark Brincat, Anthony Gartrell and Mark Lisk provided invaluable discussion for this work and Richard Gibson and an anonymous reviewer are thanked for their efforts in reviewing this paper.

References

Bailey, W.R., Manzocchi, T., Walsh, J.J., Strand, J.A., Nell, P.A., Keogh, K., Hodgetts, D., Flint, S., Rippon, J., 2002. The effects of faults on the 3-D connectivity of reservoir bodies: a case study from the East Pennine Coalfield, UK. Petroleum Geoscience 8, 263–277.

Bailey, W.R., Shannon, P., Walsh, J.J., Unithan, V., 2003. Spatial relationships between faults and deep sea carbonate mounds: the Porcupine Basin, offshore Ireland. Marine and Petroleum Geology 20, 509–522.

BHP Petroleum Pty Ltd., 1993. West Muiron-5 Well Completion Report Basic Data.

BHP Petroleum Pty Ltd., 1995a. Macedon-2 Basic Well Completion Report.

BHP Petroleum Pty Ltd., 1995b. Macedon-4 Basic Well Completion Report.

Bouvier, J.D., Kaars-Sijpesteijn, C.H., Kluesner, D.F., Onyejekwe, C.C., Van Der Pal, R.C., 1989. Three-dimensional seismic interpretation and fault sealing investigations, Nun River Field, Nigeria. American Association of Petroleum Geologists Bulletin 73, 1397–1414.

Bretan, P., Yielding, G., Jones, H., 2003. Using calibrated shale gouge ratio to estimate column heights. American Association of Petroleum Geologists Bulletin 87, 397–413.

Childs, C., Sylta, O., Moriya, S., Walsh, J.J., Manzocchi, T., 2002. A method for including the capillary properties of faults in hydrocarbon migration models. In: Koestler, A.G., Hunsdale, R. (Eds.), Hydrocarbon Seal Quantification. Elsevier, Amsterdam. Norwegian Petroleum Society (NPF), Special Publication vol. 11, pp 127–139.

Collins, P.A., 2002. Geomechanics and wellbore stability design of an offshore horizontal well, North Sea. SPE/PS-CIM/CHOA Paper 78975.

Cowley, R., O'Brien, G.W., 2000. Identification and interpretation of leaking hydrocarbons using seismic data: a comparative montage of examples from the major fields of Australia's North West Shelf and Gippsland Basin. The APPEA Journal 40 (1), 121–150.

Dewhurst, D.N., Hennig, A.L., 2003. Geomechanical properties related to top seal leakage in the Carnarvon Basin, Northwest Shelf, Australia. Petroleum Geoscience 9, 255–263.

Dewhurst, D.N., Jones, R.M., Raven, M.D., 2002a. Microstructural and petrophysical characterization of Muderong Shale: application to top seal risking. Petroleum Geoscience 8, 371–383.

Dewhurst, D.N., Raven, M.D., van Ruth, P., Tingate, P.R., Siggins, A.F., 2002b. Acoustic properties of Muderong Shale. APPEA Journal 42, 241–257.

Dewhurst, D.N., Kovack, G.E., Hennig, A.L., Bailey, W.R., Raven, M.D., Kaldi, J.G., 2004. Geomechanical and Lithological Controls on Top Seal Integrity on the Australian Northwest Shelf. In: Proceedings of the sixth North American Rock Mechanics Conference, GulfRocks04, (8 pp). Houston.

Downey, M.D., 1984. Evaluating fault seals for hydrocarbon accumulations. The American Association of Petroleum Geologists Bulletin 68, 1752–1763.

Firoozabadi, A., Ramey, H.J., 1988. Surface tension of water-hydrocarbon systems at reservoir conditions. Journal of Canadian Petroleum Technology 27, 41–48.

Fisher, Q.J., Knipe, R.J., 1998. Fault sealing processes in siliclastic sediments. In: Jones, G., Fisher, Q.J., Knipe, R.J. (Eds.), Faulting, Fault Sealing and Fluid Flow in Hydrocarbon Reservoirs. The Geological Society, London, Special Publications, vol. 147, pp. 117–134.

Gartrell, A., Lisk, M., Underschultz, J., 2002. Controls on trap integrity of the Skua Oil Field, Timor Sea. The Sedimentary Basins of Western Australia 3: Proceedings of Petroleum Society of Australia Symposium, Perth, 2002, pp. 389–407.

Gibson, R.G., 1998. Physical character and fluid-flow properties of sandstone-derived fault zones. In: Coward, M.P., Daltaban, T.S., Johnson, H. (Eds.), Structural Geology in Reservoir Characterisation, 127. Geological Society, Special Publications, London, pp. 83–97.

Hennig, A., Underschultz, J.R., Otto, C.J., 2002. Hydrodynamic analysis of the Early Cretaceous aquifers in the Barrow Sub-basin in relation to hydraulic continuity and fault seal. In: Keep, M., Moss, S.J. (Eds.), The Sedimentary Basins of Western Australia 3: Proceedings of the Petroleum Exploration Society of Australia Symposium, Perth, 2002, pp. 305–320.

Jennings, J.B., 1987. Capillary pressure techniques: application to exploration and development geology. American Association of Petroleum Geologists Bulletin 71, 1196–1209.

Jones, R.M., Hillis, R.R., 2003. An integrated, quantitative approach to assessing fault-seal risk. American Association of Petroleum Geologists Bulletin 87, 507–524.

Kovack, G.E., Dewhurst, D.N., Raven, M.D., Kaldi, J.G., 2004. The influence of composition, diagenesis and compaction on seal capacity in the Muderong Shale, Carnarvon Basin. APPEA Journal 44, 201–222.

Longley, I.M., Buessenschett, C., Clydsdale, L., Cubitt, C.J., Davis, R.C., Johnson, M.K., Marshall, N.M., Murray, A.P., Somerville, R., Spry, T.B., Thompson, N.B., 2002. The North West Shelf of Australia—a Woodside perspective. In: Keep, M., Moss, S.J. (Eds.), The Sedimentary Basins of Western Australia 3: Proceedings of the Petroleum Exploration Society of Australia Symposium, Perth, pp. 27–88.

Lothe A.E., Borge, H., Sylta, Ø., in press. Evaluation of late caprock failure and hydrocarbon entrapment using a linked pressure and stress simulator. In: J. Kaldi, & P.J. Boult (Eds.), Evaluating Fault and Caprock Seals. Hedberg Series 1.

Mildren, S.D., Hillis, R.R., Kaldi, J.G., 2002. Calibrating predictions of fault seal reactivation in the Timor Sea. APPEA Journal 42, 187–202.

Mitchelmore, L., Smith, N., 1994. West Muiron discovery, WA-155-P—new life for an old prospect. In: Purcell, P.G., Purcell, R.R. (Eds.), The Sedimentary Basins of Western Australia: Proceedings of Petroleum Exploration Society of Australia Symposium, Perth, pp. 584–596.

Needham, D.T., Yielding, G., Freeman, B., 1997. Analysis of fault geometry and displacement patterns. In: Buchanan, P.G., Nieuwland, D.A. (Eds.), Modern Development in Structural Interpretation, Validation and Modelling. Geological Society, London, Special Publications, vol. 99, pp. 189–199.

O'Brien, G.W., Woods, E.P., 1995. Hydrocarbon-related diagenetic zones (HRDZs) in the Vulcan Sub-basin, Timor Sea: recognition and exploration implications. The APEA Journal 35, 220–252.

Otto, C.J., Underschultz, J.R., Hennig, A.L., Roy, V.J., 2001. Hydrodynamic analysis of flow systems and fault seal integrity in the Northwest Shelf of Australia. The APPEA Journal 41 (1), 347–365.

Ramsey, J.G., 1967. The Folding and Fracturing of Rocks. McGraw-Hill, New York, pp. 568.

Schowalter, T.T., 1979. Mechanisms of secondary hydrocarbon migration and entrapment. American Association of Petroleum Geologists Bulletin 63, 723–760.

Scibiorski, J.P., Micenko, M., Lockhart, D., 2005. Recent discoveries in the Pyrenees Member, Exmouth Sub-basin: a new oil play fairway. APPEA Journal 45, 233–251.

Sibson, R.H., Moore, J.M., Rankin, A.H., 1975. Seismic pumping: a hydrothermal fluid transport mechanism. Journal of the Geological Society London 131, 653–659.

Smith, D.A., 1966. Theoretical considerations of sealing and non-sealing faults. American Association of Petroleum Geologists Bulletin 50, 363–374.

Smith, D.A., 1980. Sealing and non-sealing faults in Louisiana Gulf Coast Salt Basin. American Association of Petroleum Geologists Bulletin 64, 145–172.

Sneider, R.M., Sneider, J.S., Bolger, G.W., Neasham, J.W., 1997. Comparison of seal capacity determinations; conventional cores vs. cuttings. In: Surdam, R.C. (Ed.), Seals, Traps, and The Petroleum System. American Association of Petroleum Geologists Memoir, vol. 67, pp. 1–12.

Sollie, F., Rodgers, S., 1994. Towards better measurements of logging depth. Society of Professional Well Log Analysts Thirty-Fifth Annual Logging Symposium Transactions 1, D1–D15.

Sperrevik, S., Gillespie, P.A., Fisher, Q.J., Halvorsen, T., Knipe, R.J., 2002. Empirical estimation of fault rock properties. In: Koestler, A.G., Hunsdale, R. (Eds.), Hydrocarbon Seal Quantification. Elsevier, Amsterdam. Norwegian Petroleum Society (NPF) Special Publication, vol. 11, pp. 109–125.

Tindale, K., Newell, N., Keall, J., Smith, N., 1998. Structural evolution and charge history of the Exmouth Sub-basin, Northern Carnarvon Basin, Western Australia. In: Purcell, P.G., Purcell, R.R. (Eds.), The Sedimentary Basins of Western Australia 2: Proceedings of Petroleum Exploration Society of Australia Symposium, Perth, pp. 447–472.

Underschultz, J.R., Otto, C.J., Cruse, T., 2003. Hydrodynamics to assess hydrocarbon migration in faulted strata—methodology and a case study from the Northwest Shelf of Australia. Journal of Geochemical Exploration 78-79, 469–474.

Veevers, J.J., 1988. Morphotectonics of Australia's Northwestern Margin—A Review. In: Purcell, P.G., Purcell, R.R. (Eds.), The North West Shelf Australia: Proceedings of Petroleum Exploration Society of Australia Symposium, Perth, pp. 19–28.

Veneruso A.F., Erlig-Economides C., Petijean L., 1991. Pressure gauge specification considerations in practical well testing. 66th Annual Technical Conference and Exhibition of the Society of Petroleum Engineers. SPE Preprint 22752. Society of Petroleum Engineers, Richardson, Texas, USA, pp. 865–878

Watts, N., 1987. Theoretical aspects of cap-rock and fault seals for single- and two-phase hydrocarbon columns. Marine and Petroleum Geology 4, 274–307.

Yielding, G., 2002. Shale gouge ratio—Calibration by geohistory. In: Koestler, A.G., Hunsdale, R. (Eds.), Hydrocarbon Seal Quantification. Elesevier, Amsterdam. Norwegian Petroleum Society (NPF) Special Publication, 11, vol 67, pp. 1–15.

Yielding, G., Freeman, B., Needham, D.T., 1997. Quantitative fault seal prediction. American Association of Petroleum Geologists Bulletin 81, 897–917.

CSIRO PUBLISHING
www.publish.csiro.au/journals/eg *Exploration Geophysics*, 2008, **39**, 85–93

The hydrodynamics of fields in the Macedon, Pyrenees, and Barrow Sands, Exmouth Sub-basin, Northwest Shelf Australia: identifying seals and compartments*

J. R. Underschultz[1,3] R. A. Hill[2] S. Easton[2]

[1]CSIRO Petroleum, PO Box 1130, Bentley, WA 6102, Australia.
[2]BHP Billiton Petroleum, 152-158 St Georges Terrace, Perth, WA, 6000, Australia.
[3]Corresponding author. Email: james.underschultz@csiro.au

Abstract. The Barrow Group strata (Macedon Member, Pyrenees Member, and Barrow Group sandstones) of the Exmouth Sub-basin host significant accumulations of gas and liquid hydrocarbons. There is currently oil production from the Macedon sandstone at the Enfield Field and ongoing development drilling at the Stybarrow Field. Active appraisal and exploration is underway, including the multi-field Pyrenees Development. In the course of assessing these discoveries, BHP Billiton and its joint-venture partners have undertaken a hydrodynamic study in order to better understand the sealing mechanisms, the position of free-water levels (FWLs), and the likelihood of compartmentalisation within the discoveries.

Whilst the region is faulted with a predominant south-west-north-east grain, the potentiometric gradient is surprisingly flat indicating that the individual sands are hydraulically well connected. Other than the Macedon Gas Field, there is no pressure data that indicate intra-formational seals have been breached. Thus, top and bottom seal capacity is probably not limiting the pool sizes. Rather, structural spill points and fault seal capacity appear the significant factors in determining pool geometry, with the underlying aquifer being regionally connected around fault tips.

On the field-scale, the flat hydraulic gradient allows for the calculated FWLs to have a high confidence. Pressure data from the hydrocarbon phases indicate that in some cases, fault zones may compartmentalise a field into multiple pools. These areas are then targeted for additional focused geological analysis to reduce uncertainty in field compartmentalisation. The Macedon Gas Field, on the eastern edge of the play fairway, marks a change in the trapping character with intra-formational and fault seals having been breached resulting in a single continuous gas pool despite internal structural complexity. Stybarrow and Laverda-Skiddaw clearly occur as separate accumulations and the Stybarrow data define a single oil column in contrast to the potentially compartmentalized Laverda-Skiddaw field. Stybarrow represents an anomalously large oil column relative to other fields in the area and it is located on the low hydraulic head side of a sealing fault.

Key words: hydrodynamics, seal analysis, Exmouth Sub-basin, fault seal, Carnarvon Basin, Barrow Group.

Introduction

The Barrow Group strata (Macedon Member, Pyrenees Member, and Barrow Group sandstones) of the Exmouth Sub-basin host significant hydrocarbon accumulations of gas and liquids. Several discoveries over the past few years extended the play fairway defined initially by the Macedon Gas Field and has prompted a re-evaluation of the hydrocarbon systems therein (Scibiorski et al., 2005). Whilst oil production thus far is from the Macedon sands at the Enfield Field with development drilling at the Stybarrow Field, active exploration and appraisal is also underway for the multi-field Pyrenees sand discoveries. Figure 1 shows the study area and the main fields of interest. An overview of the exploration history for the Pyrenees Member is given by Scibiorski et al. (2005). They also provide a description of the stratigraphy and depositional systems for the late Tithonian to early Berriasian members of the lower Barrow Group. From early on, it was recognised that the trapping mechanisms are complex with a risk of compartmentalisation in the discovered fields. In the course of assessing these discoveries, BHP Billiton and its joint-venture partners have undertaken a hydrodynamic study with CSIRO Petroleum in order to better understand the sealing mechanisms, the position of free-water levels (FWLs), and the likelihood of compartmentalisation within the discoveries. This information guided additional focused geological analyses to further reduce uncertainty in field compartmentalisation.

Hydrodynamic data and methodology

In addition to the existing BHP Billiton geological characterisation, all available formation pressure, salinity, and temperature data was collected from well completion reports and interpreted. A summary of the data available for the study is itemised in Table 1. These data are from 42 wells (Table 2) and have had quality codes attached according to the CSIRO PressureQC methodology (Otto et al., 2001).

To achieve the project objectives the hydrodynamic evaluation was required to characterise the formation water system, the trapped static hydrocarbon phases, and the interactions between the two. Standard hydrodynamic approaches to characterising flow systems in aquifers include the analysis of pressure data, both in vertical profile (e.g. pressure-elevation plots), and within the plane of the aquifer by conversion to hydraulic head. Pressure data are supplemented with formation water analysis and formation

*Presented at the 19th ASEG Geophysical Conference & Exhibition, November 2007.

 10.1071/EG08010 0812-3985/08/020085

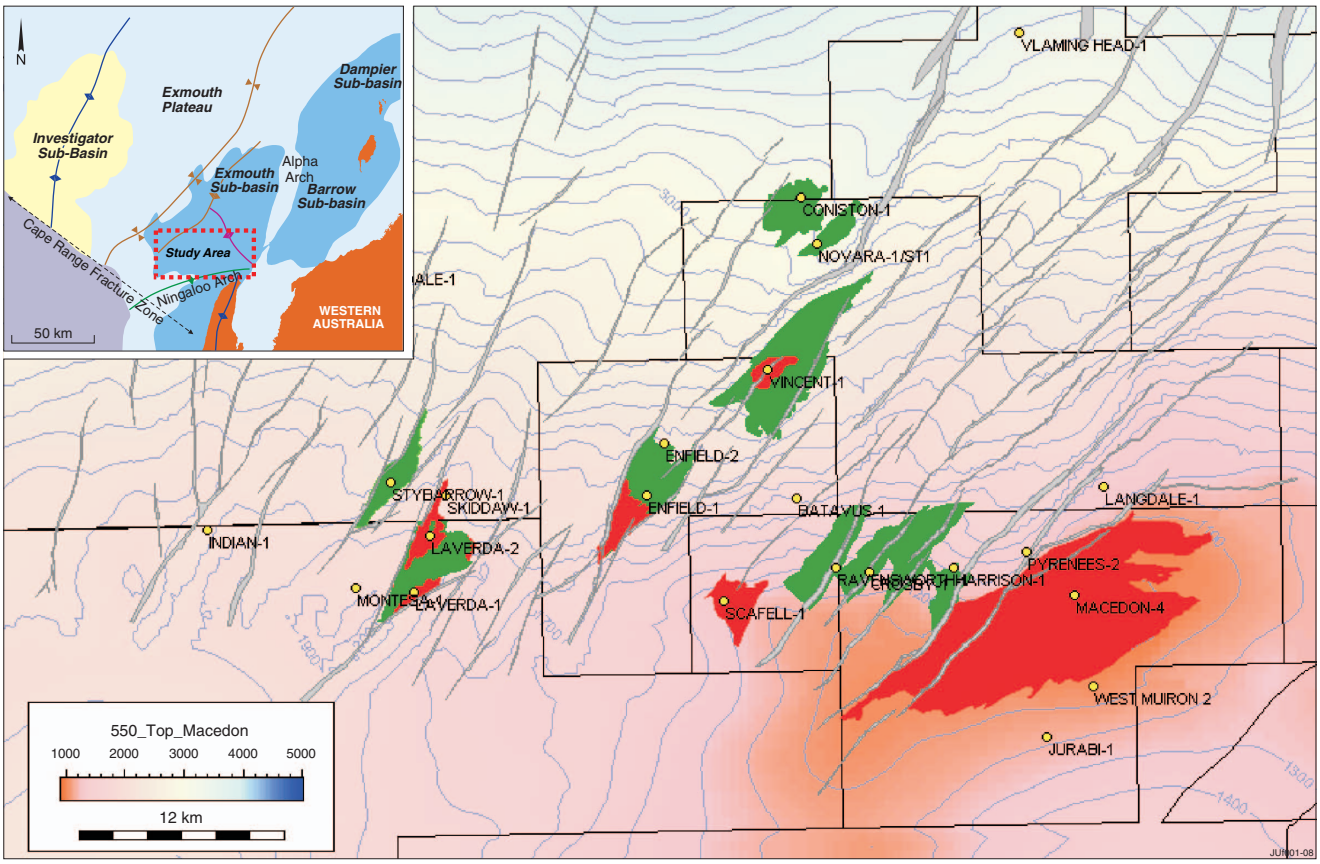

Fig. 1. Study area and depth structure map to Top Macedon Member sandstone.

Table 1. Hydrodynamic data in the study area.
BHT, Bottom-Hole Temperature; DST, Drill-stem Test; WLT, Wireline Test

Pressure and Chemistry Data Points	
DST and Production Tests	8
Formation Interval Tests	0
Wireline Pressure Tests	970
Kicks	1
Formation Water Analyses	13
Salinity Values from petrophysical log analysis	49
Temperature (BHT, DST, WLT, extrapolated BHT)	813

temperature data to aid in the evaluation of the flow system as these parameters can be related to hydrodynamic processes. Bachu and Michael (2002), Otto et al. (2001), Bachu (1995), and Dahlberg (1995) provide an overview of hydrodynamic analysis techniques. Evaluation techniques for the culling and analysis of formation water samples are described by Underschultz et al. (2002), and Hitchon and Brulotte (1994). Techniques for the evaluation of formation temperature are described by Bachu et al. (1995), and Bachu and Burwash (1991). Analysis techniques for hydrodynamic systems in faulted strata are described by Underschultz et al. (2005). Membrane (capillary) seals analysis techniques are discussed by Underschultz (2007) and Brown (2003*a*). Typical depth and gauge error to be expected from modern wireline pressure measurements are described by Brown (2003*b*), Sollie and Rodgers (1994) and Veneruso et al. (1991).

Hydrostratigraphy and pressure/head plots

The three main reservoirs of interest in this evaluation are sandstones within the Macedon and Pyrenees Members and Barrow Group. Muddy or shaly sealing zones that separate the reservoirs can be examined for their seal capacity using vertical pressure profiles if there are sufficient pressure measurements in the sands above and below a seal. Seals with high capacity are expected to correlate with a break in the vertical pressure gradient across the seal, whereas leaky seals would be expected to have little or no break. This is only a qualitative measure of the bulk seal capacity, since a seal may have high capacity but somewhere nearby there may be vertical hydraulic communication (e.g. a fault zone). In this case the pressure profile could reflect the nearby pressure communication.

By examining the vertical pressure profile for all wells with sufficient data, the geographic distribution of the relative seal capacity can be determined for each of the intra-formational seals. For example, Figure 2 shows pressure data at Stybarrow-1. There is a minor pressure break between the Barrow and Pyrenees aquifers. This is difficult to discern from the pressure data but can be observed in the hydraulic head (4 m head change). A more significant pressure break occurs between the Pyrenees and Macedon sands where an oil column is trapped in the latter. The seals above and below the Pyrenees aquifer form an important component to the trapping geometry of the Pyrenees discoveries (Scibiorski et al., 2005). The distribution of the pressure breaks across the study area were mapped and used to define the hydrostratigraphy.

Formation water salinity

It is important to understand the formation water salinity distribution since the density of the formation water changes with salinity, temperature and pressure, and the formation water density is required to calculate hydraulic head. In the event that

Table 2. Wells with hydrodynamic data in the study area.
TD, total depth

Well name	Spud date	Surface longitude	Surface latitude	Datum elevation (m)	Drillers TD (m)
BATAVUS 1	11/06/1999	114.0609138	−21.4913555	30.5	2030
CONISTON 1	26/01/2000	114.0664166	−21.3325	26	1350
CROSBY 1	3/10/2003	114.1022944	−21.5297083	26	1226
CROSBY 2	31/05/2004	114.1186556	−21.5110583	26.3	1718
ENFIELD 1	17/03/1999	113.9770527	−21.4881972	30.5	2192
ENFIELD 2	25/06/1999	113.9868055	−21.460975	30.5	2394.5
ENFIELD 3	11/09/2000	113.9792278	−21.477325	28.3	2521
ENFIELD 4	14/01/2002	113.9922417	−21.4774139	25	2240
ENFIELD 5	11/09/2002	113.9558889	−21.5092472	26.4	2150
ESKDALE 1	14/03/2003	113.826825	−21.3636139	23.5	3127
ESKDALE 2	19/04/2004	113.808725	−21.3755	22	2942
HARRISON 1	22/05/2004	114.1497917	−21.5287306	26	1600
LANGDALE 1	17/04/2005	114.2350306	−21.4872694	26	1518
LAVERDA 1	16/10/2000	113.8446917	−21.537175	28.3	2558
LAVERDA 2	30/11/2002	113.8549611	−21.5077306	22.3	2264
MACEDON 1	14/07/1994	114.1559722	−21.5569222	25	1300
MACEDON 2	1/08/1994	114.2281083	−21.5315611	25	1450
MACEDON 3	28/08/1994	114.1725833	−21.5682611	25	1180
MACEDON 4	11/10/1994	114.2153555	−21.5452222	25	1375
MACEDON 5	10/11/1994	114.2524	−21.5507166	25	1350
NOVARA 1 ST1	23/09/1982	114.0750583	−21.3572111	8	2753
PYRENEES 1	25/01/1994	114.1040416	−21.536475	22.3	1500
PYRENEES 2	28/10/1994	114.1895666	−21.5223194	25	1800
RAVENSWORTH 1	15/07/2003	114.0838306	−21.5275278	26	1432
RAVENSWORTH 2	14/06/2004	114.0926167	−21.5107861	25.45	1459
RESOLUTION 1	24/07/1979	113.6901166	−21.2989944	10.4	3797
RESOLUTION 1 ST1	25/09/1979	113.6901166	−21.2989944	10.4	3883.8
SCAFELL 1	20/02/2000	114.0188944	−21.5454972	26	1500
SKIDDAW 1	8/05/2003	113.8653778	−21.4852389	22	2192
SKIDDAW 1ST1	21/05/2003	113.8653778	−21.4852389	22	2248
STICKLE 1	8/05/2004	114.1277778	−21.5218667	26	1648
STICKLE 2	30/07/2004	114.141375	−21.505525	22	1407
STYBARROW 1	12/02/2003	113.8343194	−21.4778139	22	2477
STYBARROW 2	6/06/2003	113.8222194	−21.4924972	22	2380
STYBARROW 3	18/05/2004	113.8501194	−21.4649028	22	2522
STYBARROW 4	4/06/2004	113.8501194	−21.4649028	22	2500
VAN GOGH 1 ST1	20/09/2003	114.0825222	−21.389625	26	1526
VINCENT 1	18/12/1998	114.0460055	−21.4230361	22	1560
VINCENT 2	26/05/1999	114.0462138	−21.4374361	30.5	1490
WEST MUIRON 3	21/10/1992	114.2187888	−21.5683388	26.5	1200
WEST MUIRON 4	3/05/1993	114.2016	−21.5428888	26.5	1550
WEST MUIRON 5	23/06/1993	114.1469111	−21.5493111	26.5	1526

there are large formation water density variations within a dipping aquifer, buoyancy forces may become an important driving force which influences formation water movement (Bachu and Michael, 2002).

The region of interest has a relatively small formation water analysis dataset and many of the water samples appear to be contaminated to various degrees with drilling fluids, making the salinity measurement unreliable. These, however, can be supplemented with petrophysical log-derived salinity, which are based on the formation water resistivity. In addition, if enough vertical pressure measurements are available from within an aquifer, the vertical pressure gradient can be used to calculate the formation water density. This assumes that there is no vertical component to fluid flow (Underschultz et al., 2002). There were 52 occasions where sufficient pressure data was available from within an aquifer to estimate a formation water density. The calculated water pressure gradients range between 1.38 and 1.47 psi m^{-1} (9.52 and 10.14 kPa m^{-1}) with both the highest frequency and arithmetic average being 1.43 psi m^{-1} (9.86 kPa m^{-1}). This corresponds to a formation water salinity of ~40 000 mg L^{-1}. Hydraulic head values were calculated using a water hydrostatic gradient of 1.43 psi m^{-1} (9.86 kPa m^{-1}) for the study.

In areas where the hydrostatic gradient diverges from 1.43 psi m^{-1} (9.86 kPa m^{-1}) (e.g. Laverda-2, Figure 3) there are three possible interpretations. First, the formation water density is significantly different (due to a temperature or salinity anomaly) and the hydrostatic gradient of 1.43 psi m^{-1} (9.86 kPa m^{-1}) is locally incorrect. Second, minor intra-formational heterogeneities define minor vertical pressure breaks between individual sandstones. Third, there is a vertical component to flow.

Hydraulic head distributions

The main force that drives formation water flow in the basin is compaction (Bekele et al., 2001). As the sedimentary pile compacts, it dewaters. Formation water moves vertically out of the mud and shale horizons into adjacent sand horizons where it migrates parallel to bedding and then to eventual discharge at the sea bed. Otto et al. (2001) show that there is hydraulic communication between the Barrow and Exmouth Sub-basins

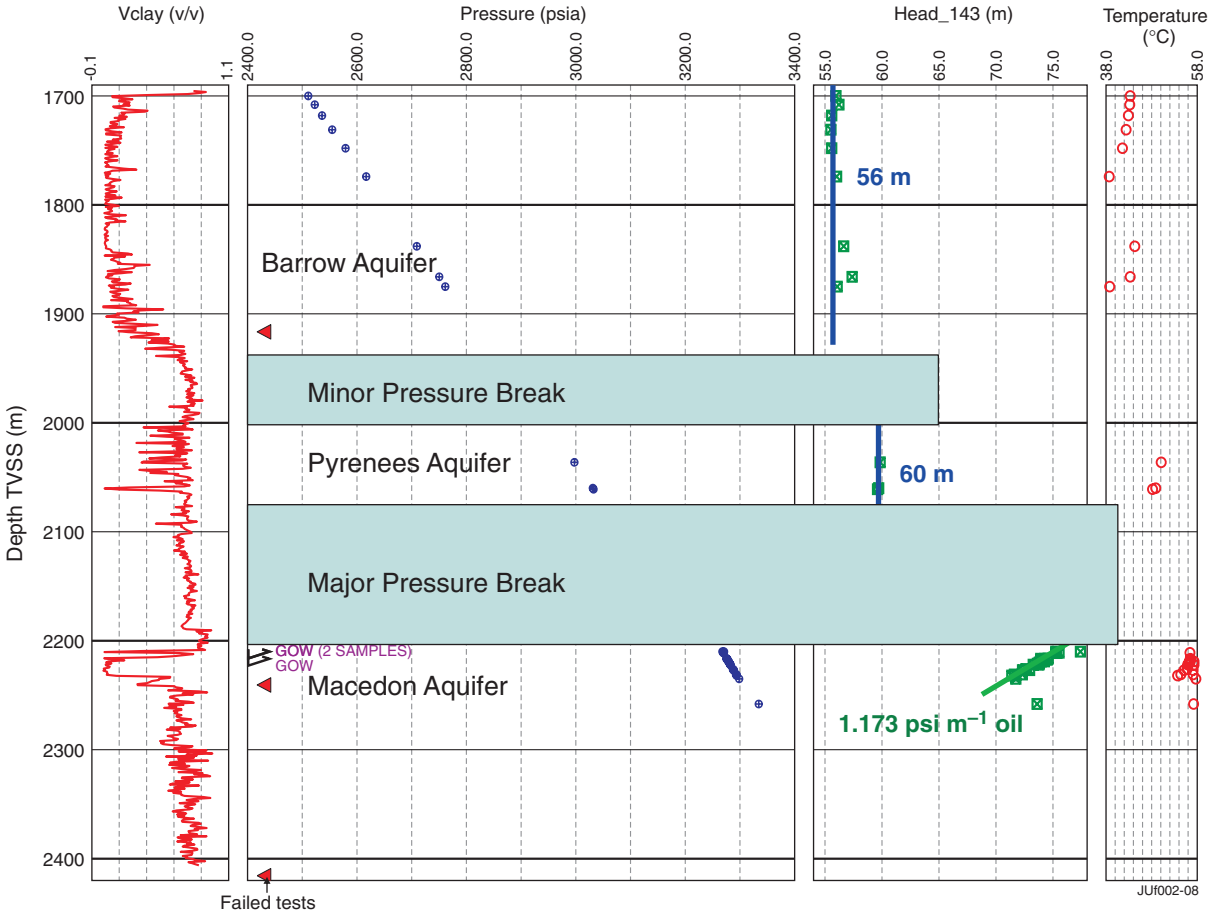

Fig. 2. Stybarrow 1 V-Clay log with pressure, hydraulic head and temperature plotted with depth. Solid red arrowheads indicate the location of failed pressure tests, and open black arrowheads indicate fluid sample recoveries.

within the Barrow Group strata. Hennig et al. (2002) show that the Barrow aquifer system in the Barrow Sub-basin (north of this study area) has the lowest hydraulic heads, that is the ultimate sink for dewatering compaction-driven fluid flow and they surmise that this system eventually discharges to the sea bed in the northern part of the greater Carnarvon Basin. This regional context of the Barrow Group hydrogeology in the Carnarvon Basin provides a framework in which to examine the pressure data of the Barrow Group Sands for this study.

To map the distribution of hydraulic head for any particular aquifer in the study area, consideration needs to be made of the data distribution relative to the location and size of faults that cut the aquifer. In this case, the frequency of faulting is greater than the frequency of the well data, and the wells tend to be clustered. This makes an interpretation of the hydraulic head distribution for any particular aquifer difficult and non-unique. However, some faults have significantly more throw than others. When contouring the hydraulic head, it was assumed that faults with larger throw have a greater chance of representing a discontinuity than smaller ones. As described by Underschultz et al. (2005), where sufficient data exist in a fault block, a hydraulic head gradient can be defined (i.e. the slope of the hydraulic head distribution) and thus the regional aquifer model is built up in a patchwork fashion.

The hydrodynamic model developed for the area of interest has important application to understanding the pressure distributions within specific field areas. At some locations, pressure data may only be available from the hydrocarbon column. Here, the pressure in the underlying aquifer can be estimated from the hydrodynamic model and then used to estimate the free-water level. Since the overall variation in hydraulic head is so low, despite the paucity of data, estimates of head from the hydrodynamic model have a low uncertainty (normally within 2 or 3 m).

Macedon Member sandstone aquifer

The hydraulic head in the Macedon Member is constrained by 18 wells that sample pressure in the aquifer. Values range from 55 to 71 m (Figure 4) making the gradients across the region very slight considering that typical gauge/depth error is equal to ~3 m of hydraulic head (~4–5 psi). The contours are dashed to reflect the high degree of uncertainty given the frequency of faulting and lack of data control. In the Laverda/Skiddaw and Crosby/Stickle areas there is sufficient data to locally define decreasing hydraulic head towards the north-east. In the Macedon region there appears to be a change in flow direction with a gradient decreasing towards the south-east. The largest change in hydraulic head over a short distance occurs between the Stybarrow and Skiddaw fields where there is a 10 m hydraulic head discontinuity across the separating fault. This suggests that the fault zone that defines the east boundary of the Stybarrow Field is not only sealing to the hydrocarbons, but is also a barrier to formation water in the aquifer at the base of the pool. In other areas where data are sparse, a hydraulic gradient is assumed to be in a similar south-west to north-east direction parallel to the main structural grain.

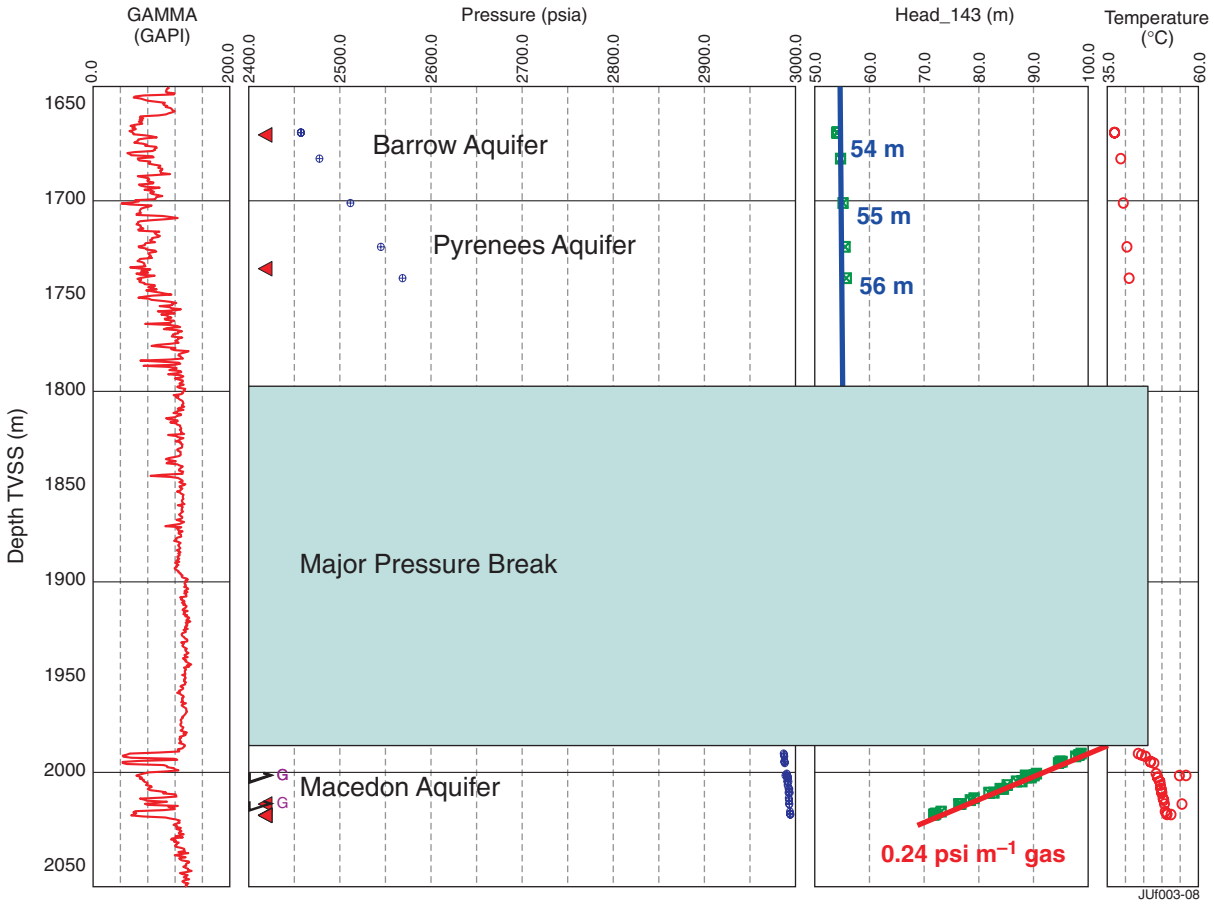

Fig. 3. Laverda 2 Gamma log with pressure, hydraulic head and temperature data plotted with depth. Solid red arrowheads indicate the location of failed pressure tests and open black arrowheads indicate fluid sample recoveries.

Pyrenees Member sandstone aquifer

The Pyrenees Member aquifer has water pressure data from 19 wells in the study area. With the exception of Laverda-2 (hydraulic head of 55 m) hydraulic head values range from 59 to 65 m resulting in a nearly flat potentiometric surface. This suggests that the aquifer has extremely good horizontal hydraulic transmissivity despite the large number of faults that cut it. Although slight, there is a hydraulic gradient from north-east to south-west across most of the area and a more southerly-directed gradient in the Ravensworth/Stickle region.

The low hydraulic head at Laverda-2 may be related to vertical hydraulic communication with the overlying Barrow Group aquifer system. The pressure plot for Stybarrow-1 (Figure 2) identifies a shale/mudstone zone on the V-clay log between the Barrow and Pyrenees sandstones, which is likely to constitute a sealing horizon. It corresponds to a difference of 4 m head between the two aquifers at that location. At Laverda 2, this seal is locally absent and the hydraulic head in the two aquifers is nearly the same (Figure 3).

Barrow Group sandstone aquifer

The stratigraphic nomenclature for the upper part of the Barrow Group is not completely consistent in the well completion reports for the area of interest. Data that was allocated to the 'Barrow Aquifer' include not only Barrow sandstones data specifically, but also any data for the Barrow Group and equivalent strata that occurs above the Pyrenees and Macedon Members.

The hydraulic head distribution for the Barrow Group Aquifer is controlled by data from 17 wells ranging between 53 and 64 m of head. There is a general decrease in hydraulic head from east to west and there is sufficient data to define a south-west-directed gradient locally in the Enfield and Laverda/Stybarrow areas.

Formation water flow relative to subcrop at the intra-hauterivian unconformity

The three reservoirs of interest (Barrow, Pyrenees, and Macedon sandstones) all subcrop against the base of the Muderong (Intra-Hauterivian Unconformity). In some cases the subcrop forms a trapping mechanism (such as for the Pyrenees Ravensworth Field). Here the formation water flow direction is away from subcrop. In other cases, fields near the subcrop are actually fault controlled (such as for the Macedon Sandstone in the Stybarrow Field). Here the formation water flow system is locally directed towards the subcrop. The presence or lack of hydraulic communication along the subcrop edge between adjacent subcropping units relates to the trapping mechanism at the subcrop. The character of this hydraulic communication can be inferred from the local formation water flow direction.

Field areas and their inter-relations

Individual fields are best characterised with a combination of multi-well pressure-elevation (or head-elevation) plots and a potentiometric surface for the aquifer. The hydraulic head maps set the context in which each field can be examined in detail. Individual fields are characterised in terms of a best estimate for the FWL, free oil level, and the likelihood of compartmentalisation. Whilst this was done for each of the fields in the study area, only selected examples are

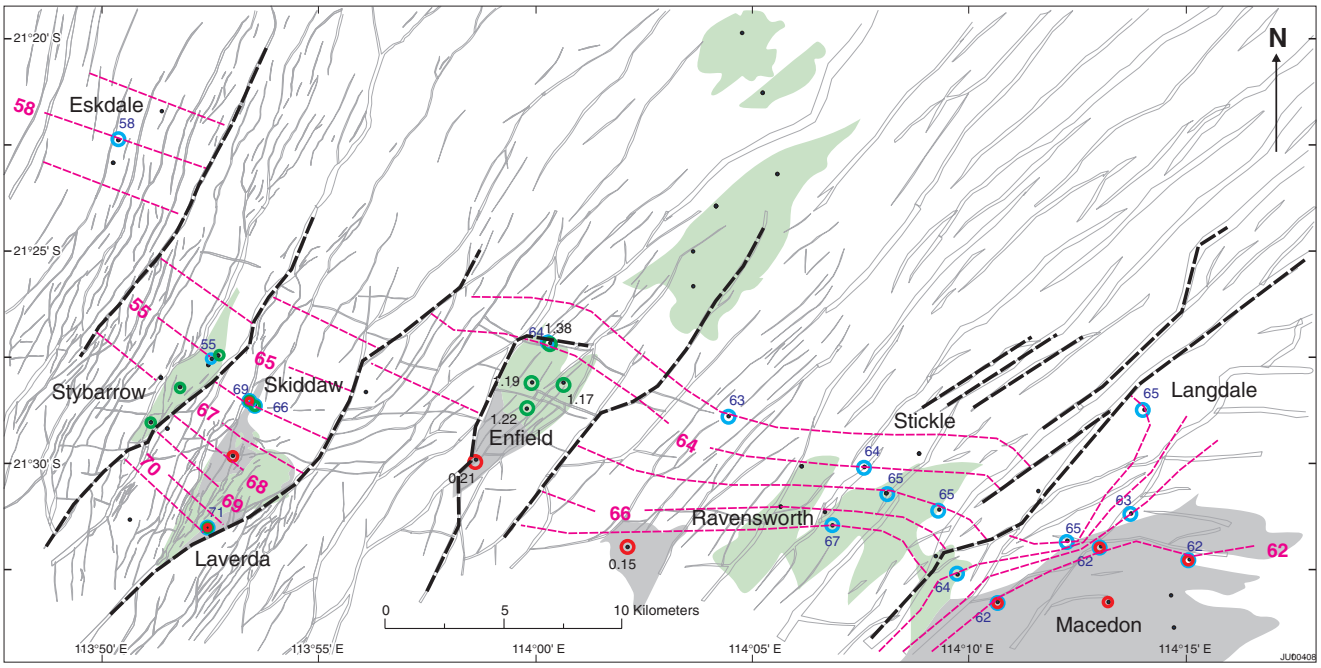

Fig. 4. Hydraulic head (m above sea level) distribution for the Macedon Sand Aquifer. Wells are depicted as black dots for which hydraulic head data is posted with open blue circles, gas pressure gradient values are posted with open red circles and oil pressure gradient values are posted with open green circles.

described that demonstrate the variable trapping styles and sealing characteristics of the region. These show how the hydrodynamic analysis can be used to identify compartmentalisation risk. The high-risk areas are then targeted for additional focused geological analysis to reduce uncertainty in field compartmentalisation.

Laverda-Skiddaw Oil and Gas Field

The Laverda-Skiddaw wells have pressure data in the Pyrenees and Macedon sandstones; however, hydrocarbons are restricted to the Macedon sandstone with the Pyrenees sandstone being water saturated. Macedon sandstone pressure data from the two Laverda and two Skiddaw wells, when plotted with elevation, can be interpreted to represent a continuous oil phase supporting three separate gas caps (Figure 5). When the same data is converted to hydraulic head and plotted with elevation, more detail can be observed with the position of the FWLs (Figure 6). From this plot, it becomes more obvious where the inflection points are between the water and oil gradients (the FWLs), but it also appears that the data do not strictly define a common oil gradient. There are two end member interpretations of the data: 1) the differences in the pressure gradients between wells are real, and the data represent three separate hydrocarbon pools; or 2) differences in the pressure gradients between wells are attributed

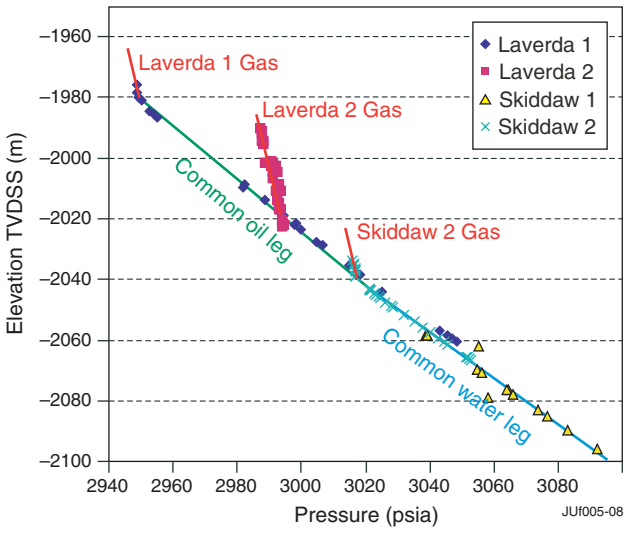

Fig. 5. Macedon Member sandstone pressure-elevation plot for Laverda/Skiddaw wells.

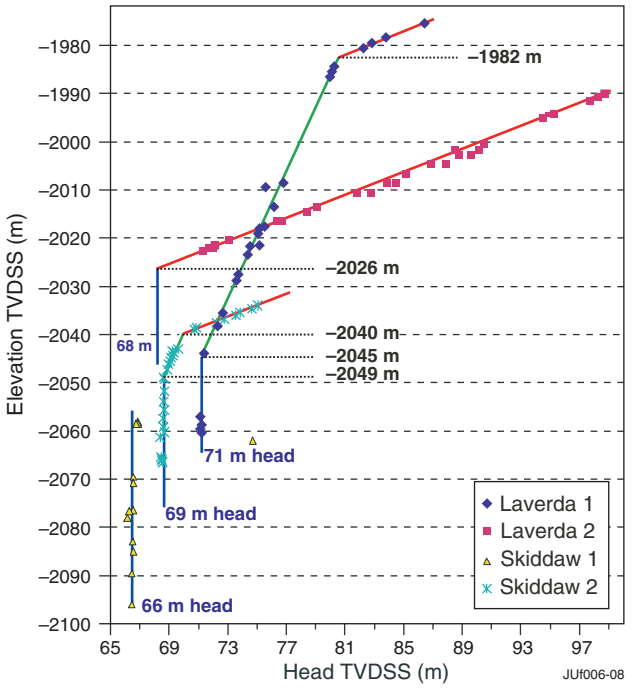

Fig. 6. Macedon Member sandstone head-elevation plot for Laverda-Skiddaw wells.

to depth and gauge error and the data can be corrected so that they converge and define three gas caps with a common oil leg and a common aquifer.

If the data are taken as correct, Laverda-1 would define a pool with an oil leg and a gas cap. The FWL is estimated to be at 2045 m tvdss and the gas-oil contact is estimated to be at 1982 m tvdss. Laverda-2 defines a gas pool with no constraint on the formation water; however a hydraulic head of 68 m is inferred from the hydrodynamic model (Figure 4) which results in an estimated FWL at 2026 m tvdss. Skiddaw-2 (sometimes referred to as Skiddaw-1ST1) defines a separate oil pool with a gas cap. In this case, the FWL is estimated to be at 2049 m tvdss and the gas-oil contact is estimated to be at 2040 m tvdss.

If the data are assumed to be subject to gauge and depth error, they can be collapsed onto a single oil pressure gradient (Figure 7). This requires a shift of Laverda-1 pressure data by 6.7 psi (46.2 kPa) and Skiddaw-2 data by 3.1 psi (21.4 kPa). As a result the FWL is interpreted at 2049 m tvdss with a common oil phase supporting three separate gas caps, with gas-oil contacts in Laverda-1, Laverda-2, and Skiddaw-2 at 1982 m tvdss, 2024 m tvdss, and 2040 m tvdss, respectively.

The two alternate interpretations of the pressure data from the Laverda-Skiddaw wells highlight the common issue in the interpretation of multi-well pressure data and obviously have significant implications on the expected connectivity and size of hydrocarbon pools. Other geological data, including in-situ stress analysis and 3D seismic interpretation of the Macedon reservoir was used to provide additional information to assess the alternative hydrodynamic models. In this case the additional analysis suggested that the pressure variations between wells are most likely due to a combination of gauge and depth errors and the risk of compartmentalisation of the field is thought to be low.

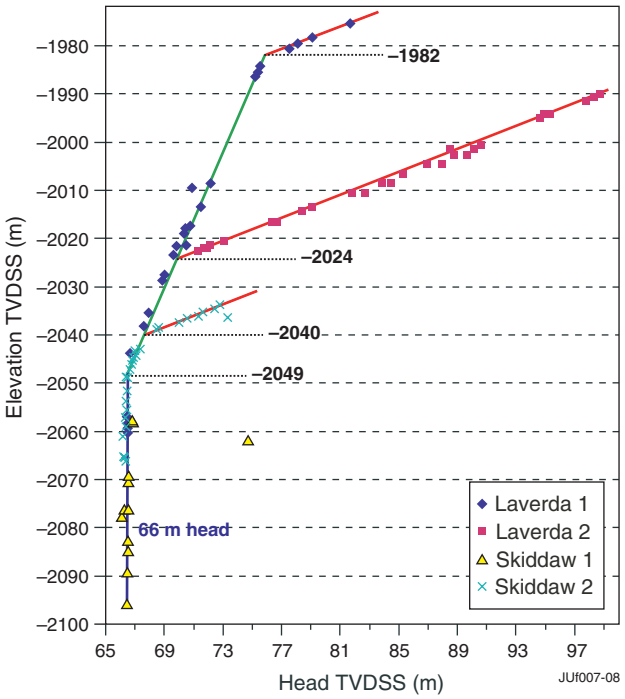

Fig. 7. Macedon Member sandstone head-elevation plot for Laverda-Skiddaw wells with the data collapsed to a common oil gradient.

Stybarrow Oil Field

The Stybarrow Field is located just west of Laverda-Skiddaw (Figure 1) and contains four wells with pressure data located across several horizons, but the hydrocarbons are reservoired in the Macedon Sandstone (Ementon et al., 2004). Figure 8 shows a hydraulic head-elevation plot with both the Stybarrow and Laverda-Skiddaw data from the Macedon Sandstone. Stybarrow and Laverda-Skiddaw clearly occur as separate accumulations and the Stybarrow data define a single oil column in contrast to the potentially compartmentalised Laverda-Skiddaw field.

A FWL is estimated at 2333 m tvdss with the Stybarrow-1, -2, -3 and -4 data all falling within 2.5 psi (17.2 kPa) of a common oil gradient across 294 m vertically. The Stybarrow data convincingly define a single continuous oil pool. By comparison, the Laverda-Skiddaw data are much less certain, as discussed above. The Stybarrow oil column is anomalously large in comparison to column heights for other fields in the region (e.g. Figure 8). Underschultz (2007) shows that the total membrane seal capacity of a fault is greater for a hydrocarbon accumulation located on the low hydraulic head side of a fault seal. The fault that seals the Stybarrow Field and separates it from the Skiddaw system to the south-east, exhibits the largest across fault head difference (10 m) of the study area, and Stybarrow is located on the low hydraulic head side. This, together with the lack of a gas cap, may explain the apparently larger seal capacity of the Stybarrow bounding fault.

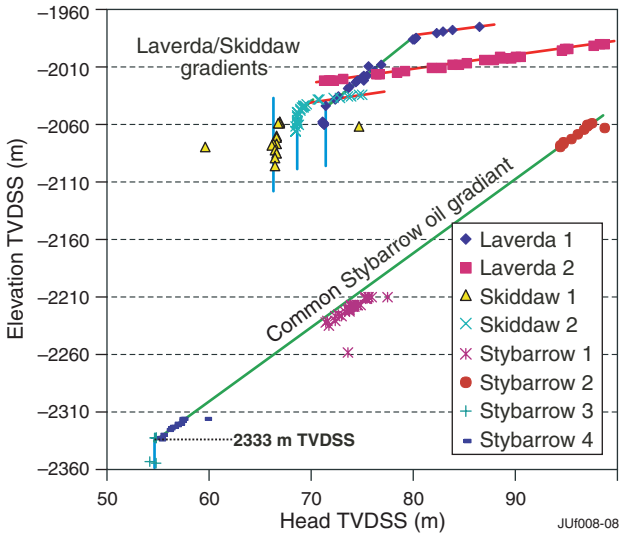

Fig. 8. Head-elevation plot for Macedon Member sandstone data from Stybarrow, Laverda and Skiddaw wells.

Macedon Gas Field

The Macedon Gas Field (Figure 1) has been studied previously by Bailey et al. (2006). It is reviewed here in relation to how the pressure data from Macedon compares with surrounding well data (Figure 9). The difference at the Macedon Field is that the lower Barrow Group intra-formational seals are either not present or have been breached. Data from seven wells define the gas column at Macedon and they all fall within ±2 psi (13.8 kPa) of a single pressure gradient. Data from Macedon-2 and West Muiron-4, from the north-west edge of the Macedon Field, have slightly higher hydraulic head in the aquifer and this changes the position of the FWL accordingly at these wells (see Bailey et al., 2006).

Other wells near the Macedon Field define separate hydrocarbon accumulations. The Langdale-1 pressure data

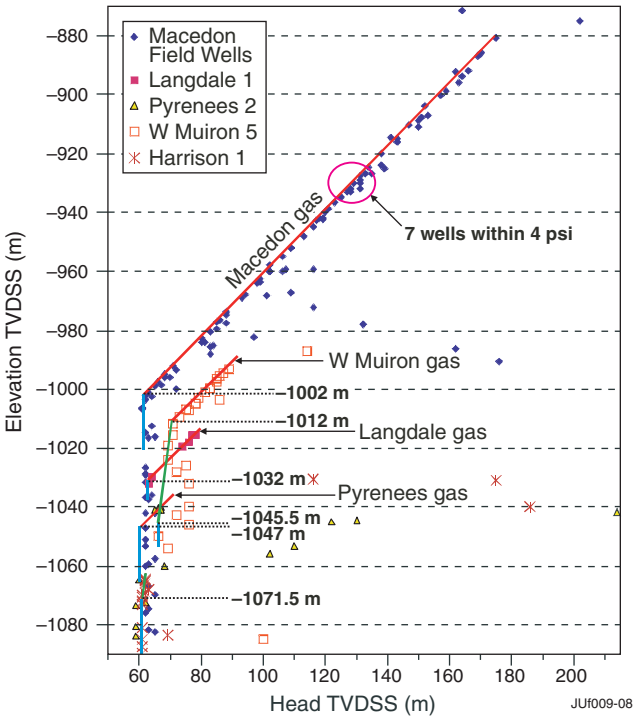

Fig. 9. Head-elevation plot for the Macedon Gas Field and adjacent wells.

define a gas column (Figure 9). The hydraulic head in the aquifer is estimated from the hydrodynamic model to be 62.5 m resulting in a predicted FWL of 1032 m tvdss. Similarly, the Pyrenees-2 gas column (Pyrenees sandstone) forms a separate pool with a FWL estimated at 1047 m tvdss. The West Muiron-5 data (Pyrenees sandstone) define a gas-oil contact at 1012 m tvdss; however, the pressure data below this elevation become poor quality and are scattered. Petrophysical analysis suggests the FWL is between 1045.5 and 1055.4 m tvdss. Finally, the pressure data from Harrison-1 (Pyrenees sandstone) define an oil column with a FWL estimated at 1071.5 m tvdss.

Conclusions

For each of the reservoirs examined (Macedon Member, Pyrenees Member, and Barrow Group sandstones), the hydraulic gradient in the aquifer is very flat with values ranging between 55 and 69 m of hydraulic head, and large regions with nearly flat hydraulic gradients. This indicates that the aquifers have excellent regional hydraulic conductivity. Vertical hydraulic communication between sands is variable with intra-formational seals affording seal capacity defined by breaks in the pressure gradient. At some locations such as Laverda-2 the intra-formational seal is locally absent and vertical hydraulic communication exists.

The frequency of faults cross-cutting the aquifer is generally greater than the frequency of pressure control points in the dataset. In local areas where there is sufficient data control to establish a hydraulic gradient within a fault block, the gradient tends to be roughly parallel with the south-west to north-east structural grain. In some cases (e.g. Stybarrow and Enfield) there is a divergence of flow with a portion of the flux heading south-west towards the subcrop edge beneath the Intra-Hauterivian Unconformity, and a portion of the flux heading north or north-east towards the basin-centred low hydraulic head. In other cases (e.g. the Pyrenees subcrop traps) the flow direction is northwards away from the subcrop.

Other than the Macedon Gas Field, there are no cases where the pressure data indicate a continuous hydrocarbon column between the Macedon, Pyrenees, and Barrow reservoirs. This suggests that where they exist, the intervening sealing horizons are water saturated and they are not controlling pool size by seal capacity (i.e. via top or bottom seal breach). In addition, the vertical seal capacity does not appear to be compromised by faulting in the sense of up-fault leakage. Rather, structural spill points and across-fault seal issues appear to be more important. The Macedon Gas Field marks a change in seal characteristics where a continuous hydrocarbon phase occurs across multiple reservoir horizons and the inter-formational seals appear to have been breached (Bailey et al., 2006). The anomalously large hydrocarbon column at Stybarrow, relative to other fields of the region, is related to the lack of a gas cap and the increased total membrane fault seal capacity on the low hydraulic head side of a fault with a large across fault hydraulic head contrast.

The use of hydrodynamic analysis proved to be a successful approach for identifying fault seal issues that pose a risk of compartmentalisation. These were then subject to additional focused geological evaluation to further constrain the uncertainty in the risk of field compartmentalisation.

Acknowledgments

The authors acknowledge BHPB Petroleum and its join venture partners for funding this work and approving it to be published. This paper has benefited from technical review by Grant Ellis and Mark Stevens.

References

Bachu, S., 1995, Flow of variable-density formation water in deep sloping aquifers: review of methods of representation with case studies: *Journal of Hydrology*, **164**, 19–38. doi: 10.1016/0022-1694(94)02578-Y

Bachu, S., and Burwash, R. A., 1991, Regional-scale analysis of the geothermal regime in the Western Canada Sedimentary Basin: *Geothermics*, **20**, 387–407. doi: 10.1016/0375-6505(91)90028-T

Bachu, S., and Michael, K., 2002, Flow of variable-density formation water in deep sloping aquifers: minimizing the error in representation and analysis when using hydraulic-head distributions: *Journal of Hydrology*, **259**, 49–65. doi: 10.1016/S0022-1694(01)00585-6

Bachu, S., Ramon, J. C., Villegas, M. E., and Underschultz, J. R., 1995, Geothermal regime and thermal history of the Llanos Basin, Colombia: *The American Association of Petroleum Geologists Bulletin*, **79**, 116–129.

Bailey, R. W., Underschultz, J., Dewhurst, D., Kovack, G., Mildren, S., and Raven, M., 2006, Multi-disciplinary approach to fault and top seal appraisal; Pyrenees-Macedon oil and gas fields, Exmouth Sub-basin, Australian Northwest Shelf: *Marine and Petroleum Geology*, **23**, 241–259. doi: 10.1016/j.marpetgeo.2005.08.004

Bekele, E. B., Johnson, M., and Higgs, W., 2001, Numerical modelling of overpressure generation in the Barrow Sub-basin, Northwest Australia: *Australian Petroleum Production and Exploration Association Journal*, **41**, 595–607.

Brown, A., 2003*a*, Capillary effects on fault-fill sealing: *The American Association of Petroleum Geologists Bulletin*, **87**, 381–395.

Brown, A., 2003*b*, Improved interpretation of wireline pressure data: *The American Association of Petroleum Geologists Bulletin*, **87**, 295–311.

Dahlberg, E. C., 1995, Applied hydrodynamics in petroleum exploration: Second edition edn: Springer-Verlag.

Ementon, N., Hill, R., Flynn, M., Motta, B., and Sinclair, S., 2004, Stybarrow oil field – from seismic to production, the integrated story so far: SPE paper 88574, SPE Asia Pacific Oil and Gas Conference Perth 2004.

Hennig, A., Underschultz, J. R., and Otto, C. J., 2002, Hydrodynamic analysis of the Early Cretaceous aquifers in the Barrow Sub-basin in relation to hydraulic continuity and fault seal. *In* M. Keep and S. J. Moss eds., The Sedimentary Basins of Western Australia 3: Proceedings of the Petroleum Exploration Society of Australia Symposium; Perth, WA, 305–320.

Hitchon, B., and Brulotte, M., 1994, Culling criteria for "standard" formation water analyses: *Applied Geochemistry*, **9**, 637–645. doi: 10.1016/0883-2927(94)90024-8

Otto, C., Underschultz, J., Hennig, A., and Roy, V., 2001, Hydrodynamic analysis of flow systems and fault seal integrity in the Northwest Shelf of Australia: *Australian Petroleum Production and Exploration Association Journal*, **41**, 347–365.

Scibiorski, J. P., Micenko, M., and Lockhart, D., 2005, Recent discoveries in the Pyrenees Member, Exmouth sub-Basin: A new oil play fairway: *Australian Petroleum Production and Exploration Association Journal*, **45**, 233–251.

Sollie, F., and Rodgers, S., 1994, Towards better measurements of logging depth: Society of Professional Well Log Analysts Thirty-Fifth Annual Logging Symposium Transactions. D1–D15.

Underschultz, J. R., 2007, Hydrodynamics and membrane seal capacity: *Geofluids*, **7**, 148–158. doi: 10.1111/j.1468-8123.2007.00170.x

Underschultz, J. R., Ellis, G. K., Hennig, A. L., Bekele, E., and Otto, C. J., 2002, Estimating Formation Water Salinity from Wireline Pressure Data: Case Study in the Vulcan Sub-basin *In* M. Keep and S. J. Moss eds., The Sedimentary Basins of Western Australia 3: Proceedings of the Petroleum Exploration Society of Australia Symposium; Perth, WA, 285–303.

Underschultz, J. R., Otto, J. C., and Bartlett, R., 2005, Formation fluids in faulted aquifers: examples from the foothills of Western Canada and the North West Shelf of Australia. *In* P. Boult and J. Kaldi eds., evaluating fault and cap rock seals. *American Association of Petroleum Geologists, Hedberg Series*, **2**, 247–260.

Veneruso, A. F., Erlig-Economides, C., and Petijean, L., 1991, Pressure gauge specification considerations in practical well testing: 66th Annual Technical Conference and Exhibition of the Society of Petroleum Engineers; Dallas, Texas. 865–878.

Manuscript received 23 September 2007; manuscript accepted 29 January 2008.

Environ Geol
DOI 10.1007/s00254-007-0941-1

ORIGINAL ARTICLE

Site characterisation of a basin-scale CO_2 geological storage system: Gippsland Basin, southeast Australia

C. M. Gibson-Poole · L. Svendsen · J. Underschultz · M. N. Watson · J. Ennis-King · P. J. van Ruth · E. J. Nelson · R. F. Daniel · Y. Cinar

Received: 31 May 2006 / Accepted: 31 January 2007

Abstract Geological storage of CO_2 in the offshore Gippsland Basin, Australia, is being investigated by the Cooperative Research Centre for Greenhouse Gas Technologies (CO2CRC) as a possible method for storing the very large volumes of CO_2 emissions from the nearby Latrobe Valley area. A storage capacity of about 50 million tonnes of CO_2 per annum for a 40-year injection period is required, which will necessitate several individual storage sites to be used both sequentially and simultaneously, but timed such that existing hydrocarbon assets will not be compromised. Detailed characterisation focussed on the Kingfish Field area as the first site to be potentially used, in the anticipation that this oil field will be depleted within the period 2015–2025. The potential injection targets are the interbedded sandstones of the Paleocene-Eocene upper Latrobe Group, regionally sealed by the Lakes Entrance Formation. The research identified several features to the offshore Gippsland Basin that make it particularly favourable for CO_2 storage. These include: a complex stratigraphic architecture that provides baffles which slow vertical migration and increase residual gas trapping and dissolution; non-reactive reservoir units that have high injectivity; a thin, suitably reactive, lower permeability marginal reservoir just below the regional seal providing mineral trapping; several depleted oil fields that provide storage capacity coupled with a transient production-induced flow regime that enhances containment; and long migration pathways beneath a competent regional seal. This study has shown that the Gippsland Basin has sufficient capacity to store very large volumes of CO_2. It may provide a solution to the problem of substantially reducing greenhouse gas emissions from future coal developments in the Latrobe Valley.

Keywords CO_2 · Storage · Gippsland Basin · Australia

C. M. Gibson-Poole (✉) · L. Svendsen · J. Underschultz · M. N. Watson · J. Ennis-King · P. J. van Ruth · R. F. Daniel · Y. Cinar
Cooperative Research Centre for Greenhouse Gas Technologies (CO2CRC), GPO Box 463, Canberra, ACT 2601, Australia
e-mail: cgibsonp@asp.adelaide.edu.au

C. M. Gibson-Poole · L. Svendsen · M. N. Watson · P. J. van Ruth · E. J. Nelson · R. F. Daniel
Australian School of Petroleum,
The University of Adelaide,
Adelaide, SA 5005, Australia

J. Underschultz
CSIRO Petroleum, PO Box 1130, Bentley,
WA 6102, Australia

J. Ennis-King
CSIRO Petroleum, Private Bag 10,
Clayton South, VIC 3169, Australia

Y. Cinar
School of Petroleum Engineering,
The University of New South Wales,
Sydney, NSW 2052, Australia

Introduction

Eighty-five percent of the electricity for the State of Victoria, southeast Australia, is generated from power stations fuelled by the extensive brown coal resources of the Latrobe Valley (DPI 2005). Whilst coal is a cheap source of energy, demand for electricity is increasing and there is concern over the contribution of greenhouse gases to the atmosphere from fossil fuel combustion. Thus, geological storage of carbon dioxide (CO_2) is being investigated by the Cooperative Research Centre for Greenhouse Gas Technologies (CO2CRC) as a possible method for storing the very large

volumes of CO_2 emissions anticipated from proposed new coal developments in the Latrobe Valley area.

A possible sink for this large source of CO_2 is the neighbouring offshore Gippsland Basin (Fig. 1), which is one of Australia's premier hydrocarbon provinces and has been producing since the 1960s. The depletion and decommissioning of some of the major oil fields is likely to coincide with the need for storage of anticipated CO_2 emissions from new coal developments in the Latrobe Valley. Enhanced oil recovery using CO_2 is not being considered by the operators for the oil fields at present, since primary recoveries are already very high.

A storage capacity of about 50 million tonnes per annum (Mt/a) for a minimum 40-year injection period is required, which provides a significant challenge of scale not previously considered. One single site will not be able to accommodate a source of this magnitude individually, so a regional solution must be found. To meet this challenge, several individual storage sites within the offshore Gippsland Basin will need to be utilised both sequentially and simultaneously.

Location and geological setting

The Gippsland Basin is an east–west trending rift basin, located in southeastern Australia, offshore from the Victorian coast (Fig. 1). It is a fairly symmetrical rift basin (Central Deep), bounded to the north and south by faulted terraces (Northern and Southern Terraces) and stable platforms (Northern and Southern Platforms) (Bernecker and Partridge 2001; Power et al. 2001) (Fig. 1).

Rifting began in the Early Cretaceous in association with the continental break-up of Gondwana along the southern margin of Australia (Rahmanian et al. 1990; Power et al. 2001). By the latest Cretaceous a post-rift marginal sag basin had developed and the upper Latrobe Group sediments (Halibut and Cobia Subgroups) were deposited under the increasing influence of the Tasman Sea, which encroached from the southeast (Fig. 2) (Rahmanian et al. 1990). The interbedded sandstones, shales and coal were deposited in alluvial plain, coastal plain, shoreface and shelf depositional environments along wave-dominated shorelines (Rahmanian et al. 1990; Thomas et al. 2003). Through the Palaeocene and Eocene the shoreline retreated to the west and northwest, and culminated in the deposition of the condensed, glauconitic Gurnard Formation as the siliciclastic sediment supply became starved (Fig. 2) (Rahmanian et al. 1990).

The transition from the Latrobe Group to the Seaspray Group is marked by a regional angular unconformity, informally termed the 'Latrobe Unconformity', created by a marked decline in the sediment supply and several separate erosional events (Fig. 2) (Rahmanian et al. 1990;

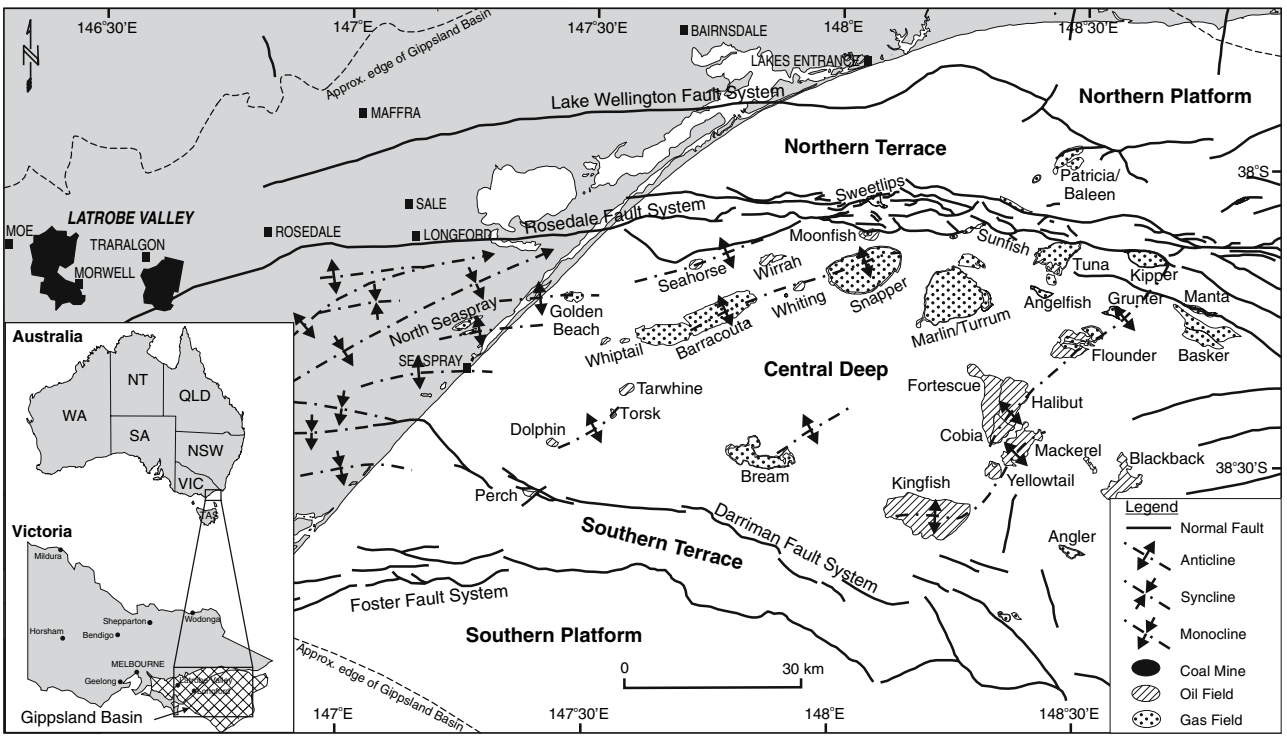

Fig. 1 Location map of the Gippsland Basin, southeast Australia, showing key tectonic elements and existing hydrocarbon fields (modified after Power et al. 2001)

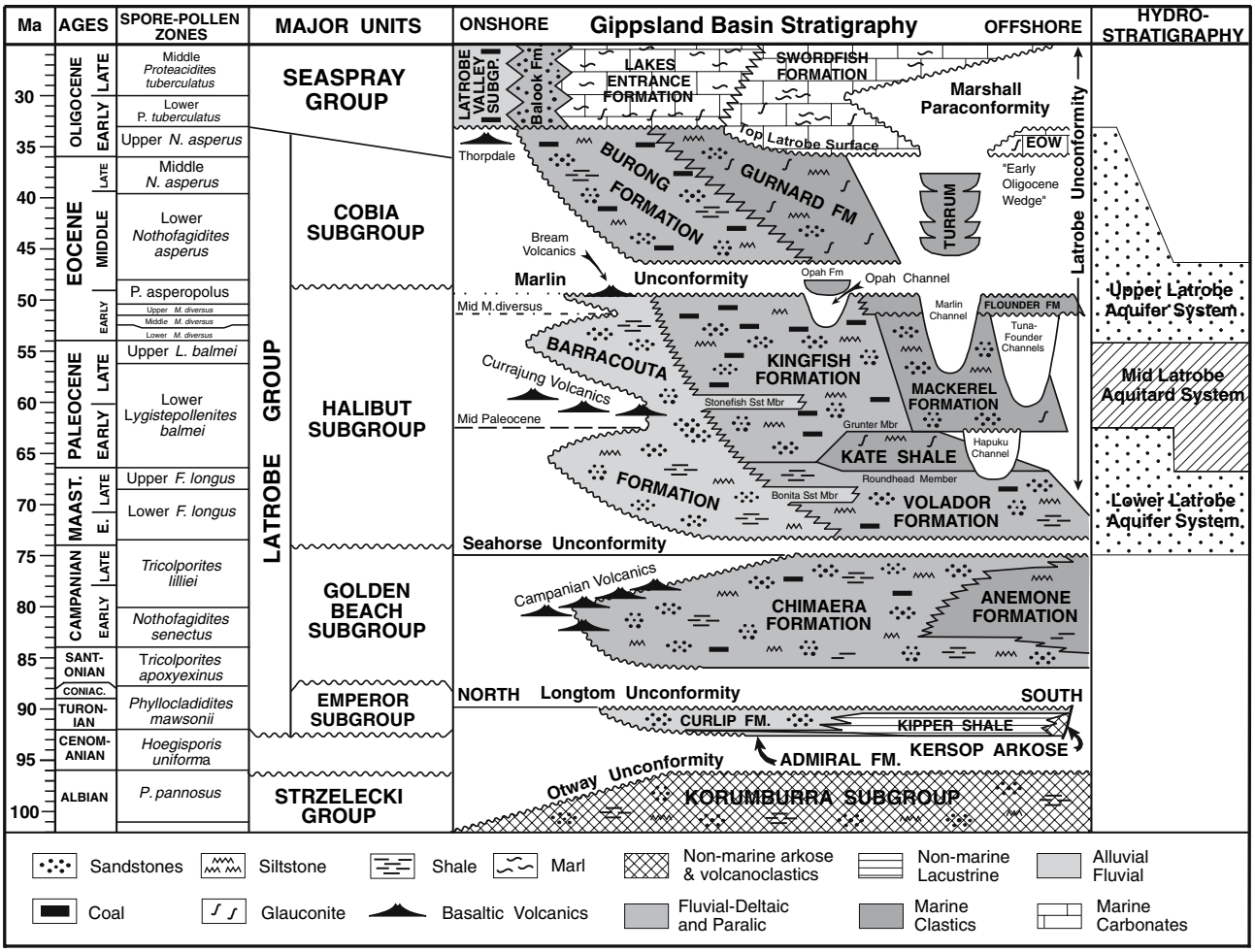

Fig. 2 Stratigraphic column of the Gippsland Basin (modified after Bernecker and Partridge 2001)

Thomas et al. 2003). Compressional tectonism started in the Late Eocene and continued through to the Middle Miocene, creating a series of NE-trending anticlines, which became the hosts for the large oil and gas accumulations. During the compressional phase, the basin continued to subside and the calcareous sediments of the Seaspray Group were deposited in shelf, slope and basinal depositional environments (Fig. 2) (Rahmanian et al. 1990; Thomas et al. 2003).

Methodology for detailed site characterisation

The subsurface behaviour of CO_2 is influenced by many variables, including reservoir and seal structure, stratigraphic architecture, reservoir heterogeneity, relative permeability, faults/fractures, pressure/temperature conditions, mineralogical composition of the rock framework, and hydrodynamics and geochemistry of the in situ formation fluids. Therefore, accurate appraisal of a potential CO_2 storage site requires detailed reservoir and seal characterisation, 3D modelling and numerical flow simulation (Root et al. 2004).

The methodology for evaluating a site for geological CO_2 storage is provided by Gibson-Poole et al. (2005) and is shown in Fig. 3. Seismic stratigraphic interpretations were integrated with wireline log correlations, detailed sedimentological core descriptions and biostratigraphy, to develop a sequence stratigraphic framework and sedimentary depositional model for each potential site. These models form the basis for the assessment of three principle aspects: injectivity, containment and capacity.

Injectivity issues include the geometry and connectivity of individual flow units, the nature of the heterogeneity within those units (i.e. the likely distribution and impact of baffles such as interbedded siltstones and shales) and the physical quality of the reservoir in terms of porosity and permeability characteristics (Fig. 3) (Gibson-Poole et al. 2005). The sedimentary depositional models derived from the sequence stratigraphic interpretation provided

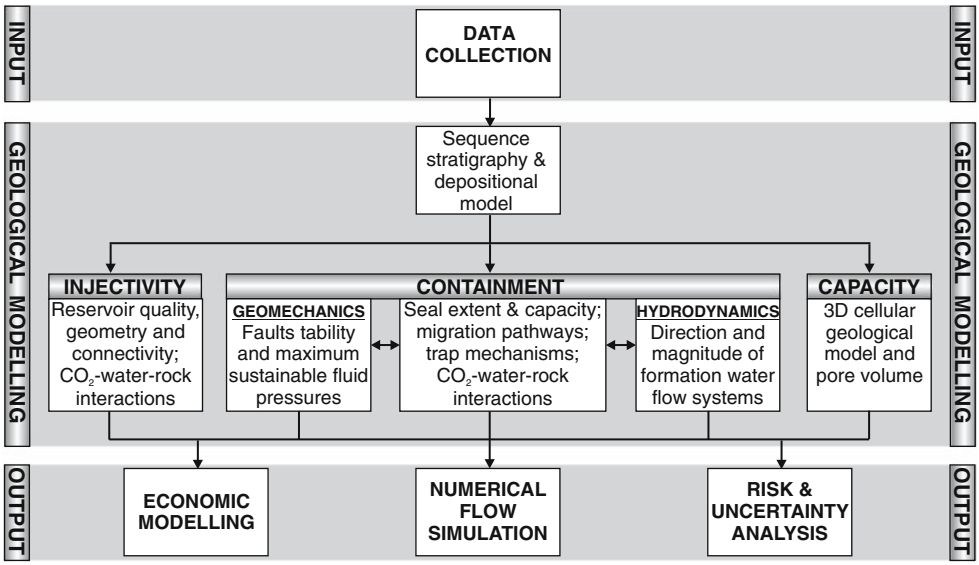

Fig. 3 Workflow for CO_2 geological storage assessment (modified after Gibson-Poole et al. 2005)

information about the reservoir distribution and the likely lateral and vertical connectivity, as the geometry and spatial distribution of individual flow units is a function of their environment of deposition. The reservoir quality was assessed via detailed analysis of core plug porosity and permeability characteristics, petrography and wireline log petrophysical interpretation. Collected core samples were also assessed petrologically by thin-section, X-ray diffraction and scanning electron microscope to ascertain potential CO_2-water-rock interactions that may have an impact on the injectivity.

Containment issues include the distribution and continuity of the seal, the seal capacity (maximum CO_2 column height retention), potential migration pathways (structural trends, distribution and extent of intraformational seals, and formation water flow direction and rate) and the integrity of the reservoir and seal (fault/fracture stability and maximum sustainable pore fluid pressures) (Fig. 3) (Gibson-Poole et al. 2005). Collected core samples were subjected to mercury injection capillary pressure (MICP) analysis to evaluate the CO_2 retention capacity of the rocks, and were assessed petrologically by thin-section, X-ray diffraction and scanning electron microscope to determine likely CO_2-water-rock interactions and the potential for mineral trapping. In situ stress and rock strength data were used to determine maximum sustainable pore pressure increases and the reactivation risk of faults in the area. The past and present formation water flow systems were characterised from pressure-elevation plots and hydraulic head distribution maps to interpret their possible impact on CO_2 migration and containment.

Potential CO_2 storage capacity can be assessed geologically in terms of available pore volume; however, the efficiency of that storage capacity will be dependent on the rate of CO_2 migration, the potential for fill-to-spill structural closures encountered along the migration path, and the long-term prospects of residual gas trapping, dissolution into the formation water or precipitation into new minerals (Fig. 3) (Gibson-Poole et al. 2005). The pore volume was estimated using standard oil industry volumetric calculation methods (e.g. Morton-Thompson and Woods 1992).

The results of the geological modelling were input into the reservoir engineering numerical flow simulations. Short-term numerical simulation models of the injection phase are needed to provide data on the injection strategy required to achieve the desired injection rates (e.g. number of wells, well design, injection pattern). Post-injection phase numerical simulations evaluate the long-term storage behaviour, modelling the likely migration, distribution and form of the CO_2 in the subsurface. The simulation models were constructed from depth-converted seismic surfaces and porosity-permeability characteristics of the intersecting wells. Shale distributions were modelled either by means of reduced vertical permeability (for injectivity simulations) or by stochastic object modelling (for simulations of short and long-term flow paths) to reflect the stratigraphic complexity. For the stochastic object modelling, Monte Carlo techniques were used to distribute shales of a chosen length and width (based on depositional environment) so as to satisfy the overall shale fraction in that interval. Short-term injectivity simulations used the IMEX Black Oil Simulator™ (CMG 2004), while the flow path simulations used the TOUGH2 code (Pruess et al. 1999). The equation of state module for TOUGH2 used in this study has been specifically designed to better represent the physical properties that drive long-term processes such as convective mixing of carbon dioxide (Ennis-King and Paterson

2005). On the other hand, IMEX, being designed for petroleum simulations, has more detailed and flexible options for well operations, which makes it more suitable for tackling some of the short-term issues around well design and injection strategy.

To complete the assessment of a particular site for its suitability for CO_2 storage, risk and uncertainly analysis and economic modelling should also be undertaken. These were also studied for this project and the results are detailed in Hooper et al. (2005).

Injection scenarios

The target reservoir intervals are the interbedded sandstones of the Paleocene-Eocene upper Latrobe Group (Halibut and Cobia Subgroups), sealed by the regionally extensive Lakes Entrance Formation (Seaspray Group). Assuming buoyancy is the primary driving force for CO_2 movement through the reservoir, an analysis of the likely CO_2 migration pathways at the top Latrobe Group (base regional seal) identified two main trends from within the Central Deep part of the basin: (1) up-dip migration from a basin centre location via the northern gas fields of Marlin, Snapper and Barracouta, and (2) up-dip migration via the southern oil fields of Fortescue, Kingfish and Bream (Fig. 4). It is envisaged that individual sites from along these two trends could be used sequentially, ramping up the volume of CO_2 stored to 50 Mt/a as power stations come online but timed such that existing hydrocarbon assets are not compromised.

A rollout plan of injection sites was devised taking into consideration techno-economic constraints such as oil and gas field depletion schedules. The first site for possible use is the Kingfish Field area. This oil field is anticipated to be depleted within the period 2015–2025 and thus available for CO_2 storage. The injection scenario assumes 15 Mt/a injection for a 40-year period, starting in the year 2015. The second site is the Fortescue Field area, also at 15 Mt/a for 40 years, commencing in 2022. The third site is the basin centre location and the northern gas fields trend (Marlin, Snapper, Barracouta), which assumes an injection scenario of 20 Mt/a for 40 years commencing in 2030. For reference, the proposed injection scenarios are 15–20 times the annual injection rate and double the overall injection period of the presently operating Sleipner project (1 Mt/a for 20 years) (Karbøl and Kaddour 1995).

The planned injection strategy for the Kingfish and Fortescue field areas involves CO_2 injection deep beneath the main oil accumulations (>500 m deeper), within the intra-Latrobe Group stratigraphy. For the basin centre site, injection is envisioned within the top Latrobe Group stratigraphy (same interval as the hydrocarbons), but nearly 20 km down-dip from the existing gas accumulations. The CO_2 injection and storage strategies proposed are intended to provide a time delay from the start of injection until the depleted hydrocarbon assets are reached, and to increase the potential storage capacity by accessing greater pore space and taking advantage of several trapping mechanisms (residual, dissolution, mineral and structural/stratigraphic trapping).

Detailed site characterisation

A detailed study was conducted on the Kingfish Field area as the first site to be potentially used (Fig. 5). The concept involves CO_2 injection deep beneath West Kingfish into the intra-Latrobe Group stratigraphy ($\sim$550–800 m deeper than the main oil accumulation). CO_2 is predicted to migrate upwards and eastwards towards the top of the Latrobe Group. Free CO_2 that reaches the base of the Lakes Entrance Formation would accumulate in the depleted Kingfish Field structural closure. If the capacity of the Kingfish closure is exceeded, and if still mobile, the CO_2 would then migrate westwards towards the structural closure of the Bream Field. This paper outlines the key results from the detailed studies on the geology, geophysics, geochemistry, geomechanics, hydrogeology and numerical flow simulations that were conducted for the regional Gippsland Basin and the Kingfish Field area.

Sequence stratigraphy and depositional model

A sequence stratigraphic approach is adopted because it focuses on key surfaces that naturally subdivide the sediment succession into chronostratigraphic units. This is vital to understanding the likely distribution and connectivity of reservoirs and seals. The approach followed here is that outlined by Van Wagoner et al. (1990), Posamentier and Allen (1999) and Lang et al. (2001), where sequences are defined as relatively conformable successions bounded by unconformities or their correlative conformities, and systems tracts are identified by key surfaces and stacking patterns, in both marine and continental settings. The sequence stratigraphic framework provides the foundation for the 3D geological models used in the numerical flow simulations.

The generic depositional model for the upper Latrobe Group is a west–east transition from non-marine to marine depositional environments (Thomas et al. 2003). An up-dip alluvial plain and adjacent coastal plain feed a wave-dominated deltaic system, with associated barrier shorelines, back-barrier lagoons and local protected embayments facing a gently dipping lower shoreface to shelf (Root et al.

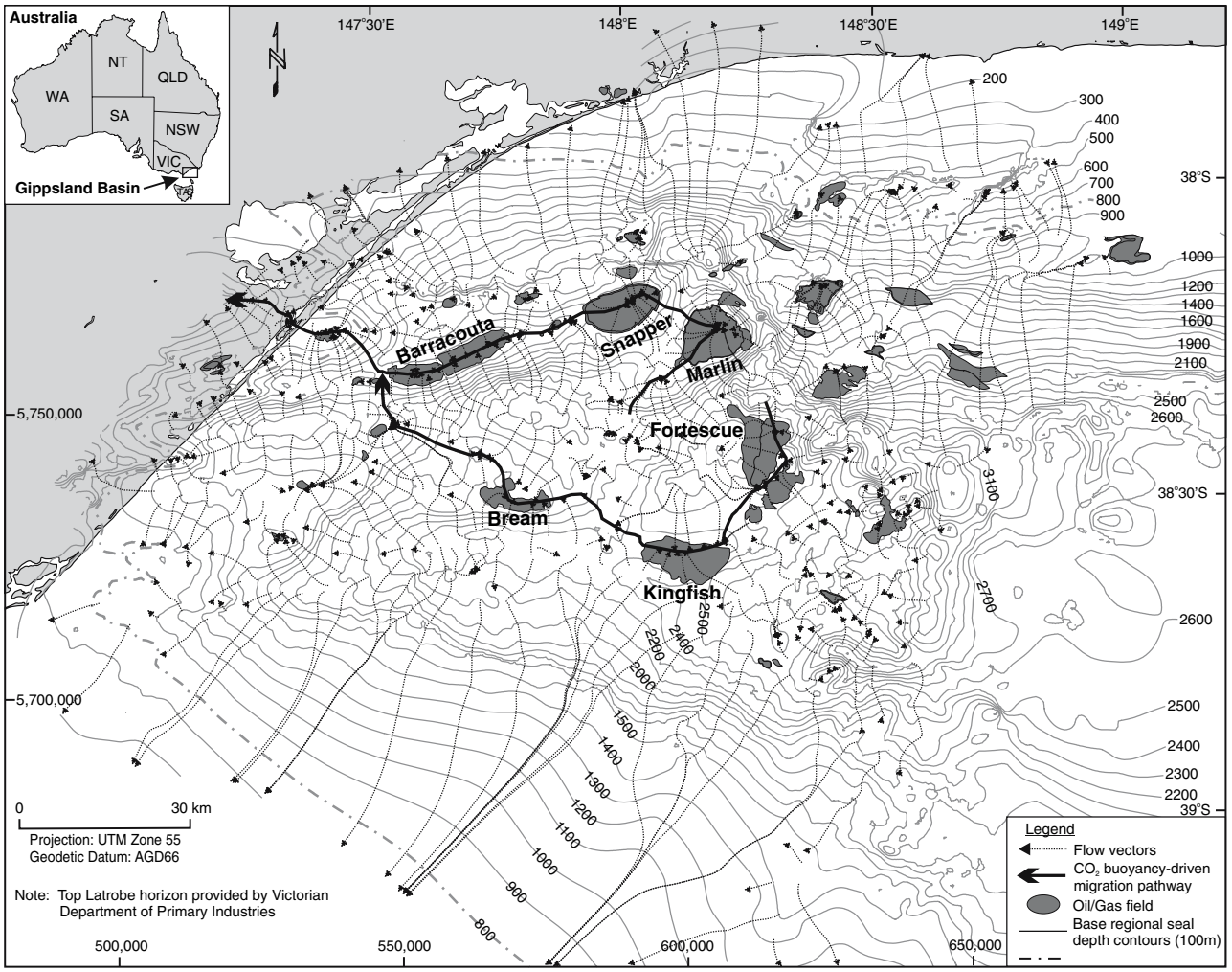

Fig. 4 Basin flow vectors and key migration pathways within the Central Deep, based on the structural geometry of the top Latrobe Group depth structure map (top Latrobe Group depth surface provided by the Victorian Department of Primary Industries)

2004). A eustatic sea level rise through the Paleocene and Eocene coincided with a steady decrease in sediment supply, resulting in a transgression of the sea with the shoreline progressively retreating to the west and northwest (Rahmanian et al. 1990). Consequently, the upper Latrobe Group is characterised by a transgressive, retrogradational

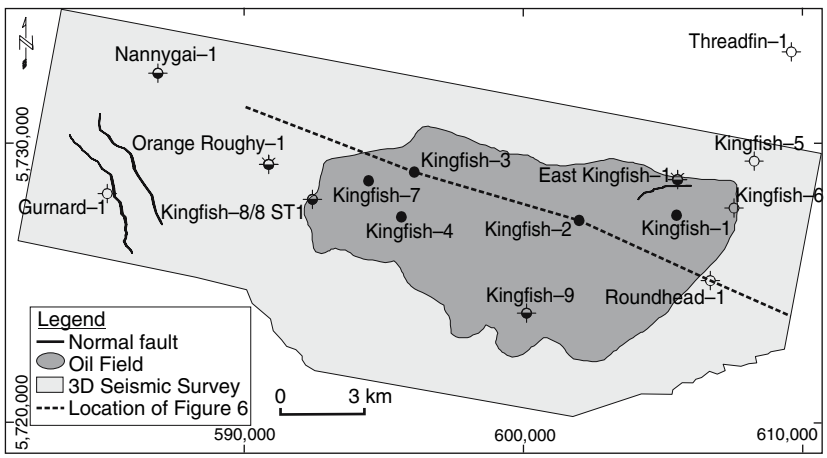

Fig. 5 Location map of the Kingfish Field and surrounding area

stratigraphic architecture and comprises numerous sequences that dip gently landward and are truncated by the Latrobe Unconformity (Rahmanian et al. 1990; Root et al. 2004).

Kingfish field area

Seven unconformity-bound sequences were identified in the Kingfish Field area Latrobe Group succession beneath the Lakes Entrance Formation regional seal (Fig. 6). Sequence 1 is representative of the Volador Formation, Sequences 2 to 6 are within the Kingfish/Mackerel Formations and Sequence 7 is representative of the Gurnard Formation. Sequences 1 to 6 are third-order sequences and are dominated by the highstand systems tracts. Each sequence has a progradational log motif and is clearly demonstrated by progradational sigmoid seismic facies at the eastern side of the field. Within each sequence, higher fourth-order sequences can be seen as transgressive–regressive cycles. Each highstand-dominated third-order sequence progressively backsteps within an overall transgressive sequence set. The sediments were deposited in coastal plain to shallow marine depositional environments along wave-dominated shorelines, transitioning from terrestrial-influenced sediments to marine-influenced sediments in a northwest-southeast direction across the field (Bernecker and Partridge 2005).

Sequence 7 (Gurnard Formation) is a transgressive–regressive cycle at the top of the Latrobe Group. It pinches out in the middle of the Kingfish Field (between the Kingfish-3 and Kingfish-2 wells), where it has been removed by subsequent erosion associated with the Latrobe Unconformity. The Gurnard Formation is a condensed, glauconitic marine shelf deposit, which acts as either a seal or a low quality reservoir depending on its location within the basin. At the Kingfish Field location it is generally considered 'non-net', although at the western end the P-1.1 reservoir is within the Gurnard Formation (Mudge and Thomson 1990). At the Bream Field the base of the formation constitutes a 'waste zone' (McKerron et al. 1998).

The shoreline position of each sequence progressively backsteps to the northwest, reflecting the overall transgressive nature of the upper Latrobe Group as the Tasman Sea increasingly encroached from the southeast. The Latrobe Group sequences are tilted structurally upwards to the east and are progressively truncated by the Latrobe Unconformity, a major basin-wide angular unconformity separating the reservoir intervals of the Latrobe Group from the overlying Seaspray Group. The fine-grained sediments of the Lakes Entrance Formation at the base of the Seaspray Group (Sequence 8) were deposited in shelf, slope and basinal depositional environments during subsequent major transgression and highstand, creating the regional seal.

Injectivity

Upon injection into a reservoir rock, the flow behaviour and migration of CO_2 will depend primarily on parameters such as the viscosity ratio, injection rate and relative

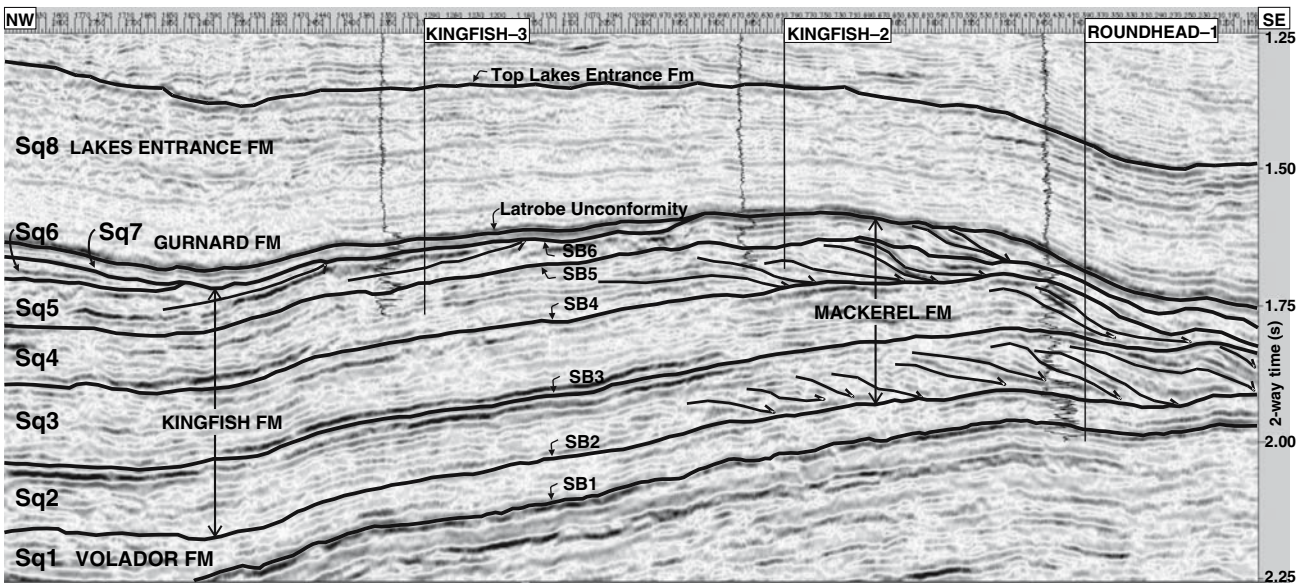

Fig. 6 Seismic cross-section through the Kingfish Field area (line G92A-3074A), showing sequence interpretation and key stratal relationships such as truncation and downlap

permeability, but also the stratigraphic architecture, reservoir heterogeneity and structural configuration of the rocks. Injectivity issues that can be assessed through the geological modelling therefore include the reservoir's quality, geometry and connectivity (Gibson-Poole et al. 2005).

Reservoir geometry and connectivity

The vertical and lateral connectivity of individual nearshore sandstone bodies is likely to be favourable, forming large-scale composite flow units. Analogue studies of modern and ancient shoreface deposits suggest individual deposit dimensions of 500–5,000 m in width and 1,000–10,000 m in length. The maximum elongation direction of the sandbodies is expected to be parallel to the palaeoshoreline (Root et al. 2004).

The fluvial channel sediments that exist in the coastal–alluvial plain deposits are commonly associated with finer-grained sediments, such as floodplain and crevasse splay deposits. As a result, fluvial deposits are characterized by greater reservoir heterogeneity, and the fluvial channel sandstone bodies are likely to exhibit poorer vertical and lateral connectivity. Analogue studies of modern and ancient fluvial deposits suggest fluvial channel belt widths of 500–2,000 m (Root et al. 2004).

Reservoir quality

Porosity and permeability

Core plug porosity and permeability data from wells in the southern oil fields area show a range of reservoir quality (Fig. 7). The Kingfish Formation sediments have porosities ranging up to 32% and permeabilities ranging up to 20,000 mD. The majority of the points lie in the 15–30% porosity and 10–10,000 mD permeability ranges, indicating good to excellent reservoir quality. The overlying Gurnard Formation has much poorer reservoir quality. Whilst porosity ranges from 8 to 27%, permeability is generally lower than 10 mD.

Petrological characterisation

The results of a previous petrological study undertaken for the GEODISC^{TM} project by Kraishan (in Root et al. 2004) were re-assessed and supplemented with new core samples obtained from the Kingfish-Bream area. Sixty-nine core samples were analysed for the diagenetic study and are listed in Table 1. The assessment indicated that the upper Latrobe Group sediments are composed mostly of quartz with significant amounts of feldspar and lithic fragments, and compositionally vary across almost the whole range of sandstone classifications (Fig. 8a). The diagenesis of the reservoir units has generally been positive for retaining high reservoir quality (Fig. 8b). Early precipitation of dolomite in the permeable sandstones has prevented compaction of the rock. Later dissolution of the dolomite during the migration of hydrocarbons and associated organic acids, combined with later feldspar dissolution, has created secondary porosity. Late-stage authigenic minerals such as quartz overgrowths and kaolinite, which can occlude porosity or close pore throats, generally only occur in minor amounts and do not contribute much to the reduction of pore volume.

Potential impact of CO_2–water–rock interactions on reservoir quality

CO_2 dissolution into the formation water allows CO_2–water–rock interactions, which will alter the mineralogy and potentially alter the physical aspects of the rock (Watson et al. 2004). This can have important implications for injectivity, as mineral dissolution may lead to migration of fine clay minerals and sand grains, or precipitation of new minerals, either of which can block or occlude the porosity and permeability of the reservoir rock.

A subset of 13 core samples from the Kingfish-Bream area were assessed in greater detail for the geochemical study (Table 1). The results indicated that the reservoir units of the Latrobe Group lack minerals which are reactive to CO_2. While rock fragments and feldspars do make up a major component of the formation mineralogy, elemental abundances indicate that the chemical composition of each mineral group is not optimal for CO_2–water–rock interactions at a rate likely to affect injectivity. For example, the feldspars are dominantly alkali, which have a very slow reaction rate, and the rock fragments are metamorphic (quartz and mica dominated), which also have a very slow reaction rate or are inert to CO_2 dissolution. Therefore, CO_2–water–rock interactions are expected to be very limited, and the injectivity of the reservoir units is unlikely to be compromised by geochemical reactions.

Containment

Before dissolution, supercritical CO_2 is less dense than water. Therefore, it will rise buoyantly through the water column, like hydrocarbons. Consequently, like hydrocarbon exploration or natural gas storage, possible CO_2 containment risks are unwanted vertical fluid migration via the top seal, faults/fractures and existing well penetrations

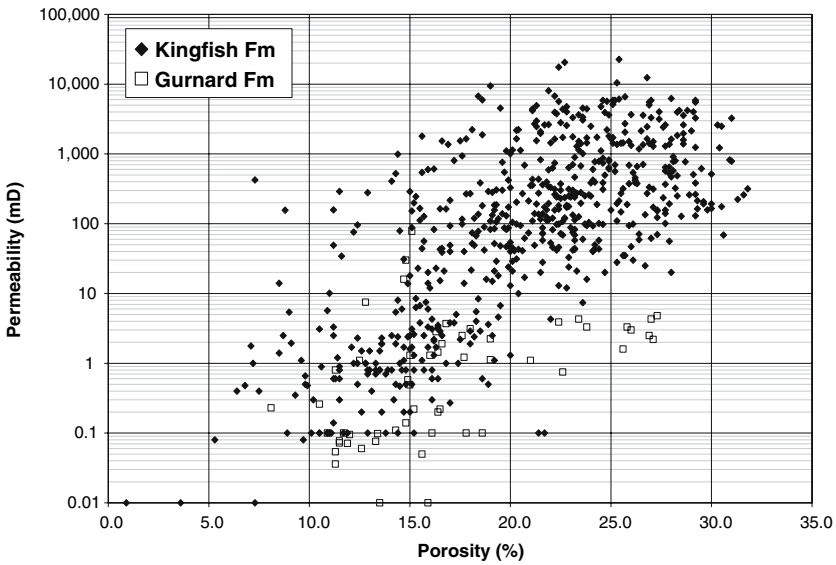

Fig. 7 Core plug porosity and permeability data for wells in the southern oil fields area for the Kingfish and Gurnard Formations

(Root et al. 2004). Containment issues that need to be assessed therefore include the extent, continuity and capacity of the seal, the likely migration pathways and trapping mechanisms and the integrity of the reservoir and seal (Gibson-Poole et al. 2005).

Seal distribution and continuity

The Lakes Entrance Formation regional seal is widespread across the offshore Gippsland Basin, with the exception of the eastern deep-water area of the Bass Canyon. It is the lowermost of four units that are distinguished within the Seaspray Group, and is lithologically composed of glauconitic, slightly calcareous and mud-rich sediments (Woollands and Wong 2001). At the Kingfish Field location, the Lakes Entrance Formation has an average thickness of 390 m.

Seal capacity

Seal capacity is an important aspect for containment of CO_2. The potential seal capacity of the regional top seals and localised intraformational seals were assessed by mercury injection capillary pressure (MICP) analysis. MICP tests are a measurement of the pressures required to move mercury through the pore network system of a core sample. The air/mercury capillary pressure data are translated to equivalent CO_2/brine data at reservoir conditions and then converted into seal capacity for CO_2, expressed as the column height that the rock would be capable of holding (sealing). Standard procedures for MICP analysis, as reviewed by Vavra et al (1992) and Dewhurst et al. (2002), were used for these studies. Thirty-one core samples were analysed by MICP, representing top seals from the Lakes Entrance, Gurnard and Turrum Formations (10 samples) and intraformational seals from within the Burong, Kingfish, Flounder and Mackerel Formations (21 samples). The samples were selected on the basis of available core material, spatial distribution across the basin and lithological variation within the formations. The calculated column heights for each of the samples tested are listed in Table 2.

The Lakes Entrance Formation regional top seal is interpreted to have good seal potential and sufficient seal capacity to successfully retain CO_2. The MICP analyses indicate that the Lakes Entrance Formation has the potential to hold back CO_2 column heights ranging from 17 to 1071 m, with an average CO_2 column height retention of 395 m. The Lakes Entrance Formation overlies the more localised top seals of the Gurnard and Turrum Formations. The properties of these formations are variable across the basin, resulting in the formations behaving as either low quality reservoir or a seal, depending on the specific depositional environment and/or diagenetic history. The Gurnard Formation sample from Bream-2 is clearly more akin to a reservoir than a seal, with a CO_2 column height of only 20 cm. However, the average CO_2 column height for the Gurnard and Turrum Formations is 360 m, which indicates good sealing potential. In the event that CO_2 migrated through the Gurnard and Turrum Formations, the CO_2 would still be successfully retained by the regionally extensive Lakes Entrance Formation.

Localised intraformational seals are present throughout the fluvial, coastal plain and nearshore marine reservoir intervals of the Burong, Kingfish, Mackerel and Flounder Formations. The MICP analyses indicate that the

Table 1 Summary of core sample petrological analyses

Well	Depth MD (m)	Formation	Reservoir/seal	Thin section	Bulk XRD	Clay XRD	XRF
Barracouta-1	1,445.00	Barracouta Fm	Reservoir	Yes	No	No	No
Barracouta-5	1,205.50	Burong Fm	Reservoir	Yes	No	No	No
Barracouta-5	1,206.70	Burong Fm	Reservoir	Yes	No	No	No
Barracouta-5	1,208.40	Burong Fm	Reservoir	Yes	No	No	No
Barracouta-5	1,209.95	Burong Fm	Reservoir	Yes	No	No	No
Barracouta-5	1,218.59	Burong Fm	Reservoir	Yes	No	No	No
Barracouta-5	1,221.75	Burong Fm	Reservoir	Yes	No	No	No
Barracouta-5	1,222.95	Burong Fm	Reservoir	Yes	No	No	No
Bream-2[a]	1,852.7	Lakes Entrance Fm	Top seal	No	Yes	Yes	Yes
Bream-2[a]	1,855.9	Lakes Entrance Fm	Top seal	No	Yes	Yes	Yes
Bream-2[a]	1,859.2	Lakes Entrance Fm	Top seal	Yes	Yes	Yes	Yes
Bream-2[a]	1,864.9	Gurnard Fm	Waste zone	Yes	Yes	Yes	Yes
Bream-2[a]	1,877.4	Burong Fm	Reservoir	Yes	No	No	Yes
Bream-2[a]	1,897.6	Burong Fm	Intra-fm seal	No	Yes	Yes	Yes
Fortescue-1	2,419.50	Flounder Fm	Reservoir	Yes	No	No	No
Fortescue-1	2,424.60	Flounder Fm	Reservoir	Yes	Yes	Yes	No
Fortescue-1	2,430.25	Flounder Fm	Reservoir	Yes	No	No	No
Fortescue-1	2,434.61	Flounder Fm	Reservoir	Yes	No	No	No
Fortescue-2	2,442.52	Gurnard Fm	Reservoir	Yes	No	No	No
Fortescue-2	2,451.45	Flounder Fm	Reservoir	Yes	Yes	Yes	No
Fortescue-2	2,471.57	Flounder Fm	Reservoir	Yes	Yes	Yes	No
Fortescue-2	2,476.35	Flounder Fm	Reservoir	Yes	No	No	No
Kingfish-7[a]	2,300.5	Flounder Fm	Waste zone	Yes	Yes	Yes	Yes
Kingfish-7[a]	2,311.3	Kingfish Fm	Reservoir	Yes	No	No	Yes
Kingfish-7[a]	2,323.2	Kingfish Fm	Reservoir	Yes	Yes	Yes	Yes
Kingfish-7[a]	2,357.2	Kingfish Fm	Intra-fm seal	No	Yes	Yes	No
Kingfish-9[a]	2,307.87	Gurnard Fm	Waste zone	Yes	Yes	Yes	Yes
Kingfish-9[a]	2,319.7	Kingfish Fm	Reservoir	Yes	Yes	Yes	Yes
Kingfish-9[a]	2,326.55	Kingfish Fm	Reservoir	Yes	Yes	Yes	Yes
Luderick-1	1,840.62	Burong Fm	Reservoir	Yes	No	No	No
Luderick-1	1,844.38	Burong Fm	Reservoir	Yes	No	No	No
Luderick-1	1,848.09	Burong Fm	Reservoir	Yes	No	No	No
Luderick-1	1,848.65	Burong Fm	Reservoir	Yes	No	No	No
Luderick-1	1,850.27	Burong Fm	Reservoir	Yes	No	No	No
Luderick-1	1,853.20	Burong Fm	Reservoir	Yes	No	No	No
Luderick-1	1,855.90	Burong Fm	Reservoir	Yes	No	No	No
Luderick-1	1,860.95	Burong Fm	Reservoir	Yes	No	No	No
Marlin-1	1,389.00	Turrum Fm	Reservoir	Yes	No	No	No
Marlin-1	1,413.05	Kingfish Fm	Reservoir	Yes	No	No	No
Marlin-1	1,415.49	Kingfish Fm	Reservoir	Yes	No	No	No
Marlin-1	1,420.31	Kingfish Fm	Intra-fm seal	Yes	No	No	No
Marlin-1	1,420.70	Kingfish Fm	Intra-fm seal	Yes	No	No	No
Marlin-4	2,248.80	Kingfish Fm	Intra-fm seal	Yes	Yes	Yes	No
Marlin-4	2,250.40	Kingfish Fm	Reservoir	Yes	Yes	Yes	No
Seahorse-2	1,487.50	Burong Fm	Reservoir	Yes	No	No	No
Seahorse-2	1,503.27	Burong Fm	Intra-fm seal	Yes	No	No	No
Snapper-1	1,267.00	Burong Fm	Reservoir	Yes	No	No	No
Snapper-5	1,402.99	Burong Fm	Reservoir	Yes	No	No	No

Table 1 continued

Well	Depth MD (m)	Formation	Reservoir/seal	Thin section	Bulk XRD	Clay XRD	XRF
Snapper-5	1,414.63	Burong Fm	Reservoir	Yes	No	No	No
Tarwhine-1	1,392.10	Gurnard Fm	Intra-fm seal	Yes	Yes	Yes	No
Tarwhine-1	1,395.00	Gurnard Fm	Reservoir	Yes	No	No	No
Tarwhine-1	1,401.18	Gurnard Fm	Reservoir	Yes	No	No	No
Tarwhine-1	1,407.58	Burong Fm	Intra-fm seal	Yes	No	No	No
Tarwhine-1	2,664.39	Barracouta Fm	Reservoir	Yes	No	No	No
Tarwhine-1	2,668.73	Barracouta Fm	Reservoir	Yes	No	No	No
Veilfin-1	3,453.58	Volador Fm	Reservoir	Yes	Yes	Yes	No
Veilfin-1	3,461.54	Volador Fm	Reservoir	Yes	Yes	Yes	No
Whiting-1	2,682.00	Kingfish Fm	Reservoir	Yes	Yes	Yes	No
Whiting-1	2,684.22	Kingfish Fm	Reservoir	Yes	Yes	Yes	No
Whiting-1	2,689.76	Kingfish Fm	Reservoir	Yes	No	No	No
Wirrah-1	1,494.00	Burong Fm	Reservoir	Yes	No	No	No
Wirrah-1	1,498.15	Burong Fm	Reservoir	Yes	No	No	No
Wirrah-1	1,500.50	Burong Fm	Intra-fm seal	Yes	No	No	No
Wirrah-1	1,503.00	Burong Fm	Reservoir	Yes	No	No	No
Wirrah-1	1,506.85	Burong Fm	Reservoir	Yes	No	No	No
Wirrah-1	1,509.70	Burong Fm	Reservoir	Yes	No	No	No
Wirrah-1	1,515.00	Burong Fm	Reservoir	Yes	No	No	No
Wirrah-1	1,515.55	Burong Fm	Reservoir	Yes	No	No	No
Wrasse-1	2,746.05	Turrum Fm	Top seal	Yes	Yes	Yes	No

[a] Sample subset used in geochemical analysis of CO_2–water–rock interactions for the Kingfish-Bream area

intraformational seals have the potential to hold back CO_2 column heights ranging from 53 to 1,191 m, with an average CO_2 column height retention of 517 m. Thus, the interbedded siltstones, shales and coals may behave as flow baffles and barriers that will hinder or slow vertical migration, encouraging the CO_2 to migrate laterally within the reservoir.

Migration pathways and trapping mechanisms

After injection ceases, the buoyancy of the free CO_2 due to its density will result in it migrating to the highest point in the reservoir. Stratigraphic heterogeneities, such as intraformational siltstones, shales and coals, have the potential to reduce the effective vertical permeability and create a more tortuous migration pathway for injected CO_2. Once CO_2 has reached the top of the reservoir, the structural geometry at the base of the overlying seal will have a strong influence on the subsequent migration direction.

Kingfish field area

The structural geometry at the top of the Volador Formation deep beneath the Kingfish Field is a westwards-plunging anticline (Fig. 9). The overlying Kingfish/Mackerel Formation sediments are tilted similarly down to the west and are progressively truncated by the Gurnard Formation and the Latrobe Unconformity. Intraformational seals within the reservoir units are aligned with this structural geometry in the western part of the field, but in the east they may form part of the sigmoidal clinoforms relating to the shoreface progradational cycles (most likely at the toes of the progrades). Figure 10 shows a schematical representation of the possible intraformational seal distribution based on the sequence stratigraphy, wireline log motifs and seismic appearance. The west to east transition from coastal plain to shallow marine depositional environments across the Kingfish Field area is reflected in the intraformational seals, which have a greater volume on the western side and then laterally pinch out towards the east as the section becomes sandier (Bernecker and Partridge 2005). The effect of the tilted structural geometry and the presence of intraformational seals suggests that CO_2 is likely to migrate upwards and eastwards by a tortuous pathway created by the stratigraphic heterogeneity until it accumulates at the top of the Latrobe Group beneath the regional seal.

Once at the top of the Latrobe Group, the migration direction of the CO_2 will be influenced by the structural geometry at the base of the regional seal, which is an

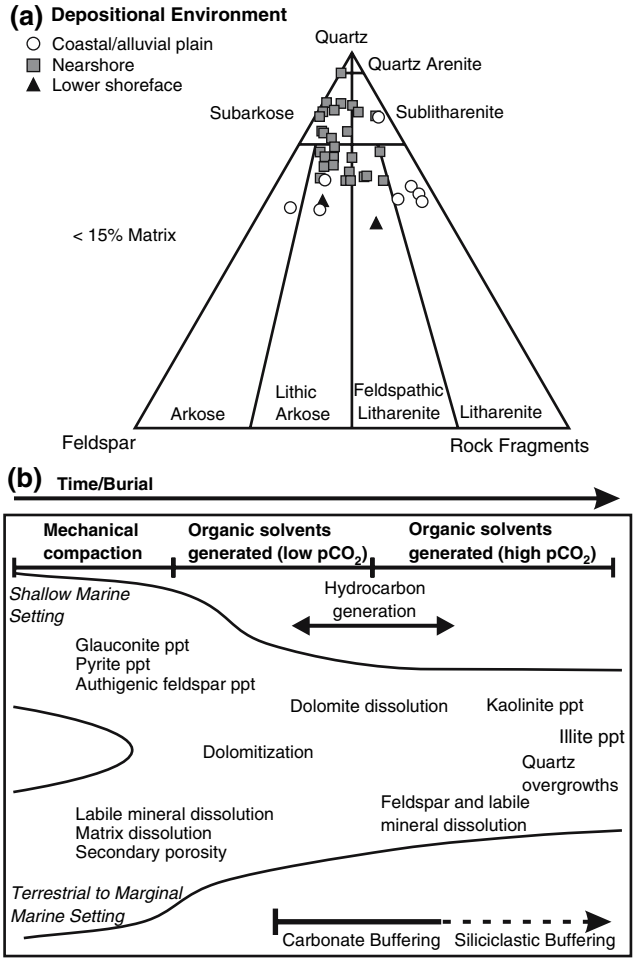

Fig. 8 **a** Ternary diagram of the various reservoir samples of the upper Latrobe Group from the northern gas fields. **b** Simplified burial diagenesis for the upper Latrobe Group reservoirs, showing the relationship between the production of low and high pCO_2 organic solvents to the diagenetic process and the past buffering capabilities of the system

eastwards-plunging anticline (opposite to the underlying structural geometry) (Fig. 11). If the storage capacity of the Kingfish Field structural closure is exceeded, the CO_2 may continue to migrate up structural dip beneath the regional seal in a westerly direction towards the structural closure of the Bream Field. This is orthogonal to the westerly-dipping intraformational baffles and barriers, which will again slow and hinder the migration of the CO_2.

The CO_2 injection and storage strategy proposed is intended to take advantage of several trapping mechanisms. The tortuous pathway created by the stratigraphic architecture within the intra-Latrobe Group is expected to effectively increase the length of the CO_2 migration pathway. This will increase the volume of pore space moved through by the CO_2, which will result in greater dissolution and residual gas trapping along the migration pathway. Once at the top Latrobe Group, the depleted Kingfish Field provides structural trapping in the anticlinal closure.

Potential impact of CO_2–water–rock interactions on containment

CO_2 introduced into the reservoir system will generate long-term CO_2–water–rock interactions. Detailed petrology can provide information on the potential mineral reactions of the CO_2 with the host rock, including dissolution, alteration and precipitation. In certain cases, mineral precipitation can lead to mineral trapping of CO_2 and increased containment security (Perkins and Gunter 1996; Watson et al. 2004).

The subset of 13 core samples from the Kingfish-Bream area were used for this geochemical study (Table 1). As discussed above, the mineralogy of the reservoir units of the upper Latrobe Group offer little to no reactive potential with CO_2. Whilst this is beneficial in terms of not inhibiting injectivity, conversely it means that there is limited potential for mineralogical trapping of the CO_2 through precipitation of carbonate minerals.

At the top of the Latrobe Group is the glauconitic marine shelf deposit of the Gurnard Formation, which acts as either a seal or a low quality reservoir depending on its location within the basin. The mineralogy of the Gurnard Formation is very different to that of the underlying Latrobe Group sediments. In addition to quartz, it also contains moderate to high concentrations of marcasite (and its polymorph pyrite), smectite and goethite, plus other minerals such as potassium feldspar, dolomite, chlorite, berthierine, glauconite and muscovite. The higher concentration of calcium, iron and magnesium bearing minerals offers significant potential for mineralogical trapping of CO_2 through precipitation of ferroan carbonate minerals (e.g. siderite). In addition, migration of the CO_2 through this low permeability reservoir is likely to slow migration rates vertically and laterally. This stratigraphic arrangement of good quality reservoirs with low reactive potential as the injection target, overlain by the low permeability yet potentially highly reactive Gurnard Formation, is an ideal reservoir system for optimising CO_2 injection and containment (Watson and Gibson-Poole 2005) (Fig. 12).

The Lakes Entrance Formation regional seal is composed co-dominantly of quartz and illitic-smectite, with one sample also containing abundant siderite cement. Mineral reactions are likely to be limited as illitic-smectite clays are weakly reactive to CO_2. It is also considered unlikely that CO_2 will enter the formation due to its low porosity and permeability characteristics and high seal

Table 2 CO_2 column heights calculated from MICP analysis

Well	Depth MD (m)	Formation	Seal type	Threshold pressure (psia)	CO_2 column height (m)
Barracouta-5	1,216.20	Burong Fm	Intraformational	488	63
Bream-2	1,852.76	Lakes Entrance Fm	Top seal–regional	607	108
Bream-2	1,855.93	Lakes Entrance Fm	Top seal–regional	5,973	1,071
Bream-2	1,859.23	Lakes Entrance Fm	Top seal–regional	100	17
Bream-2	1,864.88	Gurnard Fm	Top seal/Waste zone	5	0.19
Bream-2	1,897.50	Burong Fm	Intraformational	5,006	897
Cobia-A11	2,617.72	Kingfish Fm	Intraformational	413	53
Cobia-A11	2,618.72	Kingfish Fm	Intraformational	707	91
Drummer-1	2,485.00–2,490 (a)	Kingfish Fm	Intraformational	2,924	317
Drummer-1	2,485.00–2,490 (b)	Kingfish Fm	Intraformational	2,924	317
Fortescue-1	2,427.56	Flounder Fm	Intraformational	6,967	862
Fortescue-2	2,435.1	Lakes Entrance Fm	Top seal–regional	699	99
Fortescue-2	2,439.28	Gurnard Fm	Top seal/Waste zone	290	41
Halibut-2	2,355.80	Flounder Fm	Intraformational	2,047	285
Kingfish-7	2,300.45	Flounder Fm	Intraformational	2,950	445
Kingfish-7	2,357.20	Kingfish Fm	Intraformational	5,025	764
Kingfish-9	2,307.87	Gurnard Fm	Top seal/Waste zone	5,007	723
Luderick-1	1,861.55	Burong Fm	Intraformational	9,952	1,191
Marlin-4	2,252.80	Kingfish Fm	Intraformational	4,978	641
Seahorse-2	1,486.60	Burong Fm	Intraformational	5,970	785
Seahorse-2	1,494.85	Burong Fm	Intraformational	6,972	902
Snapper-1	1,257.86	Burong Fm	Intraformational	344	63
Tailor-1	2,420.42–2,420.57 (a)	Mackerel Fm	Intraformational	7,150	962
Tailor-1	2,420.42–2,420.57 (b)	Mackerel Fm	Intraformational	2,928	394
Tailor-1	2,420.42–2,420.57 (c)	Mackerel Fm	Intraformational	3,358	451
Tailor-1	2,420.42–2,420.57 (d)	Mackerel Fm	Intraformational	3,358	451
Tarwhine-1	1,410.24	Burong Fm	Intraformational	5,970	823
Wirrah-1	1,506.00	Burong Fm	Intraformational	708	90
Wrasse-1	2,593.56	Lakes Entrance Fm	Top seal–regional	4,165	401
Wrasse-1	2,597.26	Lakes Entrance Fm	Top seal–regional	6,969	671
Wrasse-1	2,750.87	Turrum Fm	Top seal–local	6,968	671

capacity, restricting any potential mineral reactions to the base of the seal.

Hydrodynamic analysis

Hydrodynamic modelling assesses the formation water flow systems within a basin by evaluating the degree of vertical and horizontal hydraulic communication and estimating the direction and magnitude of flow. An assessment of the virgin (pre-production) hydrodynamic regime is used to provide an understanding of the long-term (hundreds to thousands of years) influence of the formation water flow systems on the injected CO_2. An interpretation of the present-day hydrodynamic regime, which has been affected by hydrocarbon and water production, is required to evaluate the potential short-term (tens to hundreds of years) influence on the predicted migration pathway of CO_2 immediately after injection. It is assumed that once hydrocarbon/water production has ceased, the hydrodynamic flow system will gradually return to its virgin state. The injection of CO_2 into previously hydrocarbon-producing regions may speed up the aquifer pressure recovery.

Virgin and present-day hydrodynamic system

Standard hydrodynamic analysis techniques as presented by Bachu and Michael (2002), Otto et al. (2001), Bachu (1995) and Dahlberg (1995) were used for this study. New

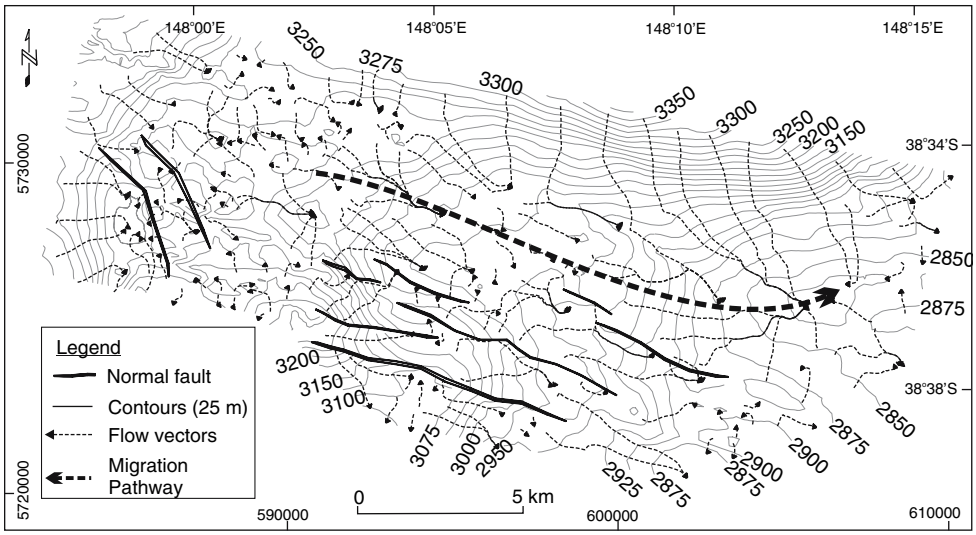

Fig. 9 Flow vectors and key migration pathway within the Kingfish Field area, based on the structural geometry of the SB2 depth structure map (top Volador Formation)

data were integrated with the data from two previous hydrodynamic studies by Underschultz et al. (2003) and Hatton et al. (2004), which formed the foundation for this study.

A model of the virgin hydraulic head distribution for the Upper Latrobe Aquifer System has been derived and is shown in Fig. 13. High hydraulic head extending eastwards from onshore subcrop reflects gravity-driven freshwater recharge from the west. This is particularly prominent within the boundaries of the Seaspray Depression and the offshore western part of the Central Deep. In the offshore Gippsland Basin high values of hydraulic head are related to a compaction-driven flow system. The onshore gravity-driven flow system and the offshore compaction-driven flow system converge into a region of low hydraulic head in the offshore Central Deep. It is speculated that this sink is connected to the Darriman Fault System on the southern edge of the Central Deep, which may then discharge to an upper aquifer or even the sea floor. Several interconnected troughs of low hydraulic head form the sink, and extend to the north and east, such as between the Snapper and Marlin Fields and between the Fortescue and Kingfish Fields.

A combination of onshore coal mine dewatering, industrial and agricultural formation water extraction, and

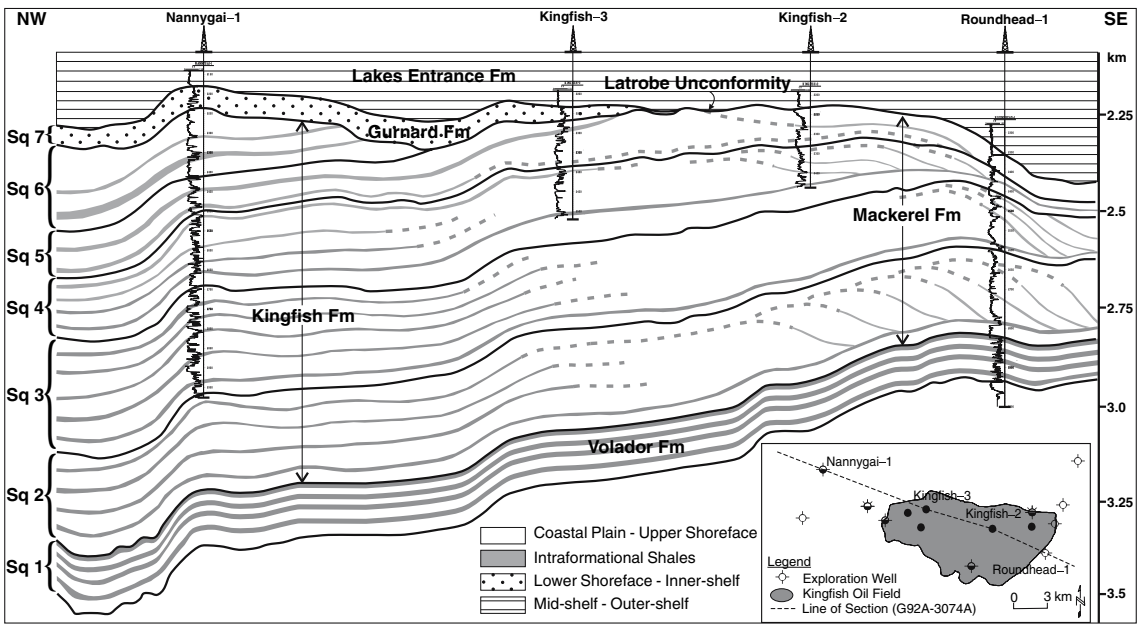

Fig. 10 Schematic representation of the possible intraformational seal distribution based on the sequence stratigraphy, wireline log motifs and seismic appearance

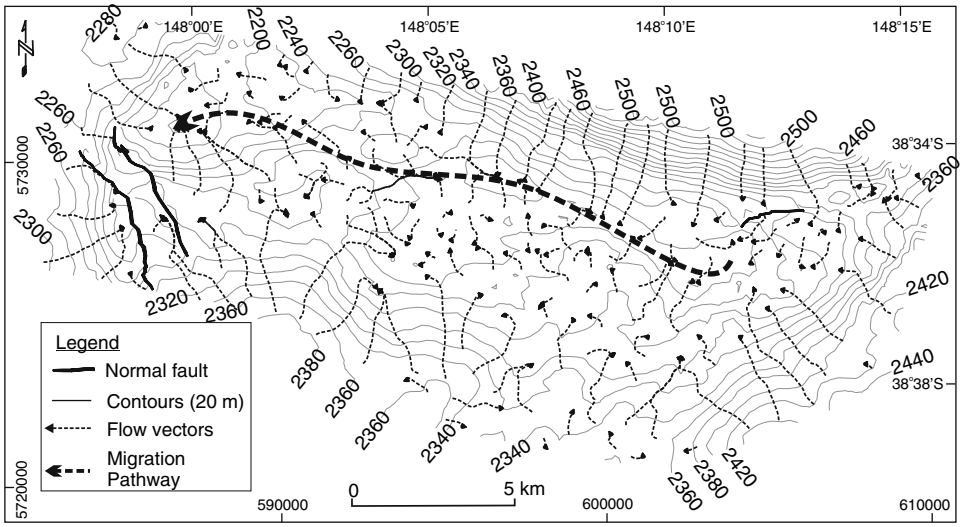

Fig. 11 Flow vectors and key migration pathway within the Kingfish Field area, based on the structural geometry of the top Latrobe Group depth structure map (base Lakes Entrance Formation regional seal)

offshore oil and gas production, have resulted in a short-term (tens to hundreds of years) transient alteration of the formation water flow system for the Upper Latrobe Aquifer System. In the absence of publicly available present-day offshore pressure data, a present-day hydraulic head distribution was estimated from the mid 1990s distribution and extrapolating the observed trend in decreasing hydraulic head with time during the 1990s (Fig. 14). In the onshore region, a depression of the hydraulic head surface occurs in the Latrobe Valley associated with coal mine dewatering. Effects of dewatering appear to be mainly confined to the Northern Terrace, suggesting the Rosedale Fault System forms a hydraulic barrier on a production time-scale. In the offshore Gippsland Basin, hydrocarbon production has resulted in a significant depression of the hydraulic head surface centred on the Fortescue to Kingfish Fields. The low hydraulic head resulting from production-induced pressure decline has altered the virgin formation water flow system so that it now flows radially inwards towards the Fortescue-Kingfish area.

Impact of hydrodynamic system on CO_2 migration and containment in the Kingfish Field area

The long-term fate of injected CO_2 is likely to be relatively unaffected by the formation water flow system, since the hydraulic gradients of the virgin hydrodynamic system are

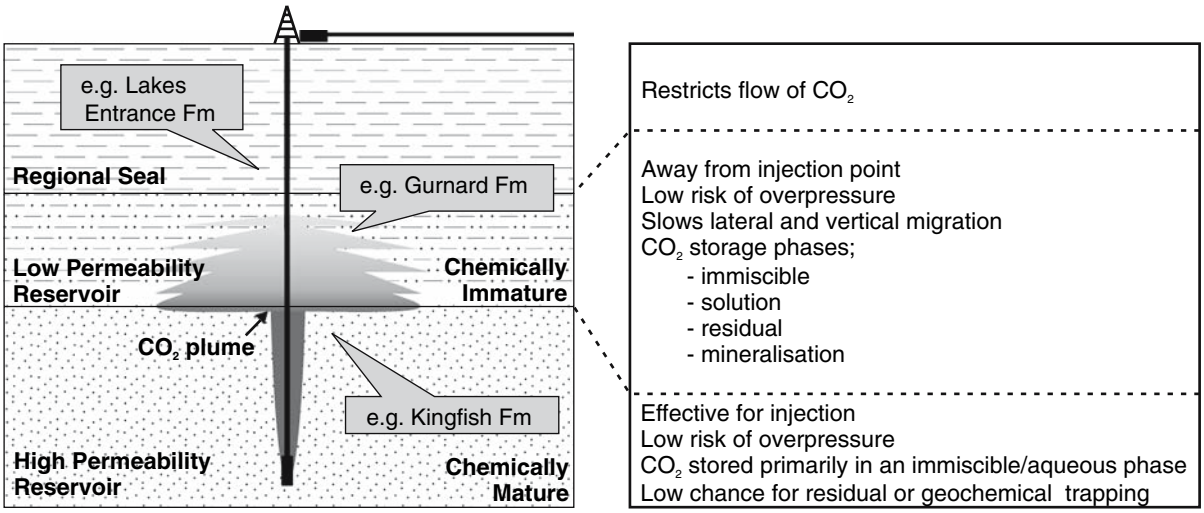

Fig. 12 Conceptual diagram of the optimised storage system for CO_2, where following buoyancy-driven vertical migration the CO_2 encounters a low permeability, chemically-immature, heterogeneous zone, slowing both the lateral and vertical migration of the CO_2 plume and promoting mineral trapping (modified after Watson and Gibson-Poole 2005)

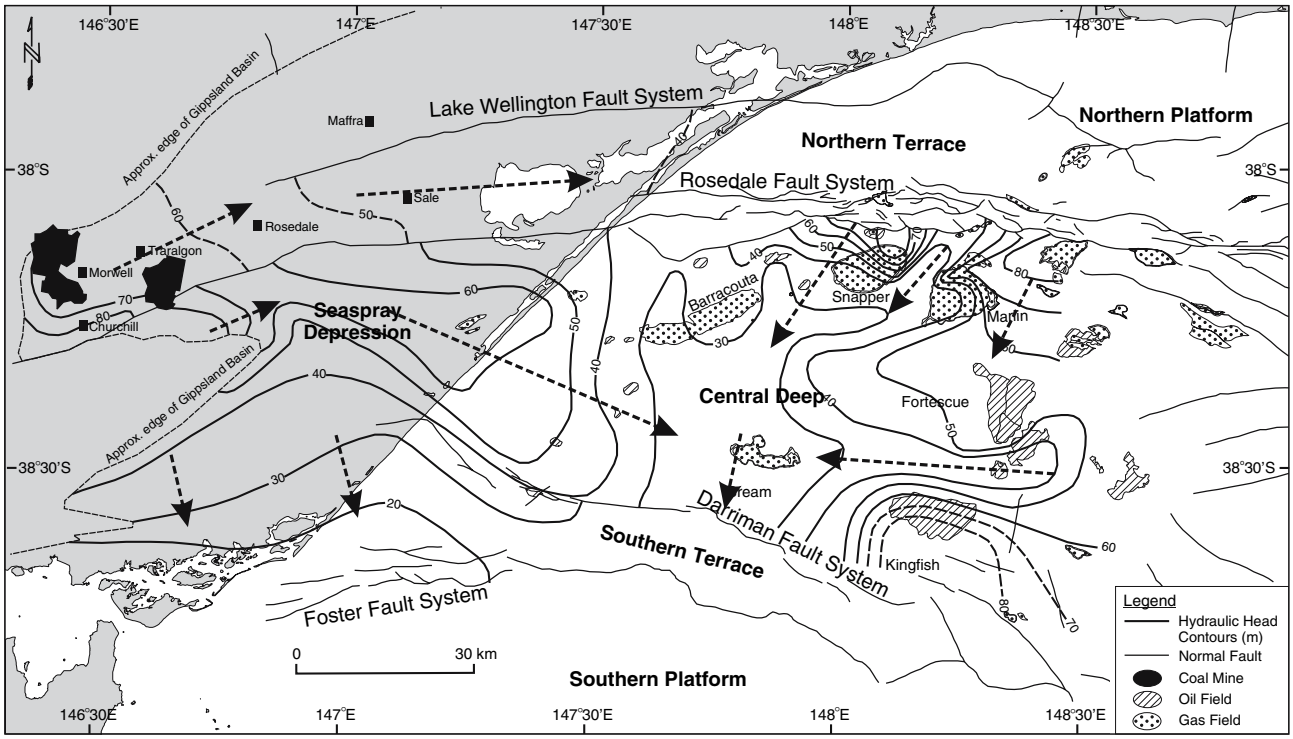

Fig. 13 Virgin (pre-production) hydraulic head distribution for the Upper Latrobe Aquifer System

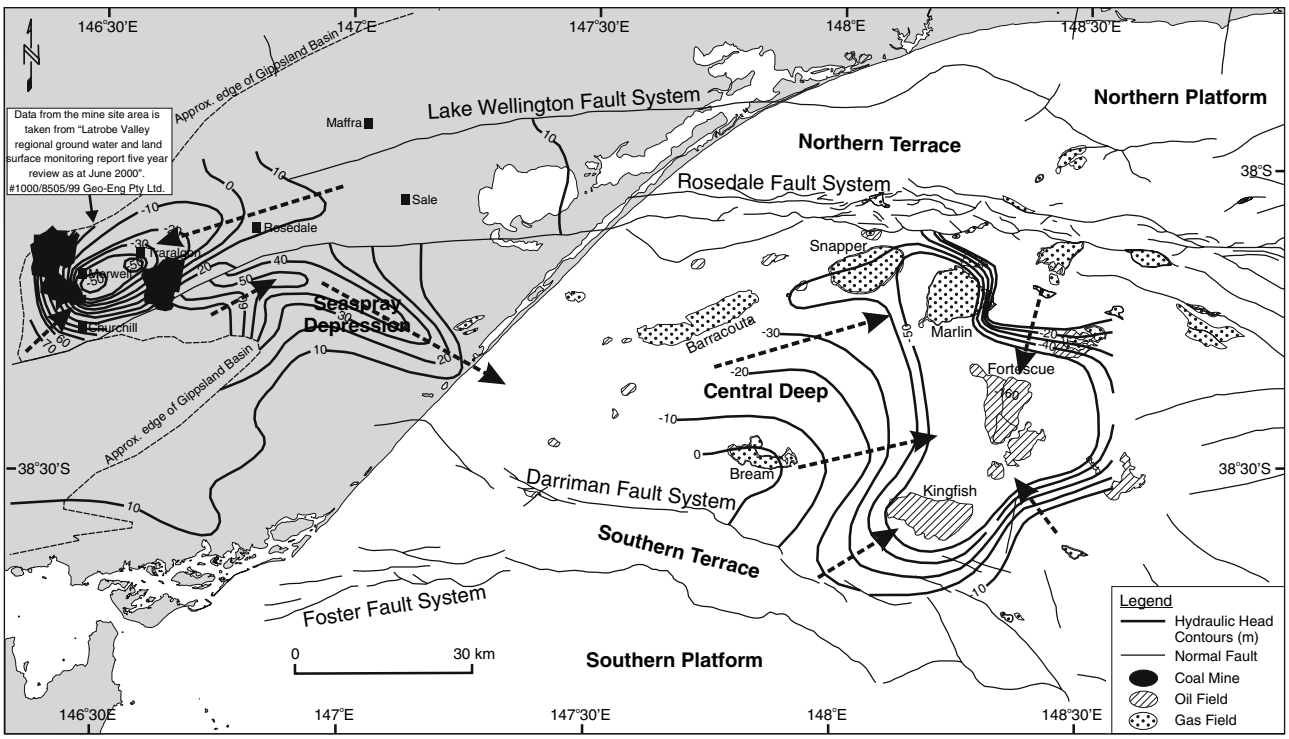

Fig. 14 Estimated hydraulic head distribution for the Upper Latrobe Aquifer System in 2004 to 2020

relatively flat compared with the structural slope of the base of the regional seal. However, pressure depletion in the vicinity of the oil-producing fields in the offshore Gippsland Basin has resulted in local steepening of the hydraulic gradient. Thus, in the short-term the driving force of the moving formation water on the injected CO_2 could significantly alter the migration direction predicted from only buoyancy drive at the base of the seal. In some cases, the driving force from moving formation water may be sufficient to entrain the CO_2 to migrate down structural dip. While this is a transient effect, aquifer recovery is not likely to occur prior to the initiation of CO_2 geological storage, so the present-day conditions need to be considered.

A tilt analysis was conducted to establish the relative strength of the up-dip buoyancy driving force versus the down-dip hydraulic driving force on injected CO_2. For the Kingfish Field area injection scenario, within the intra-Latrobe succession the hydraulic gradient is likely to be insufficient to overcome the buoyancy forces, and CO_2 will probably migrate upwards and eastwards as predicted from the structural geometry. However, once CO_2 reaches the top Latrobe Group the hydrodynamic driving force may be strong enough to entrain the CO_2 down-dip (northeastwards) towards the hydraulic low at the Fortescue Field. If this occurs it will positively impact CO_2 containment, as it will increase the migration pathway distance, allowing more pore space for storage capacity to be accessed and greater time for dissolution and mineral reactions to occur. Once the aquifer recovers and the field areas re-pressurise, the formation water flow is likely to return to a similar condition to its virgin state, and CO_2 will then migrate under the influence of buoyancy forces back towards the Kingfish Field.

The present-day flow system can therefore be used to decrease containment risk and potentially increase storage capacity if an injection and storage scenario is linked with the anticipated oil pool abandonment plans. Further numerical simulation of the flow system is required to evaluate the duration of the transient flow system, and to increase the accuracy of the predicted CO_2 migration pathways.

Geomechanical assessment

Sub-surface injection of CO_2 at pressures that exceed prevailing formation pressures may potentially reactivate pre-existing faults and generate new faults. Such brittle deformation can increase fault and fracture permeability, which could lead to unwanted migration of CO_2 (Streit and Hillis 2004). Estimates of the fluid pressures that may induce slip on faults at a potential injection site can be obtained from geomechanical risking. Such risking requires knowledge of the geomechanical model (in situ stresses and rock strength data) and the fault orientations. Details on geomechanical modelling techniques and the assessment of fault reactivation risk are described in Mildren et al (2002) and Streit and Hillis (2004).

Geomechanical model

The stress regime in the Gippsland Basin is on the boundary between strike-slip and reverse faulting, i.e. maximum horizontal stress ($\sim$40.5 MPa/km) is greater than vertical stress (21 MPa/km), which is approximately equal to minimum horizontal stress (20 MPa/km). Pore pressure is hydrostatic above the Campanian Volcanics of the Golden Beach Subgroup. The NW–SE maximum horizontal stress orientation is calculated at 139°N, which is broadly consistent with previous estimates (e.g. Hillis and Reynolds 2003; Nelson and Hillis 2005; Nelson et al. 2006) and verifies a NW-SE maximum horizontal stress orientation in the Gippsland Basin.

Geomechanical risking

Maximum sustainable pore pressure on faults and within the Latrobe Group was calculated using the FAST (Fault Analysis Seal Technology) technique (Mildren et al. 2002; Streit and Hillis 2004), and using the geomechanical model described in Table 3. The maximum pore pressure increase (Delta P) which can be sustained within the reservoir intervals of the Latrobe Group without brittle deformation

Table 3 Geomechanical model data

Scenario	Depth (m)	σ_v (MPa)	σ_H (MPa)	σ_h (MPa)	Pp (MPa)	σ_H orient (°N)	C (MPa)	μ
Faults: healed	2,300	48.3	93.2	46.0	22.5	139	8	0.78
Faults: cohesionless	2,300	48.3	93.2	46.0	22.5	139	0	0.65
Latrobe Group	2,300	48.3	93.2	46.0	22.5	139	8.8	0.67
Lakes Entrance Fm	2,300	46.2	89.1	44.0	22.5	139	2	0.60

σ_v is vertical stress, σ_H is maximum horizontal stress, σ_h is minimum horizontal stress, Pp is pore pressure, σ_H orient is the orientation of the maximum horizontal stress, C is cohesion, and μ is coefficient of friction or coefficient of internal friction for faults and intact rock respectively

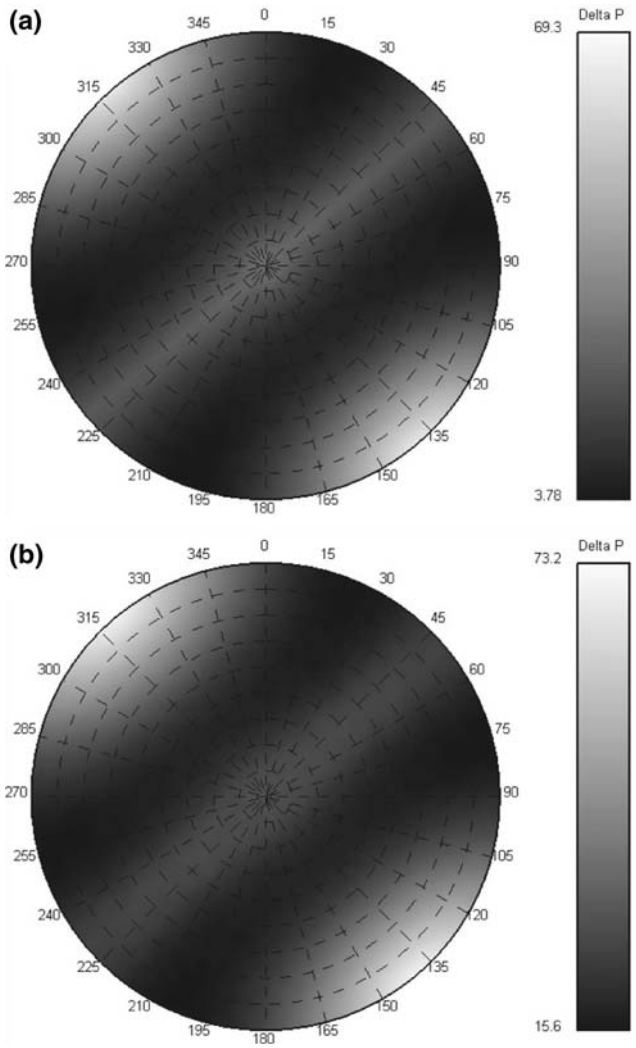

Fig. 15 Stereonets showing the reactivation risk for faults at 2,300 m in the Gippsland Basin (faults are plotted as poles to planes), for: **a** cohesionless faults—the highest reactivation risk for optimally-orientated faults corresponds to an estimated pore pressure increase (Delta P) of 3.78 MPa (~548 psi); and **b** healed faults—the highest reactivation risk for optimally-orientated faults corresponds to an estimated pore pressure increase (Delta P) of 15.6 MPa (~2,263 psi)

(i.e. the formation of a fracture) was estimated to be 14.5 MPa (~2,103 psi). The maximum pore pressure increase that can be sustained in the Lakes Entrance Formation regional seal was estimated to be 9.0 MPa (~1,299 psi). Therefore, injection is not recommended near the top of the reservoir in order to minimise the potential pore pressure build-up near the seal.

Fault reactivation risk was calculated using two fault strength scenarios: cohesionless faults and healed faults (Fig. 15). The fault orientations for high or low reactivation risk are very similar for both healed and cohesionless faults. High angle faults striking NE–SW are unlikely to reactivate in the present stress regime and have low reactivation risk. High angle faults orientated ESE–WNW and SSE–NNW have the highest fault reactivation risk potential. The highest fault reactivation risk for optimally-orientated faults corresponds to an estimated pore pressure increase (Delta P) of 3.78 MPa (~548 psi) for cohesionless faults and 15.6 MPa (~2263 psi) for healed faults. However, the Delta *P* values (maximum pore pressure increases) presented in the geomechanical assessment are subject to large errors due to uncertainties in the geomechanical model. In particular, the maximum horizontal stress and rock strength data are poorly constrained. Further work, such as laboratory testing of cores to determine failure envelopes of the fault and host rocks (e.g. uniaxial compressive strength, tensile strength), needs to be conducted to constrain the geomechanical model and reduce the uncertainties.

Fault reactivation risk for the Kingfish-Bream area

Sixteen faults have been mapped from 3D seismic data in the Kingfish-Bream area (Fig. 16). Nine of these faults cut the Latrobe Unconformity at the base of the regional seal. Six faults near the Bream Field and two faults near Gurnard-1 trend NNW-SSE. The fault near East Kingfish-1 trends SW–NE at its western tip and rotates towards E–W at its eastern tip. Seven faults were interpreted to terminate within the Latrobe Group. These faults lie south of the Kingfish Field and trend WNW–ESE to E–W. More faults are present at this stratigraphic interval, but time-restrictions meant that only a representative selection could be mapped. However, fault reactivation risk for any fault not included in this study can be analysed using the reactivation risk stereonets (Fig. 15).

Fault reactivation risk was evaluated for the 16 faults with known orientations (Fig. 16). Eight of the nine faults which cut the Latrobe Unconformity have moderate to high fault reactivation risk. Reactivation of these faults may increase fault permeability and lead to movement of CO_2 out of the Latrobe Group. However, most of the faults present are not in the predicted immediate CO_2 migration pathways and most do not cut the top seal. The fault near East Kingfish-1 has low to moderate reactivation risk and is less likely to reactivate in the present stress regime. The reactivation risk for the seven faults which terminate within the Latrobe Group is moderate to high. Reactivation of these faults may not be a containment risk because they do not appear to extend beyond the target reservoir. Nonetheless, reactivation of these intra-Latrobe faults is undesirable. An injection scenario which minimises pore pressure increases on all known faults should be chosen, such as limiting the injection rate, increasing the injection interval or number of wells, or concurrently producing water. Monitoring of pore pressure would ensure that

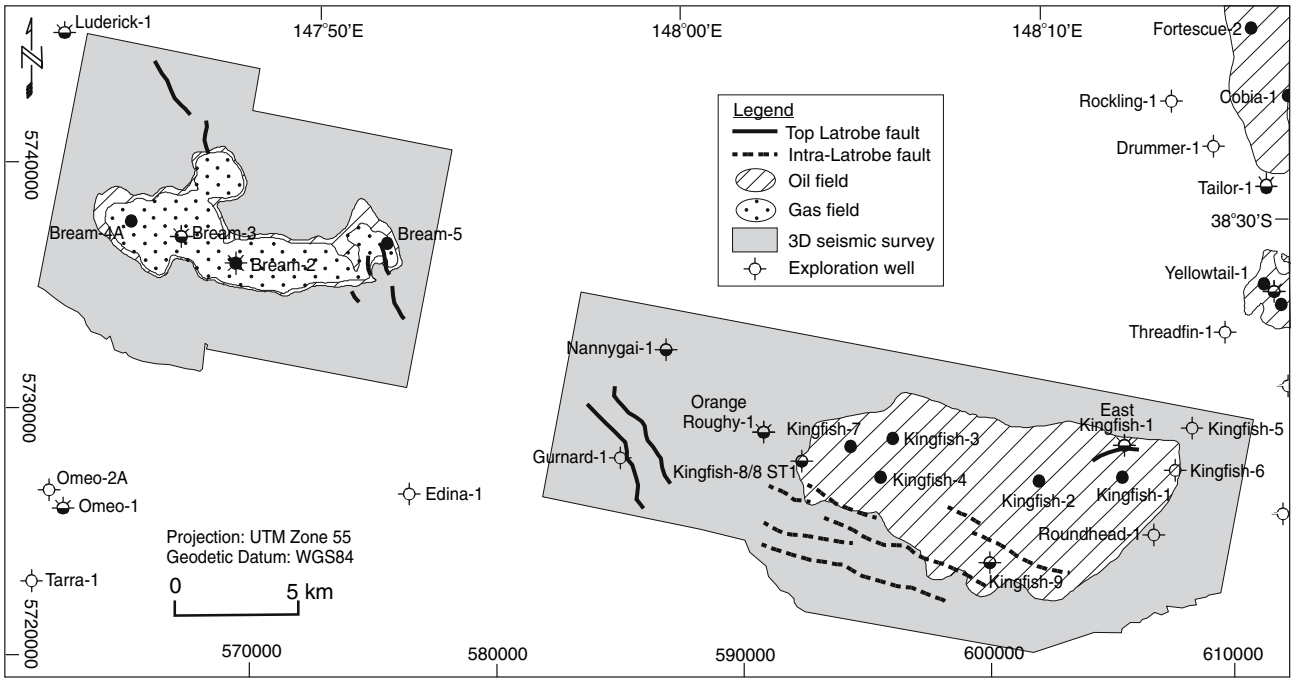

Fig. 16 Location map of interpreted faults in the Bream–Kingfish area for the top Latrobe and intra-Latrobe stratigraphic intervals

increases that may lead to slip on pre-existing faults are avoided.

Capacity

An assessment of the available pore volume in the existing hydrocarbon fields of the Gippsland Basin was undertaken to determine their possible CO_2 storage capacity once the fields are depleted. The main source of information for the properties for each of the fields was Malek and Mehin (1998), with additional data supplemented from well completion reports where necessary. The reservoir volumes presently occupied by hydrocarbons were estimated using standard oil industry volumetric calculation methods (e.g. Morton-Thompson and Woods 1992) and converted to equivalent CO_2 volumes based on reservoir-specific CO_2 formation volume factors.

The CO_2 storage capacity (available pore volume) for each of the hydrocarbon fields in the Gippsland Basin is shown in Table 4. The northern gas fields of Marlin, Snapper and Barracouta have the greatest storage potential due to the size of their structural closures. The Kingfish Field is the largest oil field, with a possible CO_2 storage capacity of about 200 Mt. The assessment shows that the existing hydrocarbon fields in the Gippsland Basin have the potential to store up to approximately 2,000 Mt CO_2. It is important to note that this number represents the structural closures only, and does not take into account the potentially significant additional capacity that could be obtained through stratigraphic trapping deeper than the structural closures, dissolution into the formation water and residual gas trapping along the migration pathways, or mineral trapping.

An estimate of the potential CO_2 storage capacity within the intra-Latrobe stratigraphy of the Kingfish Field area was also conducted to give an idea of how much additional storage capacity could be obtained by utilising more than the structural closures. The calculation method was very simplistic and used a rectangular area and average thickness for the intra-Latrobe Group intervals. As the CO_2 would be unlikely to fill the entire interval over the whole area, correction factors of 0.5 were applied to both the area and the thickness (i.e. 25% of the total volume). The corrected bulk rock volume was multiplied by average net to gross ratio and porosity values and converted to an equivalent CO_2 volume.

The results indicate that there is potential for a possible additional 685 Mt CO_2 storage capacity by utilising the intra-Latrobe stratigraphy beneath the structural closure of the Kingfish Field. This is approximately three times the capacity of the structural closure, and demonstrates how a deeper injection strategy may provide significantly more CO_2 storage capacity. This value predicts the available pore volume only, and numerical simulation is required to verify how much of the pore space is utilised (sweep

Table 4 CO_2 storage capacity of existing hydrocarbon fields in the Gippsland Basin

Field	Bulk rock volume (10^6 m^3)	Net/gross (%)	Porosity (%)	Water saturation (%)	Formation volume factor	Capacity (Mt)
Angelfish	355	59.2	14.0	57.0	0.0028490	2.5
Archer	184	67.7	13.0	53.0	0.0025516	1.5
Barracouta	7980	92.5	25.0	20.0	0.0061964	225.0
Batfish	434	87.1	25.0	23.0	0.0050806	7.1
Blackback	62	100.0	19.0	18.0	0.0027607	3.2
Bream	4212	64.1	22.0	20.0	0.0036729	122.2
Cobia	578	83.3	22.0	16.0	0.0034457	20.0
Dolphin	59	56.4	25.0	21.0	0.0049090	0.6
Flounder	2,016	79.8	21.0	23.0	0.0032449	71.5
Fortescue	3,498	69.2	20.0	22.0	0.0034331	96.7
Grunter	93	18.5	14.5	52.5	0.0028473	0.2
Halibut	2,002	61.4	22.0	16.0	0.0034457	37.2
Kingfish	6,391	74.7	21.0	18.0	0.0034577	196.5
Kipper	4,142	49.9	17.9	48.7	0.0036428	29.3
Leatherjacket	139	74.7	25.5	45.5	0.0091290	0.9
Luderick	16	100.0	24.1	20.0	0.0036114	0.8
Mackerel	4,600	91.1	20.0	22.0	0.0034457	169.1
Marlin	24,860	53.1	25.0	13.6	0.0039539	577.0
Moonfish	1,008	80.6	25.0	24.0	0.0036876	34.6
Perch	118	44.7	27.0	15.0	0.0046840	2.3
Seahorse	154	49.1	23.0	14.0	0.0037012	3.3
Snapper	16,810	58.5	24.0	15.0	0.0043158	408.8
Sunfish	240	50.0	22.0	30.0	0.0034741	4.8
Tarwhine	111	66.7	23.0	21.0	0.0044365	2.6
Tuna	1,716	37.5	18.0	37.0	0.0039111	16.4
Turrum	560	74.3	12.5	22.5	0.0034331	10.5
West Kingfish	1,216	50.0	19.0	37.0	0.0034577	9.9
West Tuna	324	91.7	24.0	35.0	0.0044365	9.2
Whiptail	36	75.0	21.5	24.0	0.0048507	0.8
Whiting	51	80.0	24.0	17.0	0.0059958	0.8
Wirrah	540	26.0	12.0	50.0	0.0031883	1.3
Yellowtail	189	100.0	18.8	33.0	0.0031394	6.8
Total						2073.2

These values represent the structural closures only and do not take into account the potential additional capacity in the pore space beneath and between the closures

efficiency). The available pore volume from both the intra-Latrobe Group and top Latrobe Group structural closure indicates there is likely to be sufficient CO_2 storage capacity for 15 Mt per annum injection for 40 years.

Numerical flow simulation

The aim of the numerical simulations was to examine the feasibility of large rates of injection at the Kingfish Field area, and to predict the migration path, ultimate long-term destination and form of the injected CO_2.

Numerical simulations of injectivity

Simulation models were constructed to test various parameters for their impact on injectivity (maximum injection rate), and to establish the number of wells required for a 15 Mt/a injection rate. A two-phase GASWATER option of the commercial IMEX Black Oil Simulator (CMG 2004) was used to model an immiscible displacement of reservoir brine with CO_2. Dissolution and residual gas saturation were not included for the sake of simplicity. Including dissolution effects may increase injectivity up to 20% (e.g. Sayers et al. 2006), so the results presented here are

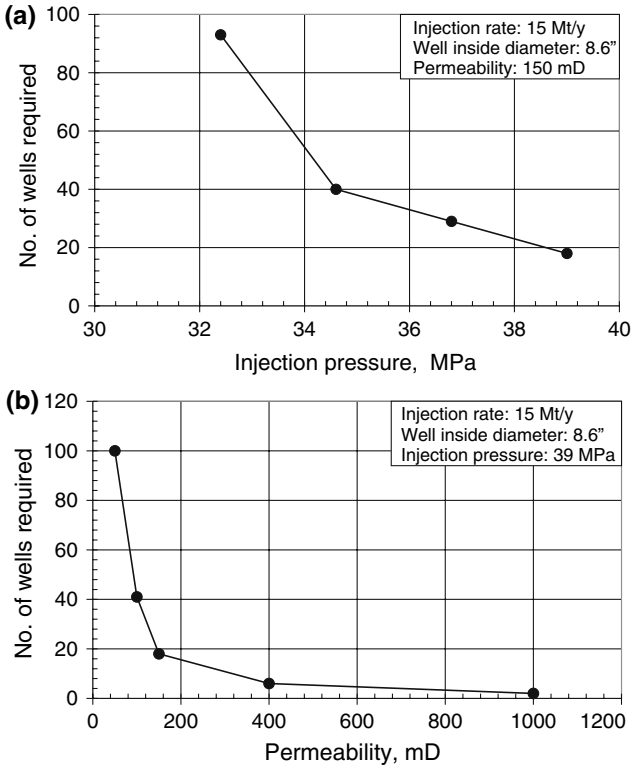

Fig. 17 Number of wells required for a CO_2 injection rate of 15 Mt/a as a function of **a** injection pressure and **b** permeability

conservative. Residual gas saturation does not have much impact in short-term injectivity simulations; it is important for long-term simulations to assess trapping phenomenon. Infinite analytical aquifers surrounded the model area to allow the outflow of brine. The shale barriers in the formations were included in the numerical model by means of a reduced vertical permeability (formation anisotropy ratio of 0.05). Simulations of 25 and 40 years were run to examine the CO_2 injectivity until injection ceased.

The simulation results from a 3D intra-Latrobe to top Latrobe model (Sequences 2 to 6) determined that 18 vertical wells are required for an injection rate of 15 Mt/a into the Sequence 2 interval at an injection pressure constrained to 90% fracture pressure (39 MPa). The effect of injection pressure on the number of vertical wells required to inject CO_2 at 15 Mt/a was also examined. This assessment indicated that constraining the injection pressure to more conservative values of the fracture pressure results in an increase in the number of wells required. For example, the number of wells required for an injection pressure at 75% fracture pressure (32.4 MPa) is more than twice that for an injection pressure at 80% fracture pressure (34.6 MPa) (Fig. 17a). Lower permeability values also result in an increased number of wells required to inject CO_2 at a rate of 15 Mt/a (Fig. 17b).

Numerical simulations of flow paths

A simulation model was devised from depth-converted seismic surfaces and average porosity, permeability and shale fraction characteristics of the intersecting wells. The stratigraphic complexity is represented in the simulations by using object modelling (explicitly generated stochastic realisations of shale distributions) to give a shale distribution that honours the overall shale fraction and the lateral extent appropriate to the depositional environment. The base of Sequence 2 (top Volador Formation) was taken as the bottom of the region of interest. The simulation code used for this study was TOUGH2 Version 2.0 (Pruess et al. 1999). For the base case simulations, the injection rate was 15 Mt/a for 40 years within the Sequence 2 interval (~550–800 m deeper than the main oil accumulation), residual gas saturation was assumed to be 20%, and the object-modelled shales were 2 km × 3 km in dimensions at a total volume fraction of 20%.

In the base case scenario modelled, the CO_2 is still contained within the intra-Latrobe Group succession after 40 years injection, migrating upwards and slightly eastwards beneath the shale units (Fig. 18a). Since the shales follow the shape of the internal surfaces, there are localised traps which retard the upward movement of CO_2 as each trap fills up to the spill-point. At around 190 years the CO_2 reaches the upper sequences (in and beneath the Gurnard Formation). From here it then spreads out laterally around the west end of the Kingfish Field (Fig. 18b). In the long-term, 1,100 years after the end of injection, the injected CO_2 has continued to drain upwards from the deep injection and has spread out into the eastern end of the Kingfish Field area and begun to migrate towards the west (and the next structural closure). At the end of the injection phase, approximately 13% of the CO_2 was dissolved into the formation water, which increased to approximately 46% after 1,000 years.

Several case variations were simulated, including changes to shale distributions, permeability and residual gas saturation. Larger shales (4 km × 6 km) decreased the effective vertical permeability, resulting in a more eastwards migration route and delayed the arrival at the top surface to around 400 years (Fig. 18c). The converse is true for a lower shale fraction, where CO_2 reached the top surface 80 years after injection ceased. Lower residual gas saturation resulted in more free CO_2 reaching the top surface and migration up-dip towards the Bream Field occurred sooner (860 years). Higher permeabilities (by a factor of three) significantly decreased the arrival time of the CO_2 at the top surface (down to 56 years) (Fig. 18d), and shallower injection (Sequence 3 interval) also gives a shorter arrival time.

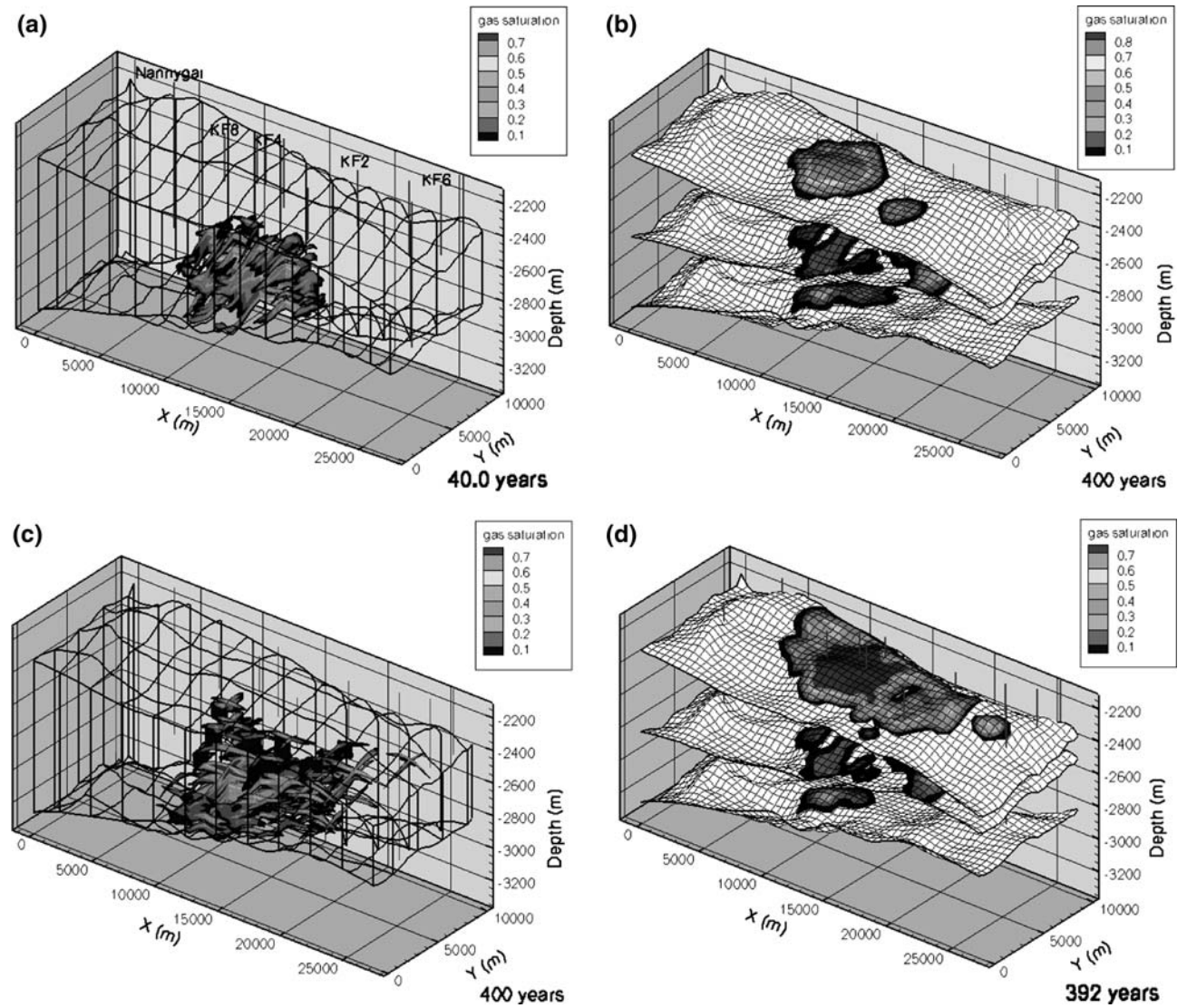

Fig. 18 Numerical flow simulation models of CO_2 saturation in the Kingfish Field area. **a** Fence diagram showing the CO_2 distribution in the base case simulation after 40 years CO_2 injection; **b** Contoured surfaces showing the lateral extent of the CO_2 in the base case simulation 400 years post-injection (the uppermost surface is the base of the regional seal); **c** Fence diagram showing the CO_2 distribution in the simulation case with larger shales 400 years post-injection; **d** Contoured surfaces showing the lateral extent of the CO_2 in the simulation case with three times higher permeability 392 years post-injection (the uppermost surface is the base of the regional seal)

The numerical simulations indicate that it is feasible to inject 15 Mt/a deep in the intra-Latrobe succession beneath the Kingfish Field area. The advantage of this strategy is a delay of about 50–200 years before the CO_2 reaches the areas from which hydrocarbons are presently being produced. In the post-injection period, the CO_2 that had migrated to the top surface was still largely contained in the Kingfish Field area after 1,000 years. In a couple of cases, it had migrated as far as the Nannygai-1 and Gurnard-1 wells. It is expected that the CO_2 would be trapped either by residual gas trapping or dissolution before it migrated as far as the Bream Field. Substantial dissolution of CO_2 (in the range 35–50%) was found to have occurred in 1,000 years.

Conclusions

Detailed studies on the geology, geophysics, geochemistry, geomechanics, hydrodynamics and numerical flow simulation were conducted in the offshore Gippsland Basin. These have yielded significant results pertinent to the suitability of the Gippsland Basin as a potential area for large-scale CO_2 geological storage. These include:

- a complex stratigraphic architecture that provides baffles which slow vertical migration and increases residual gas trapping and dissolution;
- non-reactive reservoir units that have high injectivity;
- a thin, suitably reactive, lower permeability marginal reservoir just below the regional seal to provide additional mineral trapping;
- several depleted oil fields that provide storage capacity coupled with a production-induced transient flow regime that enhances containment; and,
- long migration pathways beneath a competent regional seal.

The Kingfish Field area, in conjunction with other sites (e.g. the northern gas fields as assessed by Root et al. 2004), indicate that the Gippsland Basin has sufficient capacity to store very large volumes of CO_2. Storage of CO_2 in the Gippsland Basin may provide a solution to the problem of substantially reducing greenhouse gas emissions from proposed future coal developments in the Latrobe Valley.

Acknowledgments The authors would like to thank Barry Hooper (CO2CRC Capture Program Manager), Andy Rigg (CO2CRC Special Projects Manager) and Bill Koppe (Monash Energy) for providing guidance and support throughout this project. Adem Djakic and Peter Symes (Esso Australia) are thanked for provision of both openfile and confidential data, and for constructive criticism of the field capacity assessments. Hywel Thomas and Tom Bernecker (GeoScience Victoria, Department of Primary Industries) are also thanked for all their help and support with this project and for the provision of openfile data from the Gippsland Basin.

References

Bachu S (1995) Flow of variable-density formation water in deep sloping aquifers: review of methods of representation with case studies. J Hydrol 164:19–38

Bachu S, Michael K (2002) Flow of variable-density formation water in deep sloping aquifers: minimizing the error in representation and analysis when using hydraulic-head distributions. J Hydrol 259:49–65

Bernecker T, Partridge AD (2001) Emperor and Golden Beach Subgroups: the onset of Late Cretaceous sedimentation in the Gippsland Basin, SE Australia. In: Hill KC, Bernecker T (eds) Eastern Australian Basins symposium: a refocused energy perspective for the future. Petroleum Exploration Society of Australia, Melbourne, 25–28 November, pp 391–402

Bernecker T, Partridge AD (2005) Approaches to palaegeographic reconstructions of the Latrobe Group, Gippsland Basin, southeast Australia. APPEA J 45:581–599

CMG (2004) IMEX: IMplicit-EXplicit Black Oil Simulator User's Guide. Computer Modelling Group Ltd., Calgary, Alberta, Canada

Dahlberg EC (1995) Applied hydrodynamics in petroleum exploration. Springer, Berlin

Dewhurst DN, Jones RM, Raven MD (2002) Microstructural and petrophysical characterization of Muderong Shale: application to top seal risking. Petrol Geosci 8:371–383

DPI (2005) Minerals and petroleum—overview. http://www.dpi.vic.gov.au/dpi/nrenmp.nsf/childdocs/-C58CC29C22BD9D674A2567C4001F3676?open. Cited 1 May 2006

Ennis-King J, Paterson L (2005) Role of convective mixing in the long-term storage of carbon dioxide in deep saline formations. SPE J 10:349–356

Gibson-Poole CM, Root RS, Lang SC, Streit JE, Hennig AL, Otto CJ, Underschultz JR (2005) Conducting comprehensive analyses of potential sites for geological CO_2 storage. In: Rubin ES, Keith DW, Gilboy CF (eds) Greenhouse gas control technologies: proceedings of the 7th international conference on greenhouse gas control technologies, Volume I, Elsevier, Vancouver, 5–9 September, pp 673–681

Hatton T, Otto CJ, Underschultz JR (2004) Falling water levels in the Latrobe Aquifer, Gippsland Basin: determination of cause and recommendations for future work. CSIRO Wealth From Oceans

Hillis RR, Reynolds SD (2003) In situ stress field of Australia. In: Hillis RR, Müller RD (eds) Evolution and dynamics of the Australian Plate. Geological Society of Australia Special Publication 22 and Geological Society of America Special Paper 372:49–60

Hooper B, Murray L, Gibson-Poole CM (2005) Latrobe Valley CO_2 storage assessment—final report. CO2CRC Report No. RPT05–0108. http://www.co2crc.com.au/PUBFILES/OTHER05/LVCSA_FinalReport.pdf. Cited 30 November 2006

Karbøl R, Kaddour A (1995) Sleipner Vest CO_2 disposal— injection of removed CO_2 into the Utsira Formation. Energy Convers Manage 36:509–512

Lang SC, Grech P, Root RS, Hill A, Harrison D (2001) The application of sequence stratigraphy to exploration and reservoir development in the Cooper-Eromanga-Bowen-Surat Basin system. APPEA J 41:223–250

Malek R, Mehin K (1998) Oil and gas resources of Victoria. Petroleum Development Unit, Victorian Department of Natural Resources and Environment

McKerron AJ, Dunn VL, Fish RM, Mills CR, van der Linden-Dhont SK (1998) Bass Strait's Bream B reservoir development: success through a multi-functional team approach. APPEA J 38:13–35

Mildren SD, Hillis RR, Kaldi JG (2002) Calibrating predictions of fault seal reactivation in the Timor Sea. APPEA J 42:187–202

Morton-Thompson D, Woods AM (eds) (1992) Development geology reference manual. The American Association of Petroleum Geologists, AAPG Methods in Exploration 10

Mudge WJ, Thomson AB (1990) Three-dimensional geological modelling in the Kingfish and West Kingfish oil fields: the method and applications. APPEA J 30:342–354

Nelson EJ, Hillis RR (2005) In situ stresses of the West Tuna area, Gippsland Basin. Aust J Earth Sci 52:299–313

Nelson EJ, Hillis RR, Sandiford M, Reynolds SD, Mildren SD (2006) Present-day state-of-stress of southeast Australia. APPEA J 46:283–305

Otto CJ, Underschultz JR, Hennig AL, Roy VJ (2001) Hydrodynamic analysis of flow systems and fault seal integrity in the North West Shelf of Australia. APPEA J 41:347–365

Perkins EH, Gunter WD (1996) Mineral traps for carbon dioxide. In: Hitchon B (ed) Aquifer disposal of carbon dioxide: hydrodynamic and mineral trapping—proof of concept. Geoscience Publishing Ltd, pp 93–114

Posamentier HW, Allen GP (1999) Siliciclastic sequence stratigraphy—concepts and applications. SEPM, Concepts in Sedimentology and Paleontology 7

Power MR, Hill KC, Hoffman N, Bernecker T, Norvick M (2001) The structural and tectonic evolution of the Gippsland Basin: results from 2D section balancing and 3D structural modelling. In: Hill

KC, Bernecker T (eds) Eastern Australian Basins symposium: a refocused energy perspective for the future. Petroleum Exploration Society of Australia, Melbourne, Australia, 25–28 November, pp 373–384

Pruess K, Oldenburg C, Moridis G (1999) TOUGH2 User's Guide, Version 2.0. Earth Sciences Division, Lawrence Berkeley National Laboratory, Technical Report LBNL-43134

Rahmanian VD, Moore PS, Mudge WJ, Spring DE (1990) Sequence stratigraphy and the habitat of hydrocarbons, Gippsland Basin, Australia. In: Brooks J (ed) Classic petroleum provinces. Geological Society of London, Special Publication 50:525–541

Root RS, Gibson-Poole CM, Lang SC, Streit JE, Underschultz JR, Ennis-King J (2004) Opportunities for geological storage of carbon dioxide in the offshore Gippsland Basin, SE Australia: an example from the upper Latrobe Group. In: Boult PJ, Johns DR, Lang SC (eds) Eastern Australasian Basins Symposium II, Special Publication, Petroleum Exploration Society of Australia, Adelaide, 19–22 September, pp 367–388

Sayers J, Marsh C, Scott A, Cinar Y, Bradshaw J, Hennig AL, Barclay S, Daniel RF (2006) Assessment of a potential storage site for carbon dioxide: a case study, southeast Queensland, Australia. Environ Geosci 13:123–142

Streit JE, Hillis RR (2004) Estimating fault stability and sustainable fluid pressures for underground storage of CO_2 in porous rock. Energy 29:1445–1456

Thomas H, Bernecker T, Driscoll J (2003) Hydrocarbon Prospectivity of Areas V03–3 and V03–4, Offshore Gippsland Basin, Victoria, Australia: 2003 Acreage Release. Department of Primary Industries, Victorian Initiative for Minerals and Petroleum Report 80

Underschultz JR, Otto CJ, Roy V (2003) Regional Hydrodynamic Analysis on the Gippsland Basin. CSIRO Petroleum, APCRC Confidential Report No. 03–04

Van Wagoner JC, Mitchum RM, Campion KM, Rahmanian VD (1990) Siliciclastic sequence stratigraphy in well logs, cores and outcrops: concepts for high-resolution correlation of time facies. AAPG, Methods in Exploration Series 7

Vavra CL, Kaldi JG, Sneider RM (1992) Geological applications of capillary pressure: a review. AAPG Bull 76:840–850

Watson MN, Boreham CJ, Tingate PR (2004) Carbon dioxide and carbonate cements in the Otway Basin: implications for geological storage of carbon dioxide. APPEA J 44:703–720

Watson MN, Gibson-Poole CM (2005) Reservoir selection for optimised geological injection and storage of carbon dioxide: a combined geochemical and stratigraphic perspective. In: The fourth annual conference on carbon capture and storage. National Energy Technology Laboratory, US Department of Energy, Alexandria, 2–5 May 2005

Woollands MA, Wong D (eds) (2001) Petroleum Atlas of Victoria, Australia. The State of Victoria, Department of Natural Resources and Environment

GIPPSLAND BASIN GEOSEQUESTRATION: A POTENTIAL SOLUTION FOR THE LATROBE VALLEY BROWN COAL CO_2 EMISSIONS

C.M. Gibson-Poole[1,2], L. Svendsen[1,2], J. Underschultz[1,3], M.N. Watson[1,2], J. Ennis-King[1,4], P.J. van Ruth[1,2], E.J. Nelson[2], R.F. Daniel[1,2] and Y. Cinar[1,5]

[1]CRC for Greenhouse Gas Technologies (CO2CRC).
[2]Australian School of Petroleum, The University of Adelaide, SA 5005.
[3]CSIRO Petroleum, PO Box 1130, Bentley, WA 6102.
[4]CSIRO Petroleum, Private Bag 10, Clayton South, VIC 3169.
[5]School of Petroleum Engineering, The University of New South Wales, NSW 2052.

ABSTRACT

Geosequestration of CO_2 in the offshore Gippsland Basin is being investigated by the CO2CRC as a possible method for storing the very large volumes of CO_2 emissions from the Latrobe Valley area. A storage capacity of about 50 million tonnes of CO_2 per year for a 40-year injection period is required, which will necessitate several individual storage sites to be used both sequentially and simultaneously, but timed such that existing hydrocarbon assets are not compromised. Detailed characterisation focussed on the Kingfish Field area as the first site to be potentially used, in the anticipation that this oil field will be depleted within the period 2015–25. The potential injection targets are the interbedded sandstones, shales and coals of the Paleocene-Eocene upper Latrobe Group, regionally sealed by the Lakes Entrance Formation. The research identified several features to the offshore Gippsland Basin that make it particularly favourable for CO_2 storage. These include: a complex stratigraphic architecture that provides baffles which slow vertical migration and increase residual gas trapping; non-reactive reservoir units that have high injectivity; a thin, suitably reactive, low permeability marginal reservoir just below the regional seal providing additional mineral trapping; several depleted oil fields that provide storage capacity coupled with a transient flow regime arising from production that enhances containment; and, long migration pathways beneath a competent regional seal. This study has shown that the Gippsland Basin has sufficient capacity to store very large volumes of CO_2. It may provide a solution to the problem of substantially reducing greenhouse gas emissions from the use of new coal developments in the Latrobe Valley.

KEYWORDS

Carbon dioxide, CO_2, geological storage, geosequestration, Latrobe Valley, Gippsland Basin, Kingfish Field, Latrobe Group, Lakes Entrance Formation, sequence stratigraphy, reservoir characterisation, seal capacity, geochemical reactions, hydrodynamics, geomechanics, numerical simulation, CO2CRC.

INTRODUCTION

Eighty-five percent of the electricity for Victoria, southeast Australia, is generated from power stations fuelled by the extensive brown coal resources of the Latrobe Valley (DPI, 2005). Whilst this is a cheap source of energy, there is increasing concern over the contribution of greenhouse gases to the atmosphere from fossil fuel combustion. Thus, geological storage, or geosequestration, of carbon dioxide (CO_2) is being investigated by the Cooperative Research Centre for Greenhouse Gas Technologies (CO2CRC) as a possible method for storing the very large volumes of CO_2 emissions from the Latrobe Valley area. A recent study has focussed on storage of CO_2 emitted from the use of new coal developments in the Latrobe Valley area, which are planned to be carbon capture and storage (CCS) compatible.

The Gippsland Basin is one of Australia's premier hydrocarbon provinces, and has been producing since the 1960s (Fig. 1). The depletion and decommissioning of some of the major oil fields are likely to coincide with the need for storage for anticipated CO_2 sources from new coal developments in the Latrobe Valley. Enhanced oil recovery using carbon dioxide is not being considered for the oil fields at present, since primary recoveries are already very high. A storage capacity of about 50 million tonnes per year (Mt/y) for a minimum 40-year injection period is required, which provides a significant challenge of scale not previously considered. To meet this challenge, several individual storage sites within the offshore Gippsland Basin will need to be used both sequentially and simultaneously.

An analysis of the likely migration pathways at the top Latrobe Group (base regional seal) identified two main trends in the Central Deep: (1) migration from a basin centre location via the northern gas fields of Marlin, Snapper and Barracouta, and (2) migration via the southern oil fields of Fortescue, Kingfish and Bream (Fig. 2). It is envisaged that individual sites from along these two trends would be used sequentially, ramping up the volume of CO_2 stored to 50 Mt/y but timed such that existing hydrocarbon assets are not compromised.

A detailed study was conducted on the Kingfish Field area as the first site to be potentially used, in the anticipation that this oil field will be depleted within the period 2015–25 and thus available for CO_2 storage (Fig. 3). The concept involves CO_2 injection of 15 Mt/y for 40 years deep beneath West Kingfish into the intra-Latrobe Group stratigraphy (~550–800 m deeper than the main oil accumulation). CO_2 is predicted to migrate upwards and eastwards towards the top of the Latrobe Group. Free CO_2

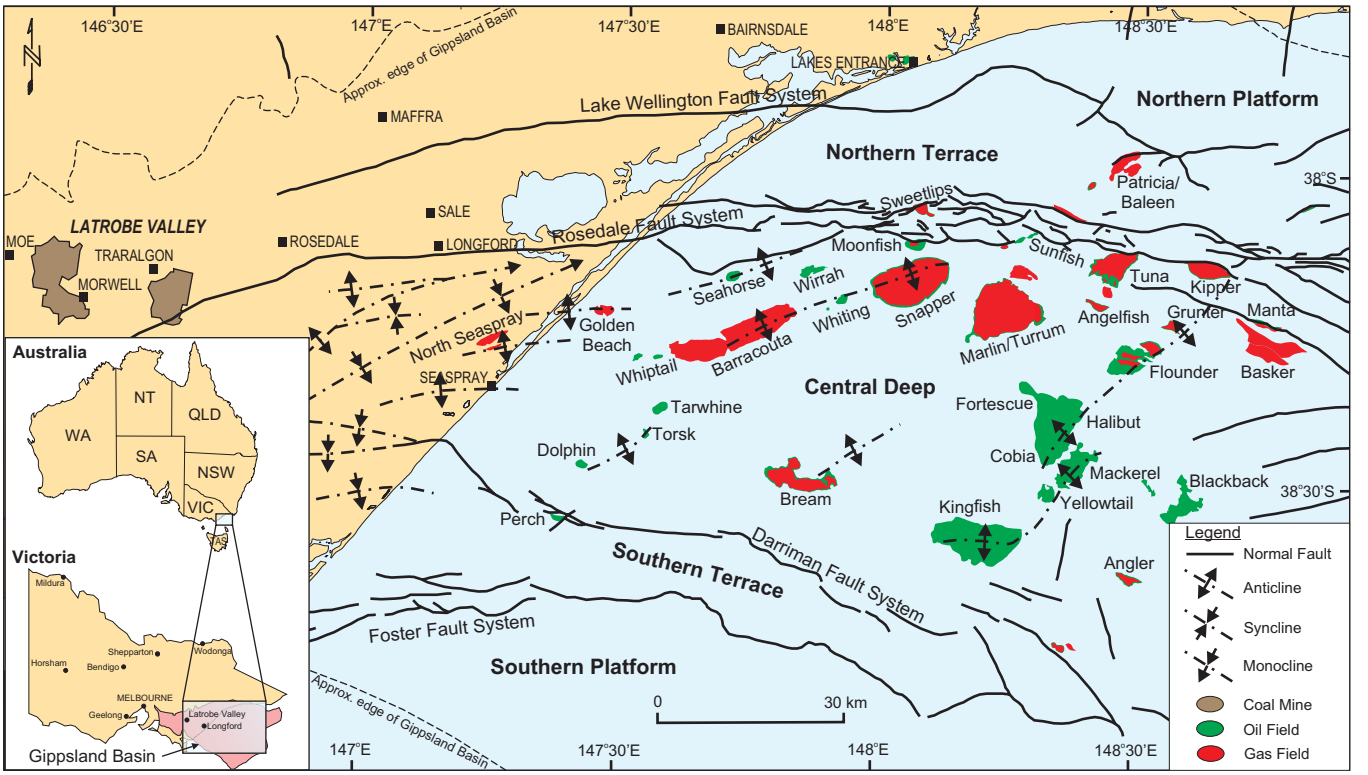

Figure 1. Location map of the Gippsland Basin, southeast Australia, showing key tectonic elements and existing hydrocarbon fields (modified after Power et al, 2001).

that reaches the base of the Lakes Entrance Formation would accumulate in the depleted Kingfish Field structural closure. If the capacity of the Kingfish closure is exceeded, and if still mobile, the CO_2 would then migrate westwards towards the structural closure of the Bream Field. This paper outlines the key results from the detailed studies on the geology, geophysics, geochemistry, geomechanics, hydrogeology and numerical flow simulations that were conducted for the Kingfish Field area.

LOCATION AND GEOLOGICAL SETTING

The Gippsland Basin is an east–west trending rift basin, located in southeast Australia, offshore from the Victorian coast (Fig. 1). It is a fairly symmetrical rift basin (Central Deep), bounded to the north and south by faulted terraces (Northern and Southern Terraces) and stable platforms (Northern and Southern Platforms) (Bernecker and Partridge, 2001; Power et al, 2001) (Fig. 1).

Rifting began in the Early Cretaceous in association with the continental break-up of Gondwana along the southern margin of Australia (Rahmanian et al, 1990; Power et al, 2001). By the latest Cretaceous, a post-rift marginal sag basin had developed and the upper Latrobe Group sediments (Halibut and Cobia Subgroups) were deposited under the increasing influence of the Tasman Sea, which encroached from the southeast (Fig. 4) (Rahmanian et al, 1990). The interbedded sandstones, shales and coal were deposited in alluvial plain, coastal plain, shoreface and shelf depositional environments along wave-dominated shorelines (Rahmanian et al, 1990; Thomas et al, 2003). Through the Palaeocene and Eocene, the shoreline retreated to the west and northwest, and culminated in the deposition of the condensed, glauconitic Gurnard Formation as the siliciclastic sediment supply became starved (Fig. 4) (Rahmanian et al, 1990).

The transition from the Latrobe Group to the Seaspray Group is marked by a regional angular unconformity, informally termed the 'Latrobe Unconformity', created by a marked decline in the sediment supply and several separate erosional events (Fig. 4) (Rahmanian et al, 1990; Thomas et al, 2003). Compressional tectonism started in the Late Eocene and continued through to the Middle Miocene, creating a series of northeast-trending anticlines, which became the hosts for the large oil and gas accumulations. During the compressional phase, the basin continued to subside and the calcareous sediments of the Seaspray Group were deposited in shelf, slope and basinal depositional environments (Fig. 4) (Rahmanian et al, 1990; Thomas et al, 2003).

METHODOLOGY

The subsurface behaviour of CO_2 is influenced by many variables, including reservoir and seal structure, stratigraphic architecture, reservoir heterogeneity, rela-

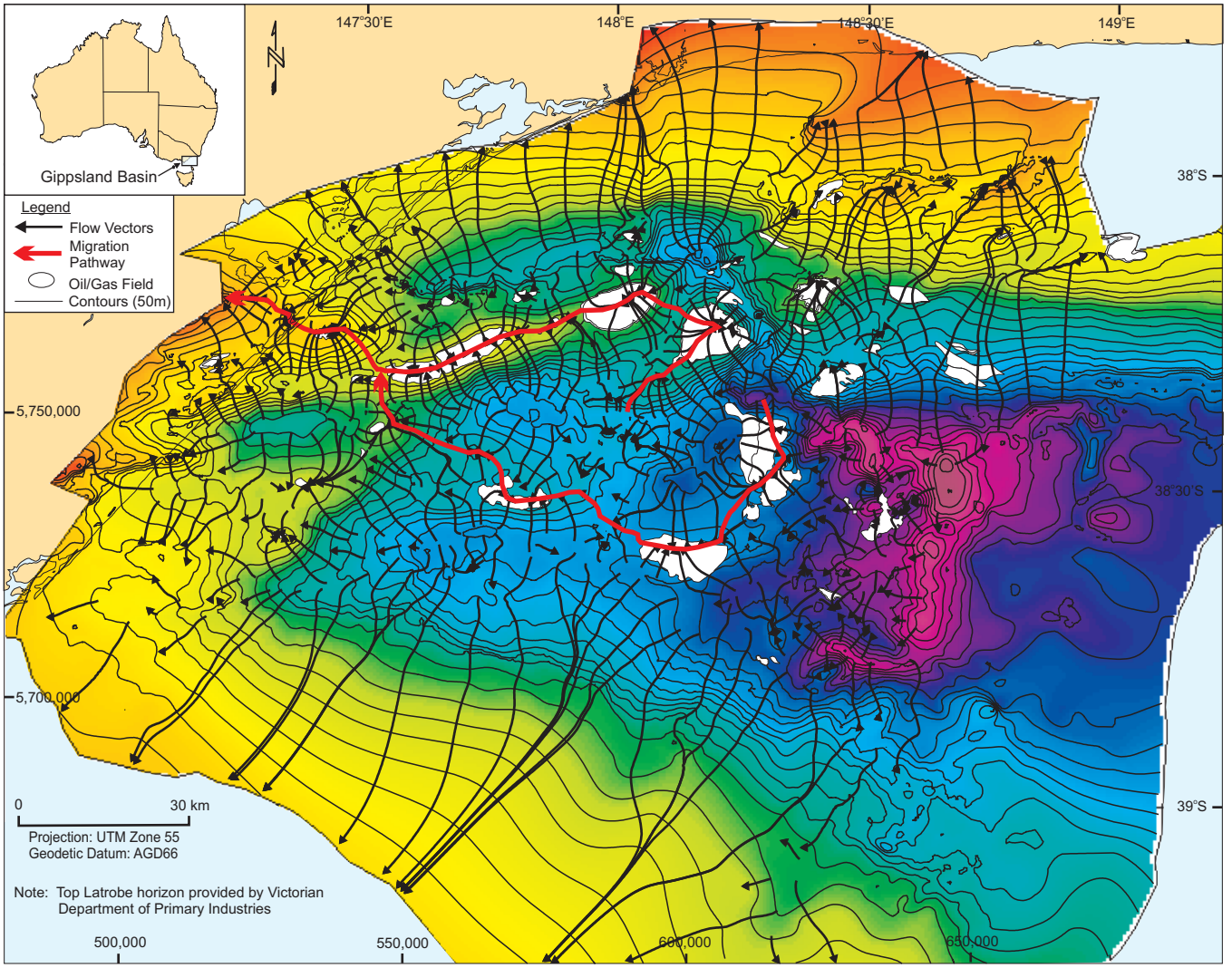

Figure 2. Basin flow vectors and key migration pathways within the Central Deep, based on the structural geometry of the top Latrobe Group depth structure map (top Latrobe Group depth surface provided by the Victorian Department of Primary Industries).

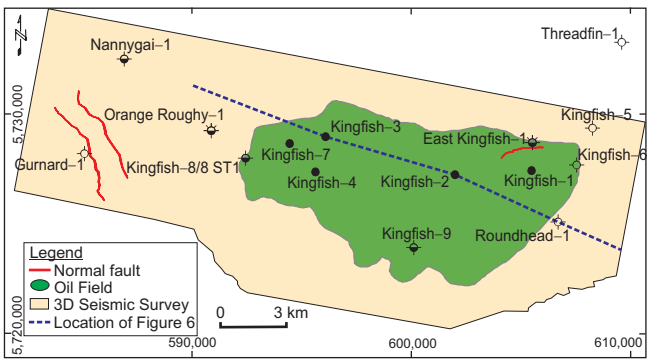

Figure 3. Location map of the Kingfish Field and surrounding area.

tive permeability, faults/fractures, pressure/temperature conditions, mineralogical composition of the rock framework, and hydrodynamics and geochemistry of the in situ formation fluids. Therefore, accurate appraisal of a potential CO_2 storage site requires detailed reservoir and seal characterisation, 3D modelling and numerical flow simulation (Root et al, 2004).

The methodology for evaluating a site for geological CO_2 storage is provided by Gibson-Poole et al (2005) and is shown in Figure 5. Seismic stratigraphic interpretations were integrated with wireline log correlations, detailed sedimentological core descriptions and biostratigraphy, to develop a sequence stratigraphic framework and sedimentary depositional model for the potential site. Collected core samples were subjected to Mercury Injection Capillary Pressure (MICP) analysis to evaluate the CO_2 retention capacity of the rocks, and were assessed petrologically by thin-section, x-ray diffraction and scanning

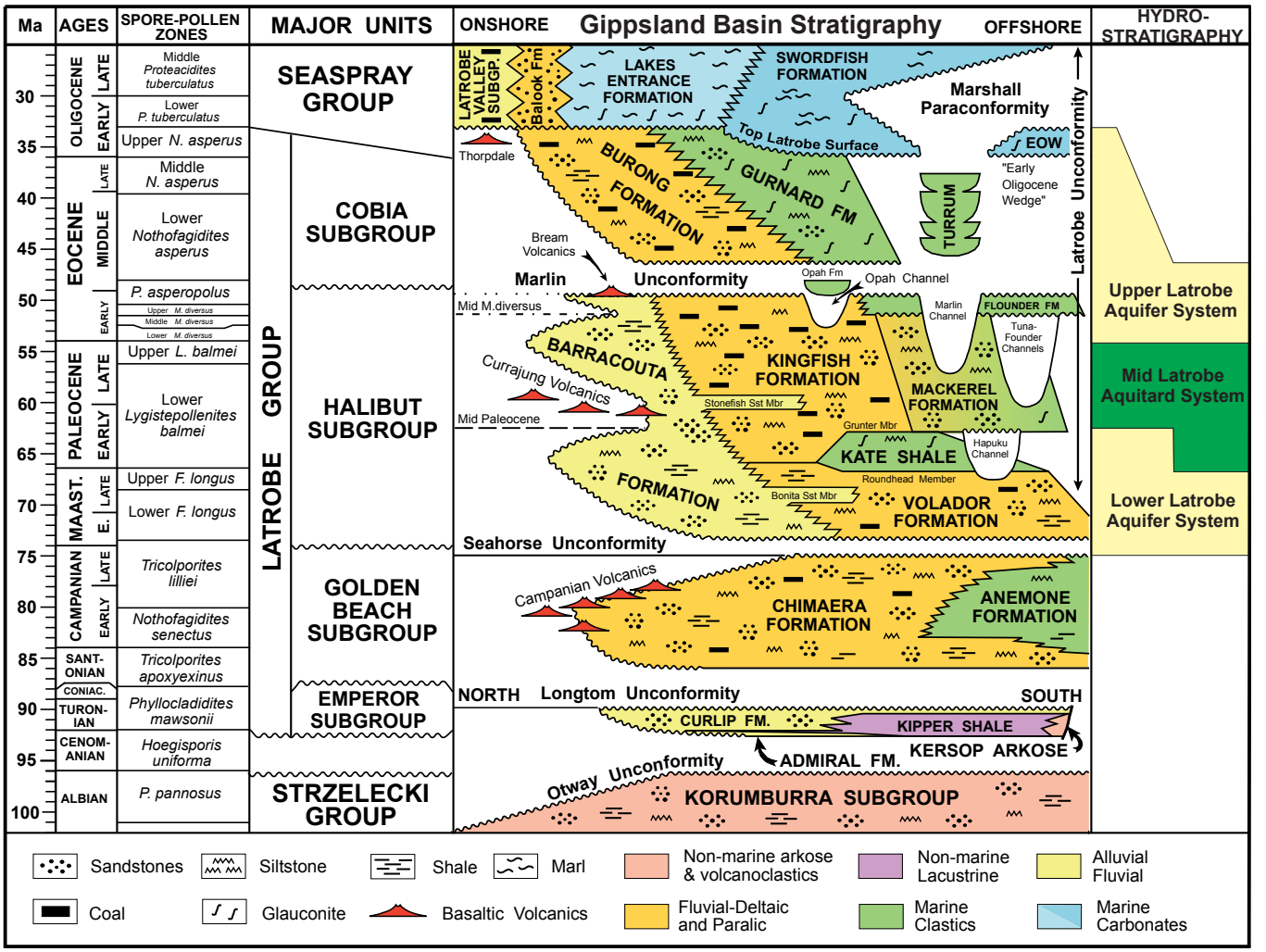

Figure 4. Stratigraphic column of the Gippsland Basin (modified after Bernecker and Partridge, 2001).

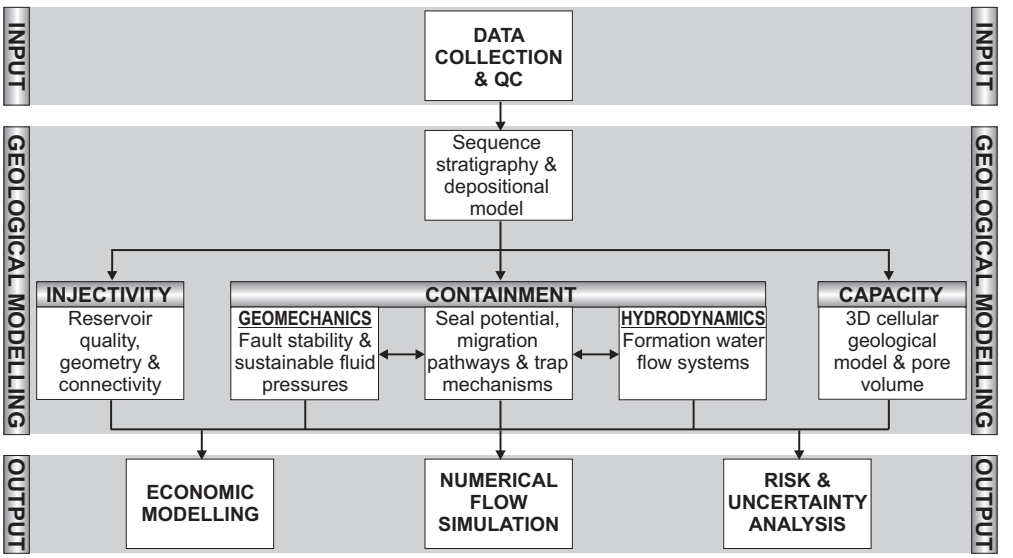

Figure 5. Workflow for CO_2 geological storage assessment (after Gibson-Poole et al, 2005).

electron microscope to ascertain potential CO_2-water-rock interactions. In situ stress and rock strength data were used to determine maximum sustainable pore pressure increases and the reactivation risk of faults in the area. The past and present formation water flow systems were characterised from pressure-elevation plots and hydraulic head distribution maps to interpret their possible impact on CO_2 migration and containment.

The results of the geological modelling were input into the reservoir engineering simulations. Simulation models were constructed from depth-converted seismic surfaces and porosity-permeability characteristics of the intersecting wells. Shale distributions were modelled either by means of reduced vertical permeability (for injectivity simulations) or by object modelling (for simulations of short and long-term flow paths) to reflect the stratigraphic complexity. Short-term injectivity simulations used IMEX Black Oil Simulator, while the flow path simulations used the TOUGH2 code.

SEQUENCE STRATIGRAPHY AND DEPOSITIONAL MODEL

A sequence stratigraphic approach is adopted because it focusses on key surfaces that naturally subdivide the sediment succession into chronostratigraphic units. This is vital to understanding the likely distribution and connectivity of reservoirs and seals. The approach followed here is that outlined by van Wagoner et al (1990), Posamentier and Allen (1999) and Lang et al (2001), where sequences are defined as relatively conformable successions bounded by unconformities or their correlative conformities, and systems tracts are identified by key surfaces and stacking patterns, in both marine and continental settings. The sequence stratigraphic framework provides the foundation for the 3D geological models used in the numerical flow simulations.

Six unconformity-bound sequences were identified in the Kingfish Field area Latrobe Group stratigraphy beneath the Lakes Entrance Formation regional seal (Fig. 6). Sequence 1 (interval D) is representative of the Kate Shale, Sequences 2 to 5 (intervals C to A) are within the Kingfish Formation and Sequence 6 is representative of the Gurnard Formation. Sequences 1 to 5 are third-order sequences and are dominated by the highstand systems tracts. Each sequence has a progradational log motif and is clearly demonstrated by progradational sigmoid seismic facies at the eastern side of the field. Within each sequence, higher fourth-order sequences can be seen as transgressive-regressive cycles. Each highstand-dominated third-order sequence progressively backsteps within an overall transgressive sequence set. The sediments were deposited in coastal plain to shallow marine depositional environments along wave-dominated shorelines, transitioning from terrestrial-influenced sediments to marine-influenced sediments in a northwest–southeast direction across the field (Bernecker and Partridge, 2005).

Sequence 6 (Gurnard Formation) is a transgressive-regressive cycle at the top of the Latrobe Group. It pinches out in the middle of the Kingfish Field (between the Kingfish–3 and Kingfish–2 wells), where it has been removed by subsequent erosion associated with the Latrobe Unconformity. The Gurnard Formation is a condensed, glauconitic marine shelf deposit, which acts as either a seal or a low-quality reservoir depending on its location within the basin. At the Kingfish Field location it is generally considered non-net, although at the western end the P–1.1 reservoir is within

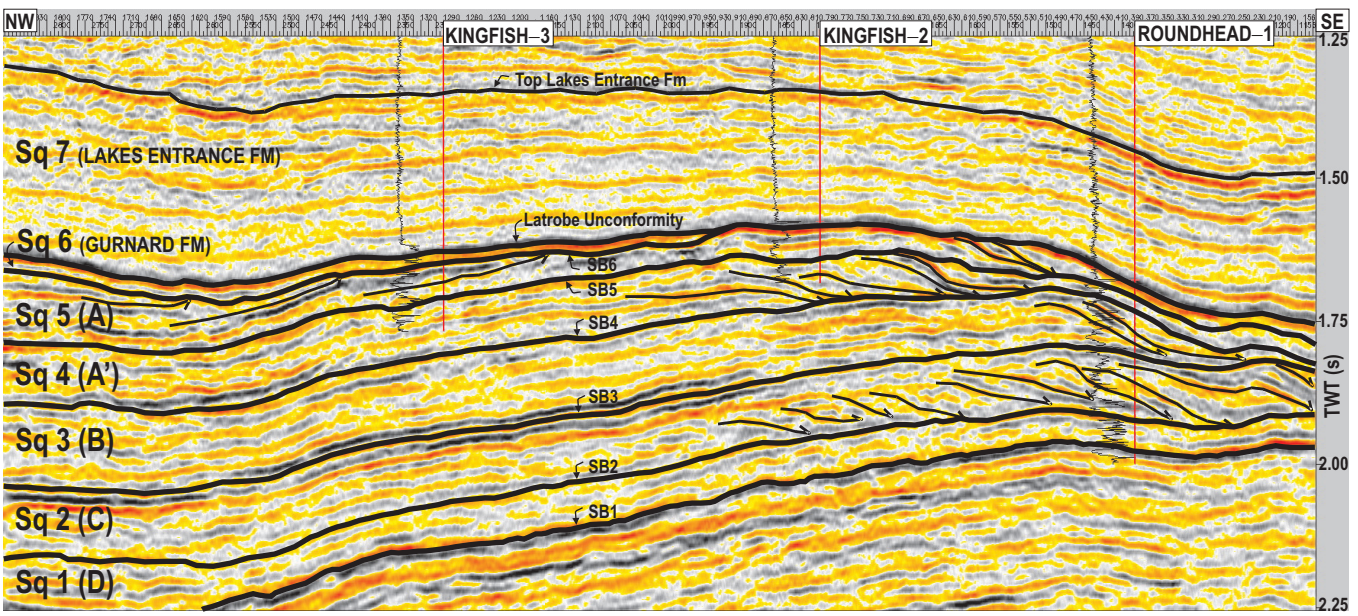

Figure 6. Seismic cross-section through the Kingfish Field area (line G92A–3074A), showing sequence interpretation and key stratal relationships such as truncation and downlap.

the Gurnard Formation (Mudge and Thomson, 1990). At the Bream Field the base of the formation constitutes a 'waste zone' (McKerron et al, 1998).

The shoreline position of each sequence progressively backsteps to the northwest, reflecting the overall transgressive nature of the upper Latrobe Group as the Tasman Sea increasingly encroached from the southeast. The Latrobe Group sequences are tilted structurally upwards to the east and are progressively truncated by the Latrobe Unconformity, a major basin-wide angular unconformity separating the reservoir intervals of the Latrobe Group from the overlying Seaspray Group. The fine-grained sediments of the Lakes Entrance Formation at the base of the Seaspray Group were deposited in shelf, slope and basinal depositional environments during subsequent major transgression and highstand, creating the regional seal.

INJECTIVITY

Upon injection into a reservoir rock, the flow behaviour and migration of CO_2 will depend primarily on parameters such as the viscosity ratio, injection rate and relative permeability, but also the stratigraphic architecture, reservoir heterogeneity and structural configuration of the rocks. Injectivity issues that can be assessed through the geological modelling therefore include the geometry and connectivity of individual flow units, the nature of the heterogeneity within those units (i.e. the likely distribution and impact of baffles) and the physical quality of the reservoir in terms of porosity and permeability characteristics (Gibson-Poole et al, 2005).

Reservoir geometry and connectivity

The vertical and lateral connectivity of individual nearshore sandstone bodies is likely to be favourable, forming large-scale composite flow units. Analogue studies of modern and ancient shoreface deposits suggest individual deposit dimensions of 500–5,000 m in width and 1,000–10,000 m in length. The maximum elongation direction of the sandbodies is expected to be parallel to the palaeo-shoreline (Root et al, 2004; Root, in prep.).

The fluvial channel sediments that exist in the coastal–alluvial plain deposits are commonly associated with finer-grained sediments, such as floodplain and crevasse splay deposits. As a result, fluvial deposits are characterised by greater reservoir heterogeneity, and the fluvial channel sandstone bodies are likely to exhibit poorer vertical and lateral connectivity. Analogue studies of modern and ancient fluvial deposits suggest fluvial channel belt widths of 500–2,000 m (Root et al, 2004; Root, in prep.).

Reservoir quality

The quality of the reservoir can be assessed through detailed analysis of core plug porosity and permeability characteristics, petrology and wireline log petrophysical interpretation.

POROSITY AND PERMEABILITY

Core plug porosity and permeability data from wells in the southern oil fields area show a range of reservoir quality (Fig. 7). The Kingfish Formation sediments have

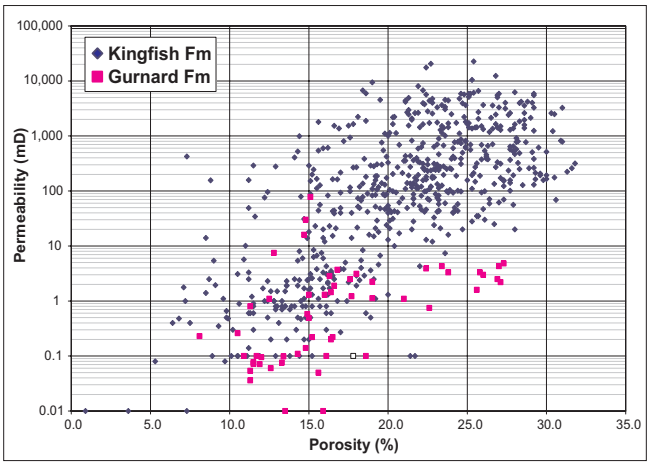

Figure 7. Core plug porosity and permeability data for wells in the southern oil fields area for the Kingfish and Gunard Formations.

porosities ranging up to 32% and permeabilities ranging up to 20,000 mD. The majority of the points lie in the 15–30% porosity and 10–10,000 mD permeability ranges, indicating good to excellent reservoir quality. The overlying Gurnard Formation has much poorer reservoir quality. Whilst porosity ranges from 8–27%, permeability is generally lower than 10 mD.

PETROLOGICAL CHARACTERISATION

The results of a previous petrological study undertaken for the GEODISC™ project by Kraishan (in Root et al, 2004; Root, in prep.) were re-assessed and supplemented with new core samples obtained from the Kingfish–Bream area. The assessment indicates that the upper Latrobe Group sediments are composed mostly of quartz with significant amounts of feldspar and lithic fragments, and compositionally vary across almost the whole range of sandstone classifications (Fig. 8a). The diagenesis of the reservoir units has generally been positive for retaining high reservoir quality (Fig. 8b). Early precipitation of dolomite in the permeable sandstones has prevented compaction of the rock. Later dissolution of the dolomite during the migration of hydrocarbons and associated organic acids, combined with later feldspar dissolution, has created secondary porosity. Late-stage authigenic minerals such as quartz overgrowths and kaolinite, which can occlude porosity or close pore throats, generally only occur in minor amounts and do not contribute much to the reduction of pore volume.

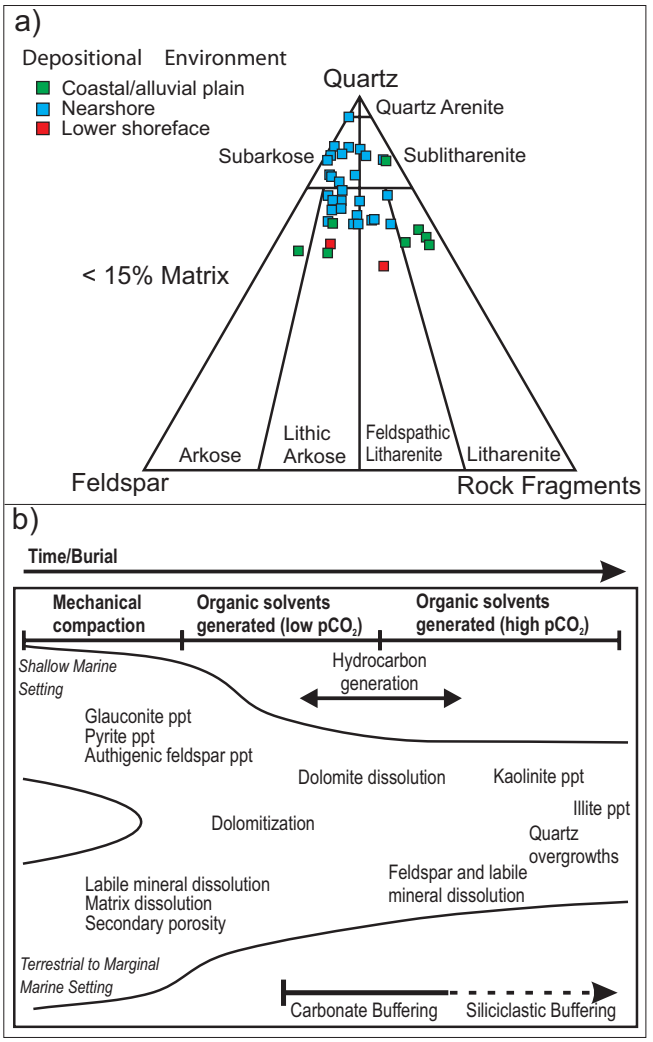

Figure 8. a. Ternary diagram of the various reservoir samples of the upper Latrobe Group from the northern gas fields, **b.** Simplified burial diagenesis for the upper Latrobe Group reservoirs, showing the relationship between the production of low and high pCO_2 organic solvents to the diagenetic process and the past buffering capabilities of the system.

POTENTIAL IMPACT OF GEOCHEMICAL REACTIONS ON RESERVOIR QUALITY

CO_2 dissolution into the formation water allows CO_2-water-rock interactions, which will alter the mineralogy and potentially alter the physical aspects of the rock (Watson et al, 2004). This can have important implications for injectivity, as mineral dissolution may lead to migration of fine clay minerals and sand grains, or precipitation of new minerals, either of which can block or occlude the porosity and permeability of the reservoir rock.

The reservoir units of the Latrobe Group lack minerals which are reactive to CO_2. While rock fragments and feldspars do make up a major component of the formation mineralogy, elemental abundances indicate that the chemical composition of each mineral group is not optimal for CO_2-water-rock interactions at a rate likely to affect injectivity. For example, the feldspars are dominantly alkali, which have a very slow reaction rate, and the rock fragments are metamorphic (quartz and mica dominated), which also have a very slow reaction rate or are inert to CO_2 dissolution. Therefore, CO_2-water-rock interactions are expected to be very limited, and the injectivity of the reservoir units is unlikely to be compromised by geochemical reactions.

CONTAINMENT

Before dissolution, supercritical CO_2 is less dense than water. Therefore, once pressures have relaxed after injection ceases, it will rise buoyantly through the water column, like hydrocarbons. Consequently, like hydrocarbon exploration or natural gas storage, a possible CO_2 containment risk is unwanted vertical fluid migration through the top seal, faults/fractures and existing well penetrations (Root et al, 2004). Containment issues that need to be assessed therefore include the distribution and continuity of the seal, the seal capacity (maximum CO_2 column height retention), potential migration pathways (structural trends and formation water flow direction and rate) and the integrity of the reservoir and seal (fault/fracture stability and maximum sustainable pore fluid pressures) (Gibson-Poole et al, 2005).

Seal distribution and continuity

The Lakes Entrance Formation regional seal is widespread across the offshore Gippsland Basin, with the exception of the eastern deep-water area of the Bass Canyon. It is the lowermost of four units that are distinguished within the Seaspray Group, and is lithologically composed of glauconitic, slightly calcareous and mud-rich sediments (Woollands and Wong, 2001). At the Kingfish Field location, the Lakes Entrance Formation has an average thickness of 390 m.

Seal capacity

Seal capacity is an important aspect for containment of CO_2. The potential seal capacity of the regional top seals and localised intraformational seals were assessed by Mercury Injection Capillary Pressure (MICP) analysis. MICP tests are a measurement of the pressures required to move mercury through the pore network system of a core sample. The air/mercury capillary pressure data are translated to equivalent CO_2/brine data at reservoir conditions and then converted into seal capacity for CO_2, expressed as the column height that the rock would be capable of holding (sealing). Standard procedures for MICP analysis, as reviewed by Vavra et al (1992) and Dewhurst et al (2002), were used for these studies. The calculated column heights for each of the samples tested are shown in Figure 9.

The Lakes Entrance Formation regional top seal is in-

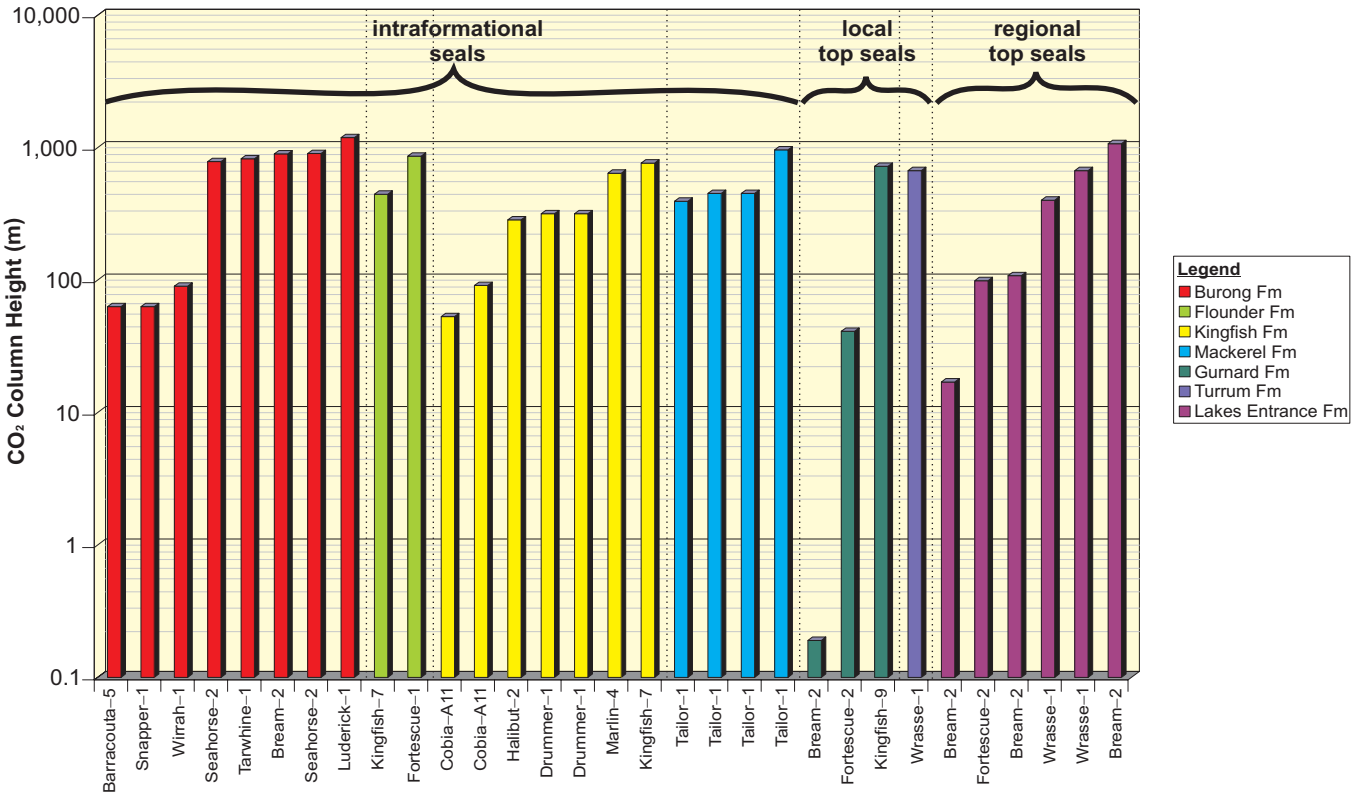

Figure 9. CO_2 column heights calculated from MICP analyses for top and informational seals.

terpreted to have good seal potential and sufficient seal capacity to successfully retain CO_2. The MICP analyses indicate that the Lakes Entrance Formation has the potential to hold back CO_2 column heights ranging from 17 m to 1,071 m, with an average CO_2 column height retention of 395 m. The Lakes Entrance Formation overlies the more localised top seals of the Gurnard and Turrum formations. The properties of these formations are variable across the basin, resulting in the formations behaving as either low-quality reservoir or a seal, depending on the specific depositional environment and/or diagenetic history. The Gurnard Formation sample from Bream–2 is clearly more akin to a reservoir than a seal, with a CO_2 column height of only 20 cm. However, the average CO_2 column height for the Gurnard and Turrum formations is 360 m, which indicates good sealing potential. In the event that CO_2 migrated through the Gurnard and Turrum formations, the CO_2 would still be successfully retained by the regionally extensive Lakes Entrance Formation.

Localised intraformational seals are present throughout the fluvial, coastal plain and nearshore marine reservoir intervals of the Burong, Kingfish, Mackerel and Flounder Formations. The MICP analyses indicate that the intraformational seals have the potential to hold back CO_2 column heights ranging from 53 m to 1,191 m, with an average CO_2 column height retention of 517 m. Thus, the interbedded siltstones, shales and coals will behave as flow baffles and barriers that will hinder or slow vertical migration, encouraging the CO_2 to migrate laterally within the reservoir.

Geochemical evaluation

CO_2 introduced into the reservoir system will generate long-term CO_2-water-rock interactions. Detailed petrology can provide information on the potential mineral reactions of the CO_2 with the reservoir rock, including dissolution, alteration and precipitation. In certain cases, mineral precipitation can lead to mineral trapping of CO_2 and increased containment security (Perkins and Gunter, 1996; Watson et al, 2004).

As discussed above, the mineralogy of the reservoir units of the upper Latrobe Group offer little-to-no reactive potential with CO_2. Whilst this is beneficial in terms of injectivity, conversely it means that there is limited potential for mineralogical trapping of the CO_2 through precipitation of carbonate minerals.

At the top of the Latrobe Group is the glauconitic marine shelf deposit of the Gurnard Formation, which acts as either a seal or a low-quality reservoir depending on its location within the basin. The mineralogy of the Gurnard Formation is very different to that of the underlying Latrobe Group sediments. In addition to quartz, it also contains moderate-to-high concentrations of pyrite (and its polymorph marcasite), smectite and goethite, plus other minerals such as potassium feldspar, dolomite, chlorite, berthierine, glauconite and muscovite. The higher concentration of calcium-, iron- and magnesium-bearing minerals offers significant potential for permanent mineralogical trapping of CO_2 through precipitation of ferroan carbonate minerals

(e.g. siderite). In addition, migration of the CO_2 through this low-permeability reservoir would slow migration rates vertically and laterally. This stratigraphic arrangement of good-quality reservoirs with low reactive potential as the injection target, overlain by the low permeability yet potentially highly reactive Gurnard Formation, is an ideal reservoir system for optimising CO_2 injection and containment (Watson and Gibson-Poole, 2005) (Fig. 10).

The Lakes Entrance Formation regional seal is composed co-dominantly of quartz and illitic-smectite, with one sample also containing abundant siderite cement. Mineral reactions are likely to be limited as illitic-smectite clays are weakly reactive to CO_2. It is also considered unlikely that CO_2 will enter the formation due to its low porosity and permeability characteristics and high seal capacity, restricting any potential mineral reactions to the base of the seal.

Migration pathways and trapping mechanisms

After injection ceases, the buoyancy of the free CO_2 due to its density will result in it migrating to the highest point in the reservoir. Stratigraphic heterogeneities, such as intraformational siltstones, shales and coals, have the potential to reduce the effective vertical permeability and create a more tortuous migration pathway for injected CO_2. Once CO_2 has reached the top of the reservoir, the structural geometry at the base of the overlying seal will have a strong influence on the subsequent migration direction.

The structural geometry at the top of the Kate Shale beneath the Kingfish Field is a westwards-plunging anticline (Fig. 11). The overlying Kingfish Formation sediments are tilted structurally upwards to the east and are progressively truncated by the Gurnard Formation and the Latrobe Unconformity. Intraformational seals within the reservoir units are aligned with this structural geometry in the western part of the field, but in the east they may form part of the sigmoidal clinoforms relating to the shoreface progradational cycles (most likely at the toes of the progrades). Figure 12 shows a schematic representation of the possible intraformational seal distribution based on the sequence stratigraphy, wireline log motifs and seismic appearance. The transition from coastal plain to shallow marine depositional environments across the Kingfish Field from west to east is reflected in the intraformational seals, which have a greater volume on the western side and then laterally pinch out towards the east as the section becomes sandier (Bernecker and Partridge, 2005). The effect of the tilted structural geometry and the presence of intraformational seals suggests that CO_2 is likely to migrate upwards and eastwards by a tortuous pathway created by the stratigraphic heterogeneity until it accumulates at the top of the Latrobe Group beneath the regional seal.

Once at the top of the Latrobe Group, the migration direction of the CO_2 will be influenced by the structural geometry at the base of the regional seal (Fig. 13). If the storage capacity of the Kingfish Field structural closure is exceeded, the CO_2 will continue to migrate up structural dip beneath the regional seal in a westerly direction towards the structural closure of the Bream Field. This is orthogonal to the westerly-dipping intraformational baffles and barriers, which will again slow and hinder the migration of the CO_2.

The CO_2 injection and storage strategy proposed is intended to take advantage of several trapping mechanisms. The tortuous pathway created by the stratigraphic architecture within the intra-Latrobe Group is expected to effectively increase the length of the CO_2 migration pathway. This will increase the volume of pore space moved through by the CO_2, which will result in greater residual gas trapping and dissolution along the migration pathway. Once at the top Latrobe Group, the depleted Kingfish Field provides structural trapping in the anticlinal closure.

Hydrodynamic analysis

Hydrodynamic modelling assesses the formation water flow systems within a basin by evaluating the degree of vertical and horizontal hydraulic communication and estimating the direction and magnitude of flow. An assessment of the virgin (pre-production) hydrodynamic regime is used to provide an understanding of the long-term (hundreds to thousands of years) influence of the formation water flow systems on the injected CO_2. An interpretation of the present-day hydrodynamic regime, which has been affected by hydrocarbon and water production, is required to evaluate the potential short-term (tens to hundreds of years) influence on the predicted migration pathway of CO_2 immediately after injection. It is assumed that once hydrocarbon/water production has ceased, the hydrodynamic flow system will gradually return to its virgin state. The injection of CO_2 into previously hydrocarbon-producing regions may speed up the aquifer pressure recovery.

VIRGIN AND PRESENT-DAY HYDRODYNAMIC SYSTEM

Standard hydrodynamic analysis techniques as presented by Bachu and Michael (2002), Otto et al (2001), Bachu (1995) and Dahlberg (1995) were used for this study. New data were integrated with the data from two previous hydrodynamic studies by Underschultz et al (2003) and Hatton et al (2004), which formed the foundation for this study.

A model of the virgin hydraulic head distribution for the Upper Latrobe Aquifer System has been derived and is shown in Figure 14. High hydraulic head extending eastwards from onshore subcrop reflects gravity-driven freshwater recharge from the west. This is particularly prominent within the boundaries of the Seaspray Depression and the offshore western part of the Central Deep. In the offshore Gippsland Basin high values of hydraulic head are related to a compaction-driven flow system. The onshore gravity-driven flow system and the offshore compaction-driven flow system converge into a region of low hydraulic head in the offshore Central Deep. It is specu-

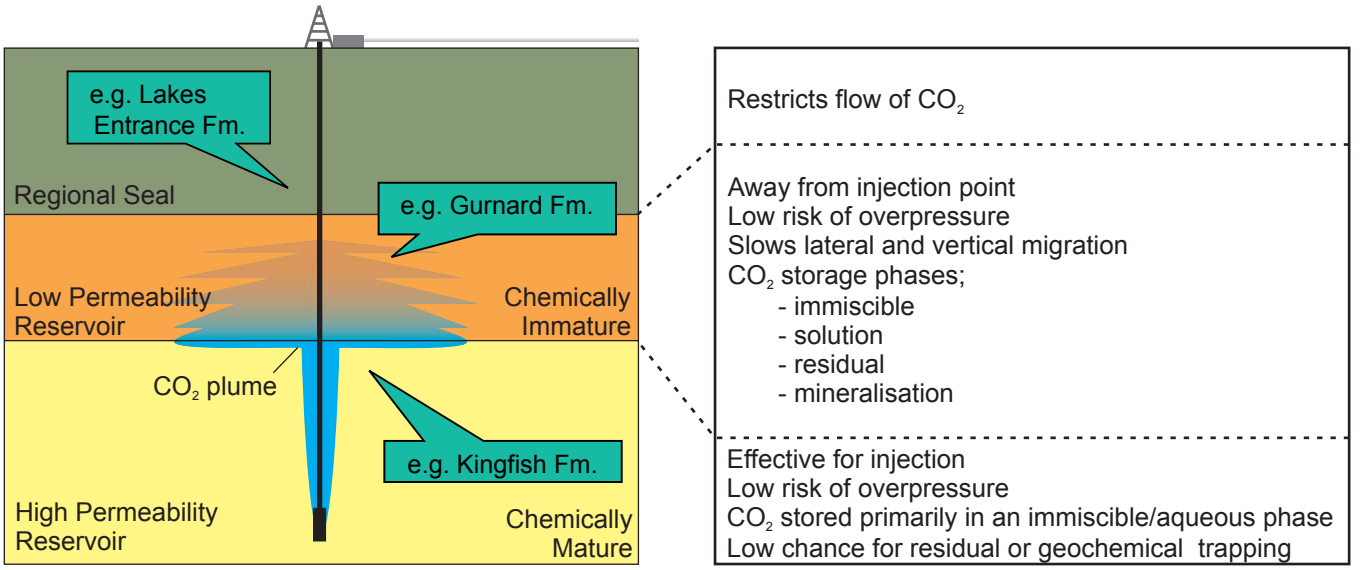

Figure 10. Conceptual diagram of the optimised storage system for CO_2, where following buoyancy-driven vertical migration the CO_2 encounters a low permeability, chemically-immature, heterogeneous zone, slowing both the lateral and vertical migration of the CO_2 plume and promoting mineral trapping (modified after Watson and Gibson-Poole, 2005).

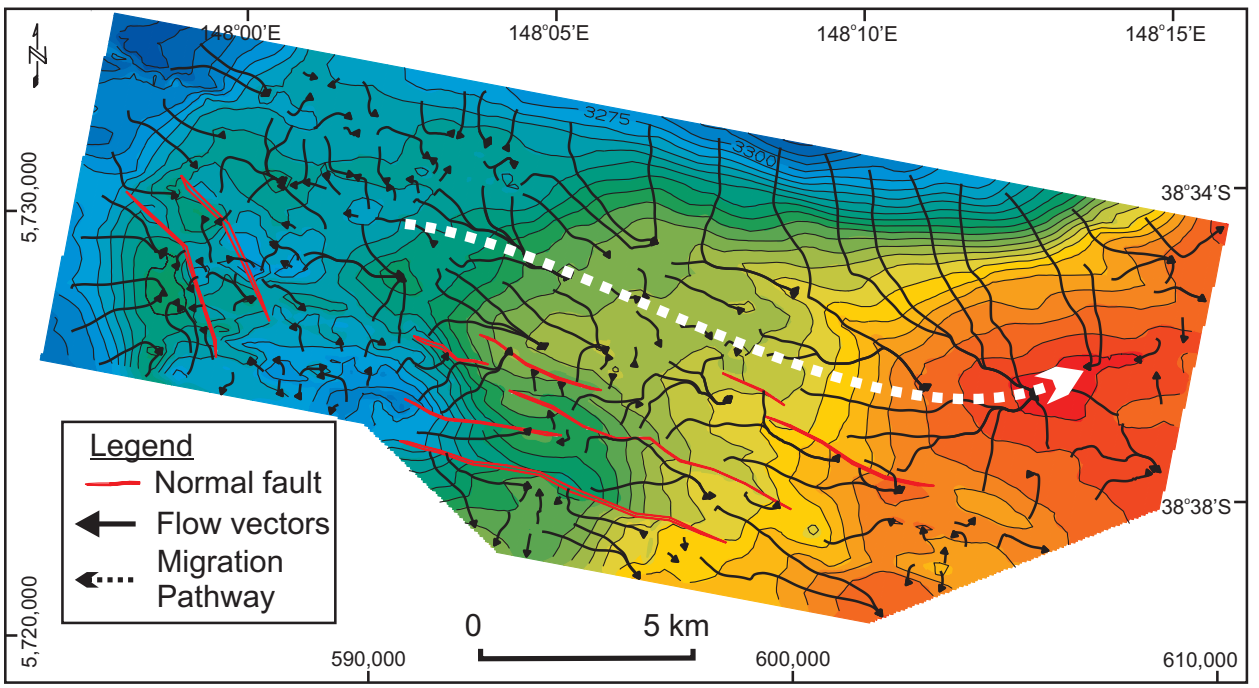

Figure 11. Flow vectors and key migration pathway within the Kingfish Field area, based on the structural geometry of the SB2 depth structure map (~top Kate Shale).

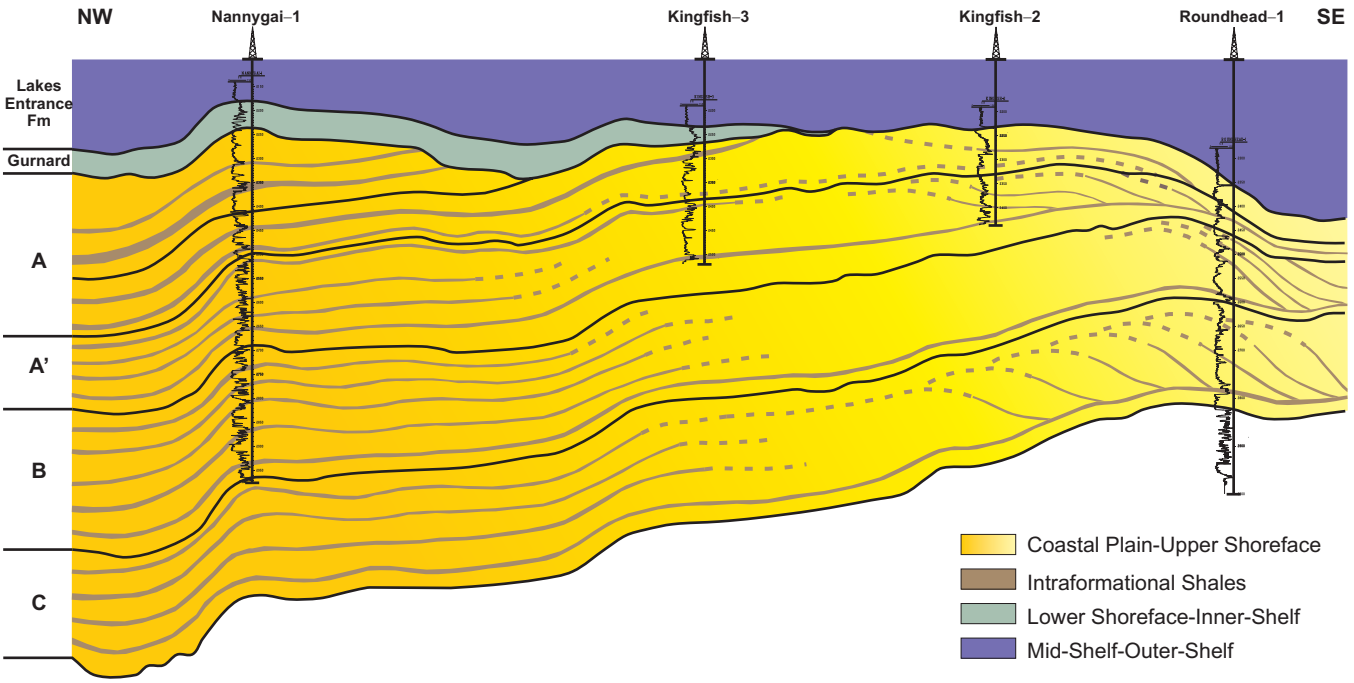

Figure 12. Schematic representation of the possible intraformational seal distribution based on the sequence stratigraphy, wireline log motifs and seismic appearance.

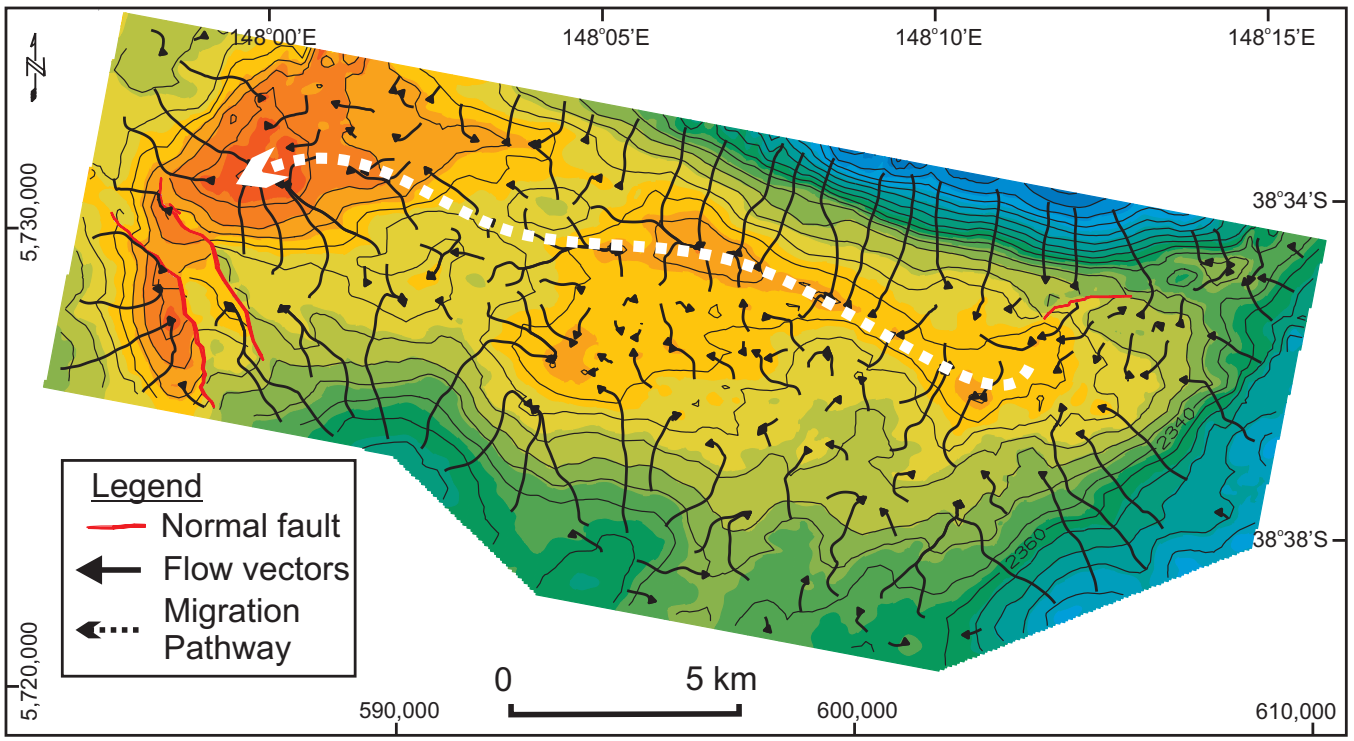

Figure 13. Flow vectors and key migration pathway within the Kingfish Field area, based on the structural geometry of the top Latrobe Group depth structure map (base Lakes Entrance Formation regional seal).

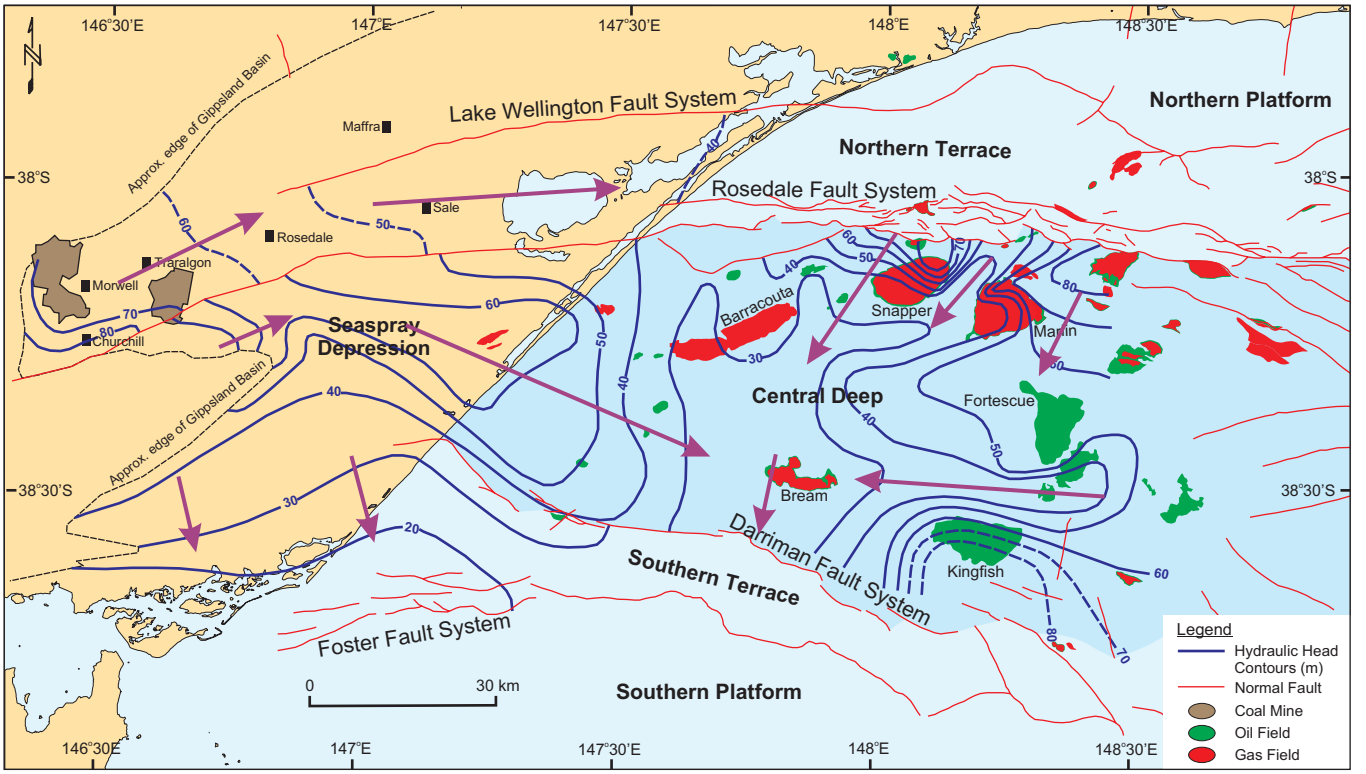

Figure 14. Virgin (pre-production) hydraulic head distribution for the Upper Latrobe Aquifer System.

lated that this sink is connected to the Darriman Fault System on the southern edge of the Central Deep, which may then discharge to an upper aquifer or even the sea floor. Several interconnected troughs of low hydraulic head form the sink, and extend to the north and east, such as between the Snapper and Marlin fields and between the Fortescue and Kingfish fields.

A combination of onshore coal mine dewatering, industrial and agricultural formation water extraction, and offshore oil and gas production, have resulted in a short-term (tens to hundreds of years) transient alteration of the formation water flow system for the Upper Latrobe Aquifer System. In the absence of publicly available present-day offshore pressure data, a present-day hydraulic head distribution was estimated from the mid 1990s distribution and extrapolating the observed trend in decreasing hydraulic head with time during the 1990s (Fig. 15). In the onshore region, a depression of the hydraulic head surface occurs in the Latrobe Valley associated with coal mine dewatering. Effects of dewatering appear to be mainly confined to the Northern Terrace, suggesting the Rosedale Fault System forms a hydraulic barrier on a production time-scale. In the offshore Gippsland Basin, hydrocarbon production has resulted in a significant depression of the hydraulic head surface centred on the Fortescue to Kingfish fields. The low hydraulic head resulting from production-induced pressure decline has altered the virgin formation water flow system so that it now flows radially inwards towards the Fortescue–Kingfish area.

IMPACT OF HYDRODYNAMIC SYSTEM ON CO_2 MIGRATION AND CONTAINMENT

The long-term fate of injected CO_2 will be relatively unaffected by the formation water flow system, since the hydraulic gradients of the virgin hydrodynamic system are relatively flat compared with the structural slope of the base of the regional seal. However, pressure depletion in the vicinity of the oil-producing fields in the offshore Gippsland Basin has resulted in local steepening of the hydraulic gradient. Thus, in the short-term the driving force of the moving formation water on the injected CO_2 could significantly alter the migration direction predicted from only buoyancy drive at the base of the seal. In some cases, the driving force from moving formation water may be sufficient to entrain the CO_2 to migrate down structural dip. While this is a transient effect, aquifer recovery is not likely to occur prior to the initiation of CO_2 geological storage, so the present-day conditions need to be considered.

A tilt analysis was conducted to establish the relative strength of the updip buoyancy driving force versus the downdip hydraulic driving force on injected CO_2. For the Kingfish field area injection scenario, within the intra-Latrobe succession the hydraulic gradient is insufficient to overcome the buoyancy forces, and CO_2 will migrate upwards and eastwards as predicted from the structural geometry. However, once CO_2 reaches the top Latrobe Group the hydrodynamic driving force is strong enough to entrain the CO_2 downdip (northeastwards) towards the hydraulic

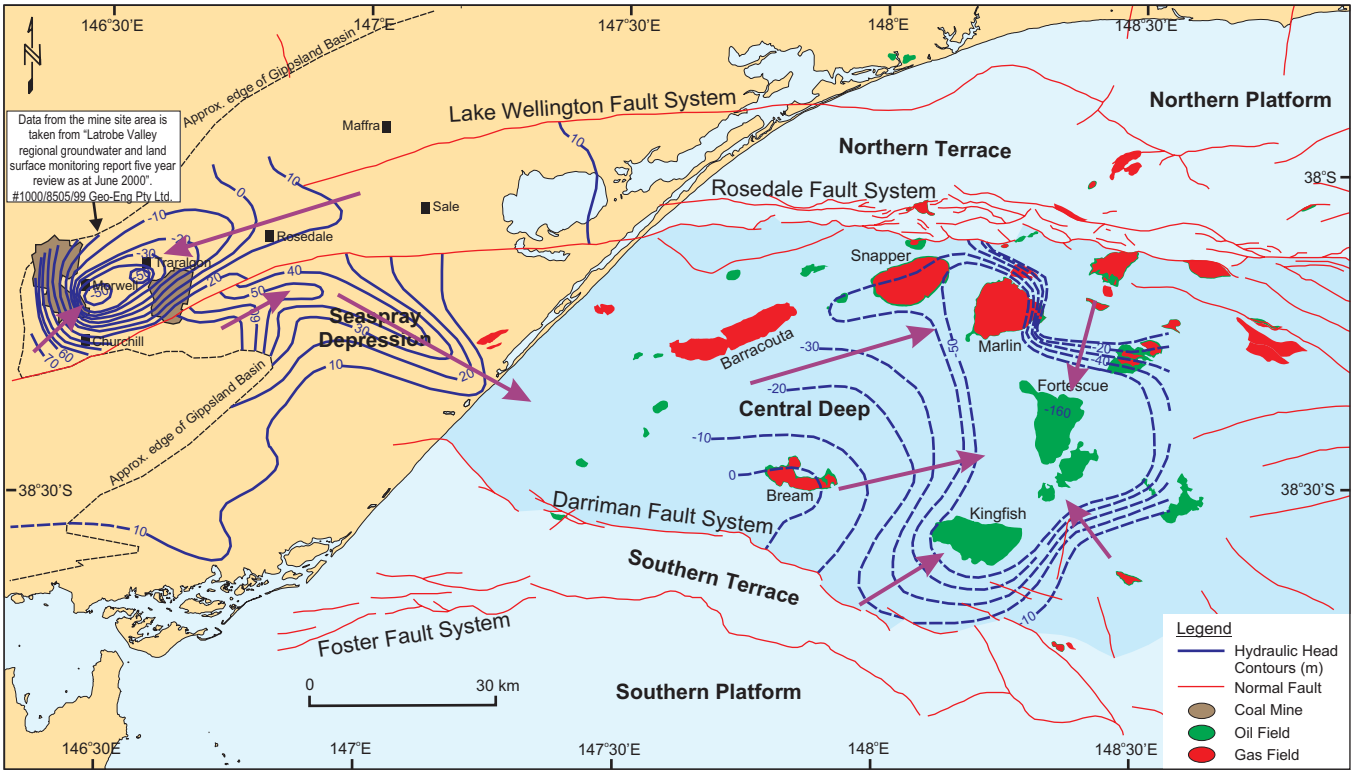

Figure 15. Estimated hydraulic head distribution for the Upper Latrobe Aquifer System in 2004 to 2020.

low at the Fortescue field. If this occurs it will positively impact CO_2 containment, as it will increase the migration pathway distance, allowing more pore space for storage capacity to be accessed and greater time for dissolution and mineral reactions to occur. Once the aquifer recovers and the field areas re-pressurise, the formation water flow is likely to return to a similar condition to its virgin state, and CO_2 will then migrate under the influence of buoyancy forces back towards the Kingfish Field.

The present-day flow system can therefore be used to decrease containment risk and potentially increase storage capacity if an injection and storage scenario is linked with the anticipated oil pool abandonment plans. Further numerical simulation of the flow system is required to evaluate the duration of the transient flow system, and to increase the accuracy of the predicted CO_2 migration pathways.

Geomechanical assessment

Sub-surface injection of CO_2 at pressures that exceed prevailing formation pressures may potentially reactivate pre-existing faults and generate new faults. Such brittle deformation can increase fault and fracture permeability, which could lead to unwanted migration of CO_2 (Streit and Hillis, 2004). Estimates of the fluid pressures that may induce slip on faults at a potential injection site can be obtained from geomechanical modelling. Such modelling requires knowledge of the geomechanical model (in situ stresses and rock strength data) and the fault orientations. Details on geomechanical modelling techniques and the assessment of fault reactivation risk are described in Mildren et al (2002) and Streit and Hillis (2004).

GEOMECHANICAL MODEL

The stress regime in the Gippsland Basin is on the boundary between strike-slip and reverse faulting, that is, maximum horizontal stress (~40.5 MPa/km) is greater than vertical stress (21 MPa/km), which is about equal to minimum horizontal stress (20 MPa/km). Pore pressure is hydrostatic above the Campanian Volcanics of the Golden Beach Subgroup. The northwest–southeast maximum horizontal stress orientation is calculated at 139° north, which is broadly consistent with previous estimates (e.g. Hillis and Reynolds, 2003; Nelson and Hillis, 2005; Nelson et al, in press) and verifies a northwest–southeast maximum horizontal stress orientation in the Gippsland Basin.

The maximum pore pressure increase (Delta P) which can be sustained within the reservoir intervals of the Latrobe Group without brittle deformation (i.e. the formation of a fracture) was estimated to be 14.5 MPa (~2103 psi). The maximum pore pressure increase that can be sustained in the Lakes Entrance Formation regional seal was estimated to be 9.0 MPa (~1,299 psi). Therefore, injection is not recommended near the top of the reservoir in order to minimise the potential pore pressure build-up near the seal.

The risk of fault reactivation was calculated using

the FAST (Fault Analysis Seal Technology) technique, which determines fault reactivation risk by estimating the increase in pore pressure required to cause reactivation (Mildren et al, 2002). Fault reactivation risk was calculated using two fault strength scenarios: cohesionless faults (cohesive strength C=0; friction coefficient μ=0.65) and healed faults (cohesive strength C=5.4; friction coefficient μ=0.78) (Fig. 16). The fault orientations for high or low reactivation risk are very similar for both healed and cohesionless faults. High-angle faults striking northeast–southwest are unlikely to reactivate in the present stress regime and have low reactivation risk. High-angle faults orientated eastsoutheast–west-northwest and south-southeast–north-northwest have the highest fault reactivation risk potential. The highest fault reactivation risk for optimally-orientated faults corresponds to an estimated pore pressure increase (Delta P) of 3.78 MPa (~548 psi) for cohesionless faults and 15.6 MPa (~2,263 psi) for healed faults. The Delta P values (maximum pore pressure increases), however, presented in the geomechanical assessment are subject to large errors due to uncertainties in the geomechanical model. In particular, the maximum horizontal stress and rock strength data are poorly constrained. Further work, such as laboratory testing of cores to determine failure envelopes of the fault and host rocks (e.g. uniaxial compressive strength, tensile strength), needs to be conducted to constrain the geomechanical model and reduce the uncertainties.

FAULT REACTIVATION RISK

Sixteen faults have been mapped from 3D seismic data in the Kingfish–Bream area. Nine of these faults cut the Latrobe Unconformity at the base of the regional seal. Six faults near the Bream Field and two faults near Gurnard–1 trend north-northwest–south-southeast. The fault near East Kingfish–1 trends southwest–northeast at its western tip and rotates towards east–west at its eastern tip. Seven faults were interpreted to terminate within the Latrobe Group. These faults lie south of the Kingfish Field and trend west-northwest–east-southeast to east–west. More faults are present at this stratigraphic interval, but time restrictions meant that only a representative selection could be mapped. However, fault reactivation risk for any fault not included in this study can be analysed using the reactivation risk stereonets (Fig. 16).

Fault reactivation risk was evaluated for the 16 faults with known orientations. Eight of the nine faults that cut the Latrobe Unconformity have moderate-to-high fault reactivation risk (Fig. 17). Reactivation of these faults may increase fault permeability and lead to movement of CO_2 out of the Latrobe Group. However, most of the faults present are not in the predicted immediate CO_2 migration pathways and most do not cut the top seal. The fault near East Kingfish–1 has low-to-moderate reactivation risk and is less likely to reactivate in the present stress regime (Fig. 17b). The reactivation risk for the seven faults that terminate within the Latrobe Group is moderate to high. Reactivation of these faults may not be a containment risk because they do not appear to extend beyond the target reservoir. Nonetheless, reactivation of these intra-Latrobe faults is undesirable. An injection scenario which minimises pore pressure increases on all known faults should be chosen.

Capacity

Potential CO_2 storage capacity can be assessed geologi-

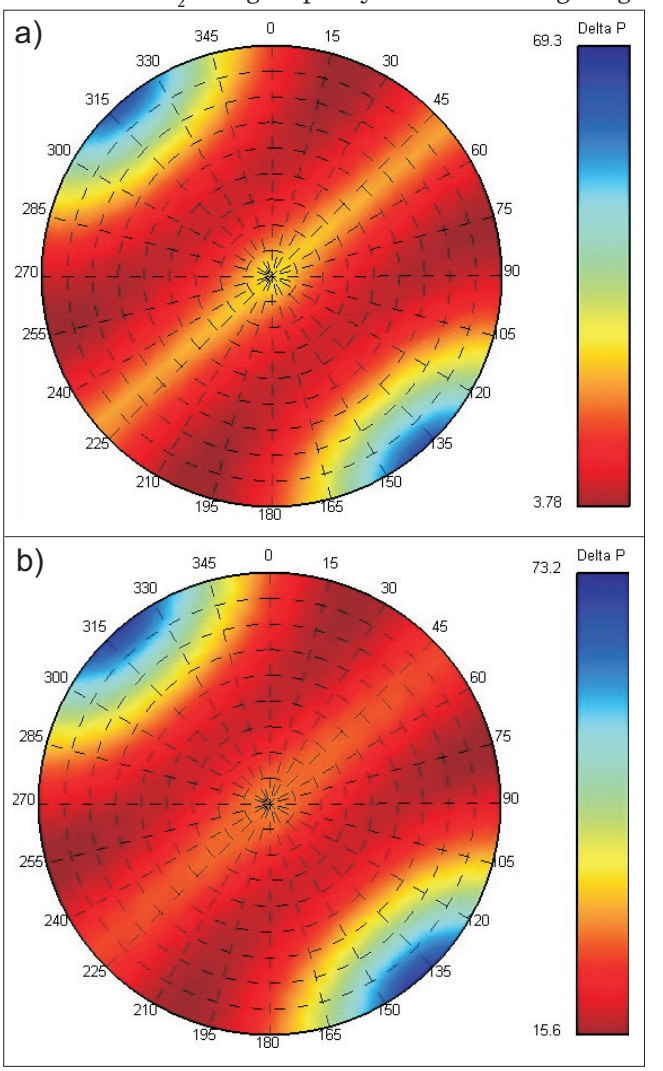

Figure 16. Stereonets showing the reactivation risk for faults at 2,300 m in the Gippsland Basin (faults are plotted as poles to planes), for: **a.** cohesionless faults—the highest reactivation risk for optimally-orientated faults corresponds to an estimated pore pressure increase (Delta P) of 3.78 MPa (~548 psi); and **b.** healed faults—the highest reactivation risk for optimally-orientated faults corresponds to an estimated pore pressure increase (Delta P) of 15.6 MPa (~2,263 psi).

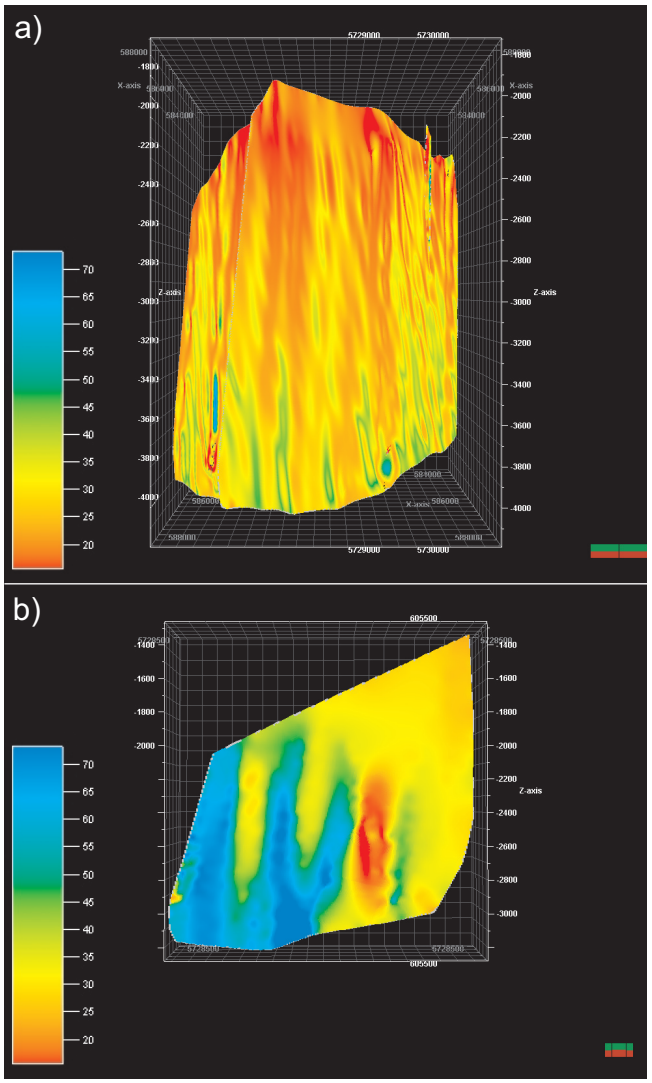

Figure 17. Reactivation risk for faults in the Kingfish Field area. Faults are coloured according to fault reactivation risk. High values of Delta P (cool colours) indicate low reactivation risk, whereas low values of Delta P (warm colours) indicate high reactivation risk. Faults shown: **a.** faults near Gurnard–1 (looking W); and, **b.** fault near East Kingfish–1 (looking N).

cally in terms of available pore volume. This provides the basis for numerical flow simulations of CO_2 injection and storage, which will give a more accurate assessment of how much of the available pore volume is actually used (sweep efficiency). The efficiency of that storage capacity will be dependent on the rate of CO_2 migration, the long-term prospects of dissolution into the formation water or precipitation into new minerals, and the potential for fill-to-spill structural enclosures encountered along the migration path (Gibson-Poole et al, 2005).

An assessment of the available pore volume in the existing oil zone of the Kingfish Field was undertaken to determine the possible CO_2 storage capacity once the field is depleted. Using reservoir property data from Malek and Mehin (1998), the reservoir volumes presently occupied by hydrocarbons were computed and converted to an equivalent CO_2 volume. An estimate of the potential CO_2 storage capacity within the intra-Latrobe succession of the Kingfish Field area was also conducted (using data derived during this study) to give an idea of how much additional storage capacity could be obtained by using more than the depleted oil field structural closure. The results indicate that there is a combined storage potential in the order of several hundred Mt of CO_2. The intra-Latrobe stratigraphy provides about three times the capacity of the structural closure, which demonstrates how a deeper injection strategy may provide significantly more CO_2 storage capacity.

These results predict the available pore volume only, and numerical simulation is required to verify the sweep efficiency. The available pore volume from both the deeper intra-Latrobe Group succession and top Latrobe Group structural closure at the Kingfish Field indicate there is likely to be ample CO_2 storage capacity for 15 Mt/y injection for 40 years.

NUMERICAL FLOW SIMULATION

The aim of the numerical simulations was to examine the feasibility of large rates of injection at the Kingfish Field area, and to predict the migration path, ultimate long-term destination and form of the injected CO_2.

Numerical simulations of injectivity

Simulation models were constructed to test various parameters for their impact on injectivity (maximum injection rate), and to establish the number of wells required for a 15 Mt/y injection rate. A two-phase GASWATER option of the commercial IMEX Black Oil Simulator (Computer Modelling Group, Canada) was used to model an immiscible displacement of reservoir brine with CO_2. The shale barriers in the formations were included in the numerical model by means of a reduced vertical permeability (formation anisotropy ratio of 0.05). Simulations of 25 and 40 years were run to examine the CO_2 injectivity until injection ceased.

The simulation results from a 3D intra-Latrobe to top Latrobe model (intervals A to C) determined that 18 vertical wells were required for an injection rate of 15 Mt/y into the C interval at an injection pressure constrained to 90% fracture pressure (39 MPa). The effect of injection pressure on the number of vertical wells required to inject CO_2 at 15 Mt/y was also examined. This assessment indicated that constraining the injection pressure to more conservative values of the fracture pressure results in an increase in the number of wells required. For example, the number of wells required for an injection pressure at 75% fracture pressure (32.4 MPa) is more than twice that for an injection pressure at 80% fracture pressure (34.6 MPa) (Fig. 18a). Lower permeability values also result in an increased number of wells required to inject CO_2 at a rate of 15 Mt/y (Fig. 18b).

Numerical simulations of flow paths

A simulation model was devised from depth-converted

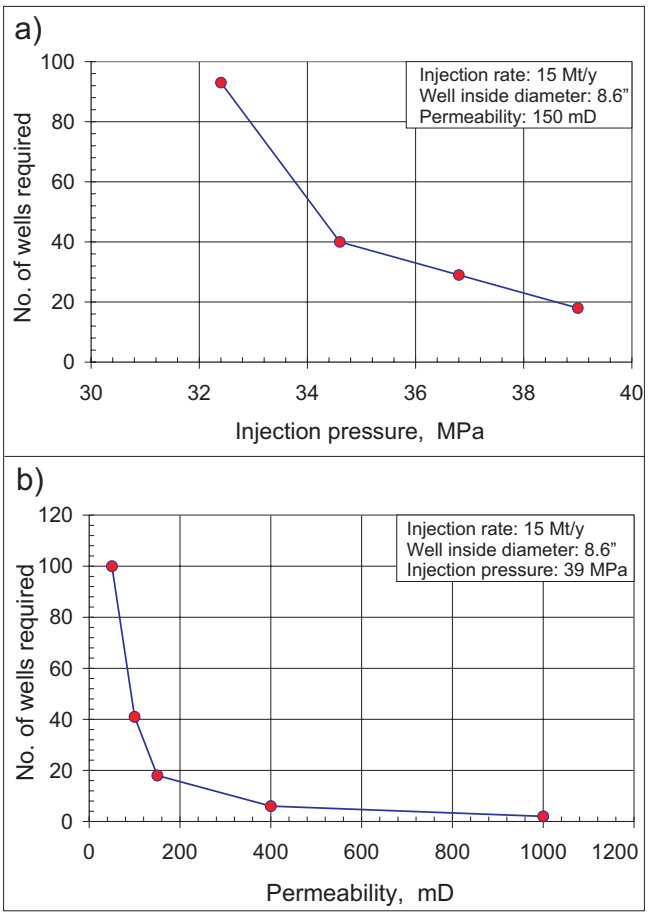

Figure 18. Number of wells required for a CO_2 injection rate of 15 Mt/y as a function of **a.** injection pressure and **b.** permeability.

seismic surfaces and average porosity, permeability and shale fraction characteristics of the intersecting wells. The stratigraphic complexity is represented in the simulations by using object modelling to give a shale distribution that honours the overall shale fraction and the lateral extent appropriate to the depositional environment. The base of the C interval (~top Kate Shale) was taken as the bottom of the region of interest. The simulation code used for this study was TOUGH2 Version 2.0 (Pruess et al, 1999). For the base case simulations, the injection rate was 15 Mt/y for 40 years within the C interval (~550–800 m deeper than the main oil accumulation), residual gas saturation was 20%, and the object-modelled shales were 2 km x 3 km in dimensions at a total volume fraction of 20%.

In the base case, the CO_2 is still contained within the intra-Latrobe Group succession after 40 years injection, migrating upwards and slightly eastwards beneath the shale units (Fig. 19). Since the shales follow the shape of the internal surfaces, there are localised traps which retard the upward movement of CO_2 as each trap fills up to the spill-point. At around 190 years the CO_2 reaches the upper sequences (in and beneath the Gurnard Formation). From here it then spreads out laterally around the west end of the Kingfish Field. In the long-term, 1100 years after the end of injection, the injected CO_2 has continued to drain upwards from the deep injection and has spread out into the eastern end of the Kingfish Field area and begun to migrate towards the west (and the next structural closure). At the end of the injection phase, ~13% of the CO_2 was dissolved into the formation water, which increased to ~46% after 1,000 years.

Several case variations were simulated, including changes to shale distributions, permeability and residual gas saturation. Larger shales (4 km x 6 km) increased the effective vertical permeability, resulting in a more eastwards migration route and delayed the arrival at the top surface to around 400 years (Fig. 19c). The converse is true for a lower shale fraction, where CO_2 reached the top surface 80 years after injection ceased. Lower residual gas saturation resulted in more free CO_2 reaching the top surface, and migration updip towards the Bream Field occurred sooner (860 years). Higher permeabilities (by a factor of three) significantly decreased the arrival time of the carbon dioxide at the top surface (down to 56 years) (Fig. 19d), and shallower injection (interval B) also gave a shorter arrival time.

The numerical simulations indicate that it is feasible to inject 15 Mt/y deep in the intra-Latrobe stratigraphy beneath the Kingfish Field. The advantage of this strategy is a delay of about 50–200 years before the CO_2 reaches the areas from which hydrocarbons are presently being produced. In the post-injection period, the carbon dioxide that had migrated to the top surface was still largely contained in the Kingfish Field area after 1,000 years. In a couple of cases, it had migrated as far as the Nannygai-1 and Gurnard–1 wells. It is expected that the carbon dioxide would be trapped either by residual gas trapping or dissolution before it migrated as far as the Bream Field. Substantial dissolution of CO_2 (in the range 35–50%) was found to have occurred in 1,000 years.

CONCLUSIONS

Detailed studies on the geology, geophysics, geochemistry, geomechanics, hydrodynamics and numerical flow simulation were conducted in the offshore Gippsland Basin. These have yielded significant results pertinent to the suitability of the Gippsland Basin as a potential area for large-scale CO_2 geological storage. These include:

- a complex stratigraphic architecture that provides baffles which slows vertical migration and increases residual gas trapping;
- non-reactive reservoir units that have high injectivity;
- a thin, suitably reactive, low-permeability marginal reservoir just below the regional seal to provide additional mineral trapping;
- several depleted oil fields that provide storage capacity coupled with a transient flow regime arising from production that enhances containment; and,

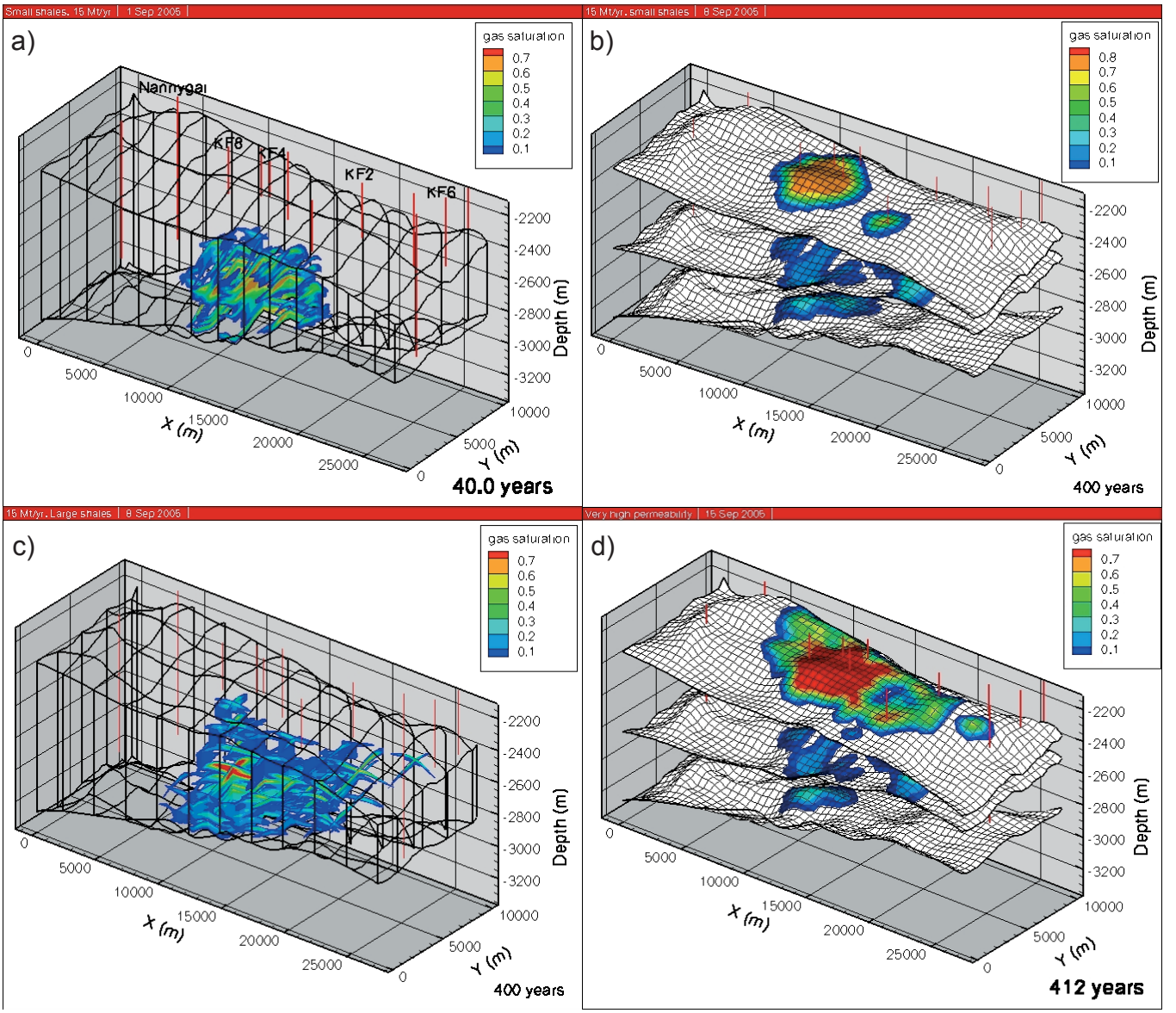

Figure 19. Numerical simulation models of CO_2 saturation in the Kingfish Field area for: **a.** base case after 40 years CO_2 injection; **b.** base case 400 years post-injection; **c.** case with larger shales 400 years post-injection; and **d.** case with 3x higher permeability 412 years post-injection.

- long migration pathways beneath a competent regional seal.

The Kingfish Field area, in conjunction with other sites—for example the northern gas fields as assessed by Root et al (2004)—indicate that the Gippsland Basin has sufficient capacity to store very large volumes of CO_2. It may provide a solution to the problem of substantially reducing greenhouse gas emissions from the use of new coal developments in the Latrobe Valley.

ACKNOWLEDGEMENTS

The authors would like to thank Barry Hooper (CO2CRC Capture Program Manager), Andy Rigg (CO2CRC Special Projects Manager) and Bill Koppe (Monash Energy) for providing guidance and support throughout this project. Adem Djakic and Peter Symes (Esso Australia) are thanked for provision of both openfile and confidential data, and for constructive criticism of the field capacity assessments. Hywel Thomas and Tom Bernecker (GeoScience Victoria, Department of Primary Industries) are also thanked for all their help and support with this project and for the provision of openfile data from the Gippsland Basin.

REFERENCES

BACHU, S., 1995—Flow of variable-density formation water in deep sloping aquifers: review of methods of representa-

tion with case studies. Journal of Hydrology, 164, 19–38.

BACHU, S. AND MICHAEL, K., 2002—Flow of variable-density formation water in deep sloping aquifers: minimising the error in representation and analysis when using hydraulic-head distributions. Journal of Hydrology, 259, 49–65.

BERNECKER, T. AND PARTRIDGE, A.D., 2001—Emperor and Golden Beach Subgroups: the onset of Late Cretaceous sedimentation in the Gippsland Basin, SE Australia. In: Hill, K.C. and Bernecker, T. (eds) Eastern Australian Basins Symposium: A Refocused Energy Perspective for the Future. PESA, 391–402.

BERNECKER, T. AND PARTRIDGE, A.D., 2005—Approaches to palaegeographic reconstructions of the Latrobe Group, Gippsland Basin, southeast Australia. The APPEA Journal, 45 (1), 581–99.

DAHLBERG, E.C., 1995—Applied Hydrodynamics in Petroleum Exploration. Springer-Verlag.

DEWHURST, D.N., JONES, R.M. AND RAVEN, M.D., 2002—Microstructural and petrophysical characterization of Muderong Shale: application to top seal risking. Petroleum Geoscience, 8 (4), 371–83.

DPI, 2005—Minerals and Petroleum—Overview [online]. Available from: http://www.dpi.vic.gov.au/dpi/nrenmp.nsf/childdocs/-C58CC29C22BD9D674A2567C4001F3676?open [accessed 1 November 2005].

GIBSON-POOLE, C.M., ROOT, R.S., LANG, S.C., STREIT, J.E., HENNIG, A.L., OTTO, C.J. AND UNDERSCHULTZ, J.R., 2005—Conducting comprehensive analyses of potential sites for geological CO_2 storage. In: Rubin, E.S., Keith, D.W. and Gilboy, C.F. (eds) Greenhouse Gas Control Technologies: Proceedings of the 7th International Conference on Greenhouse Gas Control Technologies. Elsevier, 673–81.

HATTON, T., OTTO, C.J. AND UNDERSCHULTZ, J.R., 2004—Falling Water Levels in the Latrobe Aquifer, Gippsland Basin: Determination of Cause and Recommendations for Future Work. CSIRO Wealth From Oceans. 36, unpublished.

HILLIS, R.R. AND REYNOLDS, S.D., 2003—In situ stress field of Australia. In: Hillis, R.R. and Müller, R.D. (eds) Evolution and Dynamics of the Australian Plate. GSA Special Publication 22 and GSAm Special Paper 372, 49–60.

LANG, S.C., GRECH, P., ROOT, R.S., HILL, A. AND HARRISON, D., 2001—The application of sequence stratigraphy to exploration and reservoir development in the Cooper-Eromanga-Bowen-Surat Basin system. The APPEA Journal, 41 (1), 223–50.

MALEK, R. AND MEHIN, K., 1998—Oil and Gas Resources of Victoria. Petroleum Development Unit, Victorian Department of Natural Resources and Environment. 92.

McKERRON, A.J., DUNN, V.L., FISH, R.M., MILLS, C.R. AND VAN DER LINDEN-DHONT, S.K., 1998—Bass Strait's Bream B reservoir development: success through a multi-functional team approach. The APPEA Journal, 38 (1), 13–35.

MILDREN, S.D., HILLIS, R.R. AND KALDI, J.G., 2002—Calibrating predictions of fault seal reactivation in the Timor Sea. The APPEA Journal, 42 (1), 187–202.

MUDGE, W.J. AND THOMSON, A.B., 1990—Three-dimensional geological modelling in the Kingfish and West Kingfish oil fields: the method and applications. The APEA Journal, 30 (1), 342–54.

NELSON, E.J. AND HILLIS, R.R., 2005—In situ stresses of the West Tuna area, Gippsland Basin. Australian Journal of Earth Sciences, 52, 299–313.

NELSON, E.J., HILLIS, R.R., SANDIFORD, M., REYNOLDS, S.D., LYONS, P., MEYER, J., MILDREN, S.D. AND ROGERS, C., in press—Present-day state-of-stress of southeast Australia. The APPEA Journal, 46 (1).

OTTO, C.J., UNDERSCHULTZ, J.R., HENNIG, A.L. AND ROY, V.J., 2001—Hydrodynamic analysis of flow systems and fault seal integrity in the North West Shelf of Australia. The APPEA Journal, 41 (1), 347—65.

PERKINS, E.H. AND GUNTER, W.D., 1996—Mineral traps for carbon dioxide. In: Hitchon, B. (ed) Aquifer Disposal of Carbon Dioxide: Hydrodynamic and Mineral Trapping—Proof of Concept. Geoscience Publishing Ltd, 93–114.

POSAMENTIER, H.W. AND ALLEN, G.P., 1999—Siliciclastic Sequence Stratigraphy—Concepts and Applications. SEPM, Concepts in Sedimentology and Paleontology, 7, 210.

POWER, M.R., HILL, K.C., HOFFMAN, N., BERNECKER, T. AND NORVICK, M., 2001—The structural and tectonic evolution of the Gippsland Basin: results from 2D section balancing and 3D structural modelling. In: Hill, K.C. and Bernecker, T. (eds) Eastern Australian Basins Symposium: A Refocused Energy Perspective for the Future. PESA, 373–84.

PRUESS, K., OLDENBURG, C. AND MORIDIS, G., 1999—TOUGH2 User's Guide, Version 2.0. Earth Sciences Division, Lawrence Berkeley National Laboratory, Technical Report LBNL-43134, unpublished.

RAHMANIAN, V.D., MOORE, P.S., MUDGE, W.J. AND SPRING, D.E., 1990—Sequence stratigraphy and the habitat of hydrocarbons, Gippsland Basin, Australia. In:

Brooks, J. (ed) Classic Petroleum Provinces. GSL, Special Publication, 50, 525–41.

ROOT, R.S., in prep.—Geological Model Construction for Geosequestration—Gippsland Basin, Australia. PhD thesis, The University of Adelaide, unpublished.

ROOT, R.S., GIBSON-POOLE, C.M., LANG, S.C., STREIT, J.E., UNDERSCHULTZ, J.R. AND ENNIS-KING, J., 2004—Opportunities for geological storage of carbon dioxide in the offshore Gippsland Basin, SE Australia: an example from the upper Latrobe Group. In: Boult, P.J., Johns, D.R. and Lang, S.C. (eds) Eastern Australasian Basins Symposium II. PESA, 367–88.

STREIT, J.E. AND HILLIS, R.R., 2004—Estimating fault stability and sustainable fluid pressures for underground storage of CO_2 in porous rock. Energy, 29 (9–10), 1445–56.

THOMAS, H., BERNECKER, T. AND DRISCOLL, J., 2003—Hydrocarbon Prospectivity of Areas V03-3 and V03-4, Offshore Gippsland Basin, Victoria, Australia: 2003 Acreage Release. Department of Primary Industries, Victorian Initiative for Minerals and Petroleum Report 80.

UNDERSCHULTZ, J.R., OTTO, C.J. AND ROY, V., 2003—Regional Hydrodynamic Analysis on the Gippsland Basin. CSIRO Petroleum, APCRC Confidential Report No. 03–04. 28, unpublished.

VAN WAGONER, J.C., MITCHUM, J.R.M., CAMPION, K.M. AND RAHMANIAN, V.D., 1990—Siliciclastic Sequence Stratigraphy in Well Logs, Cores and Outcrops: Concepts for High-Resolution Correlation of Time Facies. AAPG, Methods in Exploration Series, 7, 55.

VAVRA, C.L., KALDI, J.G. AND SNEIDER, R.M., 1992—Geological applications of capillary pressure: a review. AAPG Bulletin, 76 (6), 840–50.

WATSON, M.N., BOREHAM, C.J. AND TINGATE, P.R., 2004—Carbon dioxide and carbonate cements in the Otway Basin: implications for geological storage of carbon dioxide. The APPEA Journal, 44 (1), 703–20.

WATSON, M.N. AND GIBSON-POOLE, C.M., 2005—Reservoir selection for optimised geological injection and storage of carbon dioxide: a combined geochemical and stratigraphic perspective. The Fourth Annual Conference on Carbon Capture and Storage. National Energy Technology Laboratory, US Department of Energy [CD-Rom].

WOOLLANDS, M.A. AND WONG, D. (eds), 2001—Petroleum Atlas of Victoria, Australia. The State of Victoria, Department of Natural Resources and Environment, 208.

Authors' biographies next page.

THE AUTHORS

Catherine Gibson-Poole graduated BSc (Hons) geology from Royal Holloway University of London (1995) and MSc micropalaeontology from the University of Southampton (1996). She then worked as a geologist with Gaffney Cline and Associates (UK), where she was involved in geological modelling, formation evaluation, and reserves estimation and certification, as well as commercial aspects such as flotation, acquisitions and unitisations. In 1999 she joined Santos Ltd (Adelaide), working in acquisitions and divestments. Catherine commenced a PhD in 2000 at the Australian School of Petroleum (ASP), The University of Adelaide, working with the APCRC-GEODISC Program. Catherine is presently working as a researcher with the CO2CRC at ASP, producing detailed geological models of potential sites for geological storage of CO_2. Member: AAPG, PESA.

Lotte Svendsen is a researcher with the CO2CRC at the Australian School of Petroleum (ASP), The University of Adelaide, South Australia. Lotte joined the CO2CRC in 2005, after completing a MSc in petroleum geology and geophysics at the ASP. Before joining the ASP, she completed her undergraduate degree at the University of Bergen, Norway, and the Queensland University of Technology, Brisbane, Australia. Lotte's research has focussed on sedimentology, sequence stratigraphy, top and fault seals, geological modelling and CO_2 storage. Lotte is a member of AAPG, PESA and ASEG.

Jim Underschultz completed his MSc in geodynamics in 1990 at the University of Alberta. He worked as a petroleum hydrogeologist with the Basin Analysis Group at the Alberta Geological Survey from 1986 to 1994. Since 1994 he has been president of PHI Hydrodynamics Ltd in Calgary and is presently a research scientist at CSIRO Petroleum. Jim has experience with flow systems analysis in many basins worldwide. This includes non-conventional reserves of heavy oil, oil sands, low-pressure shallow gas, coal bed methane and the exploitation of pressure-depleted reservoirs. In recent years he has focussed on petroleum hydrodynamics of faulted strata and the incorporation of hydrodynamics on seals analysis. He has applied many of these aspects to geological storage of CO_2.

Max Watson is a researcher at the Australian School of Petroleum (formerly NCPGG). He completed a BSc at James Cook University in Townsville in 1998 and a BSc (Hons) at the NCPGG in 2000. His research focuses on alteration of reservoir systems by CO_2, reservoir diagenesis, seal alteration, and CO_2 migration and leakage. He is part of the CO2CRC research group. Member: AAPG and PESA.

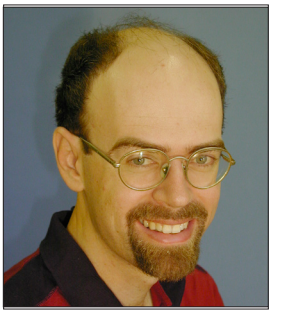

Jonathan Ennis-King completed a BSc at the University of Melbourne in 1988, with honours in applied mathematics, and a PhD at the Australian National University in 1993 in the field of theoretical colloid chemistry. Subsequently, he held postdoctoral positions at the University of Melbourne (1993–5), Lund University, Sweden (1996–7) and the Australian National University (1998–9), conducting theoretical research into colloids, polymers, polyelectrolytes and statistical mechanics. Since 1999 he has worked as a research scientist with CSIRO Petroleum, doing theoretical modelling and numerical simulation of the underground storage of carbon dioxide as part of the Australian Petroleum CRC's GEODISC project, and now as part of the CO2CRC.

Peter van Ruth is a research fellow at the Australian School of Petroleum. He graduated BSc (Hons) (1998), and PhD (2003) from Adelaide University. Peter worked for Baker Atlas as a structural geologist/geomechanical engineer (2003–04). His main research interests are in petroleum geomechanics and structural geology. Member: PESA and SEG.

Emma Nelson is a PhD student at the Australian School of Petroleum. She graduated BSc (Hons) from The University of Adelaide in 2002. Her research interests are in the application of geomechanics to the development of petroleum provinces (including hydraulic fracturing, wellbore stability and naturally fractured reservoirs). She is a member of AAPG, ASEG, PESA and SPE.

Ric Daniel graduated with a BSc in sedimentary geology from Macquarie University (1970) and with a PhD on cool-water carbonate sediments from The University of Adelaide (2002). He has worked with Baroid as a well site and drilling fluids engineer, and has worked with Flinders University and The University of Adelaide as a part-time lecturer and demonstrator. In 2001 Ric joined the Australian School of Petroleum (ASP), at The University of Adelaide, as a researcher for the APCRC Seals Program. Ric is presently working as a research fellow with the CO2CRC at ASP, investigating the seal potential of possible CO_2 storage sites. Member: Australian Quaternary Association.

Yildiray Cinar is a lecturer at the University of New South Wales. Previously, he held research positions at Stanford University, Clausthal Technical University, and Istanbul Technical University. He holds BS and MS degrees from Istanbul Technical University and a PhD degree from Clausthal Technical University, all in petroleum engineering. His present interests include experimental determination and numerical simulation of multiphase flow properties of porous media, well pressure testing and reservoir engineering. He is a member of SPE and of SCA.

15. Appendix 1: Statements from co-authors

The following papers are included as part of this thesis and have co-authors. Statements of contribution from co-authors are included for each.

1. **Underschultz, J.R.**, Otto, C.J. and Bartlett, R. (2005), Formation fluids in faulted aquifers: examples from the foothills of Western Canada and the North West Shelf of Australia. In: P. Boult and J. Kaldi eds., evaluating fault and cap rock seals: *American Association of Petroleum Geologists, Hedberg Series*, 2, 247-260.

my contribution to this publication below was mainly editorial and supervisory. The Canada part of the work was carried out by Jim Underschultz, while I had a small technical component on NWS part.

with regards

Claus

To Whom it May Concern;

My contribution to the paper co authored by Mr. James Underschultz and Dr. Claus Otto was to provide the necessary support data to undertake the interpretation of hydrodynamics as related to the The Alberta foothills stratigraphy in Western Canada. Mr Jim Underschultz did the majority of mapping and writing for the paper concerning Foothills hydrogeology in Western Canada and the above paper as noted.

Richard Bartlett
President
HydroFax Resources Ltd.

2. **Underschultz, J.R**., Otto, C. and Hennig, A. (2007), Application of hydrodynamics to Sub-Basin-Scale static and dynamic reservoir models. *Journal of Petroleum Science and Engineering*. 57/1-2, 92-105.

Jim Underschultz wrote this publication and acknowledges his co-authors who contributed to the research aspects. He is the principle investigator.

regards

Claus

To Whom it May Concern;

My contribution to the paper co authored by Mr. James Underschultz and Dr. Claus Otto was to contribute to the necessary interpretation of data to undertake the hydrodynamic studies as related to the Australian Basin studies, primarily through the PressureQC system and other case studies as referenced in the paper. Mr Jim Underschultz did the mapping and interpretation for the Gippsland Basin hydrogeology. Mr Jim Underschultz also did the majority of the supporting research and writing for this paper. My contribution to these parts were mainly editorial.

Allison Hennig
CSIRO Petroleum

_____

3. Bailey, W.R., **Underschultz J.,** Dewhurst D.N., Kovack G., Mildren S. and Raven M. (2006). Multi-disciplinary approach to fault and top seal appraisal; Pyrenees-Macedon oil and gas fields, Exmouth Sub-basin, Australian Northwest Shelf. *Marine and Petroleum Geology*, **23**, 241-259.

Jim

As for using the paper. No bother. You were indeed responsible for the hydrodynamics component & also the pressure QC behind the fault seal work. And you were responsible for the head map

Cheers
Wayne

Wayne Bailey

Co-ordinator - Structural Geology
Geology - Science & Technology
Woodside Energy Ltd.
Woodside Plaza
240 St Georges Terrace
Perth WA 6000
Australia

T: +61 8 9348 4716
F: +61 8 9214 2744

E: Wayne.Bailey@woodside.com.au

To whom it may concern,

As a co-author to the paper title outlined in yellow below, I confirm that Jim Underschultz contributed not only to the hydrodynamics part of the paper but also to extensive in depth discussions regarding the integrated model that was proposed. The discussions and conclusions of the paper were truly a joint multi-disciplinary effort, to which the hydrodynamics results significantly contributed.

Yours sincerely

Dave Dewhurst

Hi Jim,

Congratulation on your imminent submission! Here is my declaration on your behalf.

I confirm that Jim Underschultz contributed the hydrodynamics component for the paper entitled:

Multi-disciplinary approach to fault and top seal appraisal; Pyrenees-Macedon oil and gas fields, Exmouth Sub-basin, Australian Northwest Shelf. W.R. Bailey, J Underschultz, D.N. Dewhurst, G Kovack, S. Midren and M. Raven. Marine and Petroleum Geology, 2006, v. 23, 241-259.

Regards

Scotty

4. **Underschultz, J.R**., Hill, R.A. and Easton, S. (In review). The Hydrodynamics of Fields in the Macedon, Pyrenees and Barrow Sands, Exmouth Sub-Basin: Identifying Seals and Compartments. *Australian Society of Exploration Geophysicists.* 39, 2.

To whom it may concern:

Jim Underschultz undertook a proprietary study for BHP Billiton Petroleum in 2005 entitled "Hydrodynamic Analysis of the Macedon, Pyrenees and Barrow sands of the Exmouth Sub-basin". BHP Billiton supplied raw pressure, salinity and drilling data for wells not in the
public domain i.e. not held by CSIRO at the time of the original study,
in all some 42 wells were analysed. BHP Billiton also supplied some regional structure maps to help Jim interpret the potential cross-fault
communication of the various sands in the Exmouth Sub-basin. All the hydrodynamic interpretation in the study was Jim's work. The subsequent
ASEG paper (2007) entitled "Hydrodynamic Analysis of the Macedon, Pyrenees and Barrow sands of the Exmouth Sub-basin, North West Australia: identifying Seals and Compartments" was based on the CSIRO study and compiled by Jim as the lead author, I provided some regional
background on the deposition and stratigraphy of the Macedon Sands and
commented on the overall content and layout of the paper.

Robin Hill
Production Geoscience Manager

BHP Billiton Petroleum Pty ltd
Level 16 Central Park
152-158 St Georges Tce
Perth WA6000
Australia

Tel 9338 4796 (direct)
Mobile 0408 926 784
email: robin.hill@bhpbilliton.com

5. Gibson-Poole, C.M., Svendsen, L., **Underschultz, J**., Watson, M.N., Ennis-King, J., van Ruth, P.J., Nelson, E.J., Daniel, R.F., and Cinar, Y. (2007). Site Characterisation of a Basin-Scale CO_2 Geological Storage System: Gippsland Basin, Southeast Australia. *Journal of Environmental Geology*. On-line publication not yet in print. http://www.springerlink.com/content/0r4v8l4j846t5308/.

6. Gibson-Poole, C.M., Svendsen, L., **Underschultz, J**., Watson, M.N., Ennis-King, J., van Ruth, P., Nelson, E., Daniel, R., and Cinar, Y. (2006). Gippsland Basin Geosequestration: A potential solution for the Latrobe Valley brown coal CO_2 emissions. . *Australian Petroleum Production and Exploration Association Journal*, 46 (1), 241-259.

Dear Jim,

With respect to the multi-authored papers listed below, I confirm that your contribution to these papers were the sections written on the hydrodynamics.

Site Characterisation of a Basin-Scale CO_2 Geological Storage System: Gippsland Basin, Southeast Australia. Gibson-Poole, C M, Svendsen, L, Underschultz, J, Watson, M N, Ennis-King, J, van Ruth, P J, Nelson, E J, Daniel, R F, & Cinar, Y. Journal of Environmental Geology. In press.

Gippsland Basin Geosequestration: A potential solution for the Latrobe Valley brown coal CO_2 emissions. C.M. Gibson-Poole, L. Svendsen, J. Underschultz, M.N. Watson, J. Ennis-King, P. van Ruth, E. Nelson, R. Daniel, P. and Y. Cinar. The APPEA Journal, 2006, 46 (1), 241-259.

I also give permission for you to include a full copy of the APPEA paper in your thesis.

Best regards,
Catherine.

_____

Catherine Gibson-Poole
Senior Research Fellow CO2CRC
Australian School of Petroleum
The University of Adelaide
Adelaide, SA 5005
Phone: +61 8 8303 4292

Fax: +61 8 8303 4345
email: cgibsonp@asp.adelaide.edu.au

This email is sent as a confirmation that James Underschultz's contribution to the two papers listed below was to do with the hydoodynamics.

James Underschultz has my agreement to include and duplicate the APPEA paper below (in full without revision) in his PhD Thesis.

Gippsland Basin Geosequestration: A potential solution for the Latrobe Valley brown coal CO_2 emissions. C.M. Gibson-Poole, L. Svendsen, J. Underschultz, M.N. Watson, J. Ennis-King, P. van Ruth, E. Nelson, R. Daniel, P. and Y. Cinar. The APPEA Journal, 2006, 46 (1), 241-259.

Site Characterisation of a Basin-Scale CO_2 Geological Storage System: Gippsland Basin, Southeast Australia. Gibson-Poole, C M, Svendsen, L, Underschultz, J, Watson, M N, Ennis-King, J, van Ruth, P J, Nelson, E J, Daniel, R F, & Cinar, Y. Journal of Environmental Geology. In press.

If any further documentation or confirmation is neccesary, then please contact my via email or mobile.

Regards,

Lotte Myrvang (formerly Lotte Svendsen)

Lotte Myrvang

Geologist

BG Norge

Løkkeveien 103B

4007 Stavanger, Norway

+47 5120 5946 (direct)

+47 5120 5900 (operator)

+47 9480 2201 (mobile)

Email: lotte.myrvang@bg-group.com

Hi Jim,

Yes, your contribution to both the APPEA and Environmental Geology papers, which was a major component of the research, related to the hydrodynamics.

You have my permission as a co-author to include the APPEA paper in your thesis

Cheers

Max

Dear Jim,

This is to acknowledge that your contribution to the APPEA and Environmental Geology papers was to with hydrodynamics. You have my permission to include the APPEA paper in your thesis.

Yours

Jonathan

Hi Jim,

I agree that your excellent contribution to these papers related to the hydrodynamics content

You have my permission to include the APPEA paper in your thesis

Cheers

Peter

Hi Jim,

Your contribution to both the APPEA and Environmental Geology papers was of significant input and related to hydrodynamics. Yes you have my permission as a co-author to include the papers in your thesis
Regards Ric Daniel

Hi Jim,

I agree that your contribution to both articles was to do with the Hydrodynamics and you have my permission to include the APPEA paper in your thesis.

All the best

Yildiray

==========

School of Petroleum Engineering
The University of New South Wales
Sydney 2052 NSW Australia
Phone: +61-2-9385-5786
Fax: +61-2-9385-5936

16. Appendix 2: Permission letters for copyright

1. **Underschultz, J.R**., Otto, C.J. and Bartlett, R. (2005), Formation fluids in faulted aquifers: examples from the foothills of Western Canada and the North West Shelf of Australia. In: P. Boult and J. Kaldi eds., evaluating fault and cap rock seals: *American Association of Petroleum Geologists, Hedberg Series*, 2, 247-260.

Jim, we've given GSW permission to post some of our papers however, they are not the primary web site to obtain articles or information concerning AAPG. Fortunately, your email was forwarded to me at the AAPG Permissions desk.

I've attached information on seeking and granting permission. In your particular case I'll be sending you a written grant of permission (GOP) to republish your paper in it's entirety within your thesis. Please comply with section (c) "Condition of Grant of Permission" on attached.

In order to complete the GOP I'll need the title of your thesis and approximate date of completion (i.e. 2007 or 2008? is close enough).

If you have further questions please feel free to contact me directly.

Sincerely,
Mary Kay (Grosvald)
AAPG Permissions Editor
permissions@aapg.org
mgrosvald@aapg.org
(918) 560 9431

---

2. **Underschultz, J.R.**, Otto, C. and Hennig, A. (2007), Application of hydrodynamics to Sub-Basin-Scale static and dynamic reservoir models. *Journal of Petroleum Science and Engineering*. 57/1-2, 92-105.

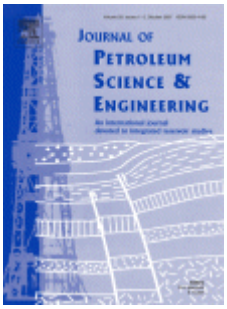

Title: Application of hydrodynamics to sub-basin-scale static and dynamic reservoir models

Author: Underschultz J.R., Otto C. and Hennig A.

Publication: Journal of Petroleum Science and Engineering

Publisher: Elsevier Limited

Date: May 2007

Order Completed

Thank you very much for your order.

This is a License Agreement between Jim Underschultz ("You") and Elsevier Limited ("Elsevier Limited"). The license consists of your order details, the terms and conditions provided by Elsevier Limited, and the payment terms and conditions.

Get the printable license.

Order Details

License Number	1833440534538

License date	Nov 21, 2007
Licensed content publisher	Elsevier Limited
Licensed content publication	Journal of Petroleum Science and Engineering
Licensed content title	Application of hydrodynamics to sub-basin-scale static and dynamic reservoir models
Licensed content author	Underschultz J.R., Otto C. and Hennig A.
Licensed content date	May 2007

Volume number	57
Issue number	1-2
Pages	14
Type of Use	Thesis / Dissertation
Portion	Full article
Format	Both print and electronic
You are the author of this Elsevier article	Yes
Are you translating?	No
Purchase order number	

Expected publication date	Feb 2008
Elsevier VAT number	GB 494 6272 12
Permissions price	0.00 USD
Value added tax 0.0%	0.00 USD
Total	0.00 USD

3. **Underschultz, J.R**. (2007). Hydrodynamics and membrane seal capacity: *Geofluids Journal*, 7, 148-158.

Thank you for your email request. Permission is granted for you to use the material below for your thesis/dissertation subject to the usual acknowledgements and on the understanding that you will reapply for permission if you wish to distribute or publish your thesis/dissertation commercially.

Best wishes
Laura Wilson.

Permissions Controller
Wiley-Blackwell
PO Box 805
9600 Garsington Road
Oxford
OX4 2ZG
United Kingdom

Fax: 00 44 1865 471150

4. Bailey, W.R., **Underschultz J.,** Dewhurst D.N., Kovack G., Mildren S. and Raven M. (2006). Multi-disciplinary approach to fault and top seal appraisal; Pyrenees-Macedon oil and gas fields, Exmouth Sub-basin, Australian Northwest Shelf. *Marine and Petroleum Geology*, **23**, 241-259.

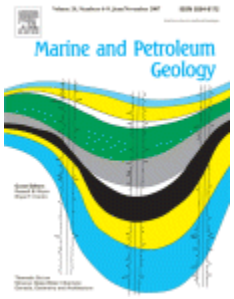

Title: Multi-disciplinary approach to fault and top seal appraisal; Pyrenees–Macedon oil and gas fields, Exmouth Sub-basin, Australian Northwest Shelf

Author: Bailey Wayne R., Underschultz Jim, Dewhurst David N., Kovack Gillian, Mildren Scott and Raven Mark

Publication: Marine and Petroleum Geology

Publisher: Elsevier Limited

Date: February 2006

Order Completed

Thank you very much for your order.

This is a License Agreement between Jim Underschultz ("You") and Elsevier Limited ("Elsevier Limited"). The license consists of your order details, the terms and conditions provided by Elsevier Limited, and the payment terms and conditions.

Get the printable license.

License Number	1833440408740
License date	Nov 21, 2007
Licensed content publisher	Elsevier Limited
Licensed content publication	Marine and Petroleum Geology
Licensed content title	Multi-disciplinary approach to fault and top seal appraisal; Pyrenees–Macedon oil and gas fields, Exmouth Sub-basin, Australian Northwest Shelf
Licensed content author	Bailey Wayne R., Underschultz Jim, Dewhurst David N., Kovack Gillian, Mildren Scott and Raven Mark
Licensed content date	February 2006

Volume number	23
Issue number	2
Pages	19
Type of Use	Thesis / Dissertation
Portion	Full article
Format	Print
You are the author of this Elsevier article	Yes
Are you translating?	No
Purchase order number	

Expected publication date	Feb 2008
Elsevier VAT number	GB 494 6272 12
Permissions price	0.00 USD
Value added tax 0.0%	0.00 USD
Total	0.00 USD

5. **Underschultz, J.R**., Hill, R.A. and Easton, S. (2008). The Hydrodynamics of Fields in the Macedon, Pyrenees and Barrow Sands, Exmouth Sub-Basin: Identifying Seals and Compartments. *Australian Society of Exploration Geophysicists*, 39, pp. 85-93.

Dear Jim

Thank you for your email.

Permission is granted for you to include this paper in your PhD thesis with appropriate acknowledgement.

Please note that *Exploration Geophysics* volume 39 no. 2, where your paper will be published in, is scheduled to be released the week starting 23 June 2008.

If you will be submitting / defending your thesis before the release of this issue of the journal, please include the following statement:

> **"Reproduced (or reprinted) with kind permission from *Exploration Geophysics* vol. 39 no. 2 (In Press). Copyright Australian Society of Exploration Geophysicists 2008. Published by CSIRO PUBLISHING, Melbourne Australia."**

Should you be submitting your thesis after the release of this volume of *Exploration Geophysics*, please replace the words *"(In Press)"* with the issue and page numbers.

Our preference is for you to include the final copyedited version of your paper, however, your supervisor should give guidance on that.

We would also appreciate it if you can cite the journal's website in your thesis. The link is http://www.publish.csiro.au/nid/224.htm

With best wishes

Carla

_____
Carla Flores
Rights & Permissions, **CSIRO** PUBLISHING
Telephone +61 3 9662 7652
Fax +61 3 9662 7595

6. Gibson-Poole, C.M., Svendsen, L., **Underschultz, J**., Watson, M.N., Ennis-King, J., van Ruth, P.J., Nelson, E.J., Daniel, R.F., and Cinar, Y. (2007). Site Characterisation of a Basin-Scale CO_2 Geological Storage System: Gippsland Basin, Southeast Australia. *Journal of Environmental Geology*. On-line publication not yet in print. http://www.springerlink.com/content/0r4v8l4j846t5308/.

Dear Sir,

With reference to your request (copy herewith) to reprint material on which Springer Science and Business Media controls the copyright, our permission is granted, free of charge, for the use indicated in your enquiry.

This permission

- allows you non-exclusive reproduction rights throughout the World.
- permission includes use in an electronic form, provided that content is
  * password protected;
  * at intranet;
- excludes use in any other electronic form. Should you have a specific project in mind, please reapply for permission.
- requires a full credit (Springer/Kluwer Academic Publishers book/journal title, volume, year of publication, page, chapter/article title, name(s) of author(s), figure number(s), original copyright notice) to the publication in which the material was originally published, by adding: with kind permission of Springer Science and Business Media.

The material can only be used for the purpose of defending your dissertation, and with a maximum of **100** extra copies in paper.

Permission free of charge on this occasion does not prejudice any rights we might have to charge for reproduction of our copyrighted material in the future.

Best wishes,

Nel van der Werf (Ms)
Assistant Rights and Permissions/Springer
Van Godewijckstraat 30 | P.O. Box 17
3300 AA Dordrecht | The Netherlands
tel +31 (0) 78 6576 298
fax +31 (0)78 65 76-300
Nel.vanderwerf @springer.com
www.springeronline.com

7. Gibson-Poole, C.M., Svendsen, L., **Underschultz, J**., Watson, M.N., Ennis-King, J., van Ruth, P., Nelson, E., Daniel, R., and Cinar, Y. (2006). Gippsland Basin Geosequestration: A potential solution for the Latrobe Valley brown coal CO_2 emissions. . *Australian Petroleum Production and Exploration Association Journal*, 46 (1), 241-259.

Dear James

Thank you for your recent enquiry regarding using certain material from the APPEA Journal.

APPEA I am afraid does not retain copyright for the individual articles so permission would have to be sought from the author(s) of that particular article.

Please advise if you require some contact details in this regard – I am sure we will be able to assist in this area.

Kind regards

Julie

Julie Hood
Director, Events
Australian Petroleum Production & Exploration Association Limited
Phone: (07) 3802 2208
Fax: (07) 3802 2209
Mobile: 0412 998 474
E-mail: jhood@appea.com.au

This letter from APPEA applies to paper 7. The co-authors statements in Appendix 1 above, also include statements on permission to reproduce the paper in this Thesis.

17. Bibliography

Jim Underschultz received his BSc (Honours) Geology in 1986 from the University of Alberta in Canada. In 1986 he commenced working with the Basin Analysis Group at the Alberta Research Council. In 1990 Jim received his MSc. in Geology/Geodynamics from the University of Alberta in Canada. In 1994 Jim moved to Hydro Petroleum Canada Ltd as a consultant in Calgary, Canada. He was promoted to Vice President of regional studies the same year. In 1995 Jim started his own company and is CEO of PHI Hydrodynamics Ltd in Calgary. In 1999 Jim took a position as senior research scientist at CSIRO Petroleum in Perth Australia in the capacity of a petroleum hydrogeologist. Currently, Jim holds the position of Stream Leader, Exploration and Appraisal in CSIRO Petroleum, Team Leader of the Hydrodynamics Group in CSIRO Petroleum and Discipline Leader of Hydrodynamics and Geochemistry programme in the CO2CRC.

With over 20 years experience, more than 30 publications and 60 conference presentations in hydrogeology, Jim has worked on the Western Canada Sedimentary Basin, the thrust-fold belt of Western Canada, the Beaufort-Mackenzie Basin, the Canadian East Coast, the Llanos Basin Colombia, most Australian basins, Lybia, Dutch North Sea, and minor examinations of other regions around the world. While primarily dealing with pressure and formation water analyses data, Jim has experience with environmental issues, numerical simulation and all aspects of basin analysis in both carbonate and clastic reservoirs. He has developed and presented field trips and short courses on Petroleum Hydrogeology and Seals Analysis and their application to exploration and production. He was the AAPG/PESA distinguished lecturer in 1999.

Recently, Jim's research interests have been in hydrodynamics related to fault and top seal analysis and the application of hydrodynamic techniques to CO_2 storage capacity estimation, containment security, and monitoring and verification. He has had close collaboration with Barry Freifeld at Lawrence Berkley National Laboratory and Sue Havorka at the Texas Bureau of Economic Geology on integrated monitoring and verification techniques implemented at the Frio II and Otway CO_2 pilot projects.